This thesis was composed by me and consists entirely of my own work.

December 1976.

PHOTOGRAPHIC PHOTOMETRY OF STAR CLUSTERS

IN THE SMALL MAGELLANIC CLOUD

Mary Kontizas

B.Sc. (GREECE, Athens)

Presented for the Degree of Doctor of Philosophy

at the University of Edinburgh

1976 December.

ABSTRACT OF THESIS

Photographic photometry of 20 star clusters and their adjoining fields has been carried out to determine the colour magnitude diagram for stellar systems in the Small Magellanic Cloud, using plates from the U.K. 1.2m Schmidt telescope. The W-N-E periphery of the Cloud has been examined.

The main difficulty of the SMC star clusters is the contamination of cluster members by stars in the surrounding field.

The evolutionary history of the star clusters seems to be similar to that of the surrounding field, implying that the background halo of the SMC is not well mixed.

Old clusters have been found over the whole Cloud exhibiting differences in the morphology of the H-B which in most cases is very well populated at the red side of the RR Lyrae stars strip.

Two more characteristics are i) the existence of very red stars (in three cases they are proved carbon stars) and ii) the large number of blue faint stars.

The metallicity has been shown to be low in the SMC but the characteristics found in the old clusters are those normally found in intermediate age clusters of our Galaxy. Thus the age of the western halo clusters is $\sim 10^9$ - 5×10^9 yrs, whereas the northern halo clusters are even younger.

The second group of clusters comprises young clusters which occupy the north part of the SMC or the north-east arm, since no young objects have been detected at the western part of this galaxy.

The colour magnitude diagrams of the clusters and the adjoining field of the north-west arm give an age estimate of this feature of about 5×10^7 yrs.

The other small young clusters in the northern side of the Cloud are objects of the SMC disc and their ages are 10^6 - 10^7 years.

To the Astronomy Department and the Royal Observatory of Edinburgh staff for being so helpful.

CONTENTS

CHAPTER III SMALL MAGELLANIC CLOUD - PREVIOUS WORK

CHAPTER IV NEW C-M DIAGRAMS OF THE SMC CLUSTERS AND THEIR SURROUNDING FIELD

INTRODUCTION

The Magellanic Clouds have always been very important objects of the southern sky and they can provide very useful material for the study of stellar evolution. They belong to our local system of galaxies and they are our nearest neighbours. The absorption in their direction is very small and the absolute magnitudes accurate to ± 0.4 mag. They contain a greal deal of objects and amongst them many star clusters. Since the powerful telescopes in the southern hemisphere started operating, an attempt has been made to study the stellar systems of both Clouds.

The Small Magellanic Cloud (SMC) is about 63 kpc from the Sun and the distance modulus is about $m-M_V = 19^m.20$ (Westerlund, 1974). This means that the limits of observations should be fainter than $V = 19^m.00$ to detect the horizontal branches of globular clusters. So far only very few globular clusters (the term old globular is more suitable for the SMC) have been studied for this reason. Kron (1956) and Lindsay (1958) provided the first lists of clusters. Arp (1958, 1958, 1959, 1959) carried out photometric and photographic photometry in order to study four rich clusters in the N-E part and the core of the SMC, i.e. NGC 361, NGC 458, NGC 330 and NGC 419. Tifft in 1963 investigated one rich cluster of the western part, the old halo cluster NGC 121 and he reached faint enough limits to get the H-B fainter, whereas Gascoigne in 1966 continued the study of the halo by producing colour-magnitude diagrams of three clusters and he wrote an extensive paper describing the first results on the behaviour of globular clusters in this galaxy.

Apart from these researchers, Westerlund (1961) studied the stellar content of the wing of the SMC carrying out photographic photometry of clusters occupying this area. He found very young objects apparently the youngest of the SMC.

Walker published two colour-magnitude (C-M) diagrams of NGC 419 (1972) and Kron 3 (1970) using electronographic magnitudes and he provided a very useful set of faint standard stars reaching a limit for V and B colours of about $22^{m}.00$.

Robertson (1975) analysed the cluster NGC 330 from both observational and theoretical points of view and he showed that it is an evolved cluster with some core Helium burning stars. De Vaucouleurs long ago and in a recent review (1972) reports that apart from the wing there is a smaller arm in the northern part of the SMC where NGC 458 is located. So it is interesting to study the stellar content of this feature and the two more clusters which are occupying this small arm.

Many researchers have studied all sorts of objects in the SMC and the Cloud's variables gave the opportunity to Miss Leavitt to establish the period-luminosity relation of Cepheids. Many RR Lyrae stars have been detected in the SMC. Graham (1975) has found that their period distribution is different than in our galaxy but similar to that of the dwarf galaxies. So a great number of very old objects belong to the SMC as well as young ones and those of intermediate age.

The study of star clusters also provides much information about the evolutionary history of the SMC. So it is very important to produce colour-magnitude diagrams of the clusters and compare them with the clusters of our Galaxy and other galaxies. Clusters of different ages have been found distributed over the whole area of the SMC.

The C-M diagrams for the old clusters cannot be fully investigated because the turn-off point occurs at very faint magnitude which is beyond the limit of detection of the large telescopes, but we can reach the horizontal branch (H-B) which is expected at about V ~ 19.00 mag and therefore it can be studied for the limits of observations are quite accurate to $V \sim 21^{m}.50$ mag.

The younger clusters of the SMC which are mainly found on the north and north-east part of the Cloud are also very interesting objects for investigation. So far their interpretation is difficult and they give C-M diagrams consisting of two distinct branches, one red giant branch and one main sequence, both at the same range of absolute magnitude.

The main problem in the interpretation of a C-M diagram in the SMC is the contamination of cluster members with their surrounding field stars. The stars are too faint to use radial velocities in order to identify the cluster members, so it was assumed that if we take a small sample of about 5 clusters close to each other in different regions of the SMC plates, they might produce the same C-M diagram for their field stars. Therefore the differences in the c-m diagrams could be due to their intrinsic properties.

New telescopes in the southern hemisphere in Chile and Australia revealed a lot more star clusters in the SMC and lists were published by Hodge and Wright (1974) and Brück (1975), bringing the total number of star clusters to 330.

Therefore the first photographic plates of the SMC provided by the U.K. 1.2m Schmidt telescope in Coonabarabran (Australia) were very useful raw material for the investigation of star clusters in this galaxy.

On each plate 330 star clusters can be detected mostly in the unvignetted area, so photographic photometry would be possible in order to determine the magnitudes of stars. Four blue and three visual plates were available and two questions had to be answered before the project of studying the star clusters and stellar content of the western and N-E periphery of the SMC, could begin.

The quality of the plates for photometry was the first problem and the photoelectric sequences existing especially for the faint limits in order to get as faint magnitudes as the Schmidt plates reach, without any dangerous extrapolations, was the second one.

The first problem could be solved because there are photoelectric standards in different parts of the SMC, published by the previously mentioned astronomers who have already studied the rich star clusters in this galaxy. The faint sequence available is only one, that by Walker which has been produced electronographically. So there was nothing else than combining these standards with the other brighter ones lying on different parts of the Cloud. The question of the quality of the plates was to be answered for making possible the combination of sets of standard stars separated on the field of the photographic plates.

Three V and three B plates have been measured and the details about the plate characteristics, the errors and accuracy have been described in chapter one of this work. It is discussed extensively which are the different sources of errors in photographic photometry and which is in particular the quality of the results of this project. The measurements have been done with a conventional Becker Iris photometer and the calibration curves by a least square fit program and hand drawn curves, where necessary. In summary the probable error of the mean photographic magnitude is ~0.03 for $V < 19^m.0$ and ~ ~$0^m.05$ for $V > 19^m.00$ whereas 0.05 throughout the B plates.

The calibration curves showed a very good agreement for the different sets of standards even for standards as far as 4^o apart from each other. The standard stars were the photoelectric sequences by Arp in 1958 for the cluster

NGC 361, by the same author in 1959 in the area of the cluster NGC 458, by Butler in 1972 in the northern part of the "bar" and "central region" of the SMC, by Tifft in 1963 for the cluster NGC 121, by Cannon in 1974 for the cluster 47 TUC and the faint electronographic sequence by Walker which has already been mentioned.

Consequently one criterion of choosing the clusters to be measured was their vicinity to the above standard sequences. The next criterion was the crowded nature of the different parts of the SMC especially near the bar and finally the clusters had to lie in the unvignetted area of the plates.

In chapter two, the observational side of galactic star cluster research work has been given. The current observational results as far as open clusters are concerned are summarised and followed by the main problems of the globular clusters. The review is mainly concerned with 3 colour photometry and the method of deriving the different parameters such as distance moduli, metal abundances and ages of star clusters.

The second part of this chapter deals with the anomalous C-M diagrams found in our own galaxy arising from the poor correlation of metal abundances and the structure of the H-B. The conjectures made so far have not given any answer to this anomaly which remains an open field for further research.

In chapter three, the main previous or current views on the SMC research are given. The star clusters in this galaxy have been discussed in more detail and all the known C-M diagrams have been interpreted.

Twenty new C-M diagrams produced in the course of this project are described in chapter four.

They have been divided into three groups according to their common characteristics such as their location on the plate or the age.

The C-M diagrams have been interpreted in as much detail as possible.

The first group comprises 11 clusters located all over the studied periphery of the SMC. They are old halo clusters and therefore they are scattered in all parts of the Cloud. The western clusters are all red halo type clusters whereas the clusters are of mixed type in the northern part.

These eleven clusters are found to have differences between themselves and especially in the structure of the horizontal branch, which of course is the only feature we can see in the C-M diagrams because the turn-off points are expected beyond the limit of observations. Some of these clusters exhibit a very conspicuous red H-B resembling the anomalous cases found in our own Galaxy which have a very rich red H-B, although they are metal poor. The existence of very red stars (some have been proved to be carbon stars) is another typical characteristic of these halo SMC clusters.

Few other clusters have a poor red H-B with some indication of blue H-B. The main difficulty of accepting or not the existence of a certain pattern in the C-M diagrams is that the field stars are mixed up with the cluster members. It also seems that the evolutionary history of the stars lying in the vicinity of the clusters is similar to that of the cluster members so in some cases the investigation of the cluster itself is very difficult.

The presence of many faint blue stars is also a problem to discuss. They can be either a significant number of blue H-B stars, or blue stragglers, which is known to be a property of intermediate age clusters in the Galaxy.

Two clusters occupy the north-east arm and their C-M diagram combined with the field stars in their vicinity shows that the age of the arm population is about 5×10^7 years.

A group of clusters around the cluster NGC 361 at the northern part of the SMC shows young objects, members of the bar or the "central region" of this galaxy.

The main results and conclusions are discussed in chapter five. The two main populations of the stellar content of the SMC (the young and the old objects) are analysed. Composite C-M diagrams for these groups are compared with similar ones in our own Galaxy or some dwarf galaxies.

Finally the charts and lists of stars measured in each cluster are given in the appendix.

CHAPTER I

PHOTOGRAPHIC PHOTOMETRY

PHOTOGRAPHIC MATERIAL - METHOD OF REDUCTION

1. The role of the Schmidt telescopes in the study of stellar photometric problems.

The photographic material of this project was obtained with the U.K. 1.2m Schmidt telescope in Siding Spring, Australia which is fully in operation since autumn 1973. The characteristics of the telescope are given in Table 1.

At first sight the Schmidt telescope appears ideally suitable for in focus photographic photometry. It provides high image quality over a wide field, of 5^{o} or greater, so that a single exposure should give images down to faint limiting magnitude with small field errors.

There are problems which can limit its possibilities. The reason is that the small size of the image makes the measured magnitude critically sensitive to certain disturbances such as errors in adjustment, focus changes and differential flexure. The plates taken by Schmidt telescopes have usually less signal-to-noise ratio than the telescopes normally used for photometry. This is due to the fact that the images are sharply circular and therefore produced by a smaller number of grains. But even so it will be important to show how much Schmidt telescopes contribute to the stellar photometry and how reliable the photometry of these new plates is.

1.1. Previous work done with Schmidt plates.

The field of Schmidt plates being so large gives an enormous amount of information down to very faint limits. Two reasons make slow the reduction of data.

TABLE 1

Parameters for the U.K. 1.2m Schmidt Telescope

Mirror diameter:	1.83 metres
Aperture diameter:	1.24 metres
Focal length:	3.07 metres
Photographic plate sizes:	356 mm square
thickness:	1 mm
Radius of curvature of focal plane:	3.07 metres
Unvignetted field radius:	147 mm = 2.73 arc degree
Plate scale:	67.1 arc sec/mm = 14.9μm/arc sec
Corrector plates:	Schott BK7 glass, corrected wavelength 4200Å; gives image diameter of about 2 arc sec with bandwidth of 1000Å centred about the corrected wavelength.

The lack of photoelectric scales and the time consuming for the measurement with isophotometers. Both handicaps can be solved. The new measuring machines like "COSMOS" in Edinburgh can speed up this difficulty and the photoelectric standards can be organised for future observational projects.

Becker in 1972 discussed many points on the role of Schmidt telescopes in the study of galactic clusters and stellar astronomy emphasising the following.

Up to the present time three-colour photometry has been applied mainly to four topics:

I. Galactic clusters:

Photographic measurements on large field plates containing at least one cluster observed photoelectrically. Out of 220 clusters 45 were observed by use of Schmidt plates. 16 of them are galactic clusters and the distance determined by Schmidt plates is almost of the same quality as the one determined photoelectrically.

II. Distribution of stars in the Galactic disc:

The application of three colour photometry for the derivation density of gradients requires a large number of stars to be measured in different galactic areas and many photoelectric scales. The first requirement can very well be solved by the Schmidt telescopes and the measuring machines.

III. Distribution of stars in the galactic halo.

IV. White dwarfs in high galactic latitudes.

The cases III and IV are solved as discussed in II.

1.2. Work on stellar photometry of the Magellanic Clouds.

Wayman (1972) also suggests the possibility of the study of the Magellanic Clouds with the large Schmidt telescopes. The main advantages are:

Both Clouds can be completely covered with no more than a dozen plates at the most, so that surveys can be completed within a reasonable period of time.

The distance of the Clouds is such that in sparse areas the stars are well enough separated but in dense areas the stellar images superimposed (2 sec of arc at the telescope corresponds to 0.5 pc).

Study of variable stars, although widely investigated, would be quite important in order to get further details, after obtaining better photoelectric sequences.

A detailed analysis of the variations on reddening over the Clouds system, from observations of blue stars is needed.

Groupings of stars of all sizes should be studied in the Magellanic Clouds. Many globular clusters exist in both Clouds and their investigation using material obtained with the Schmidt telescopes would be an important contribution.

Summarising, the main advantages of Schmidt telescopes are:

1) Homogeneous image quality over fields of 5^{o} diameters in large systems.

2) At commonly used focal ratios the sky background and extended sources can be registered with relatively short exposures.

3) The most important of all is that for a short time of observing we get an enormous amount of information on a large field plate.

1.3. Photographic material.

During the first year of operation the U.K. 1.20m Schmidt telescope at Coonobarabran, Australia, has provided a series of plates of the Small Magellanic Cloud. Three plates in each colour have been measured. The details for each plate are given in the Table 2.

TABLE 2

U.K. 1.2m SCHMIDT TELESCOPE PLATES OF SMC

Plate No.	Colour	Filter	Date	Emulsion	Exposure	L.S.T. at start
286	B	GG 385	21/22-12-73	IIaO	40 mins	$00^h\ 36^m$
287	B	GG 385	21/22-12-73	IIaO	40 mins	$02^h\ 08^m$
294	B	GG 385	25/26-10-73	IIaO	40 mins	$23^h\ 05^m$
295	B	GG 385	25/26-10-73	IIaO	40 mins	$00^h\ 0.3^m$
303	V	GG 495	29/30-10-73	IIaD	20 mins	$00^h\ 18^m$
304	V	GG 495	29/30-10-73	IIaD	20 mins	$00^h\ 56^m$
312	V	GG 495	30-10-73	IIaD	40 mins	$01^h\ 15^m$

1.4. Measurements and reductions of the photographic material.

1.4.1. Description of the instrument.

The image densities were measured with the Becker Iris photometer of the Royal Observatory of Edinburgh. Fig. 1 illustrates the main diagram of the instrument as it is described by Becker (1956).

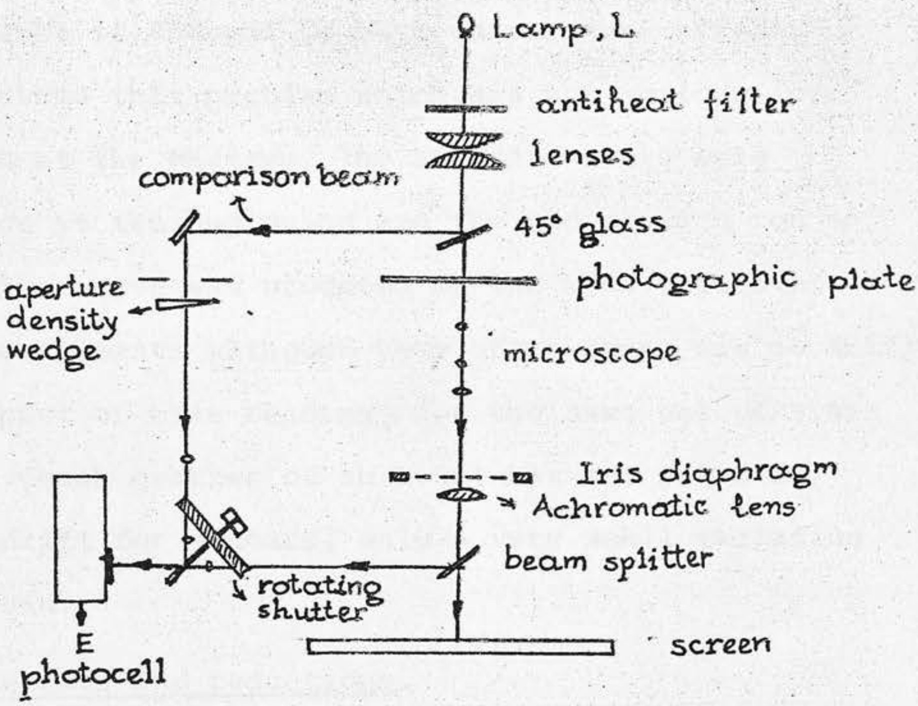

Fig. 1. Becker Iris Photometer.

The beam from the lamp L splits in two, the comparison beam and the second which passes through the photographic plate and the iris diaphragm. This latter beam splits again in two, one part goes to the screen and the other part to the rotating shutter where the comparison beam arrives too. The rotating shutter R passes the beams in rapid succession and an electronic indicator E, shows when both beams are equal in intensity.

When a star image is centred in the iris image on P, a proportion of light is absorbed and the iris diaphragm must be opened to restore equality of intensity of the two beams. An arbitrary scale attached to the iris movement gives a measure of the photographic effect of the star. This measure is independent of the brightness of the lamp L in so far as the balance of the beams is also independent. Usually during runs of several hours drifts in the zero point are observed. That is thought to be a temperature effect. In order to avoid this problem which was not serious for 4-5 hours run at the maximum, the standard stars were measured twice at the beginning and the end of each run so the calibration curve was produced by the mean values of these two measurements although very often there was no drift at all. A plot of iris readings for the same set of stars against time (each quarter of an hour) has not shown any appreciable drift for 4 hours, only a very small variation around the mean.

1.4.2. Measurements and reductions.

Each star cluster was divided into rings around the centre or sectors according to the size, trying to measure all stars in a central circular area and many field stars in order to get a sample of 400-500 stars for the rich clusters and 100-200 stars for the smaller ones. All good images of the selected areas were measured and the aim was to have an unbiased sample. Quite a few stars however, have been rejected because their images were distorted on the plate by overlappings, high background reading due to many faint stars in its vicinity or when the values found in the three plates of the same colour gave a difference in magnitude of more than $0^m.3$ - $0^m.4$ (according to the magnitude or the areas).

So for each cluster all stars were measured in one run and the standard sequence twice, once at the beginning and next at the end of the run. The drift was very small but still the mean of the two measurements was taken to produce the standard sequence's iris readings. The relationship between iris readings and photoelectric magnitude is expressed by a polynomial whose coefficients are determined by a least square solution. The degree of the best fit was chosen by the computer as the one which gave the smaller r.m.s. error, but the computer solution slightly deviates towards the faint limits of the plates, so the calibration curves have been checked and corrected by hand wherever it was necessary.

The process described above has been followed for each run of measurements and the magnitudes derived for each star have been listed. The mean of the three magnitudes derived from the V, or the B plates are the magnitudes in V and B of the measured stars.

1.5 Photometric errors and discussion on the Schmidt plate photomery.

The determination of the magnitudes of stars using an iris photometer can be constrained by the following factors which imply imperfections and errors due to the telescope, the photographic plates, the photometer and the non linearity of the iris reading calibration curve.

Although it is difficult to separate all these sources of error, it is necessary to discuss all of them in detail and give some results which show the accuracy of the photometry with the U.K. 1.2m Schmidt telescope plates of the SMC field.

The different errors involved in the photographic photometry are:

1) experimental errors due to the iris photometer.
2) errors in centering the star image in the iris diaphragm.
3) random fluctuations of the transmission coefficient of the photographic image-grain noise.
4) variations in the background density of the developed emulsion surrounding the star.
5) systematic differences in image structure, leading to differences in the transmission among images of the same magnitude in the system.
6) internal consistency of the photographic plates of the same exposure and colour.
7) drift in the iris photometer during one run of measurements.

8) optical vignetting in the telescope used to obtain the plates.

9) variations of extinction across the plate.

10) bad measures, misidentification etc.

11) non linearity of the iris reading calibration curve.

12) field errors - combination of two different standard sets separated on the plate.

13) colour equation.

1.5.1. Experimental error.

During a measurement with an iris photometer the total intensity L transmitted by the photographic image is:

$$L = \iint_A I t r . dr . d\theta$$

where $I(r,\theta)$ is the intensity of illumination of the iris image and $t(r,\theta)$ the transmission coefficient of the photographic image at the same point. As an approximation, I is constant within the iris image and is zero outside. To make a magnitude measurement, the range of integration is adjusted to make L equal to a constant Lo, the intensity of the comparison beam. The abritrary scale attached to the iris movement gives a measure A of this range of integration so the error in balancing L against Lo is minimum when $(1/L)\frac{dL}{dA}$ is maximum. For different wedge settings to balance, (a number of iris settings A of the same star accurately centred) it has been shown (Argue 1960) that the optimum iris setting for balance is not critical because a single adjustment of the comparison beam is sufficient over a range of about ten magnitudes, and the range of magnitudes involved in the present work has always been no more than 8 magnitudes.

1.5.2. Centering error.

The magnitude error is approximately proportional to the square of the off-centre distance. It is roughly independent of magnitude for a given adjustment of the comparison beam, but increases when the latter is changed, so that the iris closes more tightly around the image. This error is very difficult to be isolated or measured. But of course it was tried to centre as carefully as possible.

1.5.3. Granularity.

If we plot the magnitude difference for two runs of measurements of a set of stars against magnitude, we get the internal consistency of measurements.

If we make the same plot as previously for another sky reading and get the difference of these two plots for each magnitude, the spread of the latter is due to grain noise. Argue (1960) shows that the noise increases with greater iris settings. Many tests were carried out with the Schmidt plates to determine the optimum iris setting in order to get the minimum grain noise.

1.5.4. Variations in the background density.

The presence of the background fog around a stellar image causes the diaphragm reading to be increased and the measured magnitude to be brighter. If the fog is uniform across the plate no correction must be applied, but the presence of large background reading, due to blended faint stars or nebulosities, or discs formed by reflection for the very bright stars and anomalies of the emulsion itself should be corrected.

The most common source of this kind of error, for our plates, is the crowded nature of the field especially near the bar of the Small Magellanic Cloud (SMC) and the presence of very bright stars which affected their vicinity. So regions with uniform background and well separated stars were chosen as carefully as possible, but small variations could not be entirely avoided. In few cases the "blend stars" can amount up to 50% of all stars, and of course it is more conspicuous in the plate of the predominant colour of the cluster members.

1.5.5. Systematic differences in image structure.

In general the image structure affects the response of the iris and the magnitudes eventually are different even for stars of the same magnitude. These differences are due to different causes. One of them is small focus changes in the telescope. A second source of image distortion is a slight flexure between the main mirror and the corrector line when the tube is near a horizontal position. The atmospheric refraction, especially for long exposures is the third and usually the main cause of the distortion of the images.

In the case of the U.K. 1.2m Schmidt telescope, tests were carried out to find out which is the main source of this error. So photographs taken with usual broad band filters and photographs taken with combined filters (in order to get a narrower band) were compared and have shown that the images look different in the two cases. The broad band photographs had a slight distortion whereas the narrower band ones showed perfectly circular images.

If there is a flexure, the elongation of the images would have been the same in both cases and therefore we come to the conlusion that in the case of this particular Schmidt Telescope, the atmospheric refraction plays the major role as a source of this kind of error.

1.5.6. Internal consistency of the photographic plates of the same colour.

Figs. (2) and (3) show a plot of iris readings of the same stars from pairs of V plates of the same exposure against each other during two successive runs and B respectively. The scatter of these curves in terms of magnitude are recorded in column 3 of Table 3. Of course this scatter is due to other sources as well but each was measured at two successive runs during a short time so the conditions were exactly the same as far as the instrument is concerned.

1.5.7. Photometer drift

Measurement of a photographic plate on an iris diaphragm photometer can take several hours and a slow drift is difficult to be entirely eliminated. A correction as a function of time can be derived but it was found more convenient in practice to measure the standards a number of times during each measurement run and take the mean of their iris readings. It has been

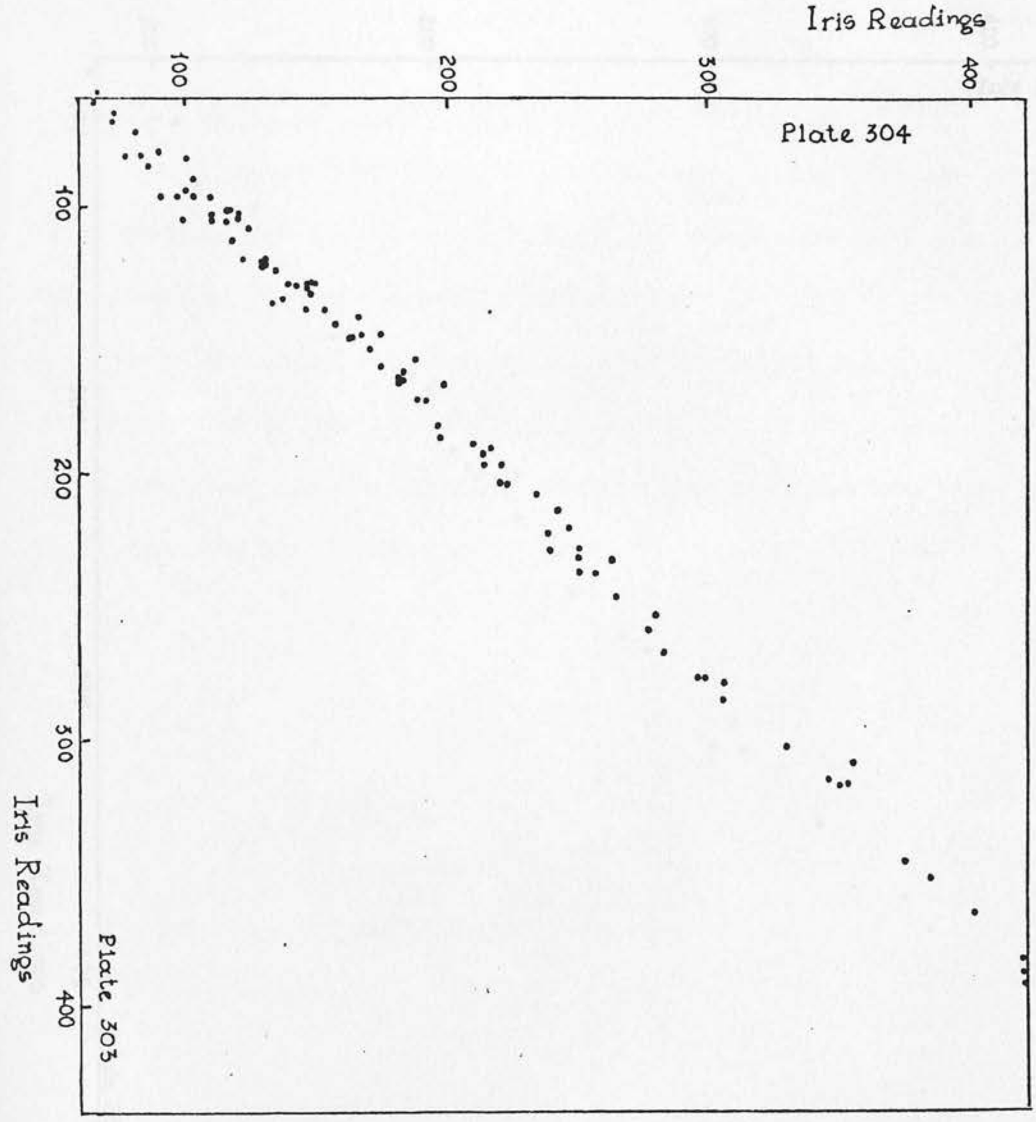

Fig. 2. Iris readings of the same stars from pairs of V plates.

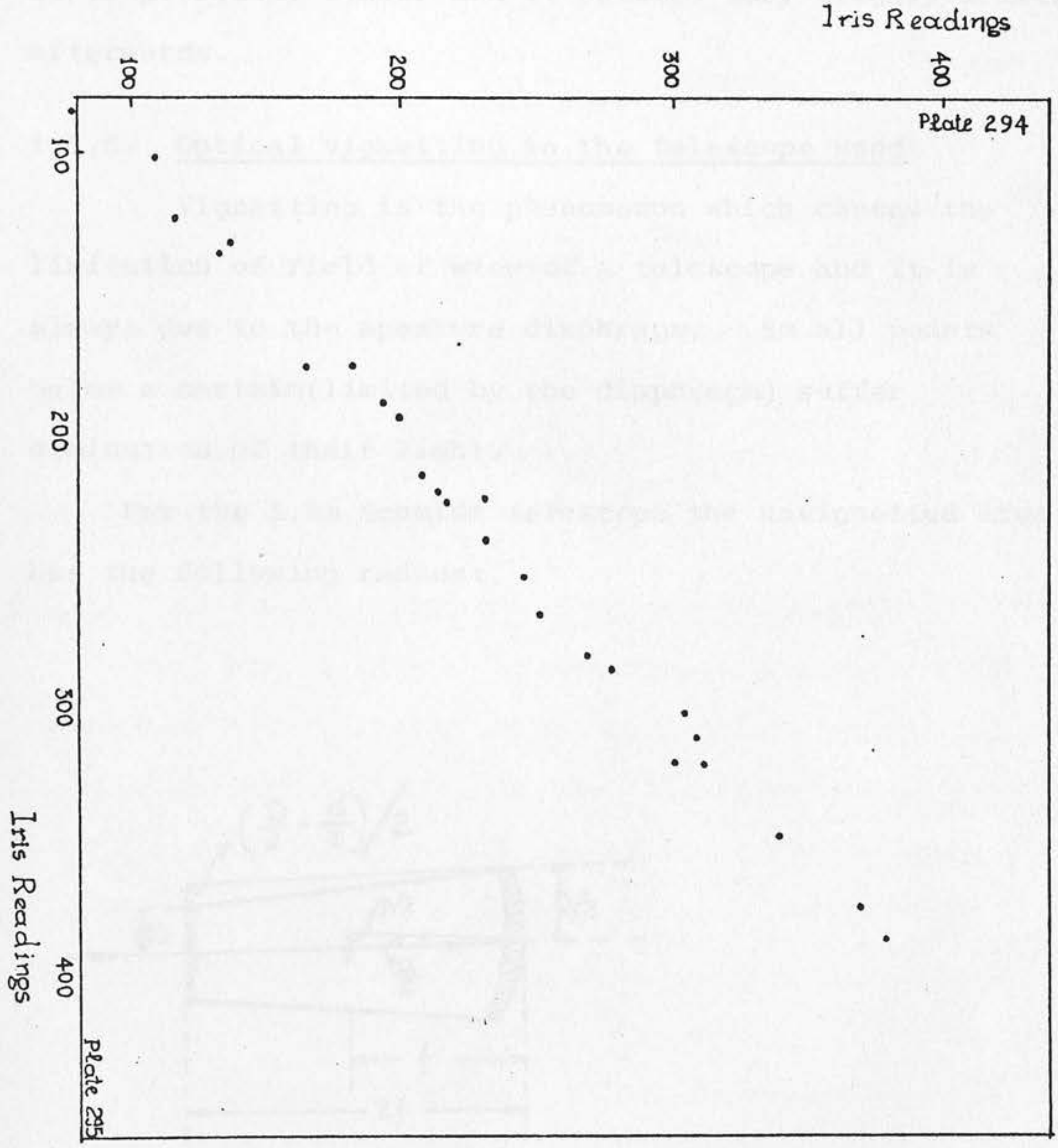

Fig. 3. Iris readings of the same stars from pairs of B plates.

found that for about four hours of continuous measurement it is perfectly stable and it becomes very slighly drifted afterwards.

1.5.8. Optical vignetting in the telescope used

Vignetting is the phenomenon which causes the limitation of field of view of a telescope and it is always due to the aperture diaphragm. So all points below a certain(limited by the diaphragm) suffer diminution of their light.

For the 1.2m Schmidt telescope the unvignetted area has the following radius:

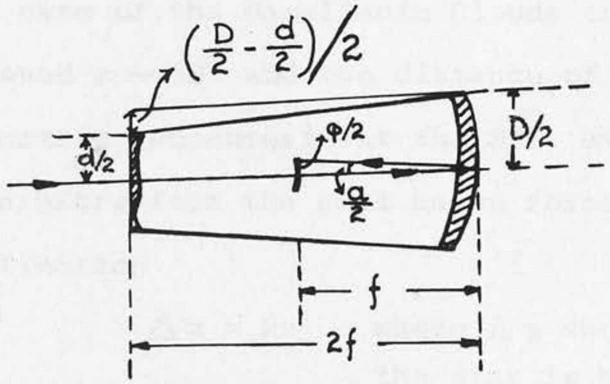

D = mirror diameter

d = aperture diameter

Fig. 4. illustrates the effect of optical vignetting on a Schmidt telescope.

From Fig. 4, applying simple geometry for the U.K. 1.2m Schmidt telescope according to the values of table 1.

$$\frac{\phi}{2} = \frac{D-d}{4} = 0.1475 = 147.5 \text{ mm}$$

$$\sin\frac{\alpha}{2} = \frac{\phi_2}{f} = 0.048045$$

$$\frac{\alpha}{2} = 2^{\circ}.73$$

So the radius of the unvignetted area is $\phi_2 = 147$ mm and our measurements and set of standards have been confined within this area. The standards nearest to the limit are the NGC 121 (Tifft, 1963) but still they occupy an area inside the critical radius.

1.5.9. Variation of extinction across the plate.

For plates taken at large zenith distances a correction for variation of extinction must be applied. In case of the Magellanic Clouds the zenith distance is around $z \sim 38^{\circ}$ and the distance of the different photoelectric sequences is at the most extreme case 4°. Therefore from the well known formula of atmospheric extinction

$\Delta m = kx$ where Δm shows how much fainter the star is because of extinction. k is the extinction coefficient and x the air mass which depends on the zenith distance of the star.

In this case we assume that two stars of the same magnitude m are about 4° apart on the plate. So $z_1 = 38^{\circ}$ and $z_2 = 42^{\circ}$ are their zenith distances. Therefore

$$\Delta m_1 = kx_1 \text{ and } \Delta m_2 = kx_2$$

For the given z_1 and z_2 we have

$$x_1 = 1.268 \text{ and } x_2 = 1.344.$$

So $\Delta m_1 - \Delta m_2 = k(x_1 - x_2) \rightarrow \Delta m_1 - \Delta m_2 = k \times 0.075.$

For the worst case of a k value of $k = \frac{1}{2}$ the difference is $\sim 0^m.035$ which introduces a very small error compared with the other photometer errors.

1.5.10. Bad measures, misidentifications etc.

These can be entirely eliminated by comparison of measured and standard magnitudes.

1.5.11. Non linearity of the calibration curve.

The non linearity of the calibration curve is the main disadvantage of the photographic emulsion as a detector. Towards the limit of the plate which is towards fainter magnitudes it looses its linearity, and the magnitudes become more uncertain. As it has already been mentioned the computer solution was always checked by hand drawn up calibration curves. If the computer fit was not satisfactory at the very faint limits, the magnitudes were read straight off the curve. The calibration is inevitably uncertain below $V > 20.0$ mag and $B > 20.50$ mag. because fainter stars are near both the photoelectric and photographic limit of detection.

The reliability of the calibration of the photographic data and the accuracy of the individual star measures can be estimated from figs. (5), (6) and (7) for three different regions on the plate.

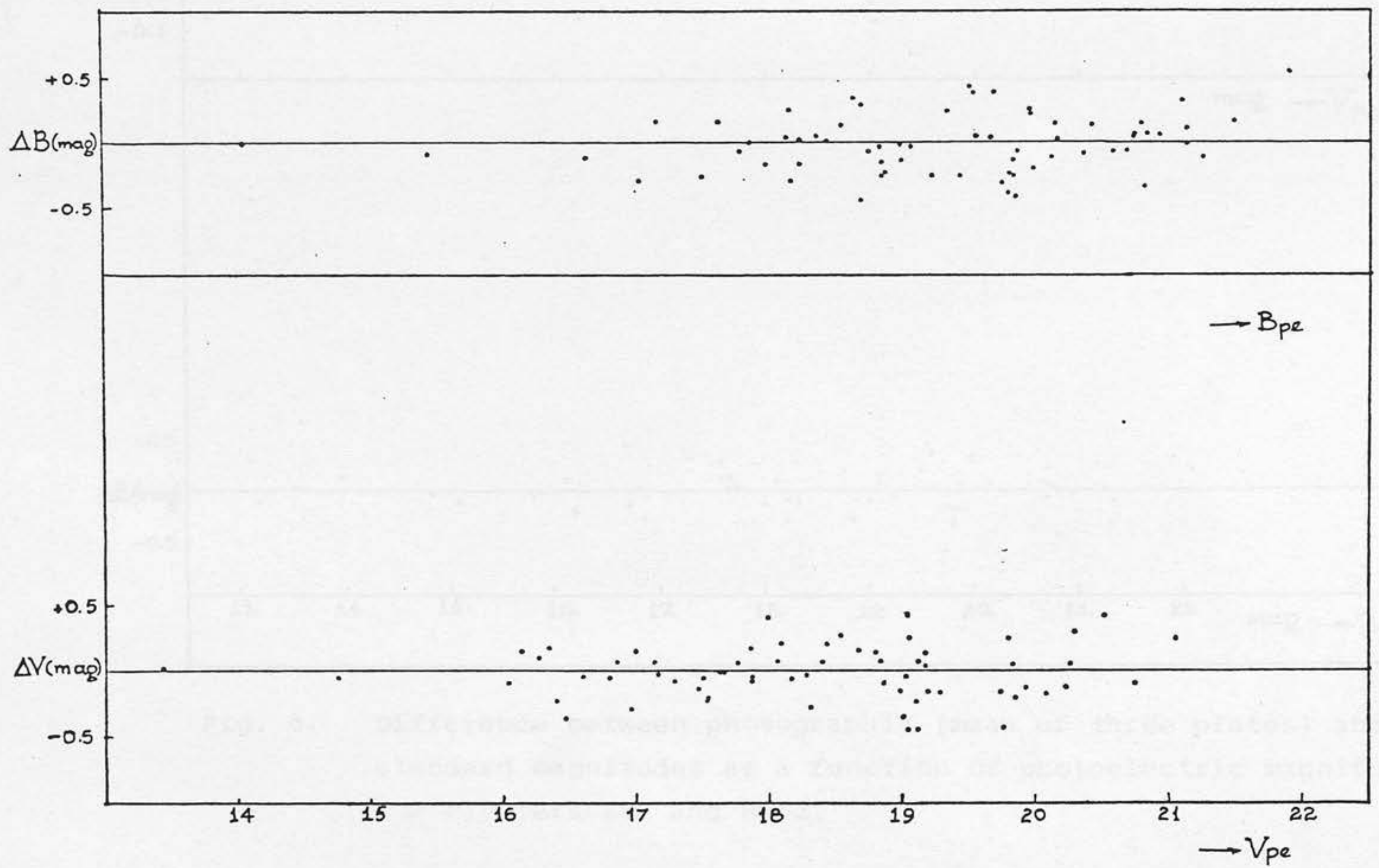

Fig. 5. Difference between photographic (mean of three plates) and standard magnitudes as a function of photoelectric magnitude for cluster L15.

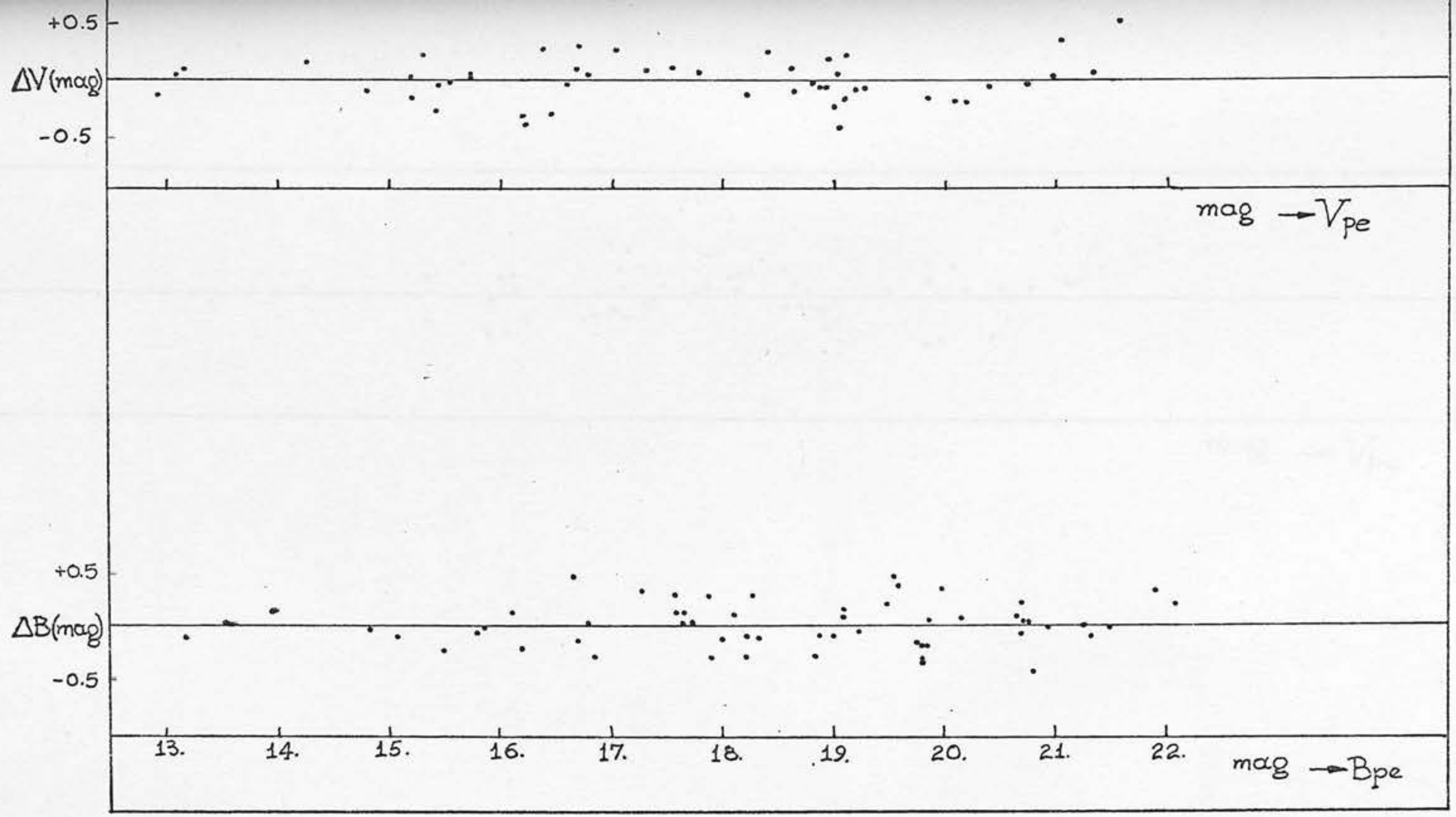

Fig. 6. Difference between photographic (mean of three plates) and standard magnitudes as a function of photoelectric magnitude for clusters L87 and HW62.

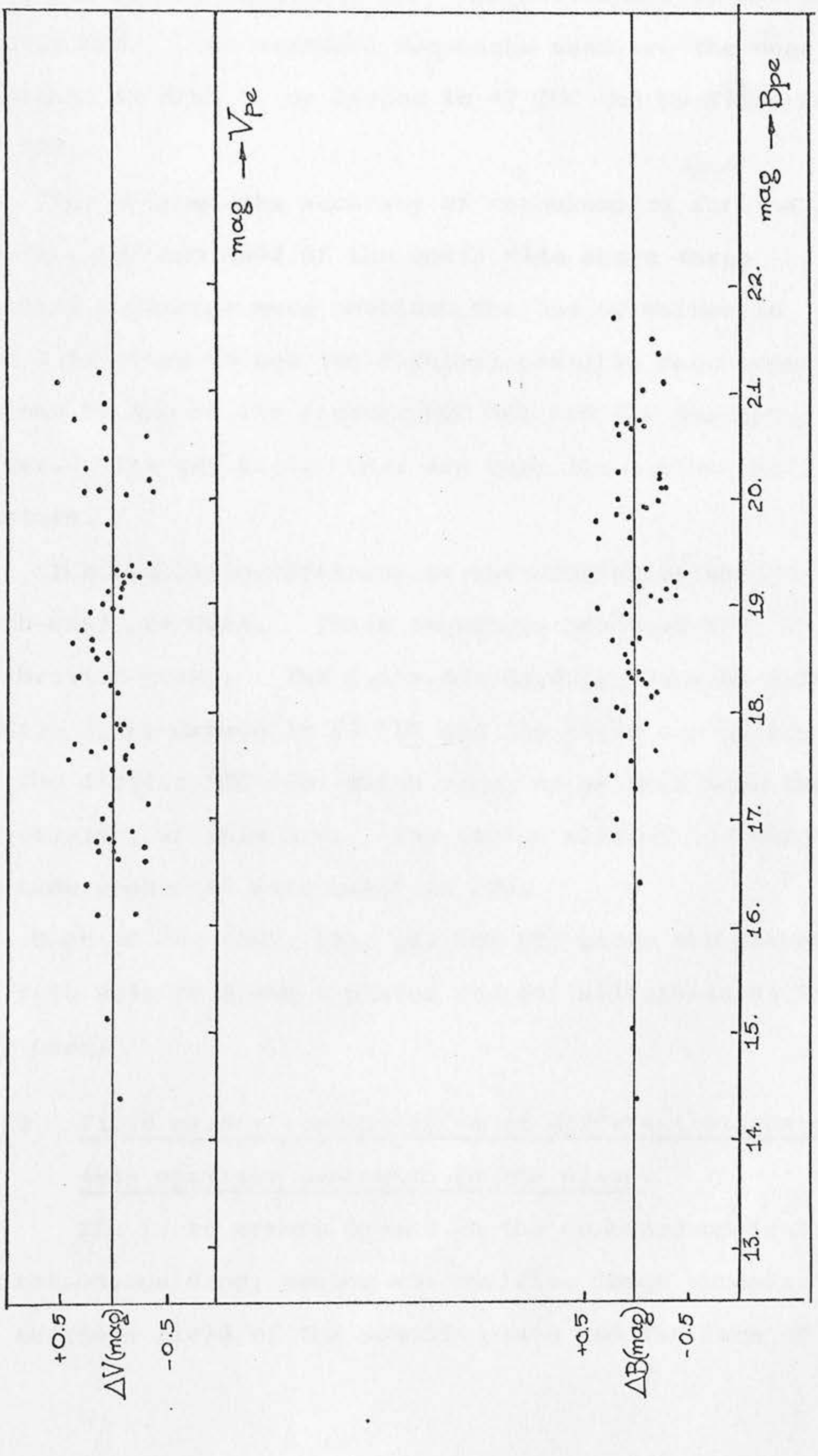

Fig. 7. Difference between photographic (mean of three plates) and standard magnitudes as a function of photoelectric magnitude for cluster HW64.

Fig. 5 illustrates the accuracy of measurements for the west side of the plate and this particular is one for the cluster L15. The standard sequences used are the ones by Walker in Kron 3, by Cannon in 47 TUC and by Tifft in NGC 121.

Fig. 6 shows the accuracy of measurements for the clusters L87 and HW62 of the north side where three standard sequences were combined, the one by Walker in Kron 3 (in order to get the faintest possible magnitudes), the one by Arp in the cluster NGC 361 and the one by Butler. The two latter ones lie near the northerly clusters.

The Fig. 7 is referring to the cluster of the north-east arm HW64. Three sequences produced the calibration curve. The faint standard sequence by Walker in Kron 3, by Cannon in 47 TUC and the third one by Arp for the cluster NGC 458, which occupies an area near the two clusters of this arm. The second cluster for which the same sequences were used is L90.

Each of the figs. (5), (6) and (7) gives the accuracy for both sets of B and V plates and for all standards in each case.

1.5.12. Field errors - combination of different standard sets spatialy separated on the plate.

The field errors depend on the combined optical aberration, guiding, seeing and emulsion image spreads. The enormous field of the Schmidt plate and the lack of many photoelectric standards demanded the combination of different photoelectric sequences separated in the extreme case by about 4^{o}. Fortunately there is no significant systematic field effect (not appreciable compared with the error introduced by other sources as crowding, photoelectric standards etc.). The main reason of this combination is the lack of faint photoelectric standards especially below V and B > 20.0 mag whereas the plate limit reaches $22^{m}.00$. So for the measurements of the faint stars and to avoid dangerous extrapolation the only faint sequence (Walker, 1972) has always been combined with the other available photoelectric standards. By a careful check of each photoelectric sequence separately it has been found that electronographically measured stars give a small error, and sometimes they are as good as a photoelectric sequence.

Fig. (8) and (9) show the calibration curves one V and one B respectively where the sets of standard stars are separated by more than 4^{o} as it is for Walker's standards in Kron 3 and Cannon's in 47 TUC which are on the west side of the SMC and Arp's standards for the cluster NGC 458 on the north-east small spiral arm. The three sets are well merged in each other and the field effects do not seem noticeable.

In Figs. (10) and (11), the calibration curves for the cluster L15 are based on standard sequences of the west side of the SMC. One V plate and one B plate

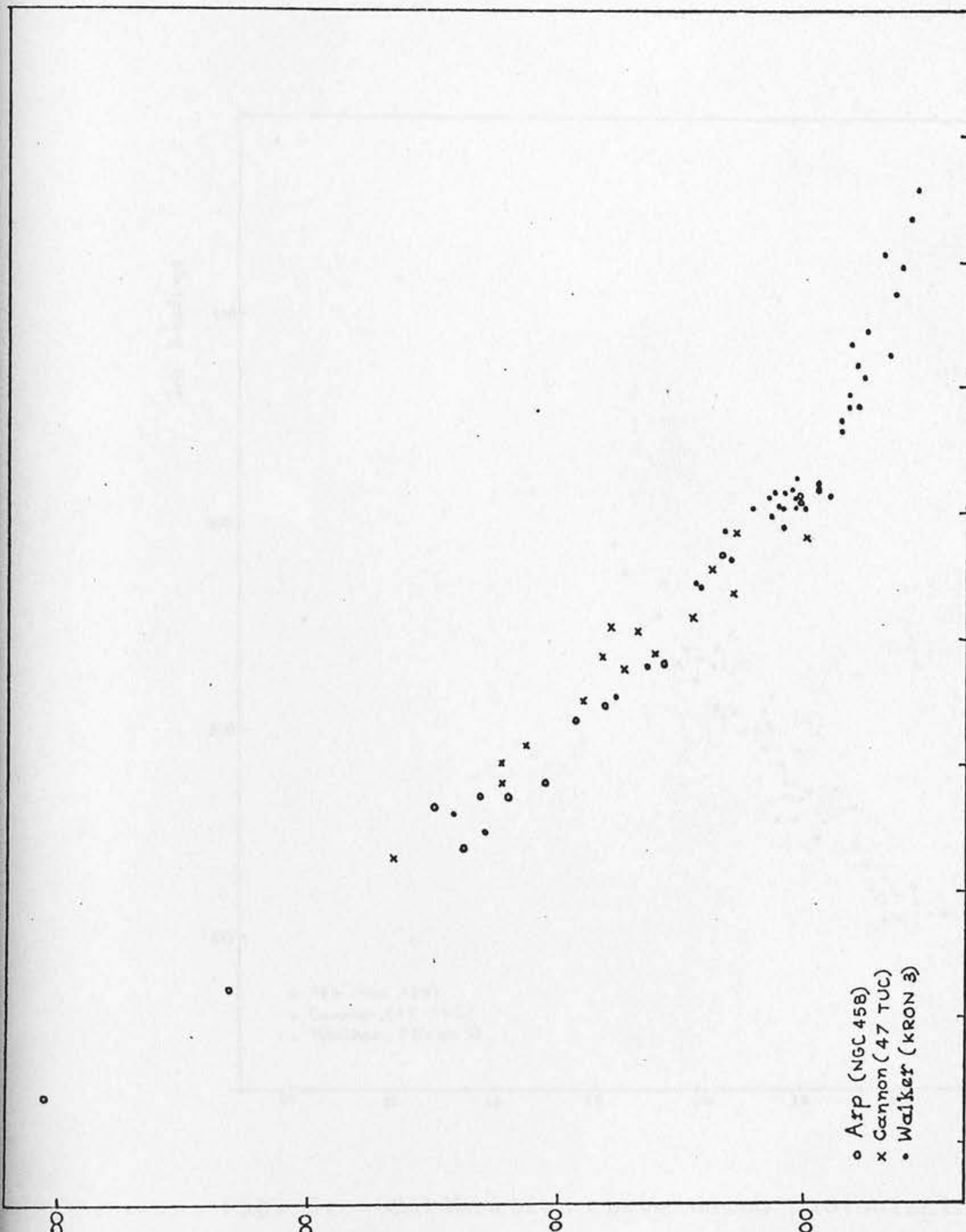

Fig. 8. Calibration curve using photoelectric V (NGC 458, 47 TUC) and electronographic (Kron 3) standard stars. The extreme distance of these sequences is about 4^{o}.

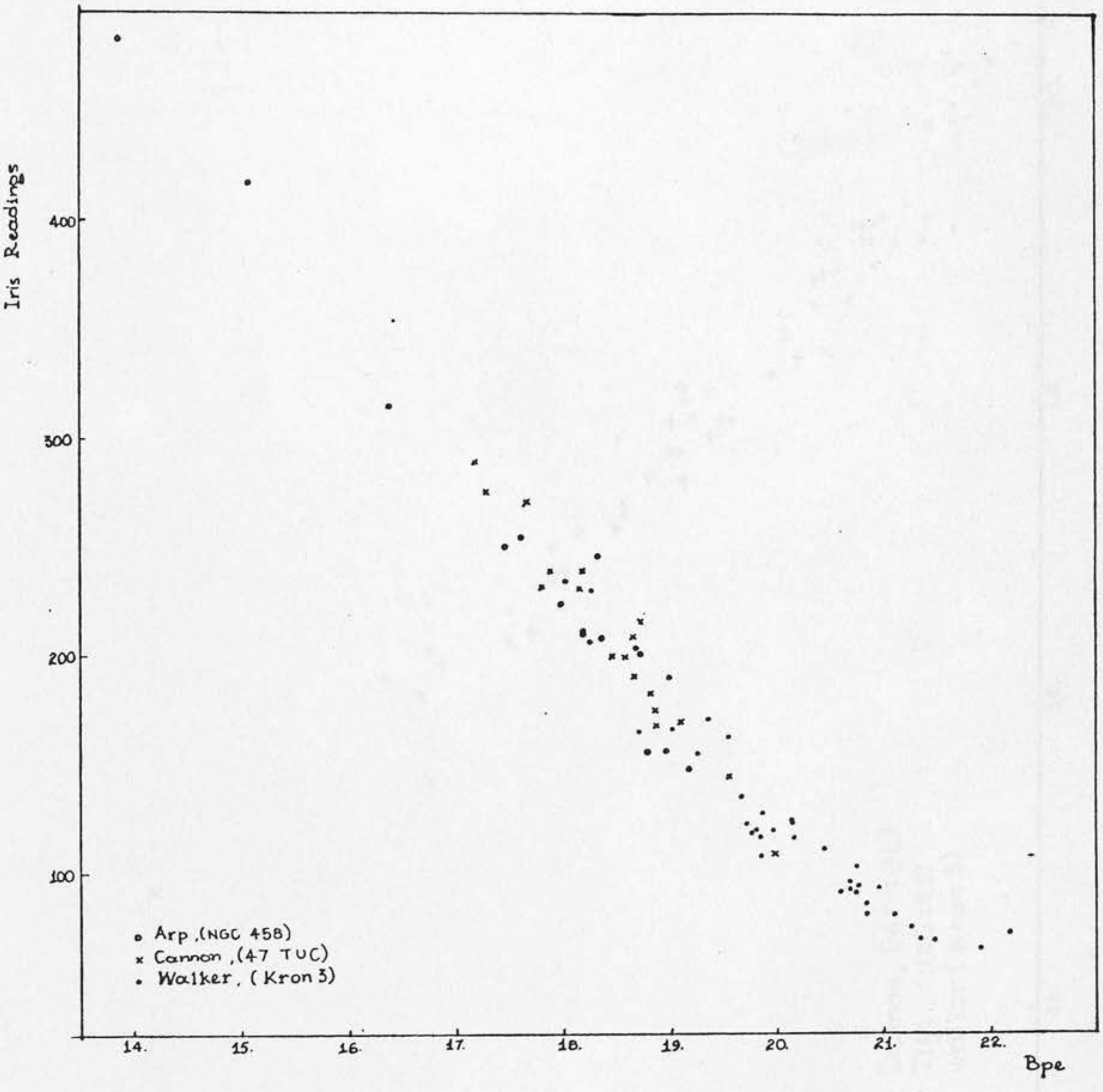

Fig. 9. Calibration curve using photoelectric B (NGC 458, 47 TUC) and electronographic (Kron 3) standard stars. The extreme distance of these sequences is about 4^{o}.

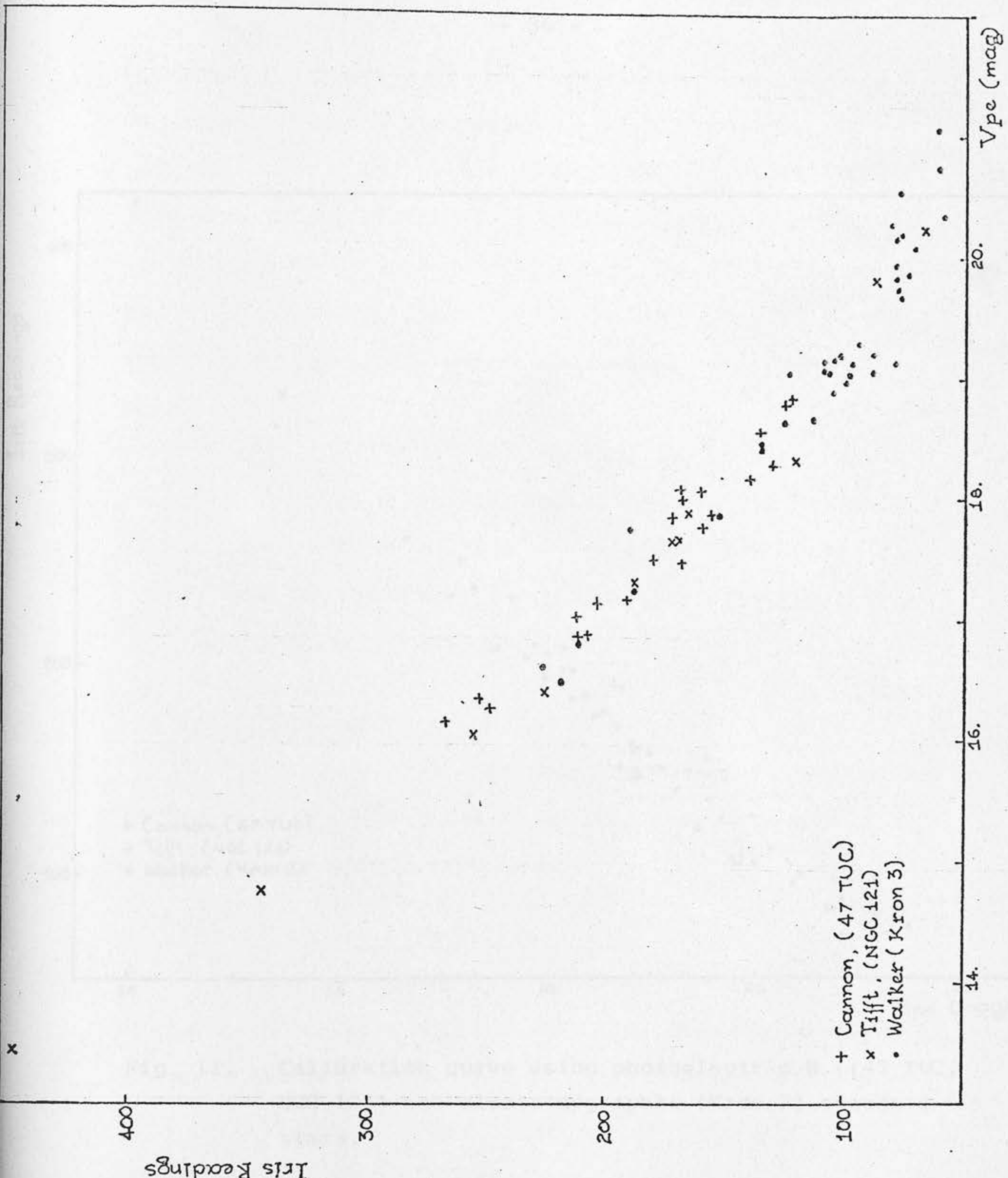

Fig. 10. Calibration curve using photoelectric V (47 TUC, NGC 121) and electronographic (Kron 3) standard stars.

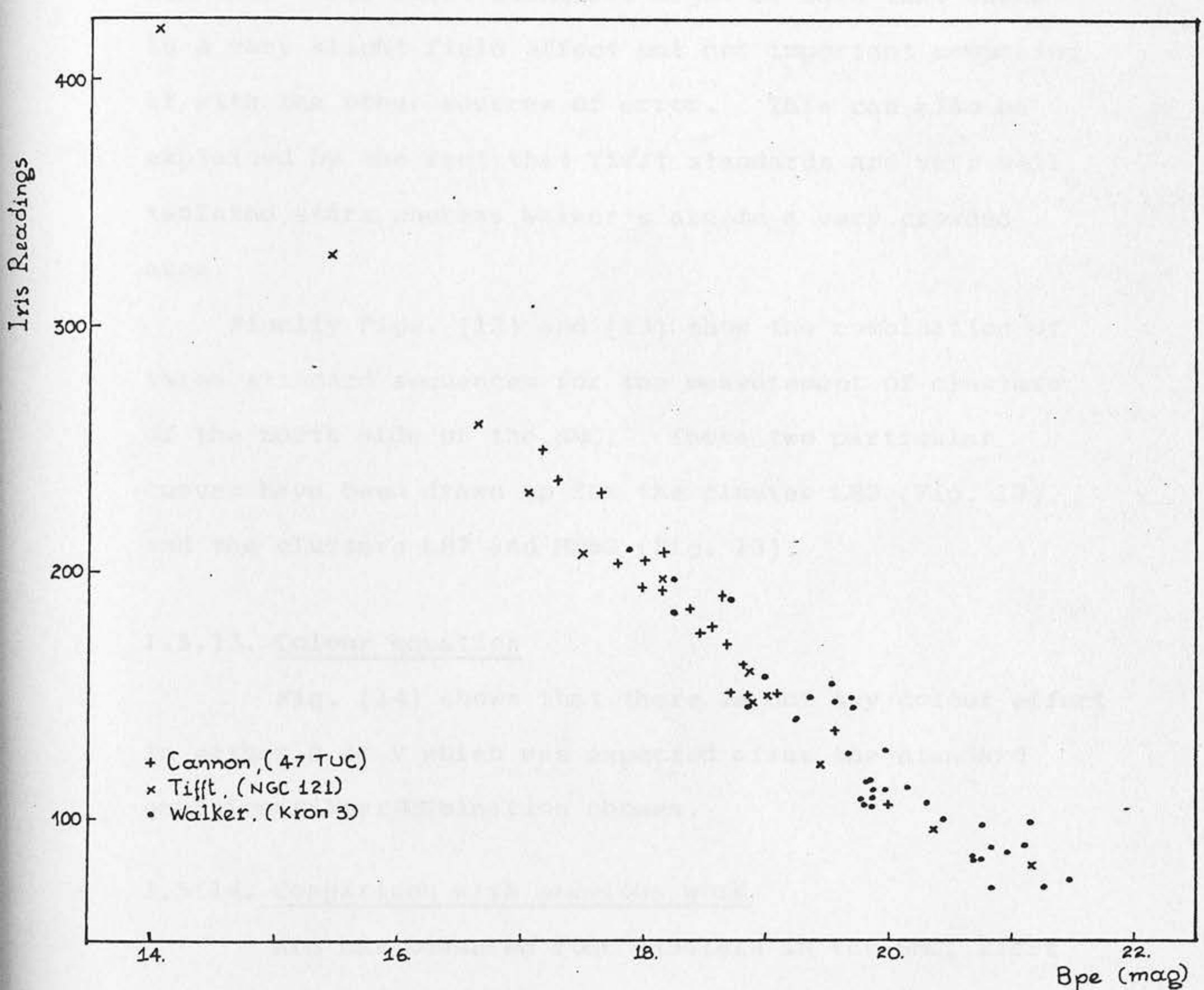

Fig. 11. Calibration curve using photoelectric B ((47 TUC, NGC 121) and electronographic (Kron 3) standard stars.

respectively show a very good agreement for the sequences by Walker in Kron 3, by Cannon in 47 TUC and Tifft in NGC 121. For Tifft standards might be said that there is a very slight field effect but not important comparing it with the other sources of error. This can also be explained by the fact that Tifft standards are very well isolated stars whereas Walker's are in a very crowded area.

Finally Figs. (12) and (13) show the combination of three standard sequences for the measurement of clusters of the north side of the SMC. These two particular curves have been drawn up for the cluster L82 (Fig. 12) and the clusters L87 and HW62 (Fig. 13).

1.5.13. Colour equation

Fig. (14) shows that there is not any colour effect in either B or V which was expected after the standard emulsion-filter combination chosen.

1.5.14. Comparison with previous work

Arp has measured four clusters in the SMC, Tifft measured the cluster NGC 121 and Walker has measured two clusters electronographically. Standard sequences have been used from all these workers for this project and our accuracy has been discussed.

Photographic values measured by Arp in NGC 361 have been compared with our photographic values for the same set of stars. The sequences used were by Arp in NGC 361,

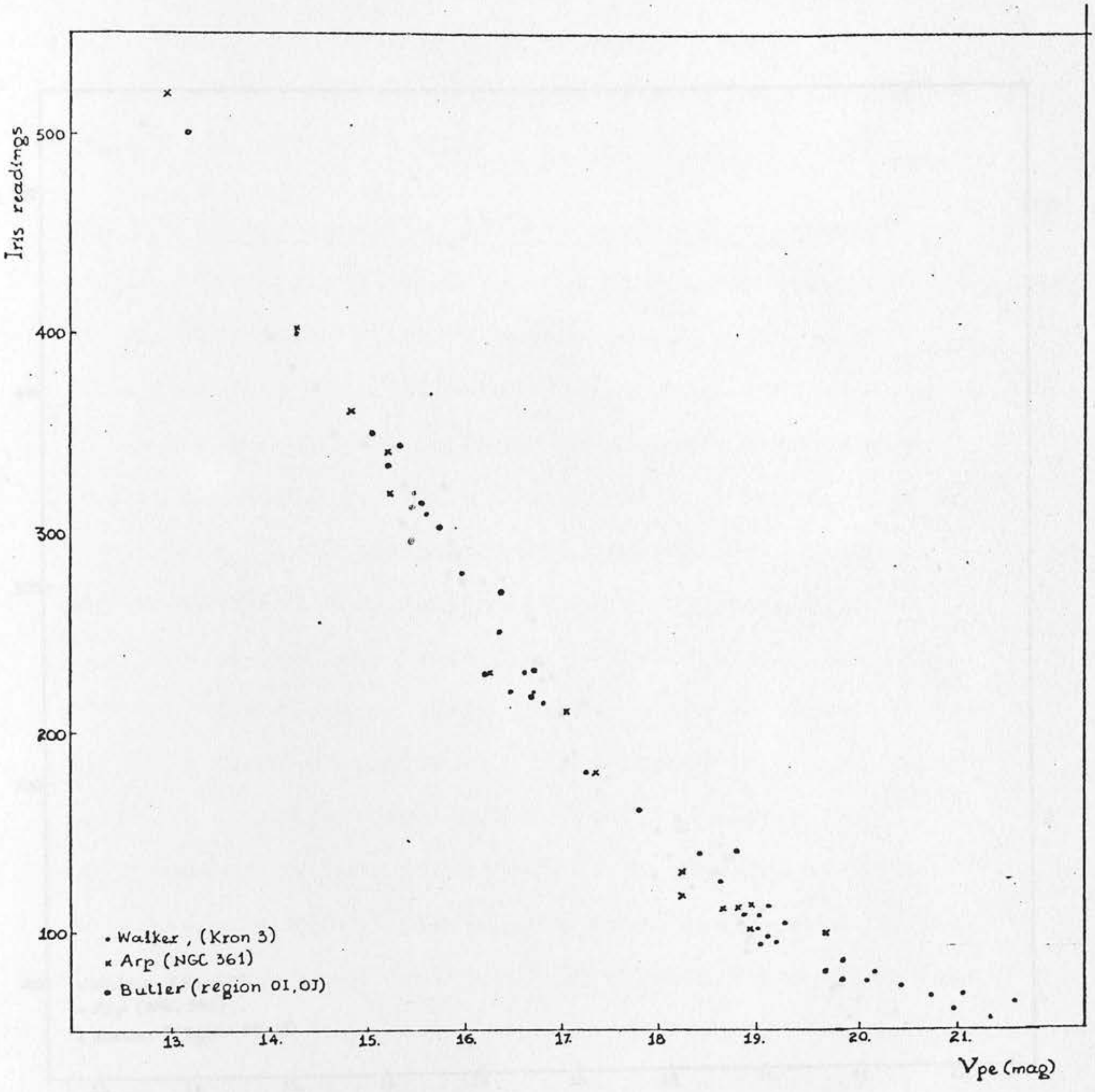

Fig. 12. Calibration curve using photoelectric V (NGC 361, Butler region) and electronographic (Kron 3) standard stars.

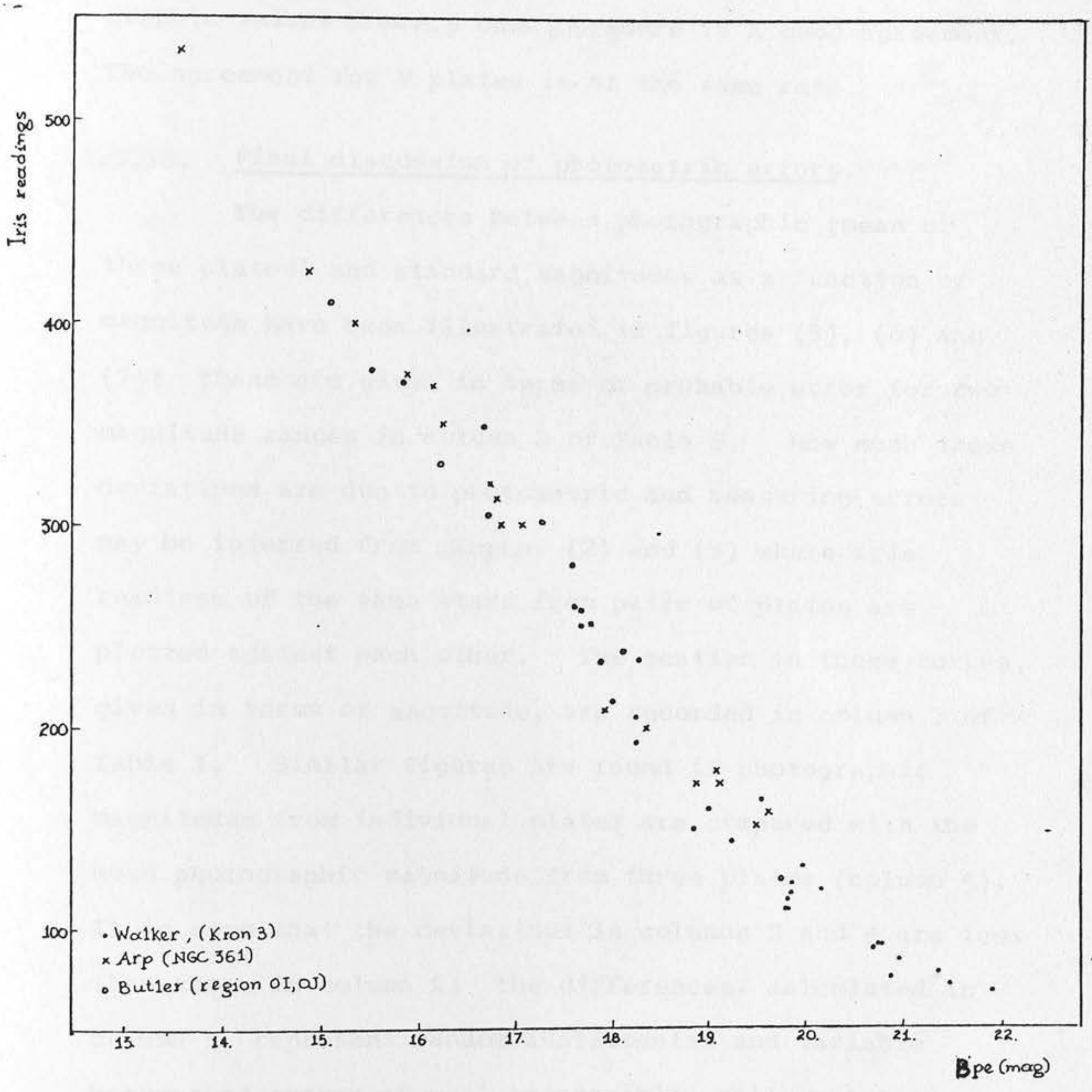

Fig. 13. Calibration curve using photoelectric B (NGC 361, Butler region) and electronographic (Kron 3) standard stars.

Walker in Kron 3 and Cannon in 47 TUC. Fig. (15) illustrates the difference of Schmidt plates' B photographic values from Arp ones and there is a good agreement. The agreement for V plates is of the same rate.

1.5.15. Final discussion of photometric errors.

The differences between photographic (mean of three plates) and standard magnitudes as a function of magnitude have been illustrated in figures (5), (6) and (7); these are given in terms of probable error for two magnitude ranges in column 2 of Table 3. How much these deviations are due to photometric and measuring errors may be inferred from Figs. (2) and (3) where iris readings of the same stars from pairs of plates are plotted against each other. The scatter in these curves, given in terms of magnitude, are recorded in column 3 of Table 1. Similar figures are found if photographic magnitudes from individual plates are compared with the mean photographic magnitude from three plates (column 4). It is seen that the deviations in columns 3 and 4 are less than those in column 2; the differences, calculated in column 5, represent random instrumental and variable background errors as well as possible small systematic differences between the standard sequences. Such residual errors are often encountered in comparisons between photoelectric and photographic photometry.

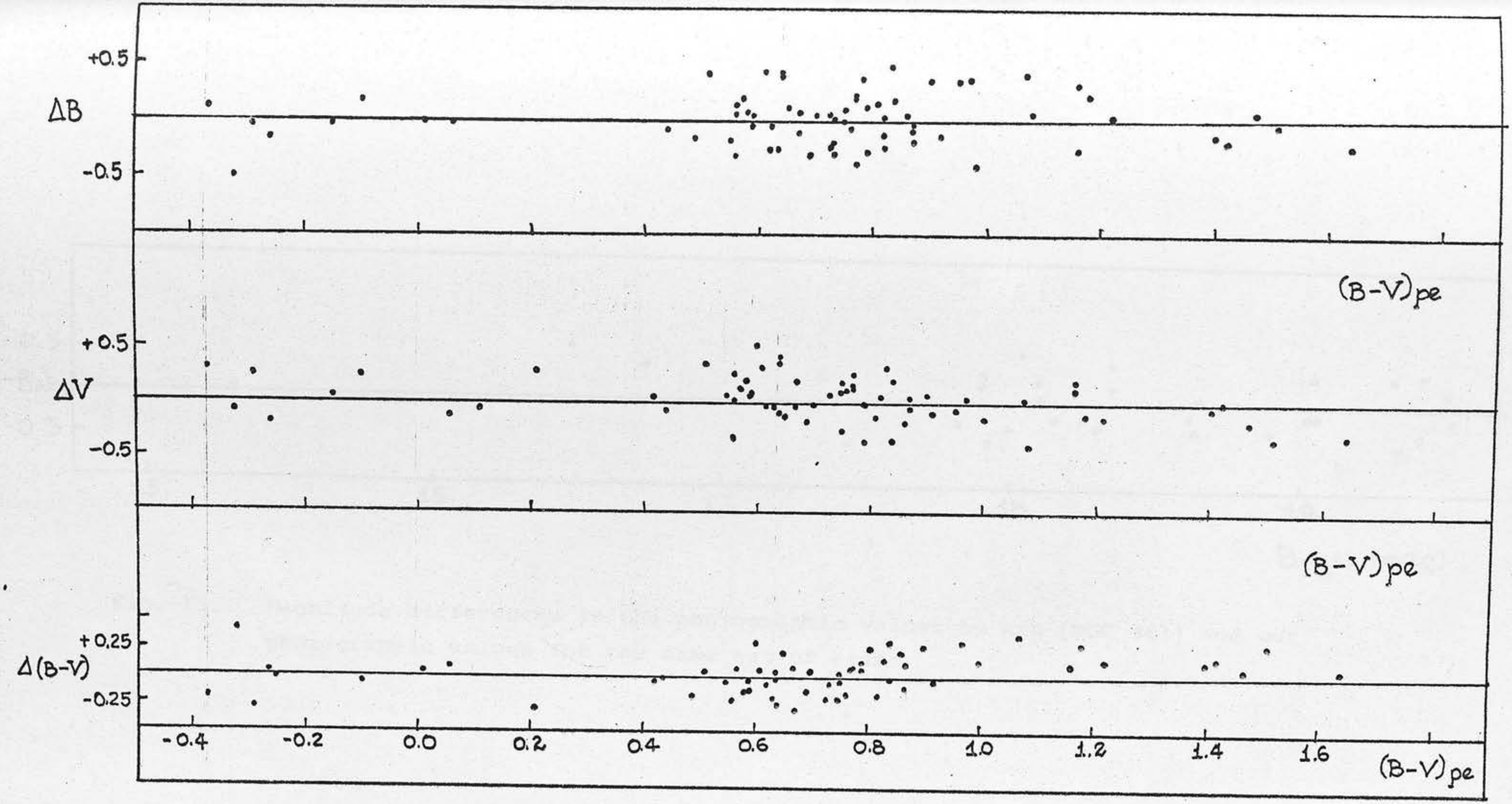

Fig. 14. Magnitude (ΔB, ΔV) and colour differences (Δ(B-V) plotted against (B-V)pe.

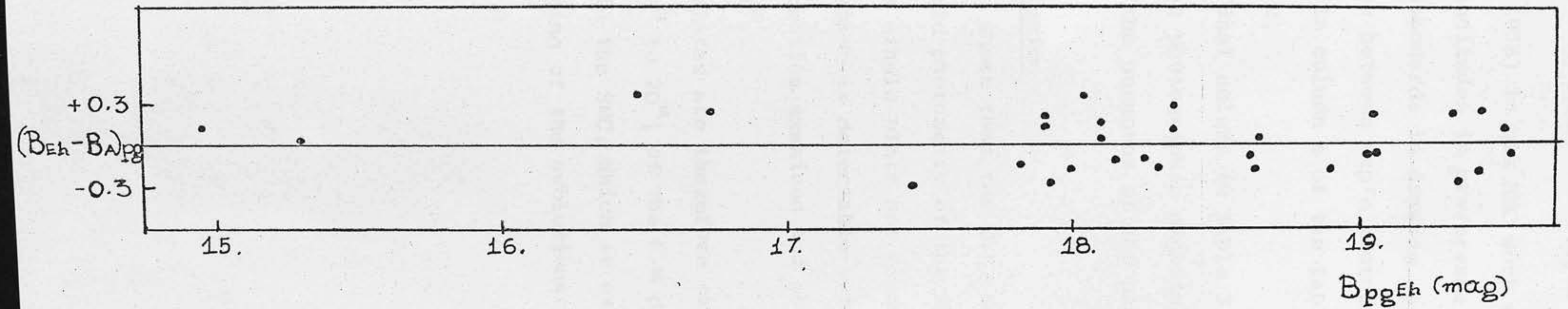

Fig. 15. Magnitude differences in the photographic values by Arp (NGC 361) and our photographic values for the same set of stars.

Arp (1958) in his SMC work adopts photographically derived magnitudes in preference to his original photoelectric standards in drawing up calibration curves. Differences between Arp's photographic magnitudes and ours are shown in column 6 of the Table 3 are less than those in column 2.

The final column in Table 3 gives the probable error of our mean photographic magnitudes which are satisfactorily small for the purposes of the planned photometric programme.

I.6. Conclusion

It is shown that the U.K. Schmidt plates are good for photographic photometry of the SMC region, the probable error on a single plate not exceeding $0^m.8$ in either B or V. No field error is detectable out to $2^o.5$ from the centre in the direction examined and photometry is possible to $B = V = 21^m$.

The plates are therefore capable of reaching the H-B at ($V = 19^m$ to 20^m) of the C-M diagrams of the globular clusters in the SMC, which is essential towards the understanding of the evolutionary history of these objects.

TABLE 3

Photometric Errors

1 Magnitude Range	2 $(\overline{pg}-pe)$	3 (pg_1-pg_2)	4 $(pg-\overline{pg})$	5 pe	6 $(pg_A-\overline{pg})$	7 $\overline{pg}$
V 19	0.12	0.05	0.05	0.10	0.07	0.03
19 V 21.25	0.15	0.07	0.07	0.13		0.05
B 19	0.14	0.07	0.07	0.12	0.12	0.05
19 B 21.5	0.18	0.10	0.08	0.16		0.05

Errors are all given in terms of probable error i.e. 0.6745 x standard or root mean square error.

Photometric sequences used

KRON 3	16.0 V 21.60	17.0 B 22.27
NGC 121	13.0 V 20.20	13.0 B 21.12
47 TUC	16.0 V 18.0	16.7 B 20.0
NGC 361	14.0 V 19.0	14.0 B 20.10
NGC 458	13.0 V 20.0	13.0 B 19.20
BUTLER'S	13.0 V 18.0	13.0 B 18.60

CHAPTER II

MAIN OBSERVATIONAL ASPECTS OF STAR CLUSTER STUDY

2.1. Stellar Groups

Star clusters are star systems which have some common characteristics. They are known to be physically connected or may be assumed from their apparent positions to constitute distinct physical organisations.

The main problems regarding their study are: a) composition. b) distribution. c) structure and cosmic position. They can be divided into two main categories:

1) stellar associations and open clusters

2) globular clusters.

2.1.1. Stellar associations and open clusters

The open clusters are usually groups with irregular shape and non-central concentration. They can be divided into two different categories according to their degree of concentration and spectral composition (Trumpler, 1930). So their members are mainly main sequence objects with some Helium core burning stars in the later types.

2.1.2. Globular clusters

These are groups with a strong central concentration and richness in faint stars.

The different types of globular cluster have been divided according to their size, luminosity, shape (which is not always circular). Their members are mainly stellar population II and their brightest members are red giants.

2.2. Ages of clusters

It has been found that open clusters contain younger stars than the globular ones. The age of a cluster is characterised by the age of its star members which are supposed to have been born simultaneously from the same initial cloud and therefore have common chemical composition and age.

The clusters have different ages which are related to some characteristic properties as follows.

a) Bright blue stars are found near interstellar gas and clouds , where they have just formed, not having time to move away.

b) Some associations with blue luminous members seem to be expanding from a common centre. The expansion rate gives an estimate of the age of the cluster.

c) In globular clusters the amount of gas is small compared with the open clusters. Therefore the redness of their members could be an estimation of their age.

Usually the older stars turn off the main sequence towards the red giant branch and in the case of old clusters the brightest members are giants whereas in open clusters the main sequence stars are the brightest members of the cluster or as bright as the red giants.

d) The kinematic properties of stars are also related to their age, i.e. the velocity of stars relative to the orbital velocity about the galactic centre. Stars in the solar neighbourhood may be arbitrarily divided into a high velocity group and a low velocity group. It has been found that the high velocity group contains many red giants and has a composite colour-magnitude diagram similar to that of globular clusters. The clusters themselves have similar properties: open clusters have low relative velocities, whereas globular clusters have high relative velocities, moving in large orbits about the galactic centre.

e) Also the distance from the galactic centre is correlated with the age of the stars. Stars with high kinetic energy may convert it into enough potential energy to overcome the gravitational attraction presented by the mass of the Galaxy. This is why the globular clusters are found very far from the galactic plane while the open, young ones, are distributed in a flat system in the galactic plane.

f) The strength of the metallic lines in the stars has been also an age criterion. Taking into account the assumption that stellar atmospheres show in general the abundances of products that were there at the time of star formation and noting that throughout time nucleosynthesis has gradually enriched the metal content of the interstellar medium, we would expect the younger stars to be richest in metals and therefore show the strongest lines. In clusters also it is found that the low velocity group stars have stronger metallic lines which is the case of open clusters, whereas the old clusters have weak metallic lines.

g) One important criterion of ages of clusters is the colour-magnitude diagram which will be discussed later in detail. It has been found that the turn-off point of a C-M diagram is a very good age criterion. It is the locus where the stars leave the main sequence to the red giant phase. The colour and luminosity of the turn-off point is redder and fainter respectively as the cluster is older. The globular clusters contain red giants brighter than the main sequence stars whereas in the open and intermediate age clusters the main sequence stars can be as bright as the giants.

2.3. Main observational results from star cluster study

The star cluster study has been done by all means of astronomical techniques but the bulk of information comes from photometry either photoelectric or photographic. Spectroscopy of bright members is also a very important source of information for the determination of the clusters abundances, and radial velocities. Colour-magnitude diagrams and two colour diagrams enable us to derive the properties of the clusters namely, age abundances, and eventually to improve the stellar evolutionary history. The spatial distribution of clusters and their kinematical properties are important for the study of structure of the galaxies and their ages.

2.3.1. Stellar associations

Observations of stellar associations are closely related to problems of their birth out of compressed interstellar clouds rich in dust and molecules and to problems of pre-main sequence evolution. Stellar associations are studied by a variety of techniques and combined observations in optical, infrared and radio wavelengths. Their kinematics is also of great interest because of the expansion from a common centre question.

So star formation problems and the structure of the Galaxy or other galaxies can be appreciable progressed by stellar associations studies.

2.3.2. Open clusters

The open clusters are the most numerous objects between the star clusters and their number is still increasing especially in the southern sky where the new large telescopes provided powerful tools of study.

The main problem of these clusters is the fact that they do not have many evolved members so the turn-off point is not always certain and therefore their age. The method of fitting the second brightest member to the Hyades C-M diagram is not always safe because the brightest blue stars are not necessarily main sequence stars but already evolved and thick shell Hydrogen burning. In young clusters the top of the main sequence is brighter than the giant branch and this difference is larger as the cluster is younger. But it can be very easily confused because in the very young clusters the evolved giants return to the blue as far as almost the main sequence and the top of the main sequence can be uncertain and look brighter than the red giant branch. As a cluster ages, both the top of the main sequence and the giant branch become redder. At the top of the main sequence as the spectral type of the brightest star moves from early B to late B, the bolometric correction decreases. The reddest giants meanwhile in changing from F to K, are radiating an increasing proportion of their light in the invisible infrared.

So clusters of an age between that of h + χ Persei (youngest ~ 1×10^6 years) and that of M41 ~ 2.8×10^7 years will have giants brighter with respect to the main sequence than will the younger or older clusters.

The young clusters are metal rich objects compared with the globular clusters. Recently spectroscopy of bright members has shown that metal deficiencies exist in some of the older open clusters.

The youngest clusters serve both as calibrators of luminosities of cepheroids and supergiant stars and as tracers of spiral structure. So the composite C-M diagram of open cluster of a certain region might produce the C-M diagram for the spiral arm of a galaxy and therefore the arm's age.

In a recent paper Harris (1976) has studied open clusters using data of the evolved stars member of 97 clusters. He produced composite C-M diagrams for stars confirmed by any means that they are members of the clusters and he divided them into six age groups, from $\log\tau = 6.6$ (4×10^6 years) to $\log\tau = 8.6$ (4×10^8 years). Thus an age scale has been built based on the evolved stars of open clusters.

Comparison of these groups with models gives the conclusion that the Hayashi track becomes bluer and brighter as Y increases or Z decreases.

It has also been shown that in the four youngest groups (4×10^6, 10^7, 2.5×10^7 and 6.3×10^7 yr.) the most striking aspect of the diagrams is that the intrinsically brightest stars are in the A-F spectral range.

Only in the two oldest age groups (1.6×18^8 and 4×10^8 yr) where the evolving stars are of the order of $2\text{-}3M_{\odot}$ do the K and M stars begin to be consistently brighter than the B, A and F stars. The group I (4×10^6 yr) has no evolved stars and group II a well defined clump of M supergiants. Groups III and IV have a large number of late type stars which shows the importance of core Helium burning in these mass ranges ($4\text{-}10M_{\odot}$). The last two groups (1.6×10^3 and 4×10^8 yr) begin to exhibit a giant branch for the G-M stars.

2.3.3. Globular clusters

From photometric studies the main physical properties of globular clusters come out. The spectroscopy of bright members give the quantity $[F_E/H]$ which determines the metal abundance of the cluster but wherever this is not possible the three colour photometry in the U, B, V gives us much information. Two-colour and colour-magnitude diagrams can give us information about:

a) The reddening in front of star clusters.

b) The age difference, or age.

c) The Helium or metal abundance.

d) Their distances.

2.3.4. The reddening values

The reddening values can be found from the two-colour diagrams of a cluster. One typical two-colour diagram is in Fig. 16 (Cannon and Stobie 1973) for the globular cluster NGC 6752. The solid line of two colour diagram comes from Michalas' models for 4 ⩾ log g ⩾ 3. The drift of the stars from this line is due to the interstellar reddening in front of the cluster.

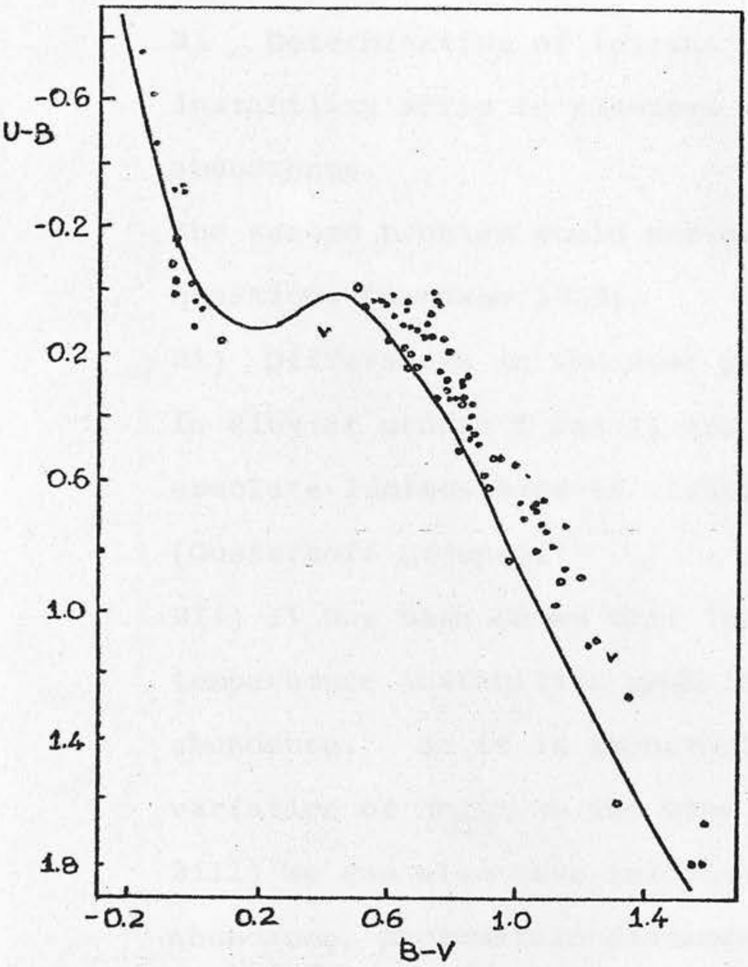

Fig. 16.
Two colour diagram for the cluster NGC 6752 (after Cannon and Stobie 1973).

Kukarkin (1974) proposed a method to calculate the interstellar reddening by the four colour photometry U, B, V, I. He proposed a way to calculate the intrinsic colours introducing three parameters X, Y and Z which are functions of the spectral type. A table is produced that gives the parameters X, Y and Z from the spectral type. And so the intrinsic values derive from the following formulae

$$X = \frac{(U-B)}{(B-V)} \qquad Y = \frac{(V-I)}{(B-V)} \qquad Z = \frac{(U-B)}{(V-I)}$$

The reddening values are important for:

1) Fitting of main sequences to obtain distances, absolute magnitudes and ages.

2) Determination of intrinsic colour of RR Lyrae instability strip in clusters of different metal abundances.

The second problem would provide answers to several questions (Sandage 1969).

2i) Differences in the mean period of RR Lyrae stars in cluster groups I and II are maybe due to different absolute luminosities of variables in the two groups (Oosterhoff groups).

2ii) It has been shown that the position of the high temperature instability edge is related to Helium abundance. So it is important to establish the variation of T_{eff} on the blue edge of the strip.

2iii) We can also have information about X and Z abundance, photometric distance module, turn-off luminosities and age.

3) The ultraviolet excess for globular cluster stars was shown to be a general feature of halo clusters and in many clusters studied subsequently. It is an index of metal abundance and there is a correlation of $\delta(U-B)$ with the Deutsch (Kinman 1959) and Morgan (1959) metallic line types.

Wallerstein and Helfer (1966) have given a preliminary calibration of $\delta(U-B) = f\left[F_E/H\right]$ for K giants which shows that $\delta(U-B)$ changes very slowly for $\left[F_E/H\right] < -1$.

2.3.5. <u>The colour-magnitude diagram (C-M)</u>

The C-M diagrams of globular clusters give information about their ages, distance modulus and metal abundances. One typical C-M diagram is the M3 (Johnson and Sandage, 1956) Fig. 17.

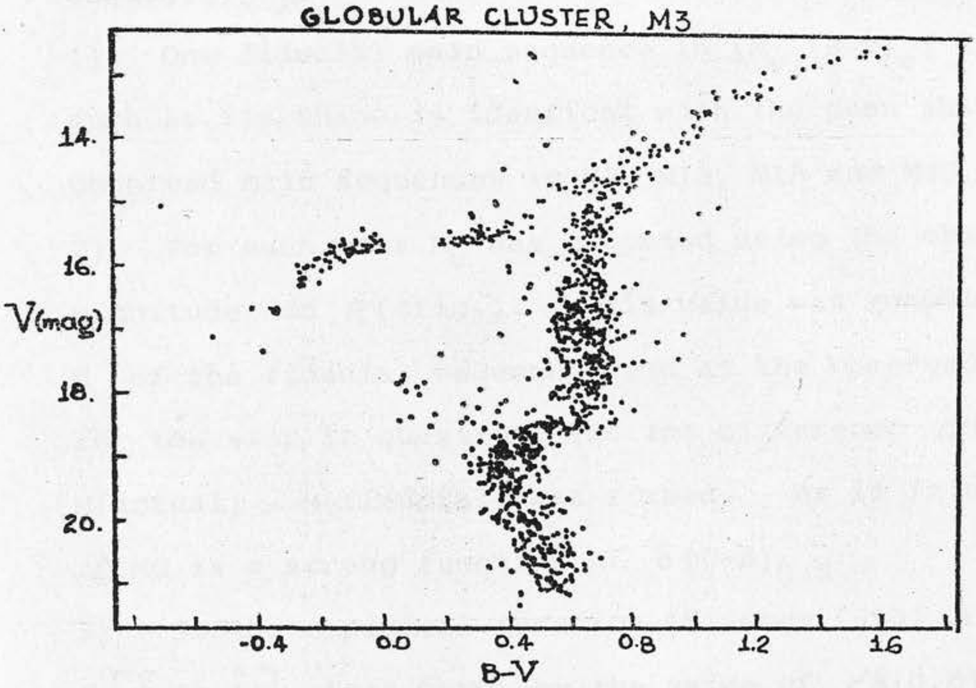

Fig. 17. The C-M diagram for cluster M3 (after Johnson and Sandage, 1956).

The determination of the physical properties by the means of the observational results is as follows:

2.3.6. Distance moduli

a) Main sequence fitting.

The distance modulus used to be assumed according to the Hyades main sequence fitting but this can lead to errors because of: i) the position of the sequence in the (M_{bol},T_{eff}) plane is sensitive to changes in X and Z. ii) Observed colours are affected by variations in Z due to line blanketing differences. One method followed by Sandage (1956) has better results and three steps are needed:

1) One fiducial main sequence in (M_v,$(B-V)_o$) is adopted such as its shape is identical with the mean shape of the observed main sequences in M3, M13, M15 and M93.

2) For each star M_v was computed using the observed V magnitude and π(trig.). This value was computed with M_v of the fiducial sequence read at the observed B-V for the star in question, and the difference ΔMU = M(actual) - M(fiducial) was formed. As it is expected ΔMU is a strong function of $\delta(U-B)_{0,6}$.

3) So the empirical function (Sandage 1956) ΔMU = $f\left[\delta(0.6)\right]$ gives $[\Delta MU]$ by the value of $\langle\delta(0.6)\rangle$.

So distance modulus comes out of combination of ΔMU, fiducial sequence and the observed C-M diagram. The weakness of the method is its high sensitivity to observational errors in E(B-V), δ(0.6) and the observed colour in main sequence.

b) Distance from independent values for $M_V(RR)$

From the observed shortest period of the Bailey type ab RR Lyrae stars in various clusters $L_{bol}(RR)$ has been calculated. These values can be changed as $L_{bol}(RR)/L_{bol}(\odot)$ so if B.C.(RR) = 0.00 the $M_{bol}(RR)$ can be found and from the observed magnitudes of RR Lyrae members of the cluster the distance modulus derives.

c) Distance from the mean magnitude of the 25 brightest stars

This method is not in use any more but it was the very first way (Arp, 1956) to estimate the distance very roughly assuming that the mean absolute magnitude of the 25 brightest stars is roughly the same for all clusters. Therefore the differences in M25 were due to the distance differences.

d) The distance determination using the clusters angular diameter

This method (Arp, 1956) is not very accurate and therefore it is used very seldom. For all clusters for which distance has been obtained and the angular diameter as well (θ in arc min) the product $D\theta$ has been found 80 in average, (θ has been the value for the isophote containing 90% of the light) and then from the mean relation

$$D\theta \approx 80$$

we obtain D very roughly.

2.3.7. Metal abundances

Metal abundance Z, is determined by spectroscopic data according to: $\left[F_e/H\right] = \log \left[F_e/H\right]_{CLUSTER} - \log \left[F_e/H\right]_{\odot}$

Another way to determine the metal abundance is by δ(U-B) as it has been discussed in paragraph 3.3.1.

The magnitude difference ΔV, between the horizontal branch and the top of the giant branch appears well correlated with abundances in the sense that the lower the metal abundance the more luminous the giants. ΔV is read off the C-M diagram as just described at $(B-V)_o$ = +1.40.

The colour of the subgiant branch, before corrections for blanketing, is also likely to be well correlated with abundances among the oldest clusters. Obviously age dispersion is important here.

The slope and length of the break between the top of the main sequence and the subgiants appears metal correlated especially in intermediate age clusters (Shleisinger, 1969). Metal rich systems seem to have a horizontal break of which the length appears to increase with abundance of metals. Metal poor clusters show a sequence inclined upward towards the red, which is well populated with stars and does not extend far toward red.

Various important age and abundance correlations have been proposed for the horizontal branch portion of the colour-magnitude diagram. It has been proposed that the colour of the branch is correlated with the abundance of metals. Metal poor systems tend to show horizontal branch populated primarily on the blue side of the cluster-variable gap with increasing metal abundance and decreasing ΔV, the branch tends to shift to a red side population and disappears entirely in metal rich galactic clusters.

2.3.8. Helium abundance determination

A method has been proposed by Sandage (1969) for the determination of Helium abundance. According to Christy's theory:

$$Y = 1.600(B-V)^{o,c}_{BE} - 0.34\,\mathcal{M}/\mathcal{M}_{\odot} - 0.16\,M_v + 0.901$$

where $(B-V)^{o,c}_{BE}$ is the colour at blue edge of the RR Lyrae strip corrected for reddening and blanketing. $\mathcal{M}/\mathcal{M}_{\odot}$ and M_v are respectively the mass and absolute magnitude of stars at this edge.

2.3.9. Age determination

The age is a sensitive function of M_{TO} (absolute magnitude of the main sequence turn-off point of the C-M diagram), Y (Helium abundance) and Z (metal abundance). Different empirical methods have been proposed to derive the age from these parameters. One example is Sandage's formula that derived from Iben and Road's models.

$$\log T_9 = \frac{\log L_{TO}/L_{\odot} + (0.92+0.11 \log Z)\,Y + 0.219 \log Z - 0.079}{0.10 \log Z - 0.59}$$

for $0 < Y < 0.3$ $\qquad 10^{-3} > Z > 10^{-5}$

L_{TO} is the main sequence turn-off luminosity where B-V is bluest and it can be found from M_{TO}.

The importance of the turn-off point for the age determination is shown in Fig. 18 where Sandage produced a composite C-M diagram for different clusters. Ages corresponding to various turn-off points are given along the right-hand ordinate.

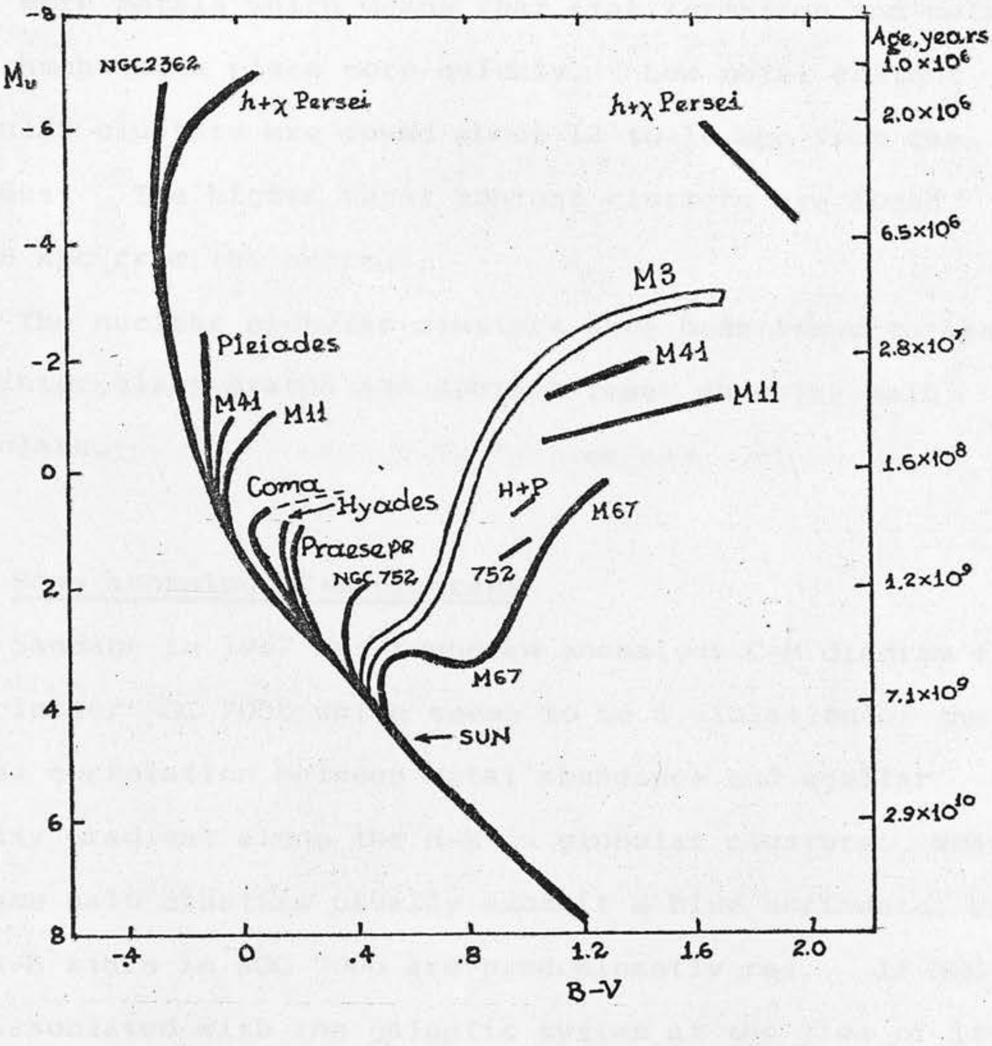

Fig. 18. A composite C-M diagram of 10 galactic clusters and 1 globular cluster. Ages corresponding to various main sequence termination points are given along the right-hand ordinate. (Sandage, 1957).

2.3.10. Some general results about globular clusters of our Galaxy.

The globular clusters are mainly found in the halo of our Galaxy except some which are near the galactic plane. The number of clusters known so far is 130. The clusters near the galactic plane have been found (Arp, 1971) to have more metals which means that star formation and metal enrichment took place more quickly. Low metal content globular clusters are found about 12 to 16 kpc from the nucleus. The higher metal content clusters are found 4 - 8 kpc from the nucleus.

The nuclear globular clusters have been found to have a fainter giant branch and contain fewer than the halo globulars.

2.4. Some anomalous C-M diagrams

Sandage in 1967 has found an anomalous C-M diagram for the cluster NGC 7006 which seems to be a violation of the unique correlation between metal abundance and stellar density gradient along the H-B in globular clusters. Whereas extreme halo clusters usually exhibit a blue horizontal branch the H-B stars in NGC 7006 are predominantly red. If NGC 7006 was associated with the galactic system at the time of its collapse toward the plane, it should be among the most metal-poor ones, because there is a relation between metalicity and the distance from the galactic plane. All spectroscopic data had indicated low metal content and the violation of the rule was the anomalous C-M diagram and especially the structure of the H-B (Fig. 19) which was exactly like the

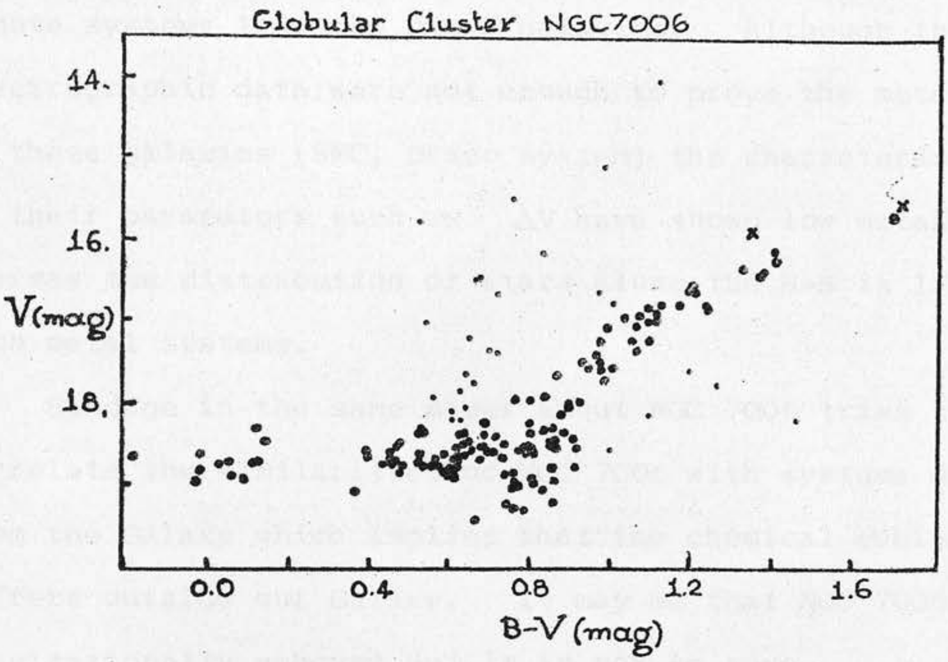

Fig. 19. C-M diagram for cluster NGC 7006 (after Sandage, 1967).

H-B of the metal rich clusters. So Sandage began to think that another parameter except metallicity should control the distribution of stars along the H-B. Two more clusters, M13 and NGC 288 (Cannon, 1974), were found to violate the rule but in the opposite way. It was then concluded (Sandage 1967) that Helium abundance should be taken into account (using the results of theoretical work by Faulkner) and be the second parameter which controls the H-B. This implies an extremely low Helium abundance for NGC 7006. Independently van den Bergh (1967 a, b) also came to this conclusion and suggested that the Helium abundance was the second parameter. It has also been found that the same sort of C-M diagrams appear in some remote systems like the dwarf galaxies. Although the spectrographic data were not enough to prove the metallicity of these galaxies (SMC, Draco system) the characteristics of their parameters such as ΔV have shown low metal content whereas the distribution of stars along the H-B is like rich metal systems.

Sandage in the same paper about NGC 7006 tries to correlate the similarities of NGC 7006 with systems distant from the Galaxy which implies that the chemical evolution differs outside our Galaxy. It may be that NGC 7006 is gravitationally unbound but it is not so sure.

After this work an effort has been made by theoreticians and observational astronomers to classify clusters according to the two suggested parameters and Hartwick presented a two dimensional classification scheme in 1968. In recent years the determination of the Helium abundance in a large number of objects has shown a remarkable degree of uniformity and the variations of Nitrogen abundance within individual galaxies have given the idea of Nitrogen being the "second parameter" wanted.

Hartwick and McClure in 1972 carried out observations of seven giant branch stars of NGC 7006 in order to get intermediate band colour indices which give amongst others the cyanogen band strength. They found that in both the surface gravity index and line-blanketing index the NGC 7006 giants are intermediate between M92 and M3. Thus only the cyanogen index indicates considerably stronger CN in this cluster than in M92 or M3. This made them think that Nitrogen abundance could be responsible for the anomalous character of NGC 7006.

In 1972 Rood produced models of the H-B trying to explain the problem theoretically. He assumed a metal abundance Z according to the globular cluster M3 which has been found to be 10 times more metal rich than the metal poorest globular cluster and 10 times less metal abundant than the known metal richest globular cluster.

He also thought that the colour extent of the evolutionary track of stars in this phase is so limited that the observed spread in colour for stars in the H-B was due to a spread in some parameter other than age along a single evolutionary track. Since some mass loss was required to have stars as blue as H-B stars it was assumed that this mass loss varied slightly from star to star while the mass of the Helium core remained constant.

Figs. 20 and 21 illustrate Rood's models transferred into colour-magnitude diagrams with a certain "observational error" to be more realistic and comparable to observational data. The effect of mass spread causes a considerable effect such as a spread in colour.

The cluster age (Fig.20) for a given X = 0.750 $Z = 10^{-3}$ affects the C-M diagram by shifting it bluewards with increasing age. This is due to the fact that M_{H-B} (mass in the horizontal branch phase) is getting smaller because M_{RG} (mass in the red giant phase) gets smaller.

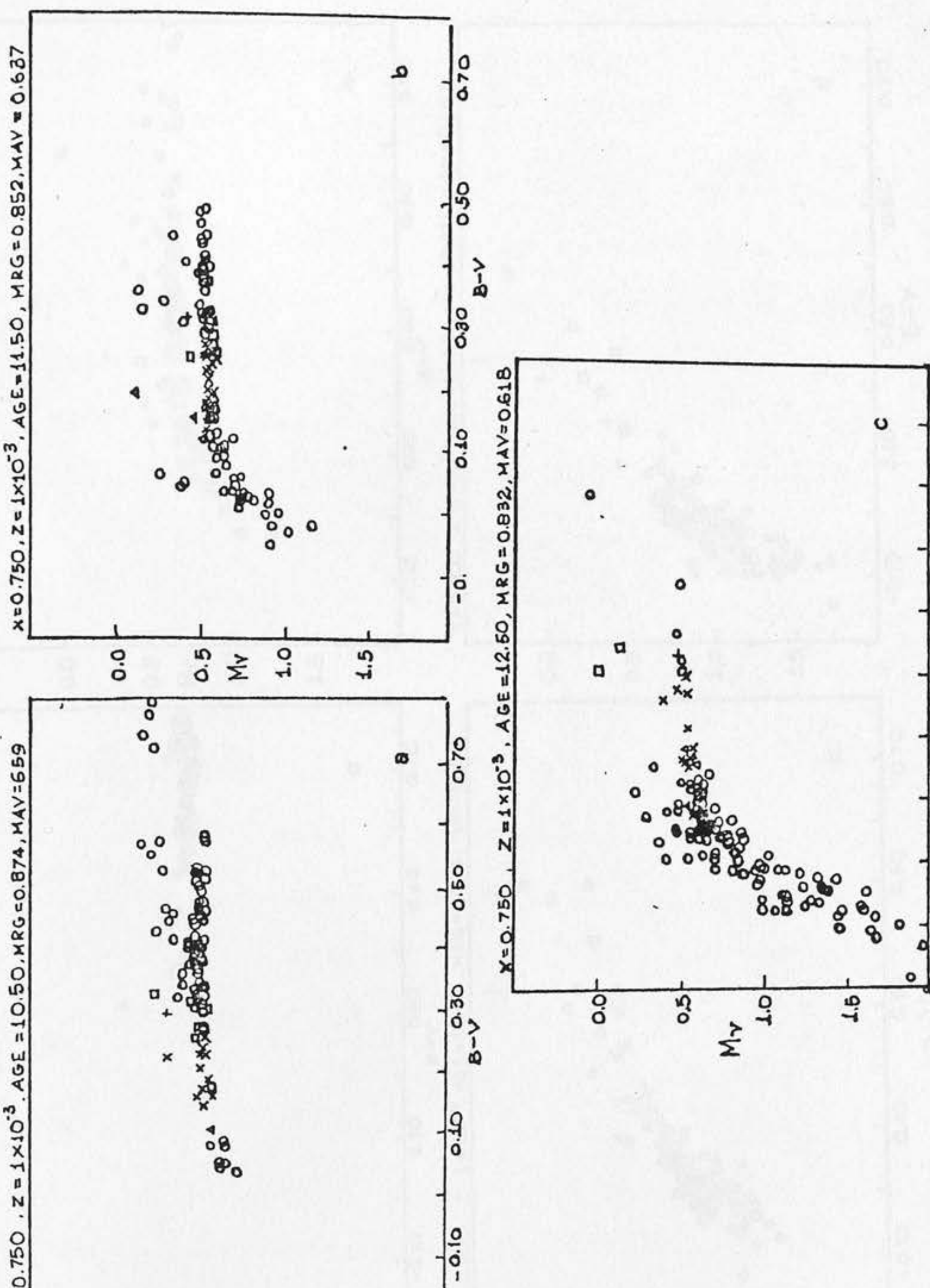

Fig. 20. The dependence of the H-B. The panels are separated by a billion years. Fig. 20b is the same as Fig. 20a with observational scatter added. (Rood, 1972.)

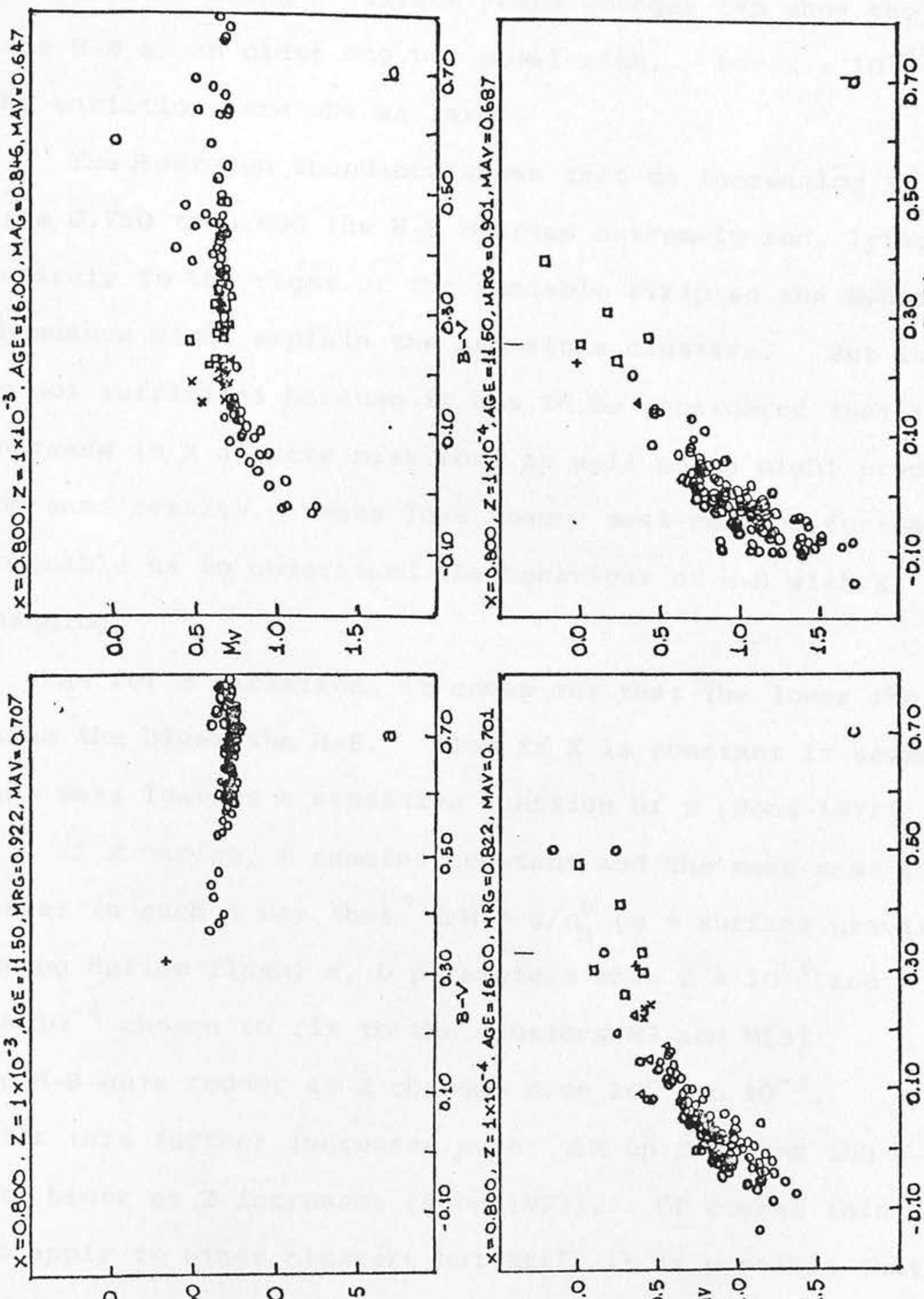

Fig. 21. Composition dependence of the H-B.

(a) The effect of increasing X by 0.05 when compared with Fig. 20b. (b) The same as (a) with mean mass loss and age adjusted. (c) The effect of an order-of-magnitude decrease in Z when compared with Fig. 21b. The mean mass loss has been decreased. When compared with Figs. 20b, Fig. 21d shows the effect of decreasing Z and the Helium abundance simultaneously (Rood, 1972).

So a cluster being a billion years younger can show the same H-B as an older one but metal rich. For $Z = 10^{-4}$ the variations are not as large.

The Hydrogen abundance shows that on increasing X from 0.750 to 0.800 the H-B becomes extremely red, lying entirely to the right of the variable strip so the Hydrogen abundance might explain the anomalous clusters. But this is not sufficient because it has to be considered that the increase in X affects mass loss as well which might produce the same results. Mass loss theory must develop further to enable us to understand the behaviour of H-B with X changing.

As for Z variations it comes out that the lower the Z value the bluer the H-B. Also if X is constant it seems that mass loss is a sensitive function of Z (Rood 1972).

If Z varies, X remains constant and the mean mass loss varies in such a way that $\Delta M = \alpha / g_h^b$ (g = surface gravity during Helium flash) α, b parameters when $Z = 10^{-3}$ and $Z = 10^{-4}$ chosen to fit to the clusters M3 and M13) the H-B gets redder as Z changes from 10^{-4} to 10^{-3}. After this further increases push ΔM up fast and the H-B gets bluer as Z increases (Rood 1972). Of course this does not apply to other clusters but still it is possible that a fair relation between Z and ΔM might explain the anomalies.

According to Simoda and Iben the Z pertinent to theoretical calculations is largely the sum of C, N, O i.e. Z_{CNO}. First it determines the rate of CN cycle, which is the dominant mode of Hydrogen burning beyond turn-off even for the Pop II abundances. It is also responsible for the dependence of Z on the opacity. But unfortunately most of the direct estimates of Z are referred to the iron-peak elements. Other metallicity indicators are based on features of C-M diagrams which must be related to Z through models which have previously assumed a constant Z_{CNO}/Z.

It is more likely that metallicity indicators based on giant branch characteristics such as $(B-V)_{o,g}$, the height of giant branch ΔV and Hartwick's parameters might be affected differently from those dependent on metallic line strengths like the Morgan (1954) classification, or the Kinman (1939) or Kron and Mayal (1960) spectral classification.

Rood's main conclusion from his theoretical work was that the variation of the H-B with Z can be explained only if one of the following is true.

i) The mean mass loss along the giant branch is some function of Z or a quantity such as surface gravity which is a function of Z.

ii) The initial Helium abundance of a cluster increases by ~ 0.05 when Z increases by an order of magnitude.

After these, the idea of a better classification of star clusters began and one conclusion is that the anomaly might be an effect of poor definition of metallicity. In 1972 Dickens has written an extensive paper about the cluster NGC 6981 where he gives a long discussion about globular clusters and their H-B characteristics. He notes that there is a rather poor correlation of H-B type with metal abundance. The metal abundance is usually judged from Deutsch-Kinman classification for individual giant stars or from ultra-violet excesses of giant stars. He also produced a code of H-B according to the distribution of stars in its different parts namely, red part-instability strip-blue H-B from 1 (predominantly blue) to 7 (predominantly red). Comparing this code for clusters well known so far with metallicity parameters it comes out that the correlation is poor and the "second parameter" is needed.

Quantities which might be expected to correlate with metal abundances are the ultra-violet excess, δ(U-B) and the absolute magnitude of the giant branch read at a given temperature as it has previously been discussed. An approximation to the latter quantity is provided by a parameter,

$$\Delta V_{corr} = \Delta V - M_{VRR}$$

where ΔV (magnitude excess above horizontal branch) read at $(B-V)_o = 1.4$ and M_{VRR} absolute magnitude of the RR variables in a cluster (i.e. the absolute magnitude of the H-B). So the correlation between Deusch class (metallicity indicators) and ΔV_{corr} seems better than the metallicity and H-B type.

Constellani et al conclude that within each H-B type there exist clusters with H-B of lower mass and higher Z, (as in M13) and clusters with stars of higher mass and lower Z (M92 case). They also found that the complete range of H-B types in globular clusters in the Galaxy can be explained theoretically by the ratio of core mass to total mass.

$$M_c/M_T = q_o$$

From about q_o = 0.9 for clusters with blue H-B to about 0.7 for clusters with red H-B.

It is therefore important to explain why q_o should vary with H-B type. Variations in Z do not appear to be the principal factor because clusters with both high and low values of Z are found with types 1-5. Variations in Y have no observational support, but assuming an increase in Y this implies decrease in M_c and hence q_o and also tendency to move the H-B stars to redder colours. The range in Y implies a range of ages amongst globular clusters, which is unlikely, or a range in mass.

All these suggestions however are not strong enough yet since theoretical and observational results are expected to provide better proofs. Spectroscopy of giant stars of different clusters would be necessary for the more accurate determination of metallicity. (Dickens, 1974).

So the "second parameter", which gives rise to anomalies in clusters like NGC 7006 or M13, remains uncertain. Theoretical models explaining the way mass loss scales with known parameters must be in progress. Either Helium variations of $\sim$ 0.03 (by mass) of age variations or perhaps a billion years would seem adequate. It is also possible that cluster concentration might somehow affect mass loss and be a second parameter and in cases like the clusters NGC 7006, it appears that they are extremely concentrated. Also reordering the clusters according to Z_{CNO} might delete the anomalies.

Recently the cluster NGC 2808 (Harris 1974) and NGC 1871 (Cannon and Stobie, Private Communication) have been found with an anomalously big gap between the blue H-B and the red H-B by Harris. This is an unusual case amongst the clusters and it can be the result of different process. Apart from the age difference which is unlikely to explain such a gap it seems that different envelope mass would explain this phenomenon. So the large M_c of red H-B stars will evolve further to the asymptotic branch whereas the blue H-B stars with low M_c cannot evolve as the previous ones and possibly they fall into white dwarfs. An unknown mass loss process probably takes place which is also very important to be studied more extensively.

CHAPTER III

SMALL MAGELLANIC CLOUD - PREVIOUS WORK

3.1. Magellanic Clouds

The two Magellanic Clouds are very well known objects of the southern sky visible by naked eye at galactic latitudes 33^{o} and 38^{o} well out of the galactic plane which is very important because the foreground visual absorption amounts only to about 0.2 mag.

The currently accepted (Westerlund, 1974) distances of the Clouds from the Sun are 50 kpc for the Large Cloud and 66 kpc for the Small Cloud. This distance is about one tenth the distance to the Andromeda nebula.

Both Clouds have irregular shapes and they both have an elongated bar without any dominant nucleus. In the literature they used to be the prototypes of "irregular Magellanic-type" galaxies. The Small Cloud has an elongated wing pointing towards the Large Cloud which contrasts with the very smooth distribution of faint stars that characterises its main bar.

De Vaucouleurs in a recent review paper (1972) describes the Magellanic Clouds as barred spirals and he claims that they may not be irregular. They both have a spiral structure characterised by a specific kind of assymetry.

The wing of the SMC contains extreme population I objects (according to Westerlund (1970)) and analogue spiral structure in the Large Magellanic Cloud can be proved by the study of the stellar content of both Clouds.

The stars in both Clouds belong to population I and population II. The wide range of ages best appear in the study of star clusters which have been found in a great variety. There are blue globular-like clusters and globulars without red H-B but many faint blue stars whereas some others exhibit only a very conspicuous red H-B.

Many bright stars scattered across the fields of the Clouds offer important material for spectroscopic studies and the study of the evolution of massive stars. They offer a unique opportunity to study and compare luminosities of supergiants, giants, main sequence stars of all types, Wolf-Rayet stars, Cepheids, eclipsing variables, Mira variables, RR Lyrae variables, globular clusters, novae and so on all at the same distance.

The mass of the Large Magellanic Cloud has been found to be from 3% - 10% of the mass of the Galaxy, whereas the Small Cloud must contain even less mass.

The abundance determination of the two Clouds have shown normal Helium abundance everywhere (Webster, 1975) whereas Oxygen abundance is lower sometimes by a factor of two or three than in our Galaxy. Metal deficiencies have been found in both clouds especially in the SMC.

In general the LMC shows a very active star formation whereas in the SMC a decline in the rate of star formation has been found.

It is then very important to clarify these problems in detail with the new data provided by the large Southern telescopes and study more carefully the satellites of our Galaxy.

The main differences in the evolutionary history of the two Clouds and our Galaxy are: (S. van den Bergh, 1975)

i) In the M. Clouds the present rate of star formation is similar to its average rate during the last $\sim 1 \times 10^{10}$ years whereas the present rate of star formation in the Galaxy is much lower than it was when the Galaxy was young.

ii) For all age groups, stars in the Magellanic Clouds have lower heavy element abundances than do their galactic counterparts.

iii) The history of cluster formation in the Galaxy and in the Magellanic Clouds was different.

For the SMC it seems that both stars and massive clusters have been forming more or less continually which means (Freeman & Munsuk, 1972) that there may not have been a great burst of star formation when the Small Cloud collapsed. The LMC appears somehow different from the SMC and started its evolution with a more violent burst of star formation.

3.2. Small Magellanic Cloud

3.2.1. Structure of the SMC

The Small Magellanic Cloud is very difficult to be analysed as far as the spiral structure is concerned because of its large inclination which is $i = 60^{\circ} \pm 3^{\circ}$ (Westerlund, 1974), although other workers have given even larger values for i.

The main features of the Small Cloud are the bar and the wing. The wing is a very confusing feature which distorts the symmetry of this galaxy and it points towards the Large Cloud.

Nevertheless the basic characteristics of Magellanic based spirals (SB) can still be recognised (de Vaucouleurs & Freeman, 1973) by direct photography, surface photometry, star counts, cluster distribution and radial velocities.

The wing is probably not in the equatorial plane of the system.

The main structure of the SMC as suggested by de Vaucouleurs consists of the bar-like core of the system elongated in p.a. 45^{o} through the optical centre, (00^{h}, 51^{m}, -73^{o}, 1950). The brightest part of the bar A is near (00^{h}, $48^{m}.5$, $-73^{o}.45$) where the gradient of the luminosity function is at maximum and the highest concentration of neutral Hydrogen is also found in this region. Another feature is the north following arm which is centred at (1^{h} $0^{m}.0$, $-72^{o}.5$). It is rich in blue supergiants and HII regions and the gradient of the luminosity function is much lower than in A. The last feature is the outer loop which is difficult to be traced because of the unfavourable inclination of the main central plane of the system and because of the inclination to the plane of the main spiral arm. But it is most clearly shown in the south-west elongated region stretching about 2^{o} of the bar and it is rich in Cepheids and red clusters. There are two possibilities (de Vaucouleurs & Freeman, 1973) one is that it forms a circular loop around the main body and the other that it is a spiral arc south west of the bar. Later on, in the present project it appears more likely to accept the first possibility. The main peculiarity of the SMC is the assymetric "wing".

In Fig. 22 (de Vaucouleurs & Freeman, 1973) the spiral structure of the SMC is illustrated with all possible arms and orientation of this galaxy.

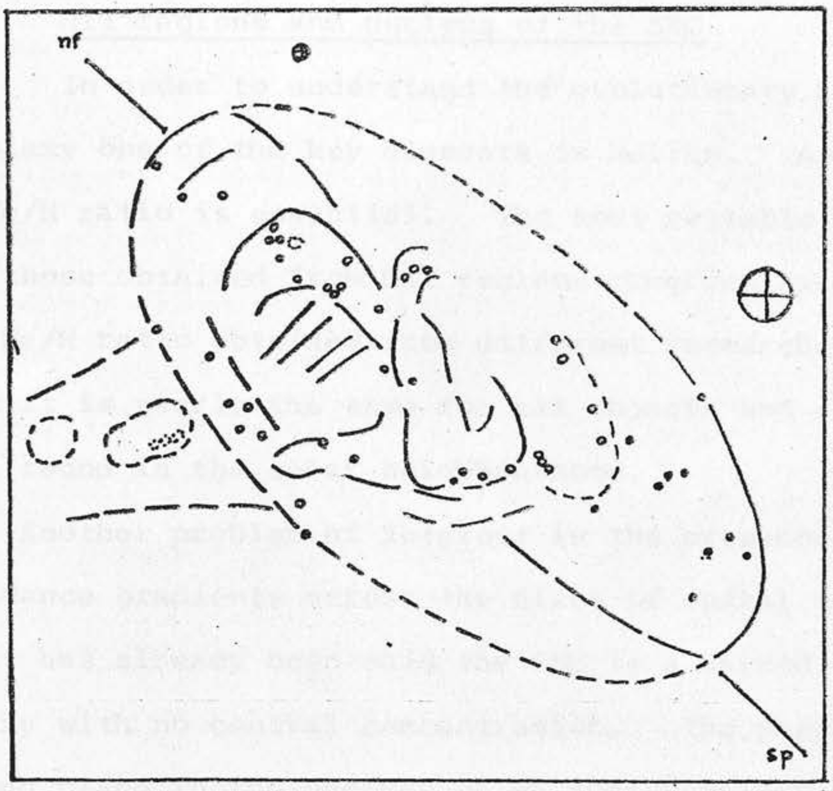

Fig. 22. The spiral structure of the SMC (after de Vaucouleurs & Freeman, 1973).

Basically the main characteristics of this kind of galaxy is a strong assymetry of the spiral structure about the bar axis in which one major arm dominates the spiral pattern, while two or three smaller and a shorter arm emerge from the other extremities of the bar.

The radial velocity of the SMC is on average ± 170 km/sec and foreground galactic stars have radial velocity + 50 km/sec. At the distance of either Cloud, a cross-wire motion of as much as 20 km/sec leads to an annual proper motion,

$\mu = 7 \times 10^{-5}$ sec of arc, far below our limits of detection. Hence any star with a measurable proper motion is almost sure to be a foreground star (Bok, 1966).

3.2.2. HII regions and nucleus of the SMC

In order to understand the evolutionary history of a galaxy one of the key elements is Helium. An examination of He/H ratio is essential. The most reliable determinations are those obtained from HII regions observed optically. The He/H ratio obtained from different researchers shows that it is nearly the same for all objects and similar to that found in the solar neighbourhood.

Another problem of interest is the presence of chemical abundance gradients across the discs of spiral galaxies. As it has already been said the SMC is a barred spiral galaxy with no central concentration. The phenomena taking place in the nucleus of an active galaxy are: violent motions of gaseous clouds, considerable excess of radiation in the ultraviolet, relatively rapid changes of brightness, expulsion of jets and condensations. The presence of these processes is described by the words activity of the nucleus. No sign of such activity has been found in the SMC.

The SMC HII regions are mostly diffuse with relatively little fine structure on scales down to 10 arc sec and only weak central concentrations (Davies et al., 1976). The neutral Hydrogen is found similar in density for the SMC and the LMC and it seems difficult to see why the HII regions and star formation are different. The explanation might be found in the history of the SMC. It is now established that a strong tidal interaction has taken place between our Galaxy and the Magellanic Clouds. Such an interaction is more disruptive for objects with smaller mass and as a consequence the SMC is more strongly affected. This passage occurred at 2-3 x 10^8 years ago and its effect could still be evident in terms of a lower rate of star formation and HII region production. It has also been found that the tongue of HI and HII regions projecting to the east of the main body of the SMC is not so prominent optically; it is therefore composed of younger material than the main body.

3.2.3. Planetary nebulae in the SMC

The study of planetary nebulae (Webster, 1975 report) in the SMC shows that the Oxygen abundance in the planetaries is lower by a factor of two or three, which indicates that the heavy element production has been less rapid in the SMC than in the Galaxy. Nitrogen also has been found deficient (Sanduleak, 1972) in the planetary nebulae.

3.2.4. Supernova Remnants (SNR's)

Two SNR's have been identified in the SMC and ten shell sources which might be possible SNR's. (Davies, 1976).

3.2.5. Variable stars

The Magellanic Clouds are famous objects because it was in them that Miss Leavitt established the period-luminosity relation for Cepheids. This relation has led to a long series of investigations and the most recent one is whether the Cepheids in the Clouds have the same composition as our Galaxy. The discovery of RR Lyrae stars in the Clouds is of fundamental importance for the study of the SMC, the actual variables and the distance scale. So the different kind of variables will be discussed separately.

a.5.1. RR Lyrae stars

The first astronomers who discovered RR Lyrae stars in the SMC are Thackeray and Wesselink who were followed by a recent extensive study by Graham (1975).

Graham searched an area of $1^{o} \times 1^{o}.3$ in an outlying region of the SMC around the cluster NGC 121. He found that the period distribution is unlike that found anywhere in the Galaxy and resembles most closely the variables in the Leo II dwarf galaxy. There is also some evidence that for a given period the SMC variables tend to have smaller amplitudes than Galactic RR Lyrae stars. The mean blue magnitudes of the SMC variables peak sharply at $\langle B \rangle = 20^{m}.0$. The mean $\langle \bar{B} \rangle$ for all RR Lyrae variables with known periods and with $\langle B \rangle \rangle 19^{m}.00$ is $19^{m}.95$. Measurements of the yellow plates give a similar mean $\langle \bar{V} \rangle = 19^{m}.57$ for this same group. The mean absolute magnitude is $+0^{m}.6 \pm 0^{m}.25$. A search for RR Lyrae variables in the field of the SMC between the clusters NGC 362 and NGC 361 has given quite similar results. So it is likely that RR Lyrae stars are distributed rather evenly over the

SMC and concentrate neither towards the central bar nor toward the centre of the SMC system.

In the area of the cluster NGC 121 there are no Cepheid variables , . no young OB stars or HII regions, no open clusters. These characteristics and the C-M diagram of the field signify that there has been no star formation in the area more recently than 10^9 years ago. However, the space density of the RR Lyrae stars, a factor of 10 greater than that in the Galactic halo, indicates that a strong component of old population II is present and that a considerable amount of star formation has occurred during an earlier period, far from the present main body of the SMC.

Again the similarity of RR Lyrae variables distribution with the dwarf galaxy Leo II might be explained by the lack of an active nucleus in these dwarf galaxies.

b. Cepheid variables in the SMC

The SMC contains many Cepheids which are different from the ones investigated in our own Galaxy. The main properties of SMC Cepheids are:

1) In the SMC many Cepheids have periods between 1.5 and 4 days which is rather uncommon for the Milky Way.

2) The B-V colours of the SMC Cepheids are bluer than those in the Galaxy by about 0.1 mag. for periods shorter than 10 days.

3) The amplitude of these short period, blue SMC Cepheids are very large, reaching 1.6 mag.

The Cepheid instability strip (M_{bol}, $\log T_{eff}$) diagram is likely the same for all galaxies. However the filling of the strip may differ from galaxy to galaxy due to differences in the evolutionary tracks. Thus the bluer Cepheids in the SMC result from their penetrating deeper into the strip than the galactic Cepheids. This explains points (1) and (2) (Sandage and Tammann, 1971).

c. Other variable stars in the SMC

One object with H and FeII emission and suspected T_iO absorption has been found in the SMC and may belong to the VV Cephei class which are an interesting class of long period binary stars consisting of a cool supergiant and an OB star with low density gas and they are believed to be high mass objects.

Feast has also reported (1974) some long-period (period 127 days) Cepheid stars in the SMC which present the anomaly of being too red for the assigned types.

3.2.6. Carbon stars in the SMC

A large number of carbon stars were discovered (Westerlund,1972), whereas few very red stars appeared in the globular clusters, something most unusual for our Galaxy. In 1973 Feast and Evans carried out spectroscopic observations of stars with (B-V) $\sim$ 2.0 or greater in the clusters NGC 121, NGC 419 and Kron 3 and have revealed that some of them are carbon stars. Their absolute magnitude is $M_V = -3.0$. Some simple statistics show that these stars are more likely to be cluster members. Such stars have been detected in ω Cen and in the intermediate age clusters which means either that the SMC globular clusters are younger than their counterparts in the Galaxy or their chemical composition is different.

3.2.7. Dust content in the SMC

The foreground absorption in the direction of the SMC is very small and it is of the order of $E_{B-V} = 0.07$ with standard deviation $0^m.01$. The dust content appears remarkably low in relation to their gas content.

The dust-to-gas ratio in the SMC varies a lot according to the different researchers. They have given values of 10 to 100 times smaller than in the Galaxy (MacGillivray, 1975, Butler, 1972, van den Bergh 1974).

The differences in the value of the ratio E_{B-V}/N_H for the Galaxy and the Magellanic Clouds could be interpreted as evidence that either the Magellanic Clouds are less evolved than the Galaxy, or that the mixing of the interstellar medium in the Magellanic Clouds is less efficient. Because of that it is expected that metals are underabundant in this galaxy.

3.3. Stars and stellar systems in the SMC

The stellar content and the star clusters are the aim of this project so a detailed review of the work which has been done on this subject will be reported. Star clusters are distributed all over the body of the SMC and the number of such objects is increasing as the new large telescopes in the South hemisphere are in operation during the last few years.

3.3.1. Catalogues of the SMC clusters

Star clusters in the SMC have been listed by several workers. Many of them are included in the NGC catalogue, in the IC catalogues and a few of them in the Bailey's catalogue of Bright Clusters and Nebulae (1908). Shapley and Miss Wilson (1925) compiled an exhaustive catalogue of non-stellar objects in the SMC. In 1935 Miss Mohr found seven more objects classified as clusters. Kron in 1956 gave the first detailed catalogue of 69 objects only four new ones and with the aid of a blink comparator he divided the clusters into predominantly red or predominantly blue ones. It also gave a very rough estimate of diameters and some remarks referring to the central concentration, based upon the appearance of the object on the plates, its colour and brightness.

The clusters of the Small Magellanic Cloud were 116 in a catalogue by Lindsay in 1958 from material which was obtained from ADH plates (Boyden Observatory) of long exposure centred on the Cloud. In his catalogue the right ascension and declination are given and additionally the photographic (wherever possible) magnitudes, estimate of the diameter in arc min and other reference numbers for each cluster if possible.

In 1971, 18 more clusters in the wing of the SMC were reported by Westerlund and Glaspey.

Since the operation of the new big telescopes in the Southern hemisphere a search started for new objects in the Small Magellanic Cloud. The first paper with a catalogue of new clusters appeared in 1974 by Hodge and Wright where they listed 86 more bringing the total number of catalogued clusters to 220. The material of this catalogue was provided by plates of Cerro Tololo Interamerican Observatory's Curtis Schmidt Telescope.

These objects were missed in previous searches either because of their compactness, which can cause them to appear as stars because of poor seeing, or because of the faintness of their stars. They give positions, diameters and descriptions for each individual cluster.

The most recent catalogue is by Brück (1975) from plates of the U.K. 1.2m Schmidt telescope in Australia. The field of these plates is $6^{o} \times 6^{o}$ and 160 clusters out of 220 of Hodgewright catalogue have been identified whereas 170 further clusters were found. All objects were examined visually on U, B and V plates to provide estimates of brightness, colour and size by the aid of a blink comparator. Maps and complete lists of this catalogue have been published in 1976.

The cluster members recorded in this project refer to the catalogue where they first appeared or they are best known. The letter L in front of the cluster number means that the numbers refer to Lindsay catalogue, HW means number from the Hodge-Wright catalogue and E means number from the Brück catalogue.

3.3.2. <u>Subsystems of the SMC and related clusters studied previously</u>

The stellar content of the SMC has been studied by Westerlund (1970) according to the evident spatial distribution of the different subsystems. These are mainly the bar, the wing, the central system and the halo. The clusters studied previously and the new clusters studied in this project are noted in Fig. 23 except three small clusters by Andrews, in the vicinity of the cluster NGC 371.

Arp (1958a, 1958b, 1959a, 1959b) was the first who carried out photoelectric and photographic photometry and studied four rich clusters in the N-E part of the SMC, i.e. NGC 361, NGC 458, NGC 330 and NGC 419. Tifft (1963) studied next a globular cluster of the western part NGC 121 and he reached faint enough limits to get the H-B and fainter. Gascoigne in 1966 produced the C-M diagrams of 3 SMC globular clusters and wrote an extensive paper with the first results on the behaviour of the globular clusters in this galaxy.

Apart from these researchers, Westerlund (1961) studied the wing of the SMC carrying out photographic photometry of clusters occupying this area. He found very young objects,

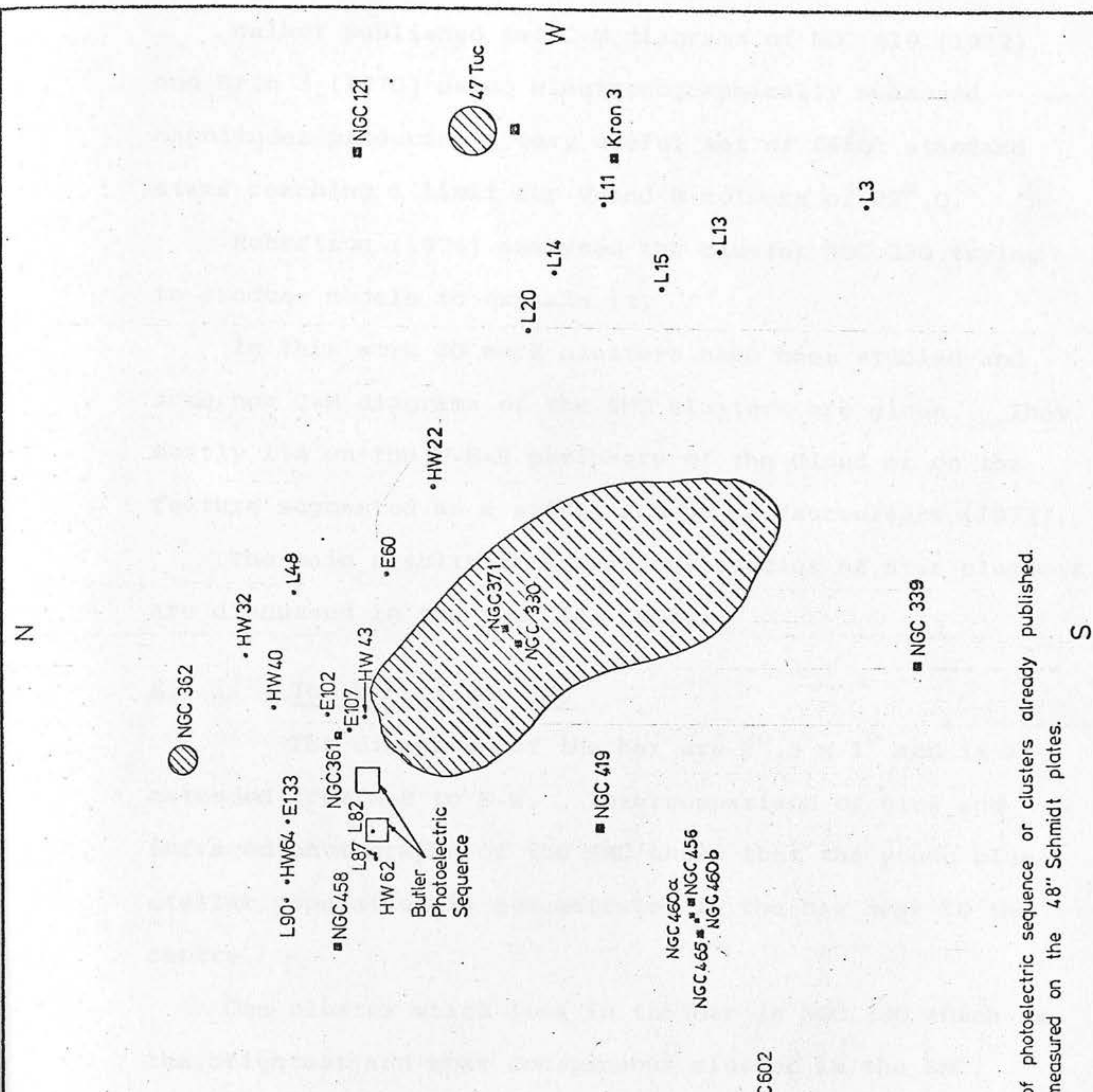

Fig. 23. A schematic diagram of the SMC of the U.K. Schmidt plate. The location of photoelectric sequences or clusters measured by previous workers is identified by squares. The dots show the location of clusters measured for the first time on the U.K. Schmidt plates.

apparently the youngest of the SMC.

Walker published two C-M diagrams of NGC 419 (1972) and Kron 3 (1970) using electronographically measured magnitudes producing a very useful set of faint standard stars reaching a limit for V and B colours of $22^{m}.0$.

Robertson (1974) analysed the cluster NGC 330 trying to produce models to explain it.

In this work 20 more clusters have been studied and some new C-M diagrams of the SMC clusters are given. They mostly lie on the W-N-E periphery of the Cloud or on the feature suggested as a spiral arm by de Vaucouleurs (1973).

The main results from previous studies of star clusters are discussed in the next few pages.

a. <u>The bar of the SMC</u>

The dimensions of the bar are $2^{o}.5 \times 1^{o}$ and it is extended from N-E to S-W. Intercomparison of blue and infrared photographs of the SMC shows that the young blue stellar population is concentrated in the bar near to the centre.

One cluster which lies in the bar is NGC 330 which is the brightest and most conspicuous cluster in the SMC. The members of this cluster are bluer and very luminous. Arp has first given the C-M diagram of this cluster and he concluded that it differs from the galactic ones and this should be due to a different chemical composition (Arp 1958). Robertson (1974) measured again the cluster NGC 330 and he tried to make models explaining the C-M diagram of the cluster (Fig. 24). It is an extremely young cluster

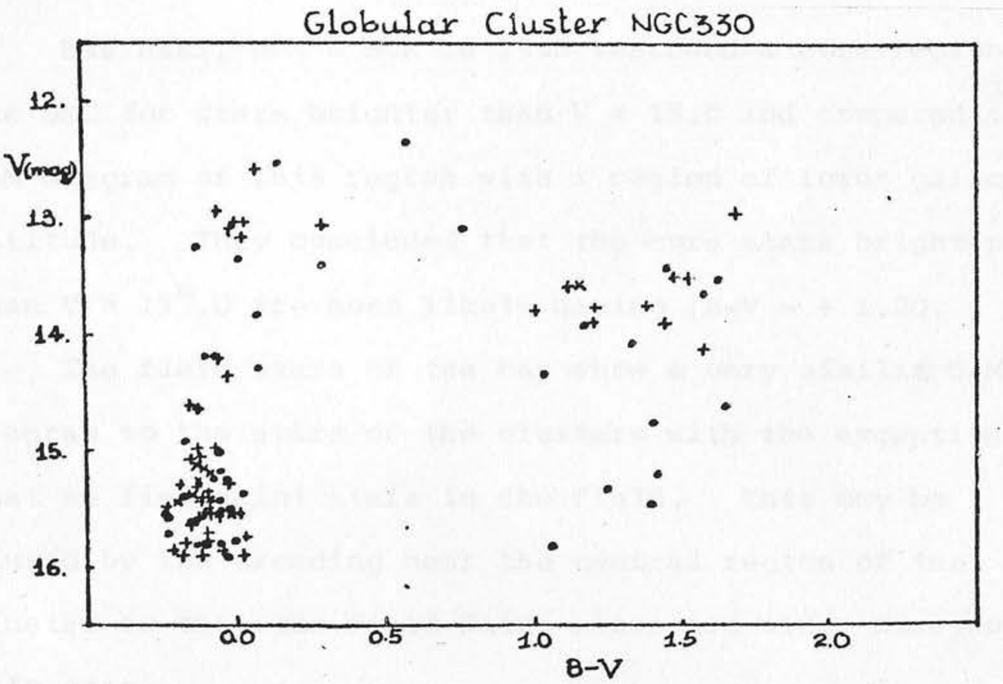

Fig. 24. Colour-magnitude diagram for NGC 330. The filled circles represent stars in region B and the pluses and crosses represent stars in region A (the crosses are the poor values or eye estimates).

with some members burning Helium in their core, which explains the existence of a gap in the main sequence. He also reports that the blue supergiants in NGC 330 are somewhat bluer than NGC 2004 in the LMC which has almost identical C-M diagram.

This implies lower Z for the SMC than the LMC or the Galaxy. Feast (1972) has studied spectroscopically the bright main sequence stars of NGC 330 and he has shown that almost all stars with $-3^m.2 < M_1 < -4.^m2$ are B_e stars. This implies that the diagram needs correction for the rotational distortion of the diagram. We have estimated that the age of the cluster is 5×10^6 years using Schlesinger models (1969).

Basinski, Bok & Bok in 1966 searched a core region of the SMC for stars brighter than V = 15.0 and compared the C-M diagram of this region with a region of lower galactic latitude. They concluded that the core stars brighter than V = $15^{m}.0$ are most likely having (B-V ~ + 1.20.

The field stars of the bar show a very similar C-M diagram to the stars of the clusters with the exception that we find faint stars in the field. This may be caused by the crowding near the central region of the cluster or that the field faint stars are older foreground halo stars.

The bluesness of the stars of this region gives some evidence that the bar is a site of present star formation in this galaxy. Another evidence of this conclusion is that the bar contains a significant amount of neutral Hydrogen (Hindman 1967).

Many stellar OB associations are found in the bar, while the compact clusters tend to occur in the centre (Brück 1975).

Andrews produced C-M diagrams of three small clusters (Fig. 25) in the vicinity of NGC 371 where many Cepheids have been discovered. The region is dominated by supergiant stars and these represent a very young population. Some red giants are also present as it always happens for all regions of the SMC. The age of these objects seems younger than that of NGC 330. Especially C_1 and C_3 which have not many giants seem to be purely

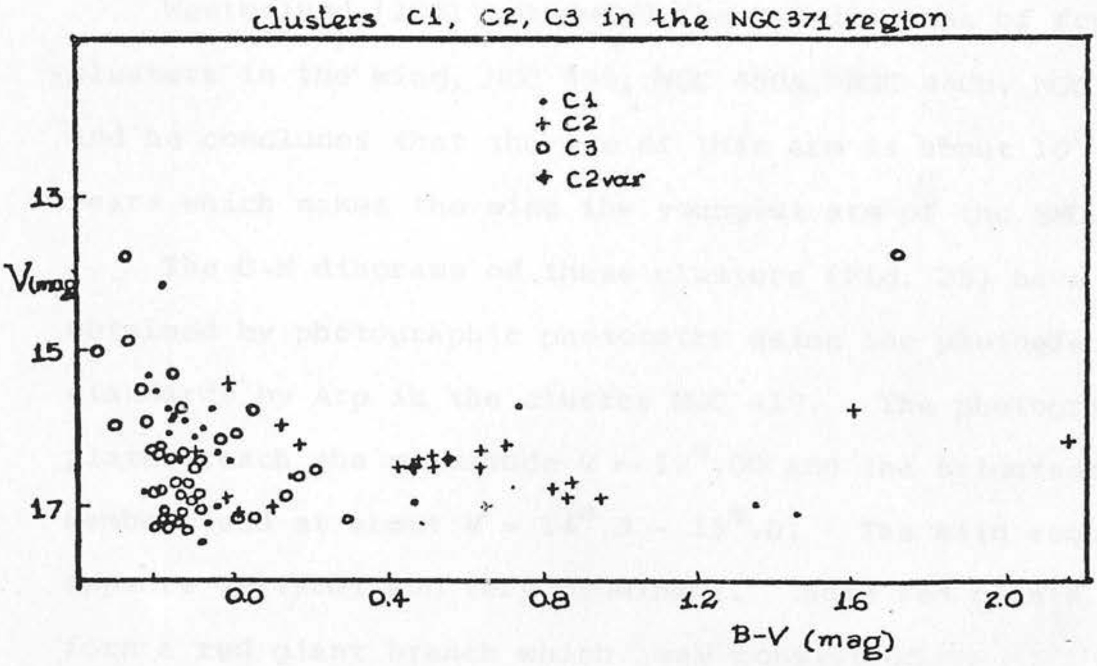

Fig. 25. C-M diagrams of three clusters C1 (dots), C2 (crosses), C3 (open circles) in the vicinity of NGC 371. (Andrews, 1971).

main sequence objects where no evolved Helium burning stars appear, whereas C2 seems to have rather pure population objects where the red giant stars form an horizontal kind of branch very narrow in brightness but extended in colour. Of course C2 is a different object, a halo type possibly.

b. <u>The wing of the SMC</u>

The wing extends from the cluster NGC 419 towards the LMC direction and its dimensions are $6^{\circ} \times 1^{\circ}$.

It contains mainly extreme population I stars and almost all of them are blue stars. The star systems found on it are mainly stellar OB associations. It seems that the wing contains the youngest clusters found in the SMC.

Westerlund (1961) produced the C-M diagrams of four clusters in the wing, NGC 456, NGC 460a, NGC 460b, NGC 465 and he concludes that the age of this arm is about 10^6-10^7 years which makes the wing the youngest arm of the SMC.

The C-M diagrams of these clusters (Fig. 25) have been obtained by photographic photometry using the photoelectric standards by Arp in the cluster NGC 419. The photographic plates reach the magnitude $V \sim 19^m.00$ and the brightest members end at about $V = 14^m.3 - 15^m.0$. The main sequence appears vertical and very prominent. Some red giants also form a red giant branch which may consist of field stars. The age suggested is 10^7 years. Two very red stars of $M_V = -3.2$ and $B-V = +3.0$ and $M_V = -1.5$, and $B-V = +2.8$ were detected and he suggested that they are foreground carbon stars.

c. <u>The central system of the SMC</u>

The central system is assumed flat and circular (Westerlund, 1972) of diameter 7^o and the centre lies near the cluster NGC 419. The extent of the "central system" is based upon the classification of(Gascoigne 1966) intermediate age globular clusters. Of course it is difficult to classify the clusters of this region because the C-M diagrams are distorted by the foreground stars.

The only known C-M of clusters of the central system are for NGC 458, NGC 419 and NGC 361 studied first by Arp (1958, 1959). Walker (1972) gave the C-M diagram of NGC 419 electronographically.

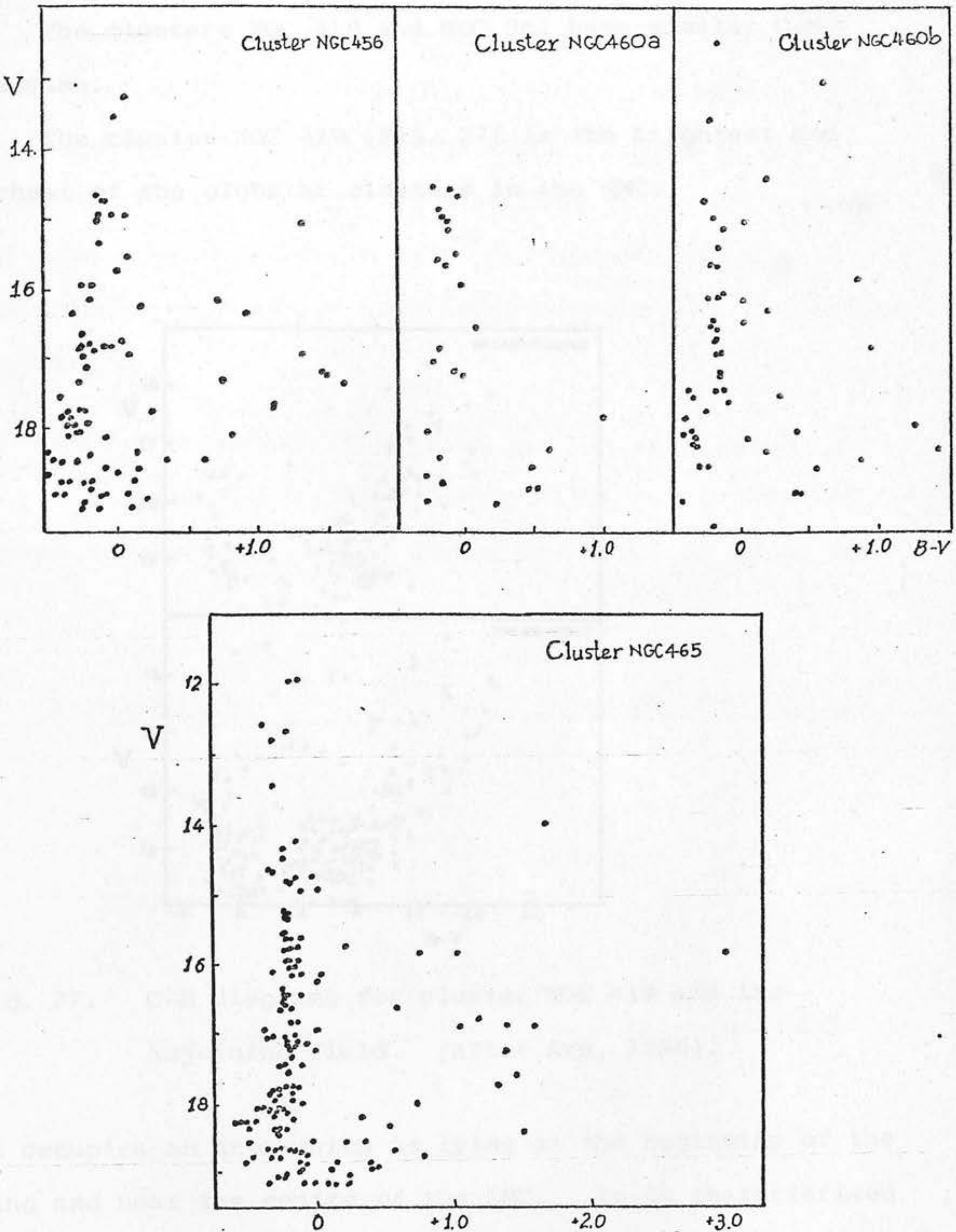

Fig. 26. Colour-magnitude diagram for NGC 456, NGC 460a, NGC 460b, NGC 465. (Westerlund, 1961).

The clusters NGC 419 and NGC 361 have similar C-M diagrams.

i. The cluster NGC 419 (Fig. 27) is the brightest and richest of the globular clusters in the SMC.

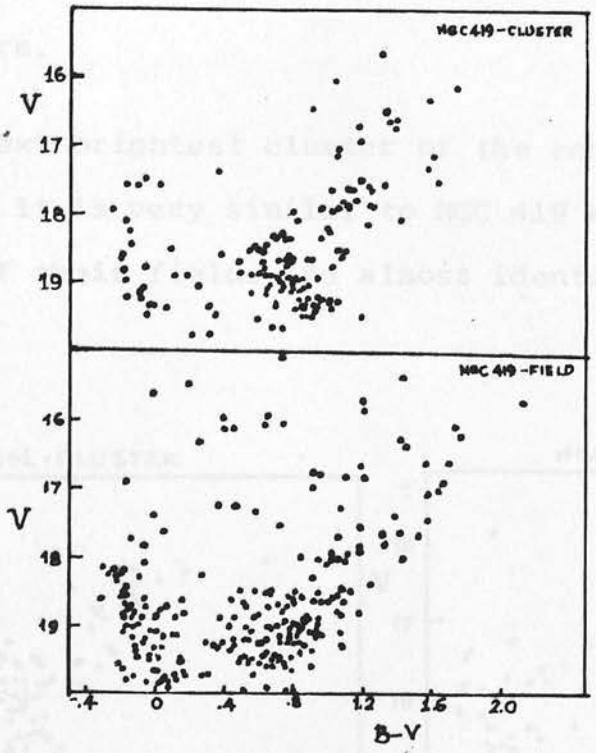

Fig. 27. C-M diagrams for cluster NGC 419 and its adjoining field. (after Arp, 1958).

It occupies an area which is lying at the beginning of the wing and near the centre of the SMC. It is characterised by a strong red giant branch extending to redder stars than found in our Galaxy. The field contains numerous main sequence stars which are probably background stars belonging to the main body of the SMC. Walker (1970) in his interpretation reports that this cluster is similar to

Kron 3 or NGC 2209 of the LMC.

As it is discussed before, Feast and Evans reported that the very red star which is at the central region of the cluster with $M_V = -3\overset{m}{.}0$ is a carbon star. The comparison of NGC 419 with its counterparts in our Galaxy would give a certain answer about the age of this cluster, because carbon stars have been detected only in intermediate age clusters.

ii. The next brightest cluster of the central system is NGC 361. It is very similar to NGC 419 and the C-M diagrams of their fields are almost identical. (Fig. 28)

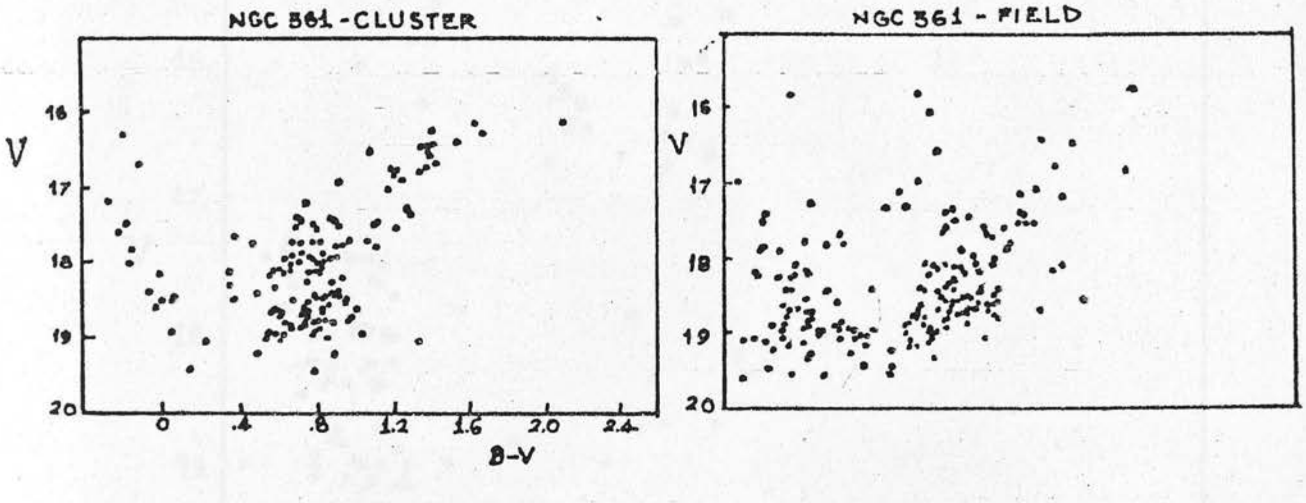

Fig. 28. C-M diagram for cluster NGC 361 and its adjoining field (after Arp, 1959).

So the conclusion is that apart from the differences between the two clusters, the stellar content where they are embedded is quite of the same kind.

The cluster itself consists of a red giant branch starting from B-V = $1^m.6$ and V = $16^m.0$ and curving down to a subgiant branch that runs between B-V = 0.7 to 0.8 mag from V = $18^m.0$ to fainter magnitude.

iii. The third cluster of the central system is NGC 458 (Fig. 29), (Arp, 1959).

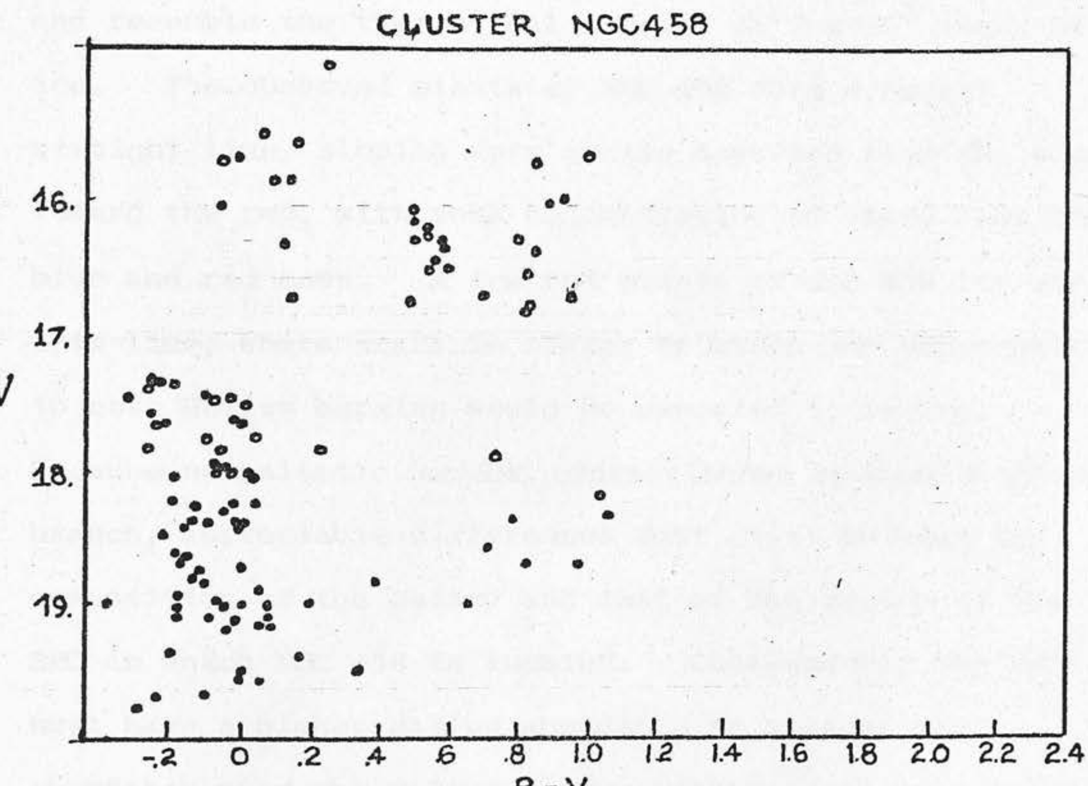

Fig. 29. C-M diagram for cluster NGC 458 (After Arp, 1959).

This cluster occupies the area of the second spiral arm of the SMC in the N-E side of this galaxy. Arp has studied this cluster and the produced C-M diagram appears in Fig. 29. It seems a young cluster with some evolved stars and its age is 2×10^7 years. The diagram of NGC 458 is somewhat bluer than expected in our own Galaxy but it is very likely that the metallicity of the star members is much lower in this cluster and the SMC in general.

Later in 1969 Schlesinger tried to match the C-M diagram of NGC 458 with his model (part II) and he suggested that the evolved stars are Helium-burning stars and resemble the theoretical cluster of 7×10^7 years of age. The observed giants of NGC 458 form a nearly straight line, sloping very gently downward from the blue toward the red, with some concentration of stars near the blue and red ends. A few red giants of NGC 458 lie above this line where stars in stages of evolution subsequent to core Helium burning would be expected to evolve. Because no galactic or SMC cluster shows so blue a giant branch, appreciable differences must exist between the composition of the Galaxy and that of the region of the SMC in which NGC 458 is located. Consequently the SMC must have a higher Helium abundance or a lower metal abundance than the Galaxy. The latter seems more likely after recent investigations about the Helium abundance in the SMC which has been reported to be normal.

The C-M diagram of the field is like that of NGC 361 and NGC 419 fields which is an evidence that this is in general the characteristic C-M diagram of the stellar content of the SMC "central system".

d. <u>The halo of the SMC</u>

The halo of the SMC is spherical of 7^{o} diameter.

i) Gascoigne in 1966 has published an extensive paper on the globular clusters of the SMC where he presents their main characteristics and differences from the ones of the Galaxy. He measured four globular clusters of the SMC halo and produced their C-M diagrams. These diagrams are illustrated in Figs. 30a, b, c, d, e, f, g. All these clusters

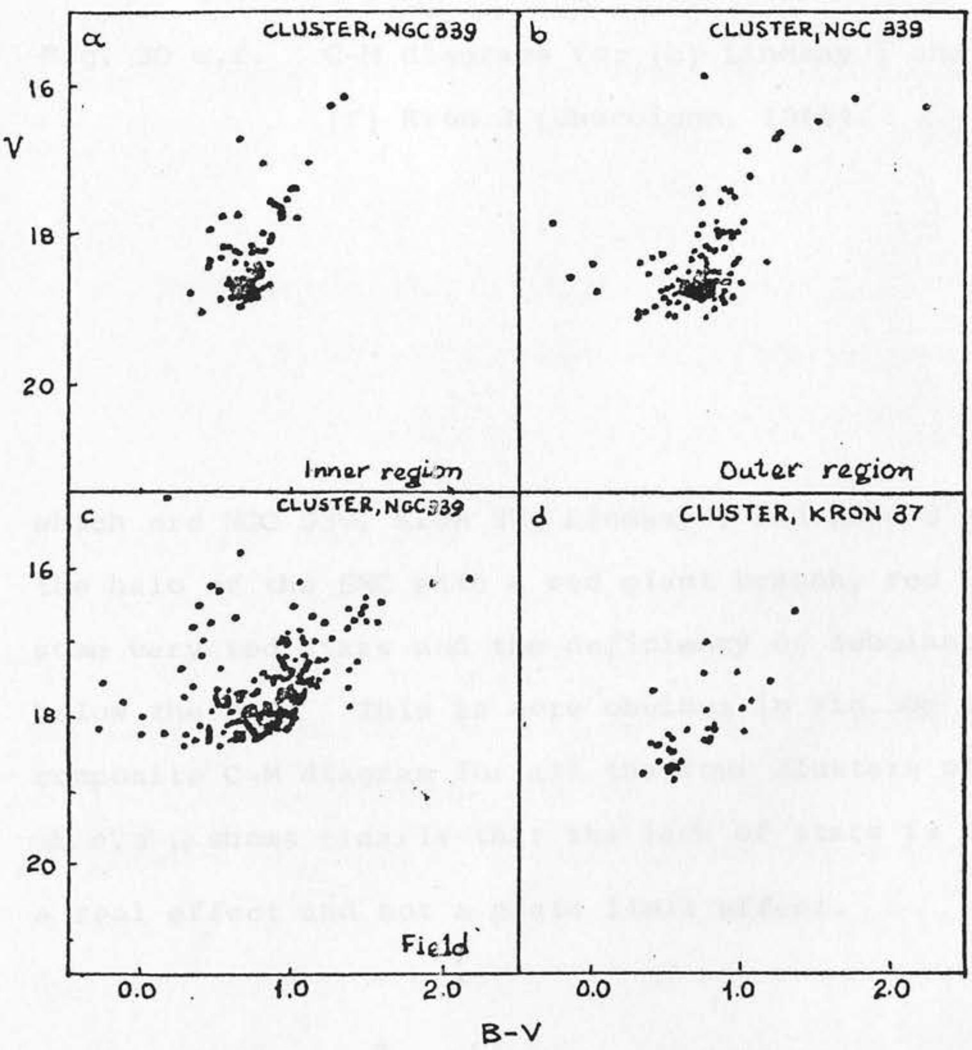

Figs. 30a, b, c, d. C-M diagrams for (a),(b),(c), NGC339, (d) Kron 37 (Gascoigne, 1966).

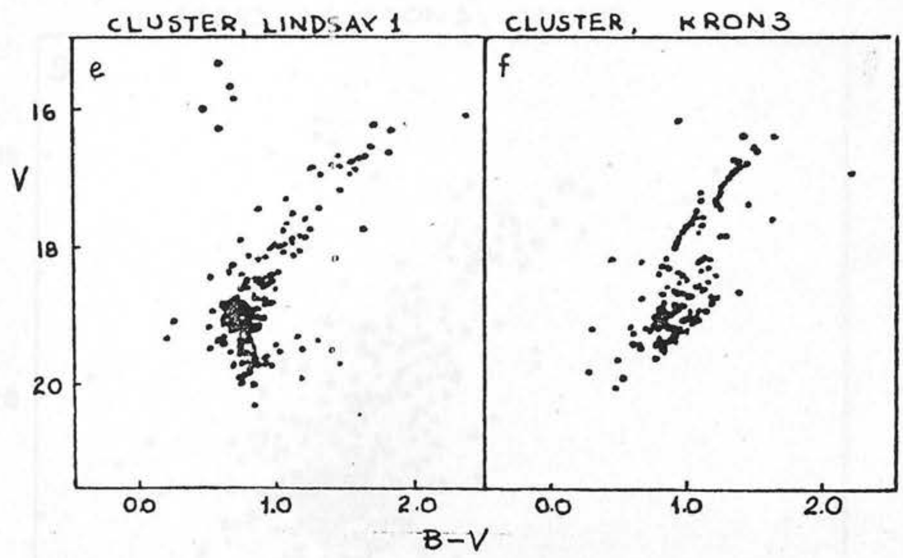

Fig. 30 e,f. C-M diagrams for (e) Lindsay 1 and (f) Kron 3 (Gascoigne, 1966).

which are NGC 339, Kron 37, Lindsay 1 and Kron 3 belong to the halo of the SMC with a red giant branch, red H-B, some very red stars and the deficiency of subgiant stars below the H-B. This is more obvious in Fig.30g where the composite C-M diagram for all the four clusters of Fig. 30 a, d, e, f, shows clearly that the lack of stars is probably a real effect and not a plate limit effect.

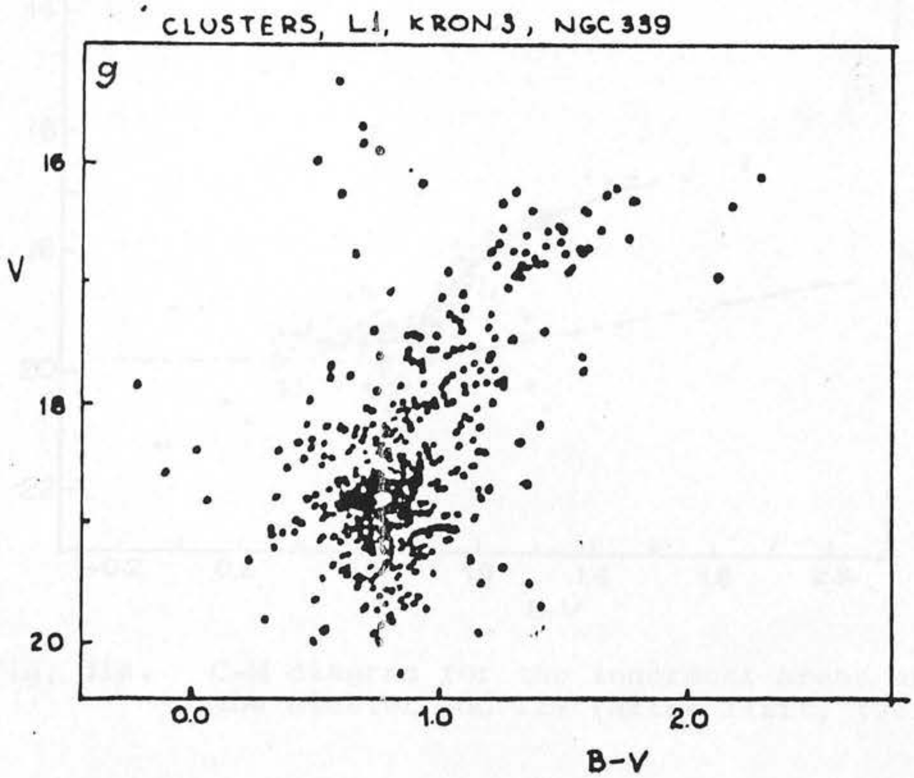

Fig. 30g. Composite C-M diagram for the Clusters L1, Kron 3 and NGC 339 (after Gascoigne, 1966).

ii) The second cluster very well known of the western side of the SMC is NGC 121. Tifft (1963) has studied it very carefully and produced a very good set of C-M diagrams starting from the central region of the cluster up to the vicinity of the globular cluster 45 TUC. Fig. 31a illustrates the diagram of the central region where mostly members of the cluster are present whereas in Fig. 31b the next rings have more faint stars but the giant branch is blended with field stars.

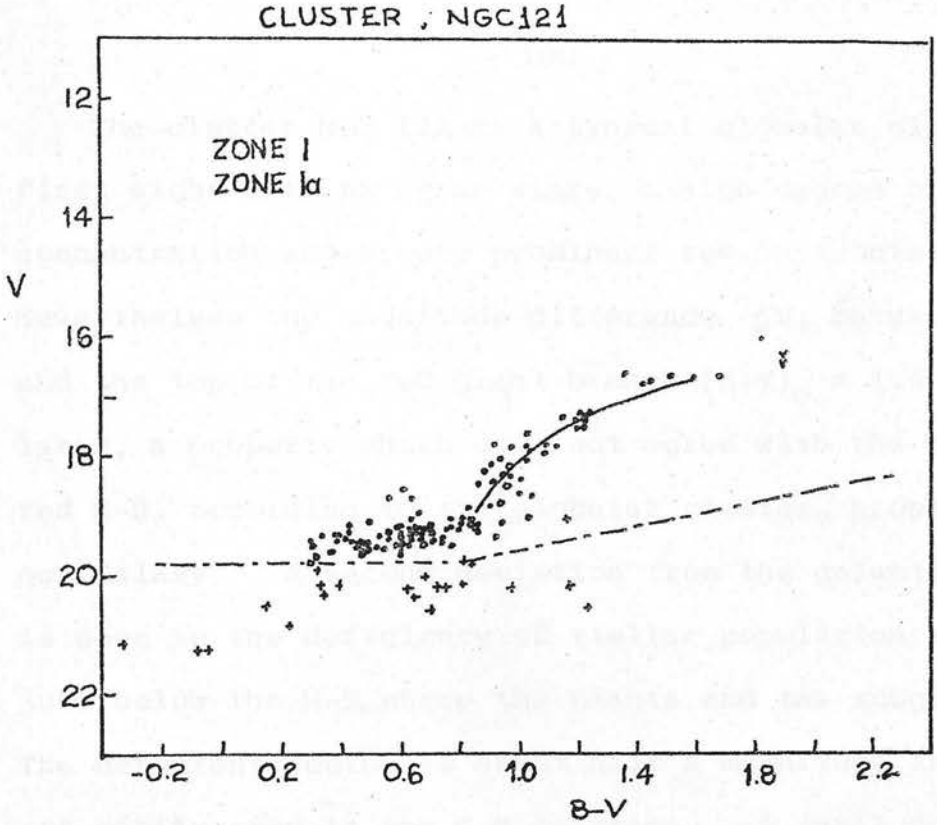

Fig. 31a. C-M diagram for the innermost areas of the cluster NGC 121 (After Tifft, 1963).

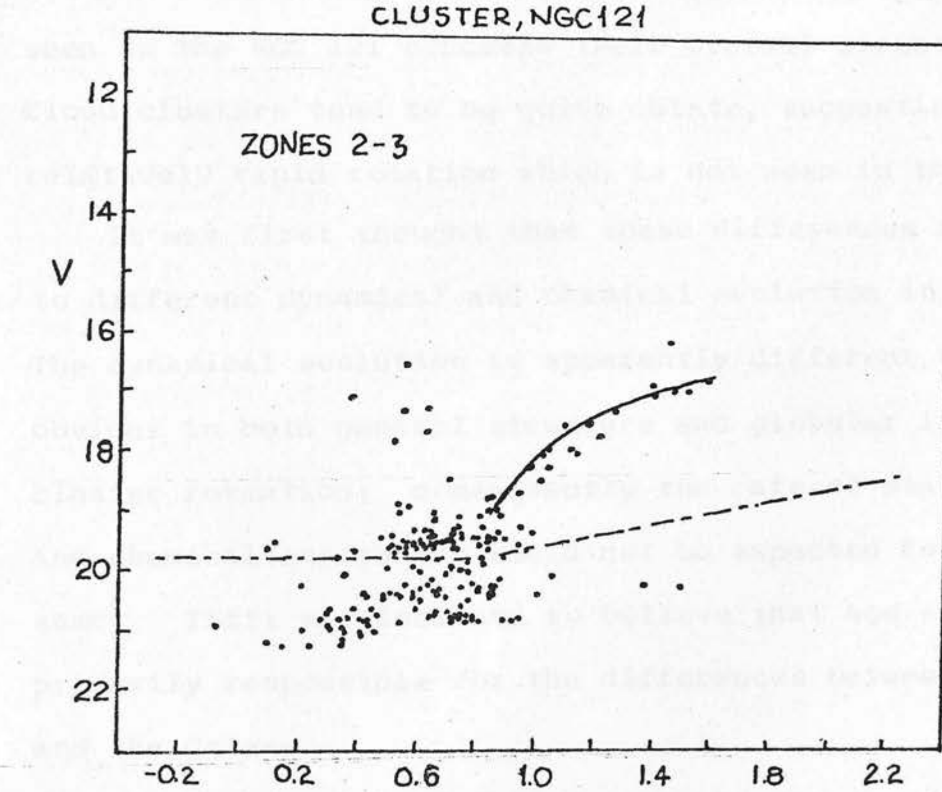

Fig. 31b. C-M diagram for stars of the outer regions of the cluster NGC 121. This diagram contains primarily physical member of NGC 121 but begins to show a significant field component (after Tifft, 1963).

The cluster NGC 121 is a typical globular cluster at first sight with RR Lyrae stars, a high degree of concentration and a very prominent red horizontal branch. Nevertheless the magnitude difference ΔV, between the H-B and the top of the red giant branch $(B-V)_o = 1.4$ is quite large, a property which does not agree with the extremely red H-B, according to the globular cluster properties in our Galaxy. A second deviation from the galactic pattern is seen in the deficiency of stellar population at the point, just below the H-B, where the giants and the subgiants merge. The deficient region is about half a magnitude in width and easily seen in the C-M diagrams. A small deficiency of stars at this point is seen in galactic globulars but it is generally fairly weak. One final difference, between galactic and Cloud globular-like clusters, easily seen in the NGC 121 concerns their overall structure. Cloud clusters tend to be quite oblate, suggesting relatively rapid rotation which is not seen in the Galaxy.

It was first thought that these differences are due to different dynamical and chemical evolution in the SMC. The dynamical evolution is apparently different and quite obvious in both general structure and globular like cluster formation; consequently the rate of star formation and chemical enrichment would not be expected to be the same. Tifft was inclined to believe that age effects are primarily responsible for the differences between the SMC and the Galaxy.

Two carbon stars detected again by Feast and Evans belong to the cluster NGC 121. One is a variable star of period $140^d.2$ and $\langle V\rangle = 16.4$, $\langle B\rangle - \langle V\rangle = 1.9$ and the second star has a period of $112^d.4$ and $\langle V\rangle = 16.4$, $\langle B\rangle - \langle V\rangle = 1.9$ and $\Delta V = 0.25$. The existence of carbon or very red stars in the SMC cluster is becoming a very frequent case and it seems that we must take it into consideration.

iii) The C-M diagram the most recent (Fig. 32) of Kron 3 is given by Gascoigne (1976) from plates of the AAT Anglo-Australian Telescope. Walker (1970) has also given electronographically measured, the C-M diagram of the same cluster. It is more likely that Fig. 32 represents better the cluster members being produced by plates with higher resolution and consequently exhibiting stars occuping areas near the nucleus of the cluster.

One carbon star has been reported by Feast and Evans with V = 16.48 and B-V = +2.37. The C-M diagram of the cluster exhibits a red H-B. The uncertainty about the integrated colour which seemed bluer than the C-M diagram by Walker could explain is solved; many faint blue stars with $V > 20^m.30$ appear, which contribute to make the integrated light bluer.

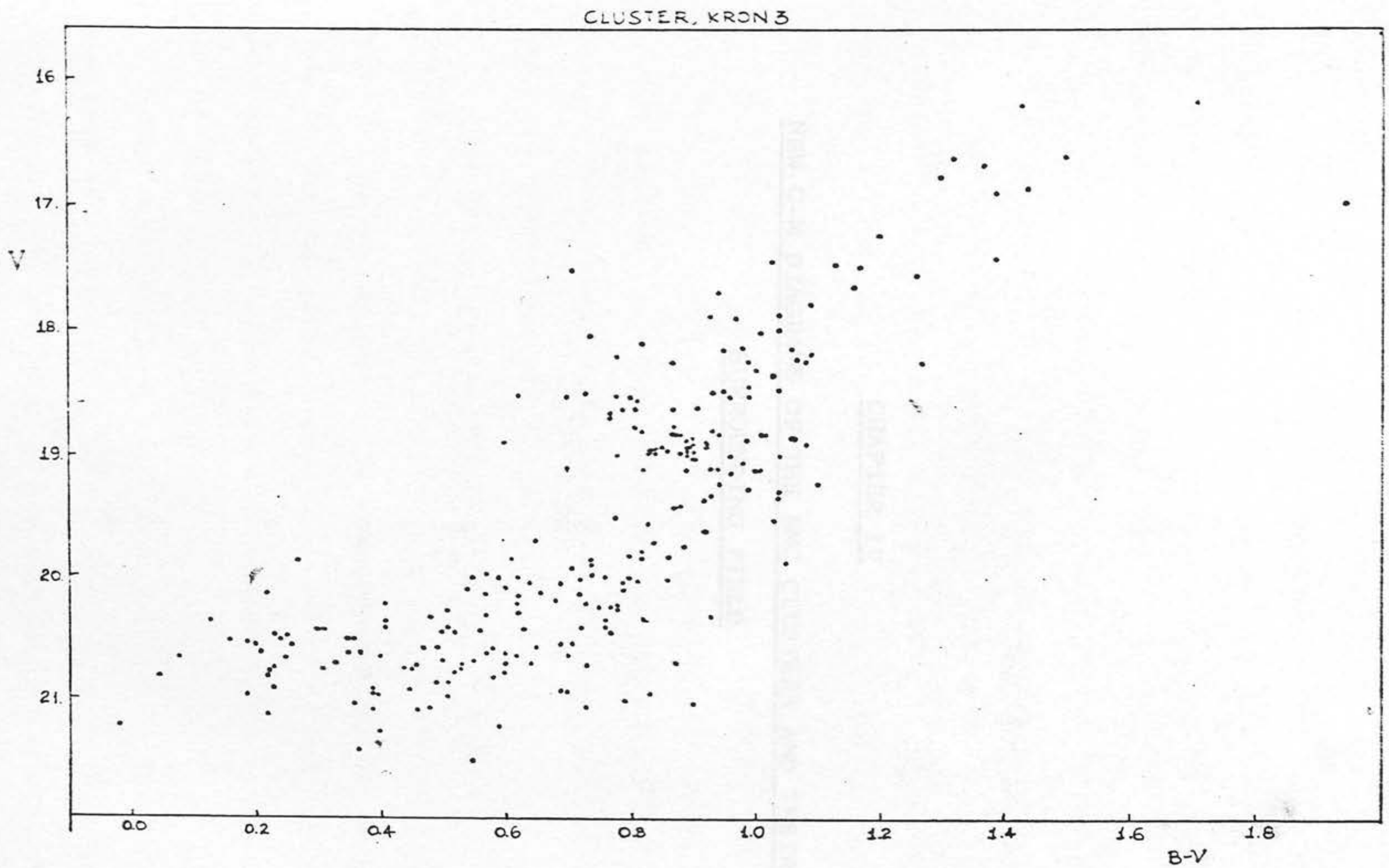

Fig. 32. C-M diagram for cluster Kron 3 (Gascoigne, 1976)

CHAPTER IV

NEW C-M DIAGRAMS OF THE SMC CLUSTERS AND THEIR SURROUNDING FIELD

4. Introduction

The U.K. 1.2m Schmidt telescope has provided good raw material for the study of star clusters in the SMC. The accuracy of the photometry discussed in the first part is not excellent but good enough to derive useful C-M diagrams and make some more assumptions for the problems of the evolutionary history of the SMC.

The faint limit of the Schmidt plates is about 2-3 magnitudes more than most of the plates taken so far for the study of star clusters in this galaxy with the exception of Walker's electronographic magnitudes, Tifft's NGC 121 and the latest Gascoigne's AAT plates. The limit of the previous diagrams used to be at about $18^{m}.50$ exactly where the H-B is expected to occur. So the advantage of this new material is that the H-B is detected and its behaviour can be studied, especially as far as its variations from cluster to cluster. So some more evidence arises about the halo population of the SMC.

The next possibility, which was given by the Schmidt plates, is to study the stellar content of the feature reported as spiral arm by de Vaucouleurs in the north-east side of the SMC central system. Two clusters lying on this spiral arm would give information about the kind and age of this stellar system.

The main problems which make difficult the study of the clusters and surrounding fields are the crowded nature of this region and the uncertainty of whether we are looking at cluster members or a blend of field and cluster stars with the same evolutionary history. This problem can be minimised by studying a large sample of clusters of a certain area and therefore assuming that the differences between the C-M diagrams are different because of their intrinsic properties, providing that the C-M diagram of the field over a large region would be similar for all clusters.

The problem discussed already is the lack of good photoelectric sequences and especially for the faint limits. So the selection of clusters to be measured was difficult for taking into account two main problems; they had to be near one of the existing photoelectric sequences and to occupy a not crowded area.

Finally, the clusters chosen to be measured are (Fig. 23) L3, L13, L15, L11, L14, L20, which occupy the west part of the SMC halo, HW22, E60, L48, HW32, E102, E107, HW43, E133, L82, L87, HW62 which lie on the northern part of the SMC and the last two L90 and HW64 located on the small spiral arm of the north-east part of the SMC.

The adopted distance modulus is m-M = 19.20 according to Westerlund (1974) and the reddening is $E_{B-V} = 0.12$ (Butler, 1972).

These twenty C-M diagrams have been divided into three main categories according to their main common characteristics or their location on the plates. Their C-M diagrams have been produced and lists of measured stars with maps are given. (Appendix).

4.1. First Group

This group comprises stars clusters from the western and northern part of the SMC which are classified as old halo type objects with differences in the structure of the H-B, the only feature which provides criteria of ages or abundances for the time being. We need to get much fainter magnitudes to have the complete C-M diagram and the turn-off points reliably.

4.1.1. The cluster L11

In this section the most characteristic C-M diagram is of L11. This cluster is a globular cluster at the western side of the SMC. It is very near to the cluster Kron 3 and toward the central region of the SMC. About 300 stars have been measured around the centre of the cluster, in three regions.

The region measured has been divided into rings of equal area (where the central $r_1 = 1.2$ arc min) and the number of stars per ring was plotted (Fig. 33) against distance from the centre. The curve shows a very sudden cut-off at about $r_3 = 2.3$ arc min) which is most likely the limit of the cluster. Three C-M diagrams have been produced where regions 1 and 2 represent the cluster according to Fig. 33. The C-M diagram of both regions 1 and 2 (Fig. 34) is very characteristic for the SMC. It resembles the cluster NGC 121 (Tifft, 1963) with an extremely dense red H-B which extends in colour from B-V $\sim$ 0.6 to B-V $\sim$ 1.0 but quite narrow in brightness.

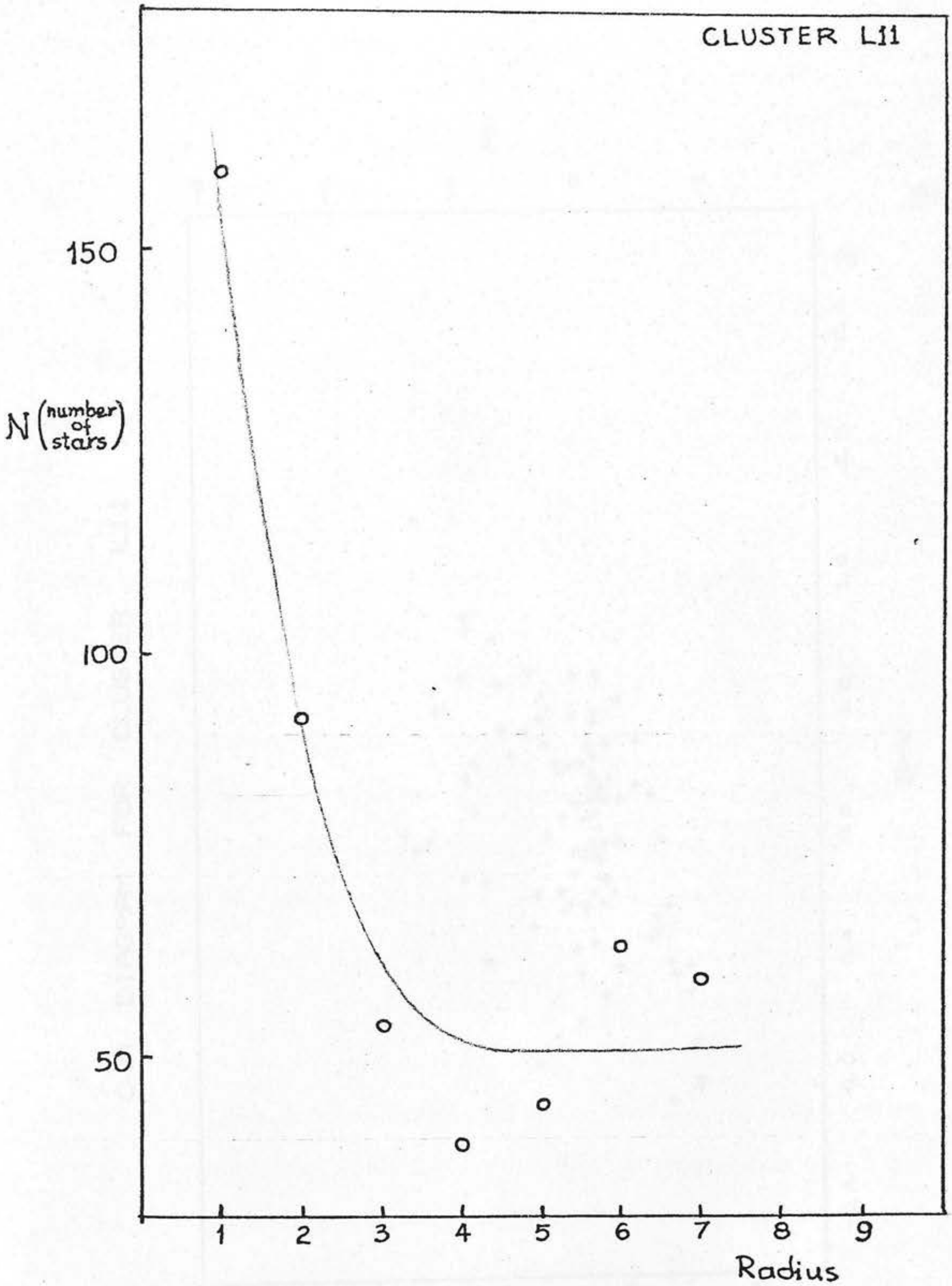

Fig. 33. Number of stars in circular regions of equal area and around the cluster L11. All stars down to $V \sim 21^m.0$ have been taken into account. The abcissa gives the number of each radius (r_o is the centre and $r_1 \sim 1'.2$ arc min).

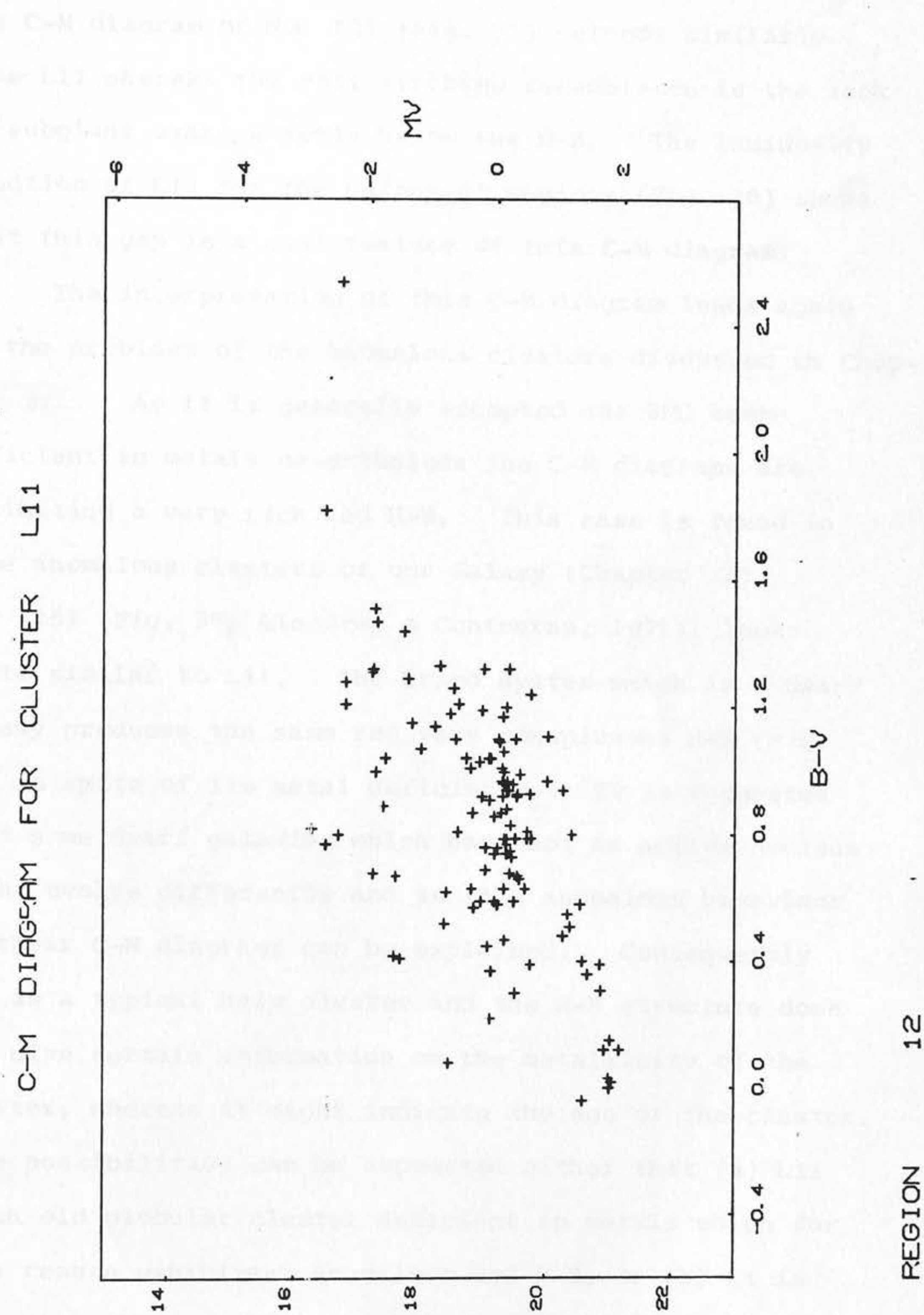
C-M DIAGRAM FOR CLUSTER L11
REGION 12
V
14
16
18
20
22
MV
-6
-4
-2
0
2
B-V
-0.4
0.0
0.4
0.8
1.2
1.6
2.0
2.4

Fig. 34.

The giant branch terminates at $M_V = -2\overset{m}{.}5$ and B-V = +1.60. The C-M diagram of NGC 121 (Fig. 31) extends similarly like L11 whereas the most striking resemblance is the lack of subgiant stars exactly below the H-B. The luminosity function of L11 for the different regions (Fig. 36) shows that this gap is a real feature of this C-M diagram.

The interpretation of this C-M diagram leads again to the problems of the anomalous clusters discussed in Chapter 2. As it is generally accepted the SMC seems deficient in metals nevertheless the C-M diagrams are exhibiting a very rich red H-B. This case is found in some anomalous clusters of our Galaxy (Chapter 2). NGC 1261 (Fig. 37, Alcaino & Contreras, 1971) looks quite similar to L11. The Draco system which is a dwarf galaxy produces the same red very conspicuous H-B (Fig. 35) in spite of its metal deficiency. It is suggested that some dwarf galaxies which have not an active nucleus might evolve differently and so this anomalous behaviour of their C-M diagrams can be explained. Consequently L11 is a typical halo cluster and the H-B structure does not give certain information on the metallicity of the cluster, whereas it might indicate the age of the cluster. Both possibilities can be supported either that (a) L11 is an old globular cluster deficient in metals which for some reason exhibitsan anomalous red H-B, or (b) it is a younger cluster which has been evolved differently because of the poor activity of the SMC nucleus.

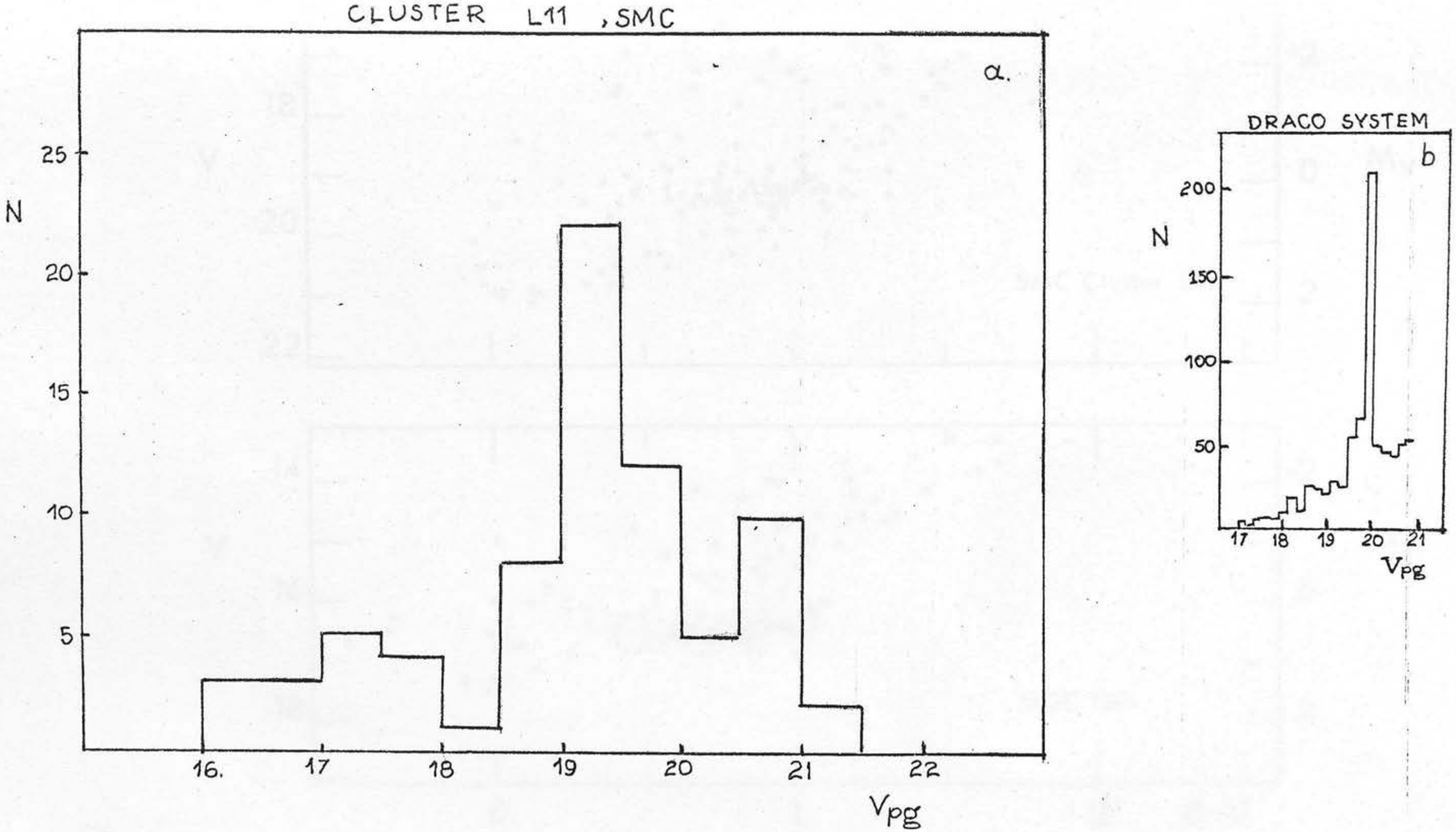

Fig. 36. a)Luminosity function in V for the SMC cluster L11.
b)Luminosity function in photovisual light of Draco system (after Baade & Swope, 1961).

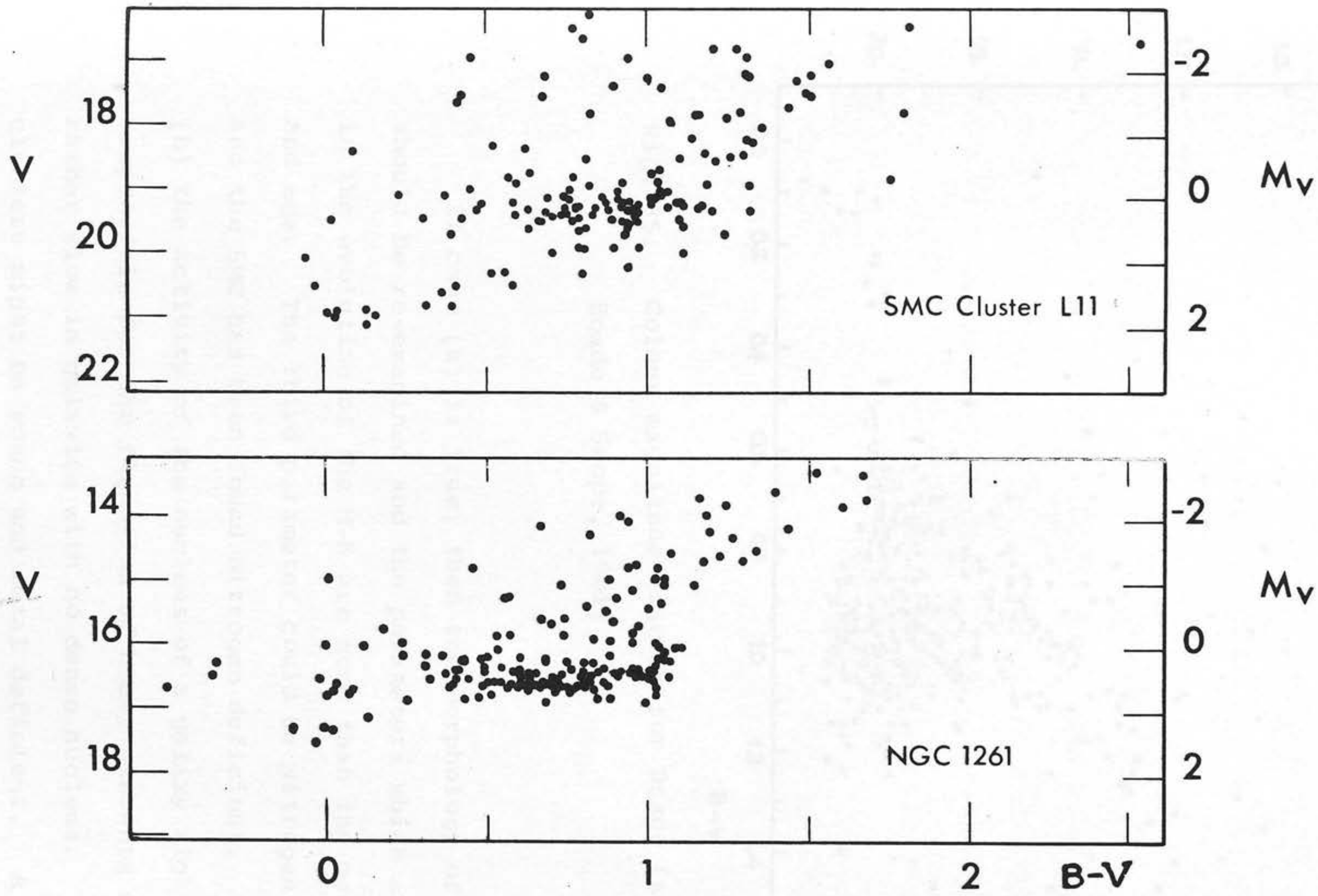

Fig. 37. Comparison of the C-M diagrams for the clusters L11 (SMC) and NGC 121 (Alcaino & Contreras, 1971).

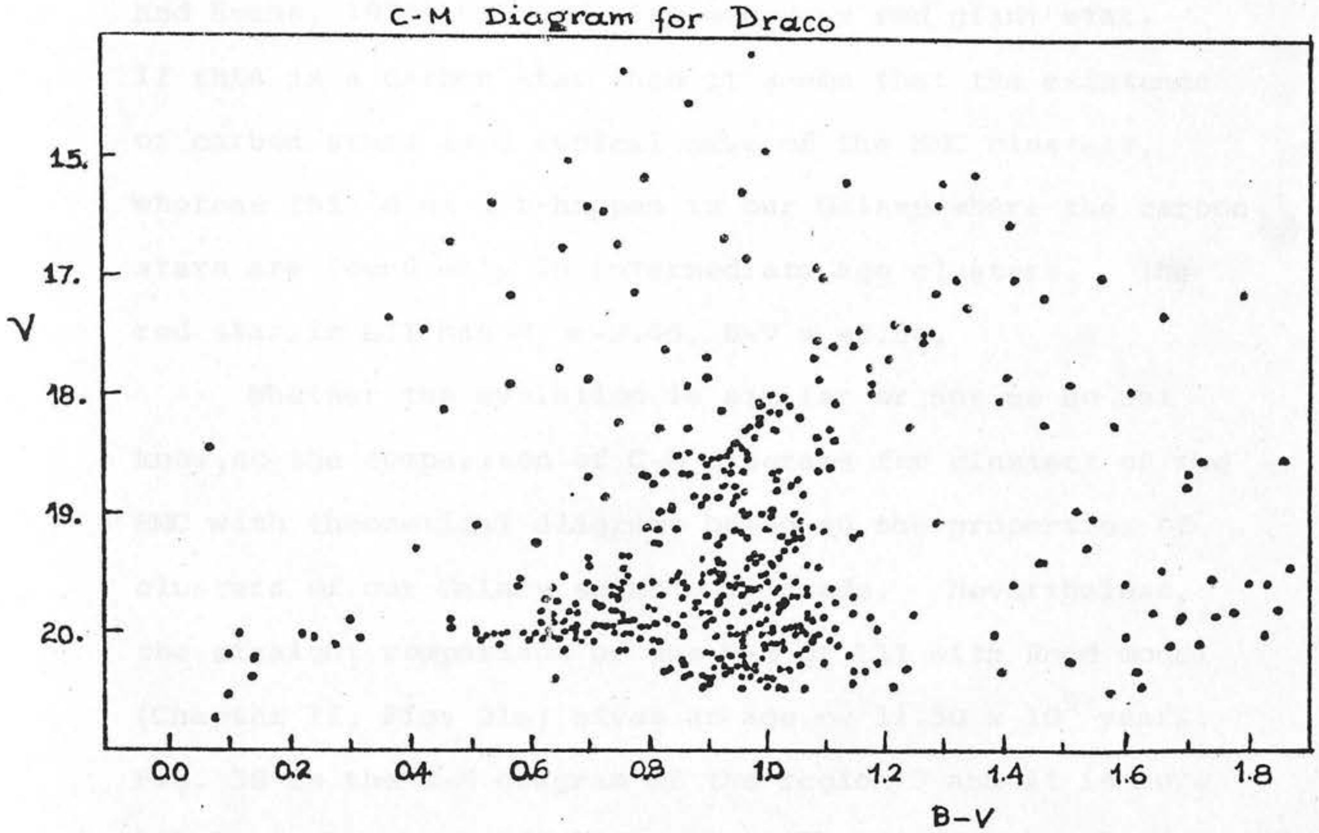

Fig. 35. Colour magnitude diagram for Draco (after Boade & Swope, 1961).

If case (a) is true, then the morphology of the H-B should be re-examined and the parameters which are involved in the evolution of the H-B are more than the metallicity and age. The third parameter could be Nitrogen abundance and the SMC has been found Nitrogen deficient. In case (b) the activity of the nucleus of a galaxy might be responsible for the formation of heavy elements which is rather slow in galaxies with no dense nucleus. So the clusters might be young and metal deficient. A fact supporting the idea of a younger age is the existence of carbon stars in the globular clusters of the SMC(Feast and Evans, 1973) L11 has also one very red giant star. If this is a carbon star then it seems that the existence of carbon stars is a typical case of the SMC clusters, whereas this does not happen in our Galaxy where the carbon stars are found only in intermediate age clusters. The red star in L11 has $M_V = -2.45$, $B-V = +2.54$.

Whether the evolution is similar or not we do not know, so the comparison of C-M diagrams for clusters of the SMC with theoretical diagrams based on the properties of clusters of our Galaxy seems very crude. Nevertheless, the straight comparison of the H-B of L11 with Rood model (Chapter II, Fig. 21a) gives an age $\sim 11.50 \times 10^9$ years. Fig. 38 is the C-M diagram of the region 3 and it is more likely to have many field stars. The diagram has less bright red giants but the H-B is still very conspicuous. So the star members of the cluster must be quite similar with the field stars. The field stars of this part of the SMC will be discussed later on as well. Fig. 39 illustrates the composite C-M diagram for all regions and stars measured. The main part still very prominent is the red H-B which is the most striking feature of this plot.

4.1.2. The cluster HW40

The second cluster of the SMC which is similar to L11 is HW40, one of the northern side, small and containing very faint stars. The most conspicuous feature of its C-M diagram is a red H-B like concentration of stars extending from $B-V = +0.45$ to $B-V = +1.0$. The red giants are very few and some main sequence stars are also

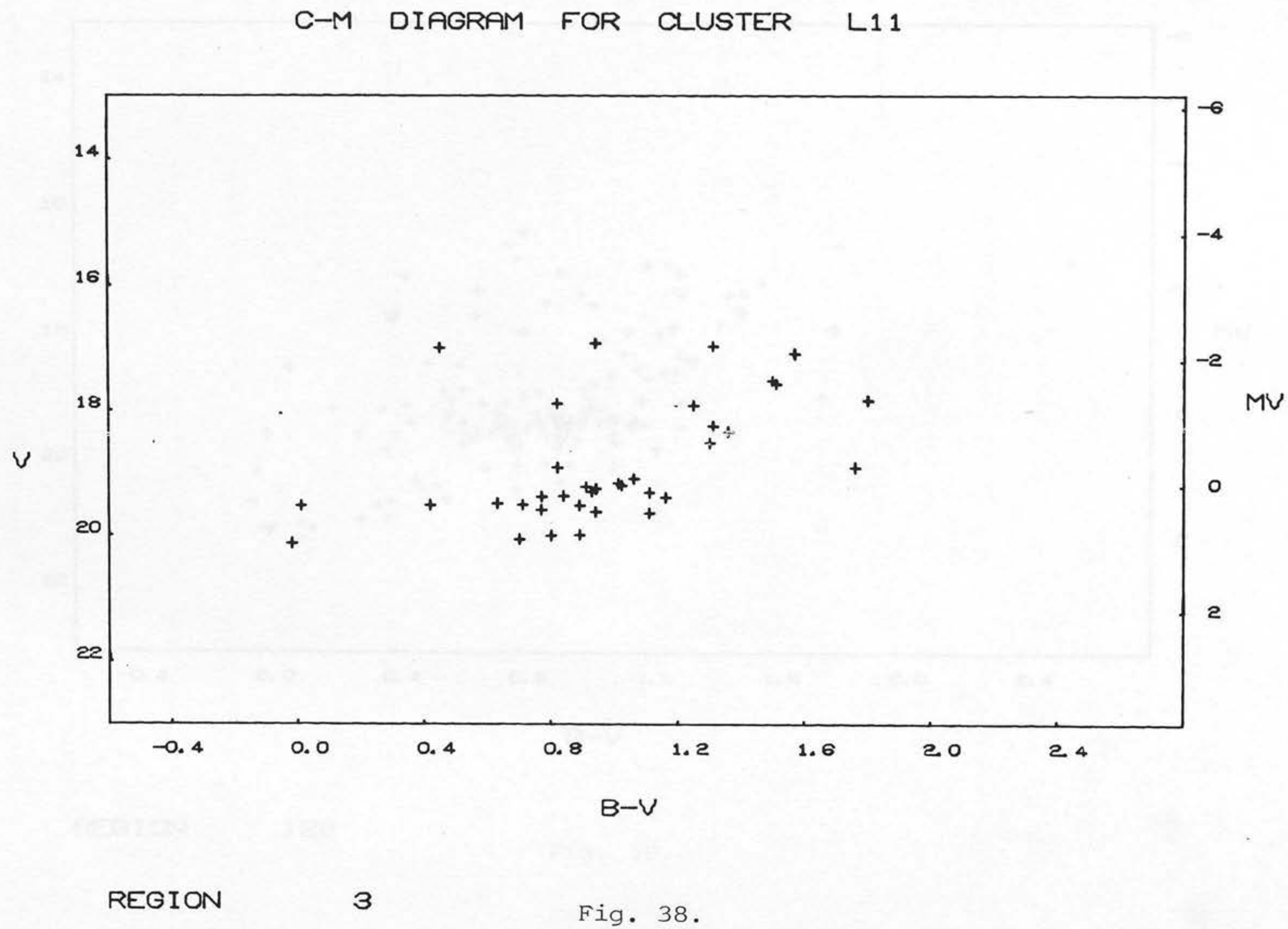
C-M DIAGRAM FOR CLUSTER L11
V
14
16
18
20
22
MV
-6
-4
-2
0
2
-0.4
0.0
0.4
0.8
1.2
1.6
2.0
2.4
B-V
REGION 3

Fig. 38.

C-M DIAGRAM FOR CLUSTER L11

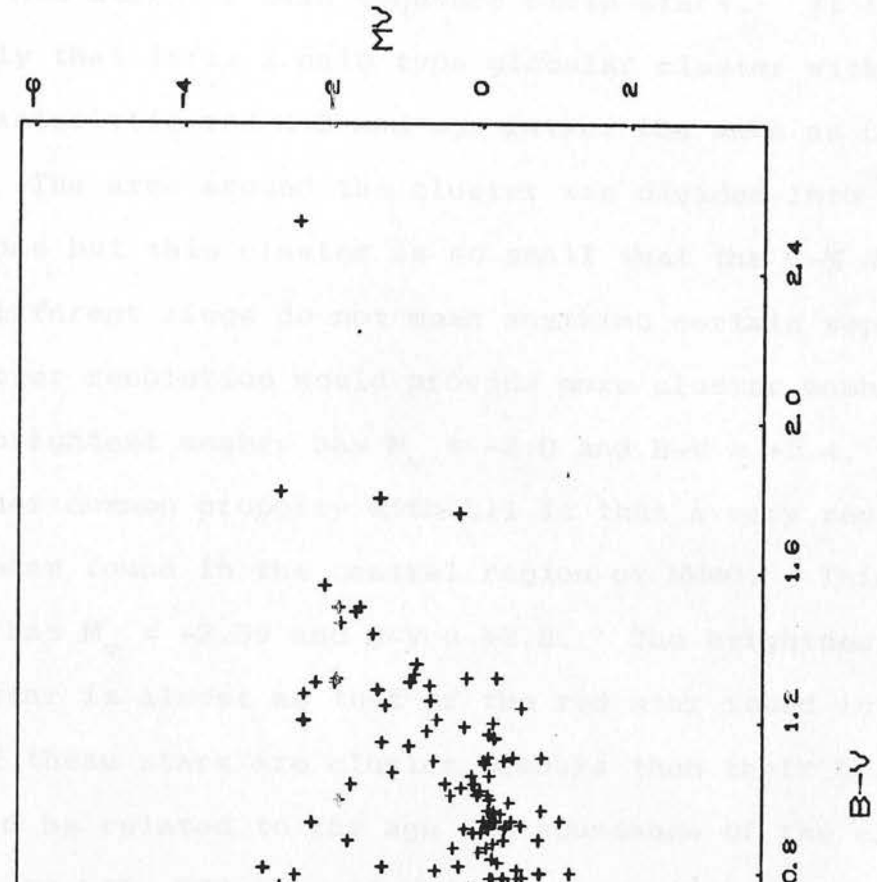

REGION 122

Fig. 39.

present (Fig. 40).

It is not certain whether some of the blue stars are blue H-B stars or main sequence field stars. It is more likely that it is a halo type globular cluster with a characteristic red H-B and age rather the same as L11.

The area around the cluster was divided into three regions but this cluster is so small that the C-M diagrams of different rings do not mean anything certain separately. A better resolution would provide more cluster members. The brightest member has M_V = -2.0 and B-V = +1.4. Another common property with L11 is that a very red star has been found in the central region of HW40. This red star has M_V = -2.59 and B-V = +2.8. The brightness of this red star is almost as that of the red star found in L11. So if these stars are cluster members then their brightness should be related to the age and abundance of the cluster.

So L11, NGC 121 and HW40 are a kind of globular halo type clusters of the SMC.

Fig. 41 illustrates the C-M diagram for the outer region which has diameter about ~1.5 arc min. The stars are very few because the crowding made difficult the detection of faint stars. In Fig. 42 all stars are present. They must be field stars and some cluster members too. The predominent stellar content of this region seems to be population II stars, of halo type, like in L11 or NGC 121. The composite C-M diagram for the outer regions of these three clusters (Fig. 43) show these characteristics discussed in L11 or NGC 121.

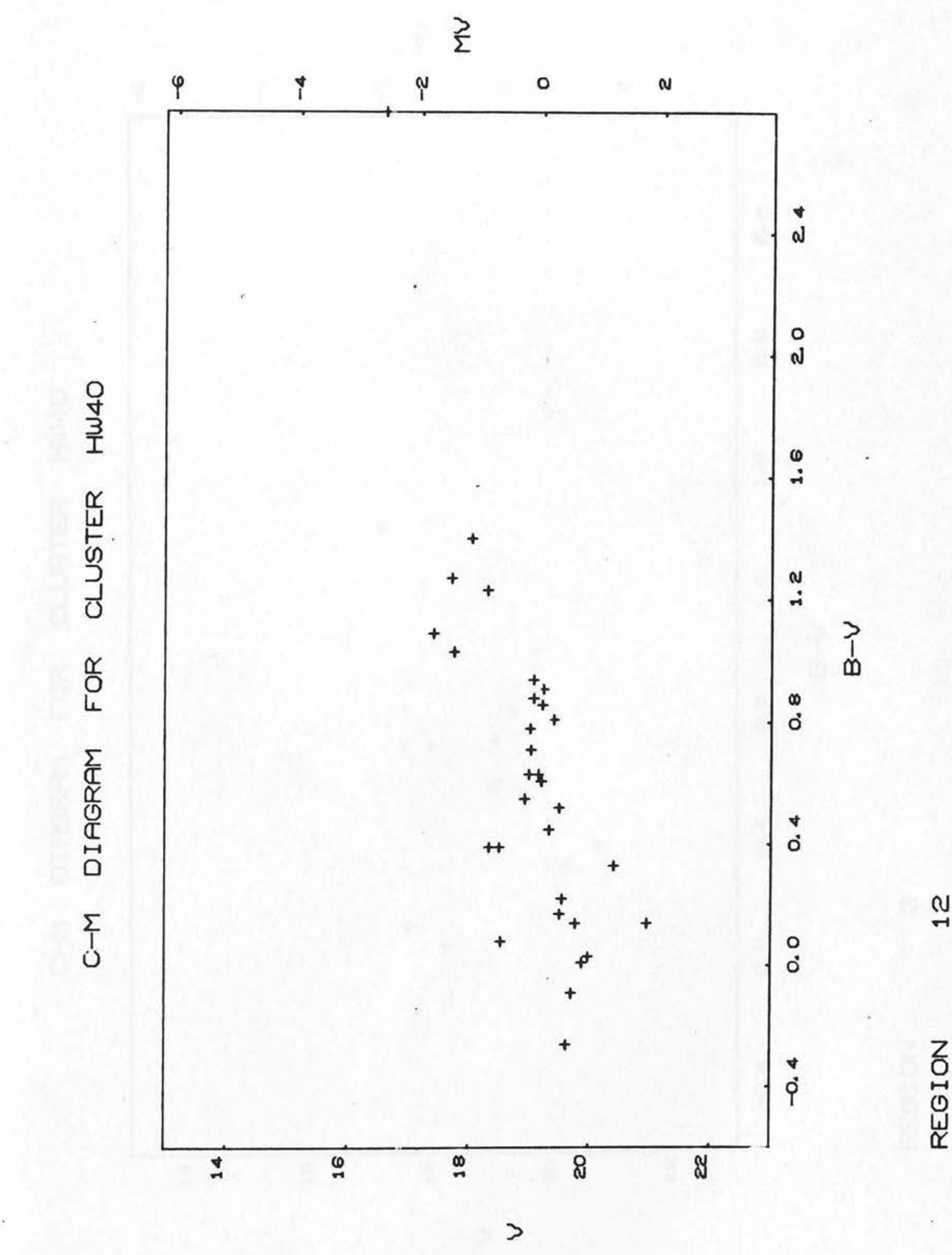
C–M DIAGRAM FOR CLUSTER HW40
REGION 12
B–V
V
MV
-0.4 0.0 0.4 0.8 1.2 1.6 2.0 2.4
14 16 18 20 22
-6 -4 -2 0 2

Fig. 40.

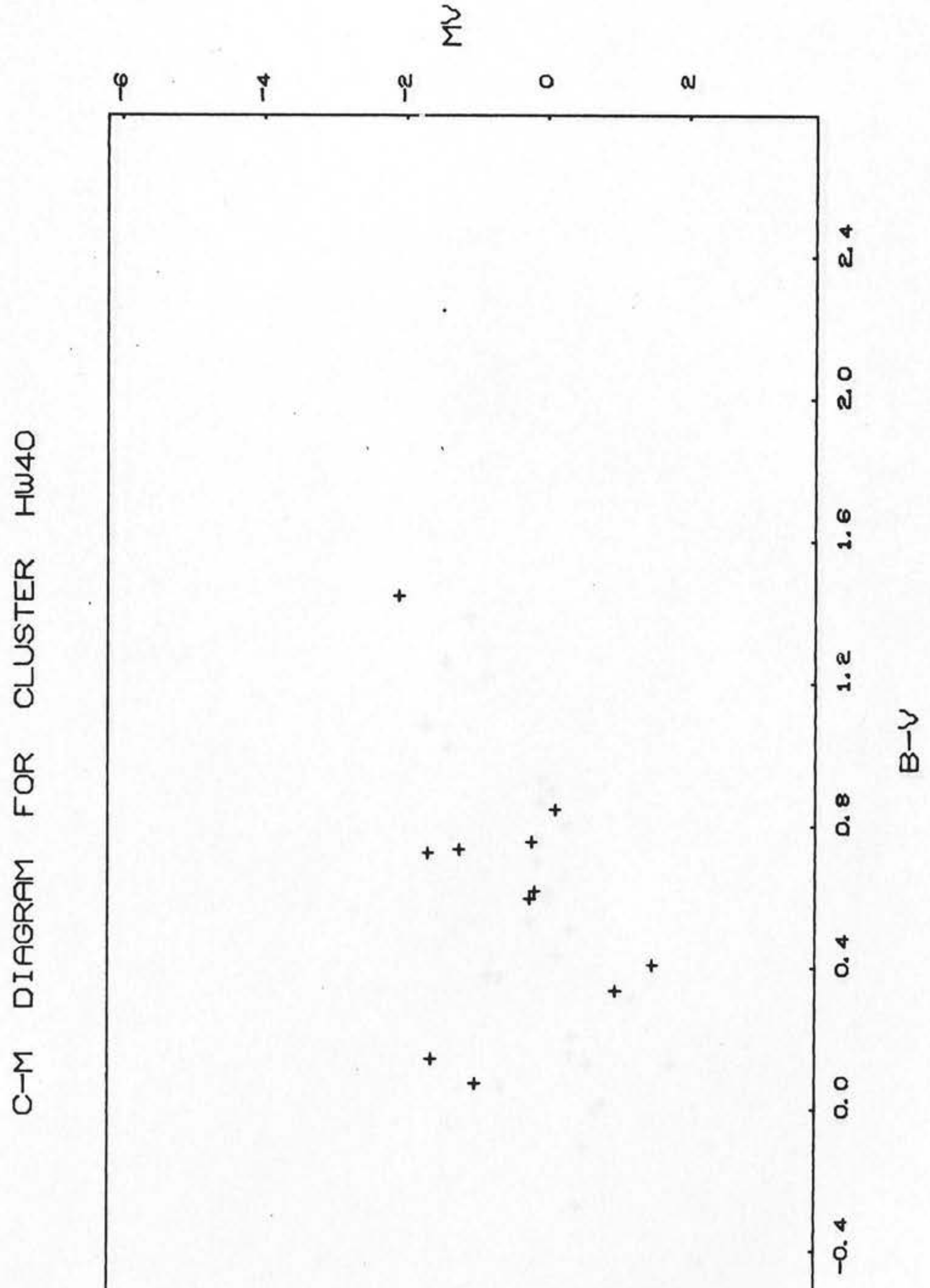
C-M DIAGRAM FOR CLUSTER HW40
REGION 3
B-V
V
MV
-0.4
0.0
0.4
0.8
1.2
1.6
2.0
2.4
14
16
18
20
22
-6
-4
-2
0
2

Fig. 41.

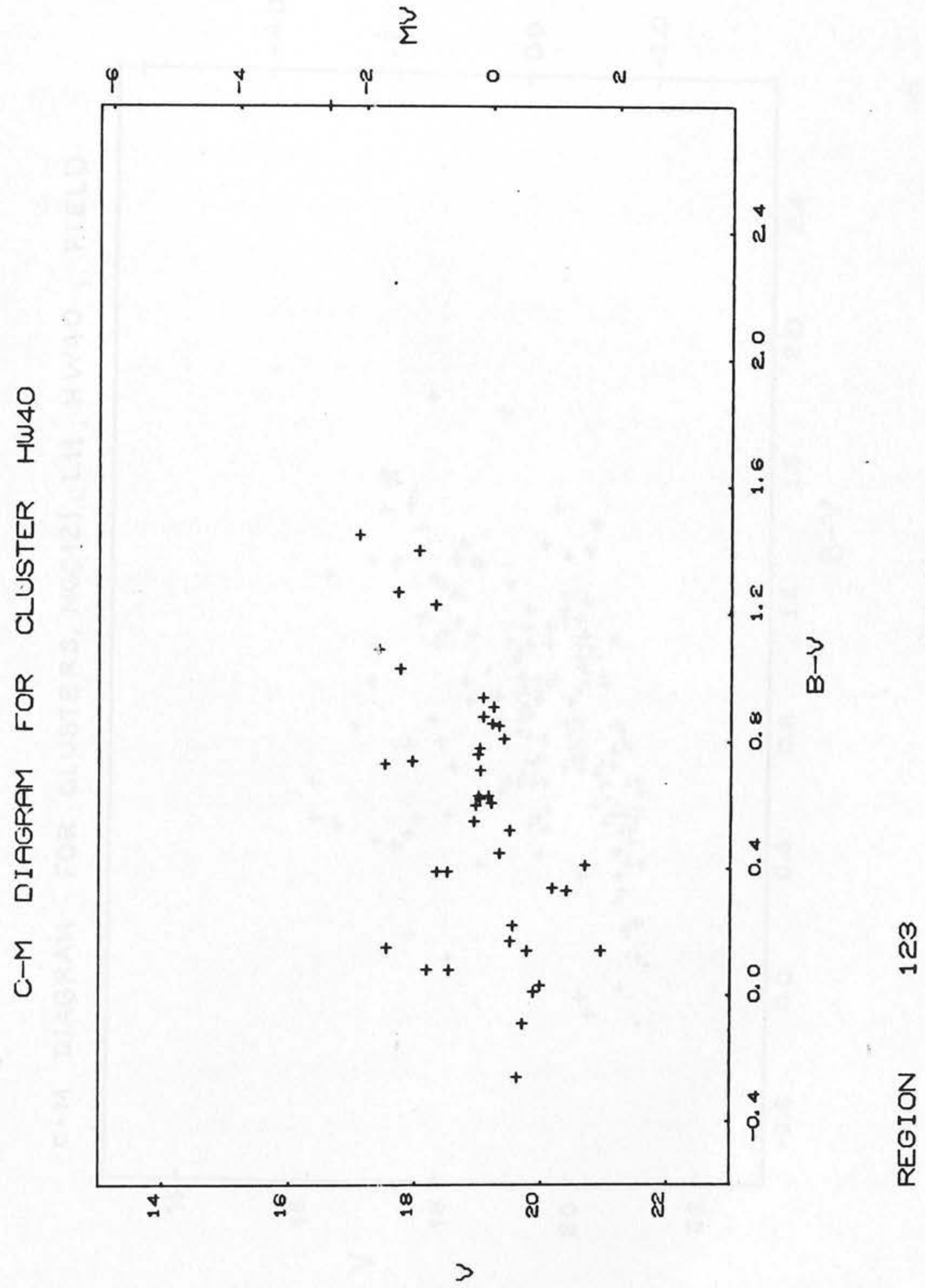
C-M DIAGRAM FOR CLUSTER HW40
V
14
16
18
20
22
MV
-6
-4
-2
0
2
B-V
-0.4
0.0
0.4
0.8
1.2
1.6
2.0
2.4
REGION 123

Fig. 42.

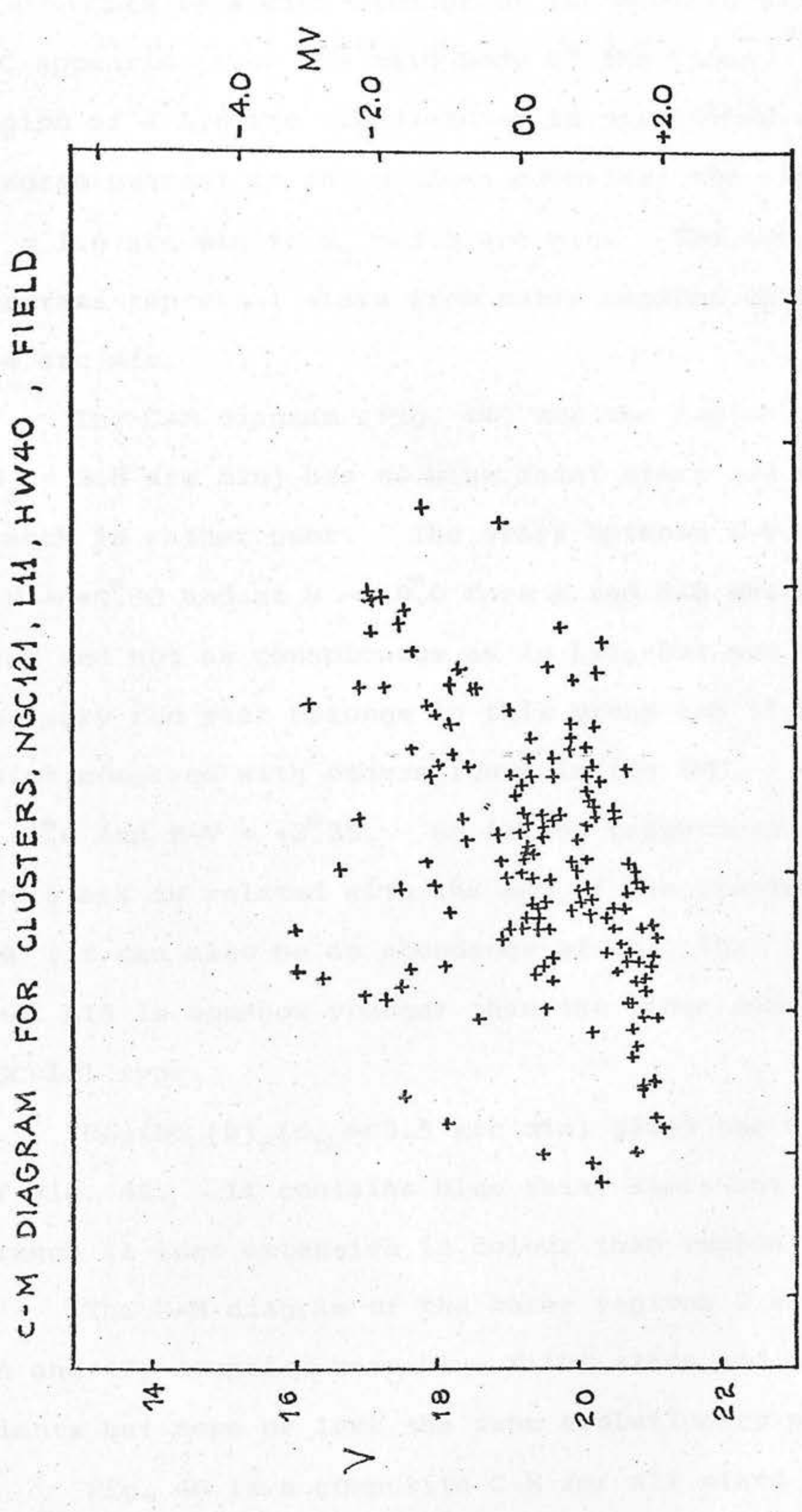
C-M DIAGRAM FOR CLUSTERS, NGC121, L11, HW40 , FIELD
MV
-4.0
-2.0
0.0
+2.0
V
14
16
18
20
22
B-V
-0.4
0.0
0.4
0.8
1.2
1.6
2.0
2.4

Fig. 43.

4.1.3. The cluster L15

L15 is a rich cluster of the western side of the SMC appearing near the main body of the Cloud. A central region of a 1.6 arc min diameter is unresolved so the C-M diagram nearest to the nucleus comprises one ring between d_1 = 1.6 arc min to $d_b \sim$ 3.5 arc min. The two more C-M diagrams represent stars from outer regions up to $d_{out} \sim$ 8.4 arc min.

The C-M diagram (Fig. 44) for the region (a) (d_a = 2.8 arc min) has no blue faint stars and the giant branch is rather poor. The stars between B-V ~ 0.42 and B-V ~ +0^m.80 and at V ~ 19^m.0 form a red H-B which is rather weak and not as conspicuous as in L11, but not negligible. One very red star belongs to this group and it is very faint compared with others found in the SMC. It has M_V = -1^m.0 and B-V = +2^m.25. So if the brightness of these red stars is related with the age of the clusters in the SMC (it can also be an abundance effect) then one could say that L15 is somehow younger than the other clusters of NGC 121 type.

Region (b), ($d_b \sim$ 3.5 arc min) gives the C-M diagram of Fig. 45. It contains blue faint stars but the giant branch is less extensive in colour than region (a).

The C-M diagram of the outer regions 2 and 3 (Figs. 46 and 47) comprises more blue faint stars and less red giants but more or less the same evolutionary pattern.

Fig. 48 is a composite C-M for all stars measured in the cluster L15 and the surrounding field. The main

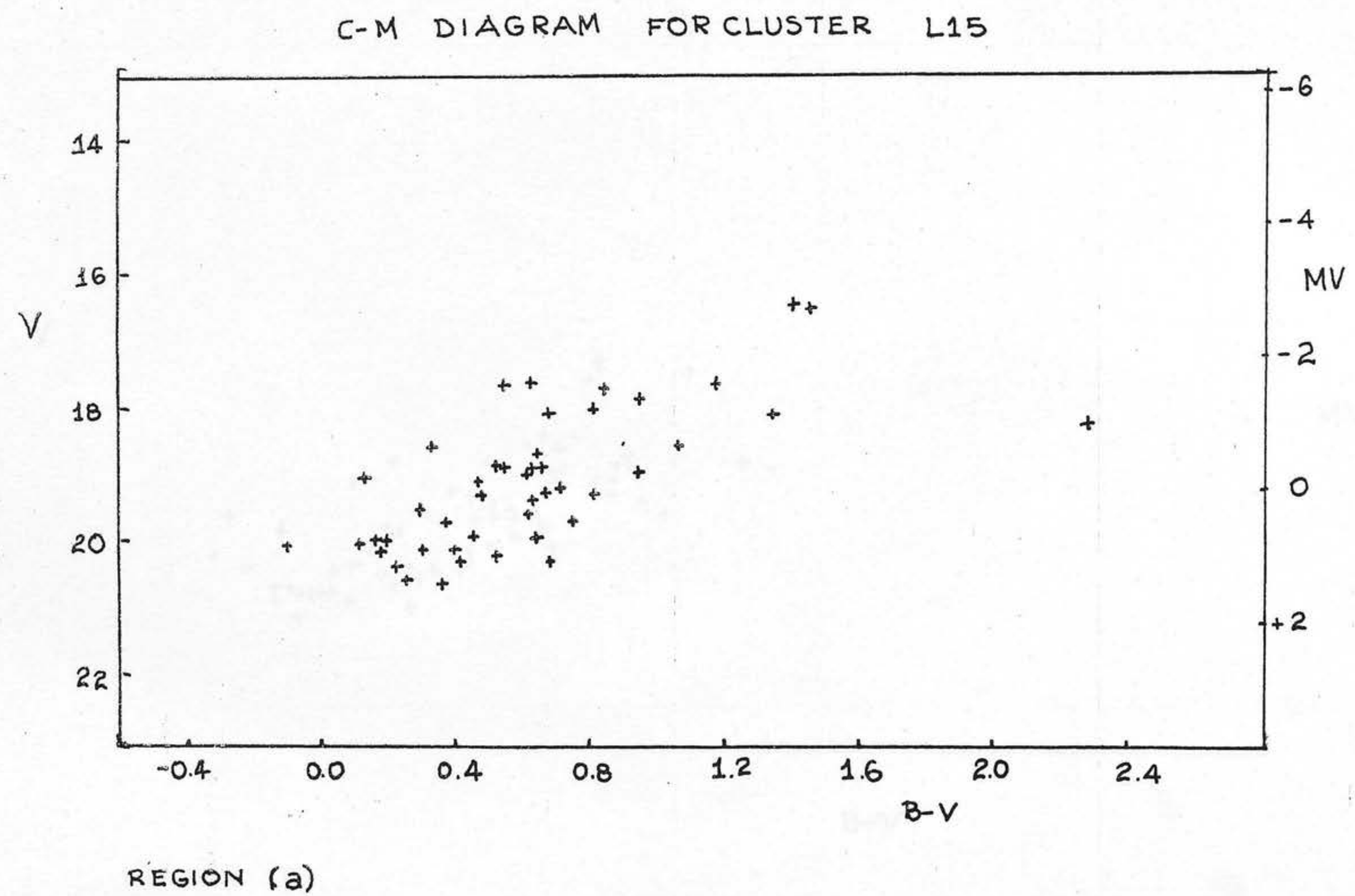
C-M DIAGRAM FOR CLUSTER L15
V
14
16
18
20
22
MV
-6
-4
-2
0
+2
-0.4
0.0
0.4
0.8
1.2
1.6
2.0
2.4
B-V
REGION (a)

Fig. 44.

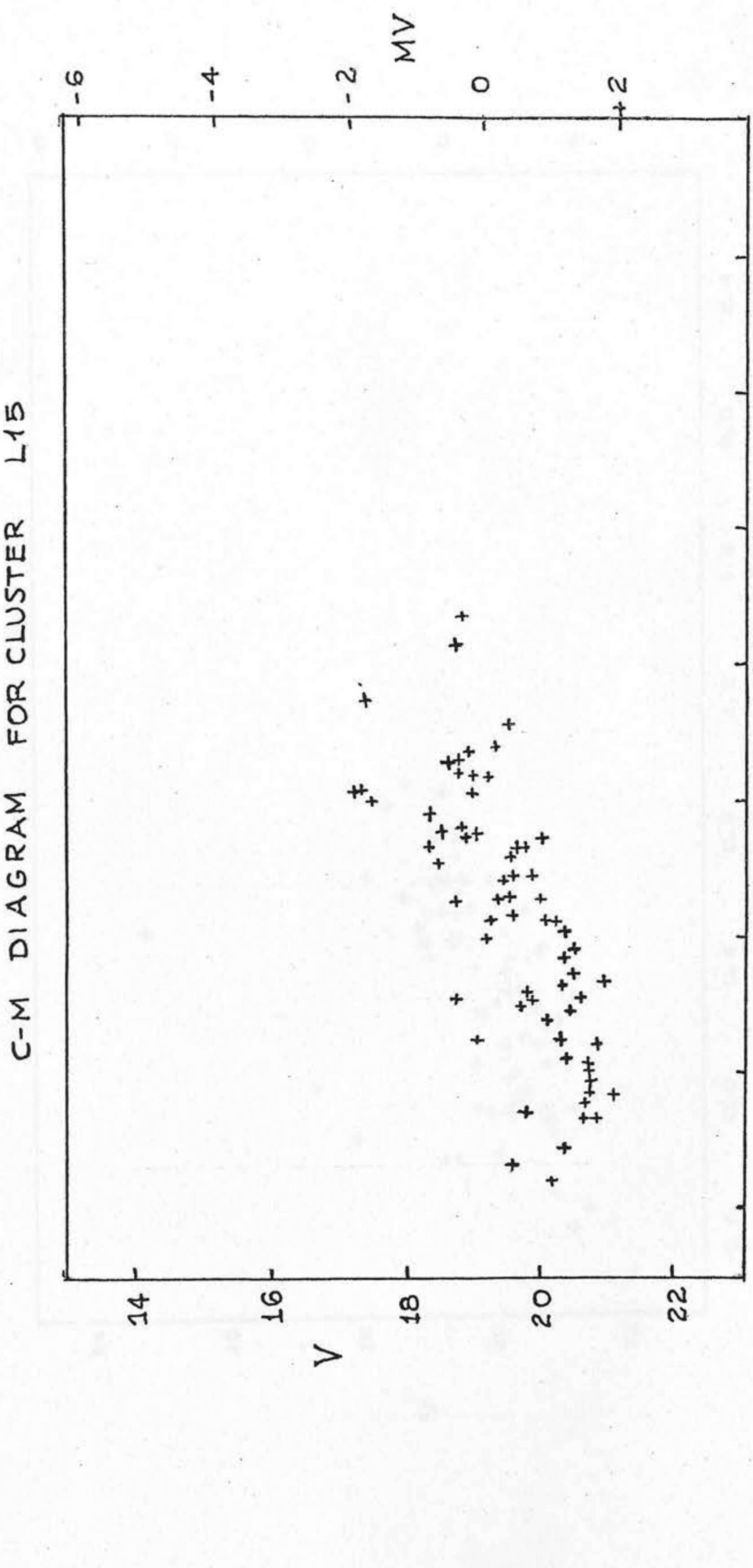
C-M DIAGRAM FOR CLUSTER L15
REGION (b)
V
14
16
18
20
22
MV
-6
-4
-2
0
2
B-V
-0.4
0.0
0.4
0.8
1.2
1.6
2.0
2.4

Fig. 45.

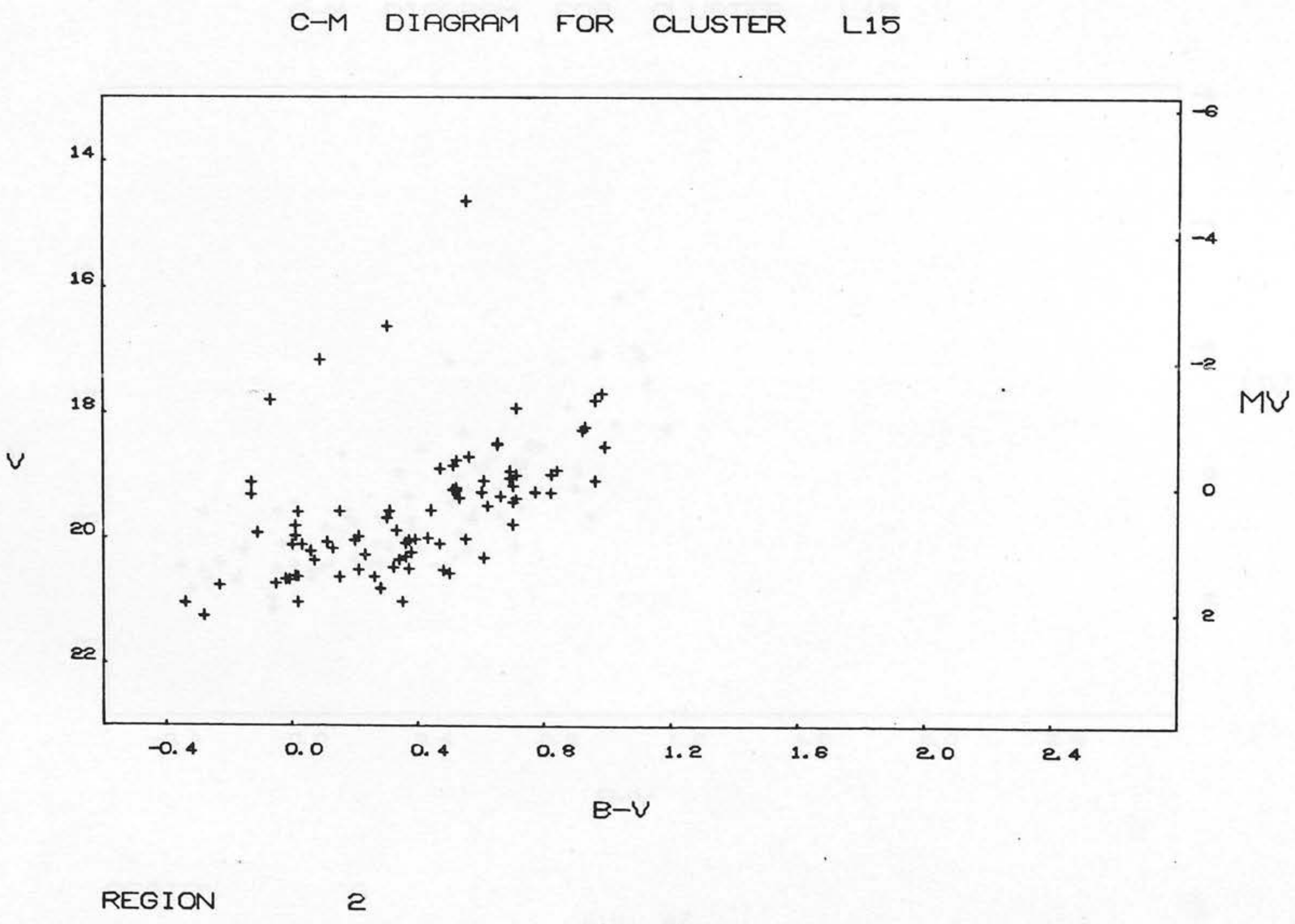
C–M DIAGRAM FOR CLUSTER L15
14
16
18
20
22
V
-6
-4
-2
0
2
MV
-0.4
0.0
0.4
0.8
1.2
1.6
2.0
2.4
B–V
REGION 2

Fig. 46.

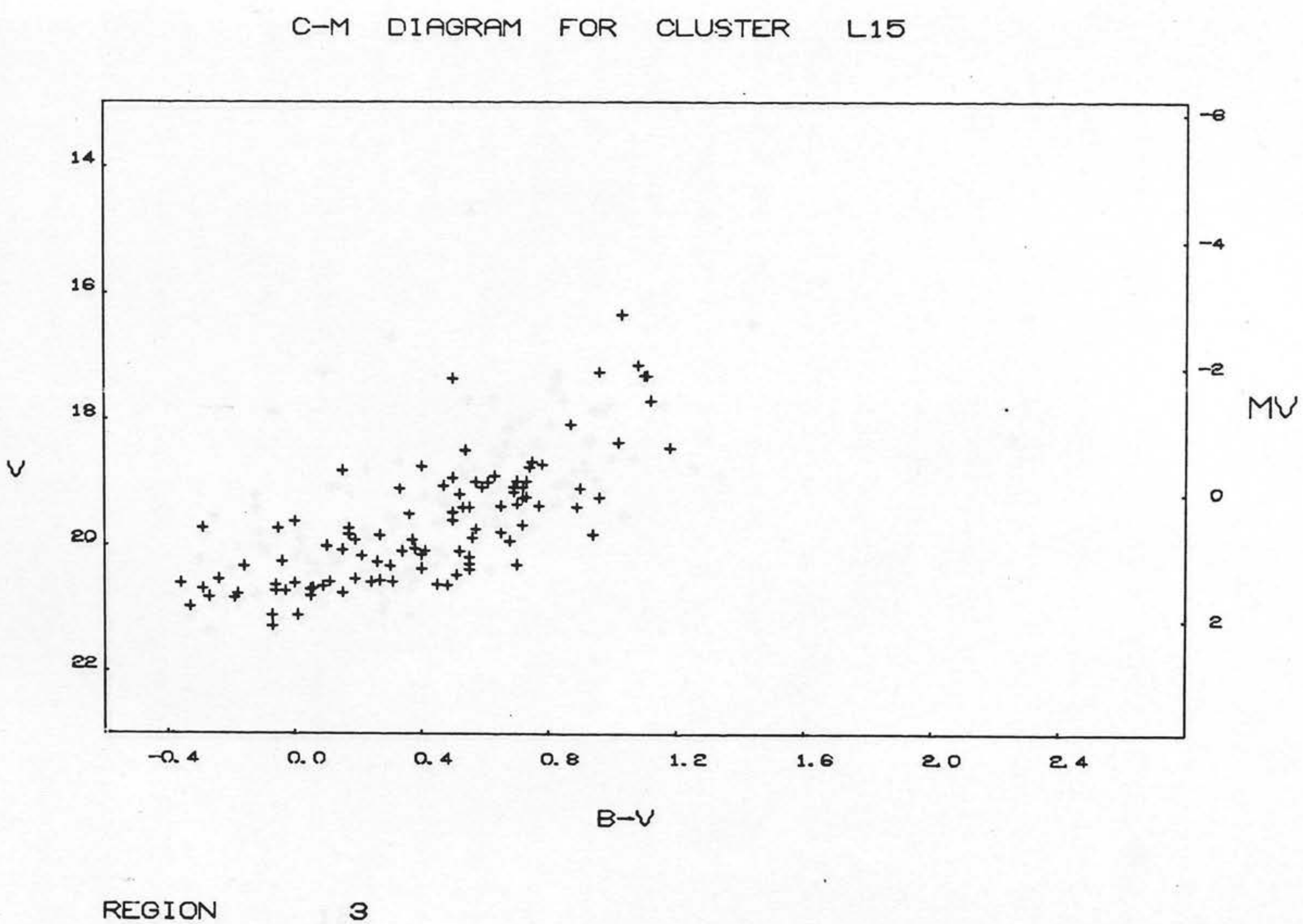
C–M DIAGRAM FOR CLUSTER L15
V
14
16
18
20
22
MV
-6
-4
-2
0
2
-0.4
0.0
0.4
0.8
1.2
1.6
2.0
2.4
B–V
REGION 3

Fig. 47.

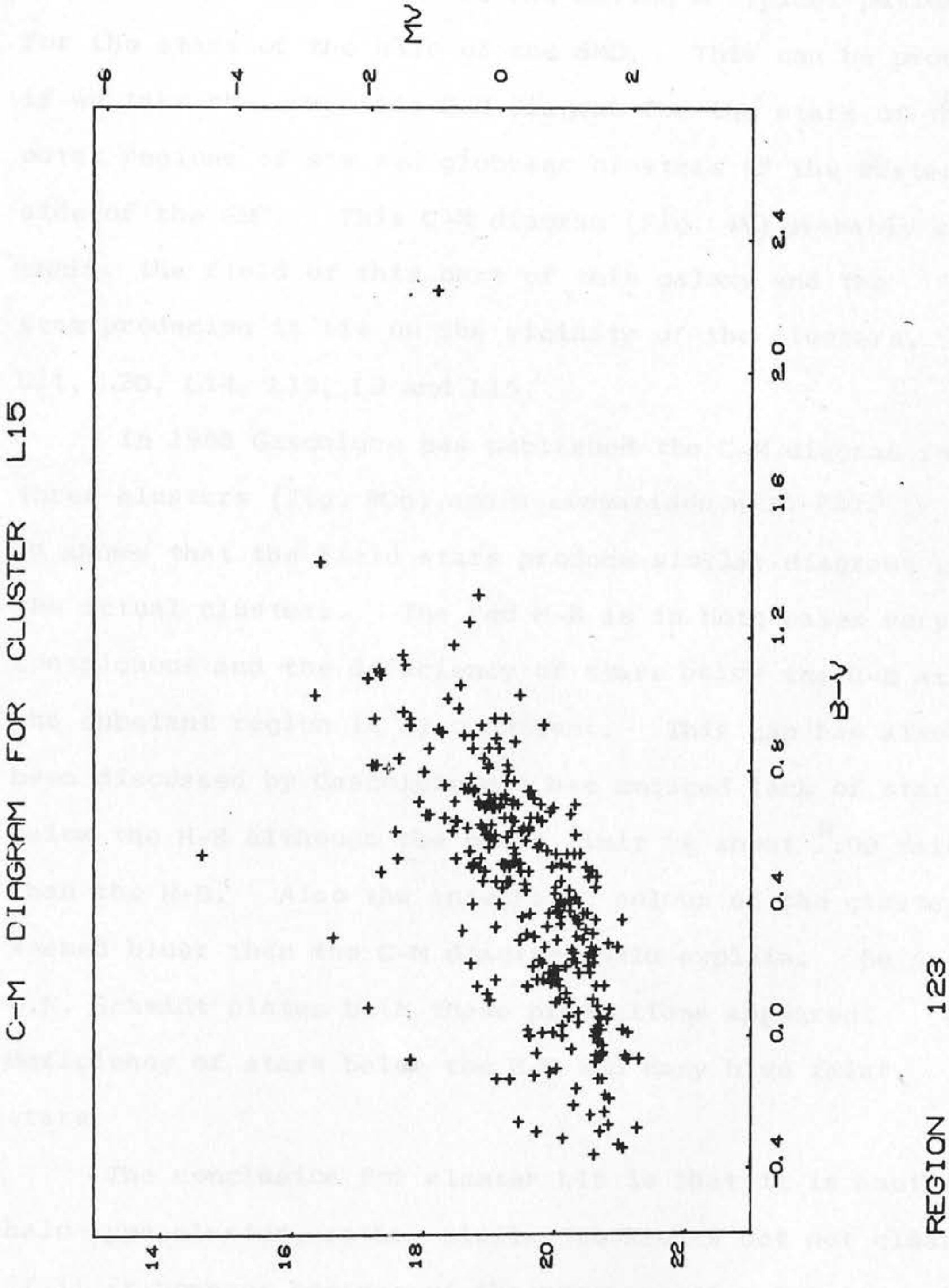
C-M DIAGRAM FOR CLUSTER L15
REGION 123
V
MV
B-V
14
16
18
20
22
-6
-4
-2
0
2
-0.4
0.0
0.4
0.8
1.2
1.6
2.0
2.4

Fig. 48.

difficulty has always been the contamination of cluster members with field stars. So in C-M diagrams like Fig. 48 it is more likely that we are having a typical pattern for the stars of the halo of the SMC. This can be proved if we take the composite C-M diagram for the stars of the outer regions of six red globular clusters of the western side of the SMC. This C-M diagram (Fig. 49) probably represents the field of this part of this galaxy and the stars producing it lie on the vicinity of the clusters, L11, L20, L14, L13, L3 and L15.

In 1966 Gascoigne has published the C-M diagram for three clusters (Fig. 30g) and a comparison with Fig. 49 shows that the field stars produce similar diagrams to the actual clusters. The red H-B is in both cases very conspicuous and the deficiency of stars below the H-B at the subgiant region is also evident. This gap has also been discussed by Gascoigne who has noticed lack of stars below the H-B although the plate limit is about $1^{m}.00$ fainter than the H-B. Also the integrated colour of the clusters seemed bluer than the C-M diagram would explain. So in the U.K. Schmidt plates both these predictions appeared: deficiency of stars below the H-B and many blue faint stars.

The conclusion for cluster L15 is that it is another halo type cluster, rather similar to Kron 3 but not clear if it is younger because of the presence of a fainter red star and the weaker red H-B.

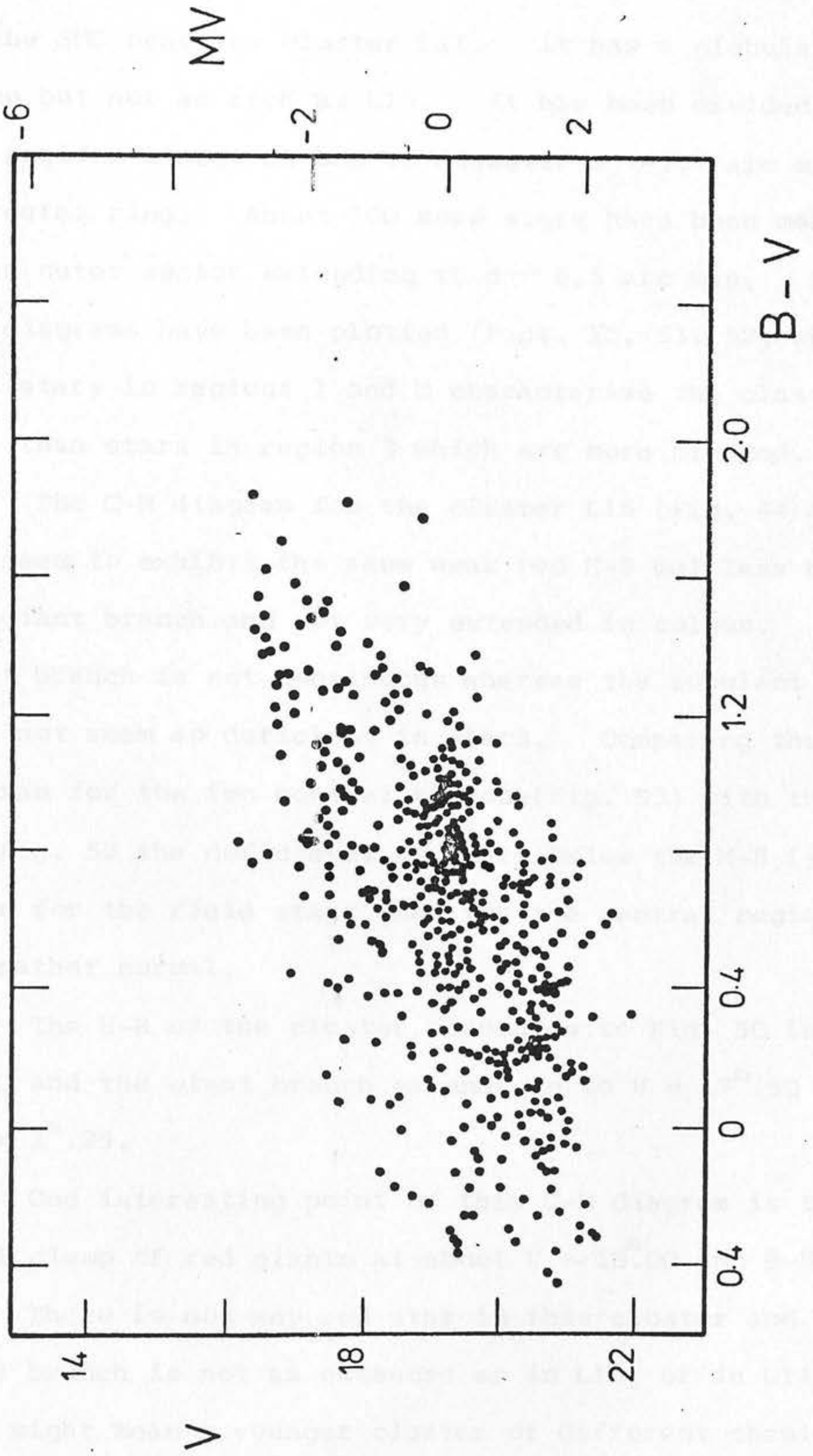

Fig. 49. C-M diagram of the western field of the SMC.

4.1.4. <u>The cluster L14</u>

Cluster L14 is another cluster of the western side of the SMC near the cluster L11. It has a globular like shape but not as rich as L15. It has been divided into two regions a central one of diameter $d_c \sim 1.7$ arc min and one outer ring. About 100 more stars have been measured in an outer sector extending to $d \sim 5.5$ arc min. So three C-M diagrams have been plotted (Figs. 50, 51, 52) which show that stars in regions 1 and 2 characterise the cluster much more than stars in region 3 which are more blended.

The C-M diagram for the cluster L15 (Fig. 44) and L14 (Fig. 50) seem to exhibit the same weak red H-B but less bright red giant branch and not very extended in colour. The giant branch is not continuous whereas the subgiant region does not seem so deficient in stars. Comparing the C-M diagram for the two central regions (Fig. 53) with that of the Fig. 52 the deficiency of stars below the H-B is more clear for the field stars than for the central regions which are rather normal.

The H-B of the cluster according to Fig. 50 is at $V \sim 19^m.50$ and the giant branch extends up to $V = 17^m.50$ and $B-V = 1^m.25$.

One interesting point of this C-M diagram is the small clump of red giants at about $V \sim 18^m.00$ and $B-V \sim 0^m.95$.

There is not any red star in this cluster and the giant branch is not as extended as in L15, or in L11. This might mean a younger cluster or different chemical composition or just a random statistical effect.

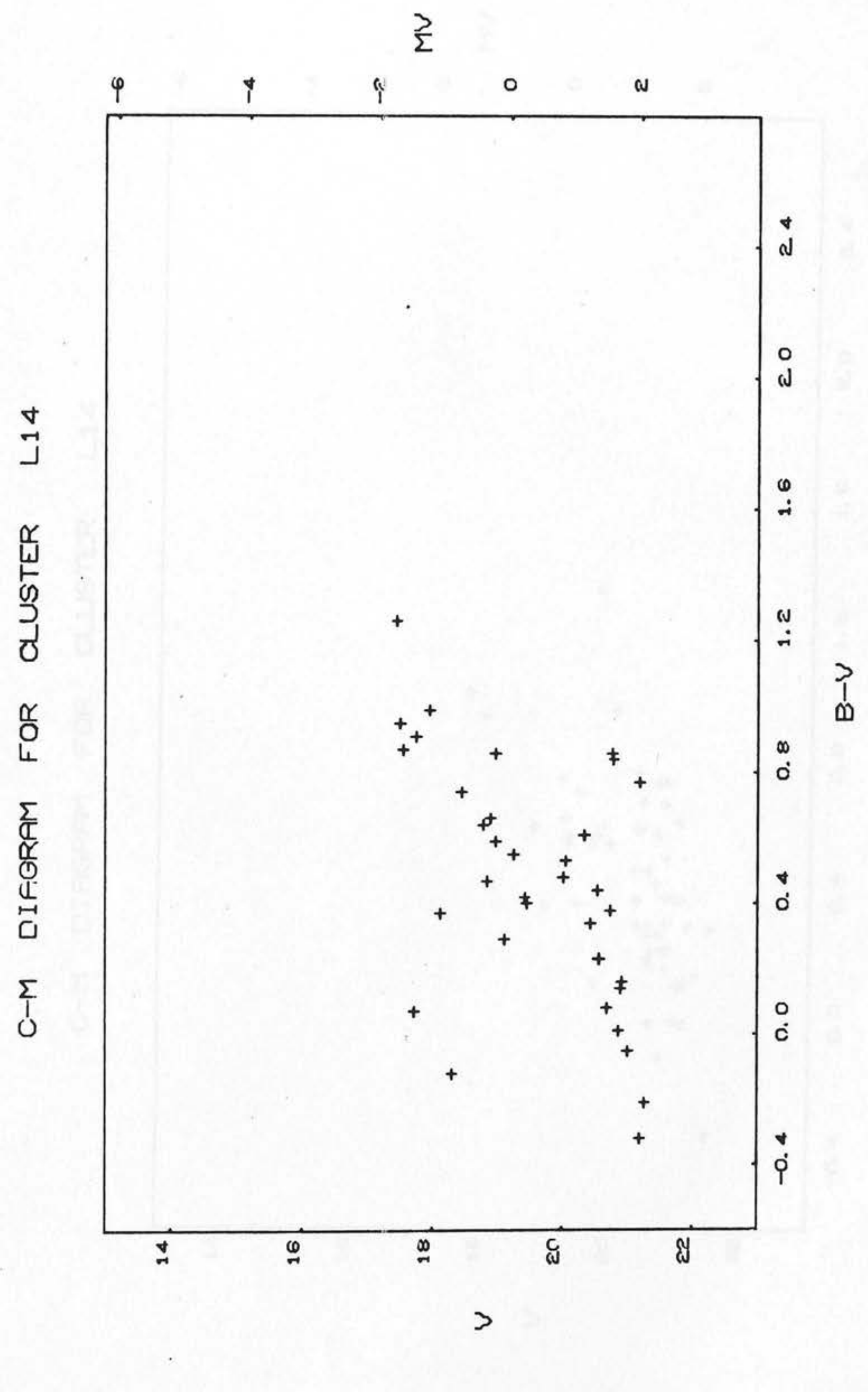
C-M DIAGRAM FOR CLUSTER L14
REGION 1
V
MV
B-V
14
16
18
20
22
-6
-4
-2
0
2
-0.4
0.0
0.4
0.8
1.2
1.6
2.0
2.4

Fig. 50.

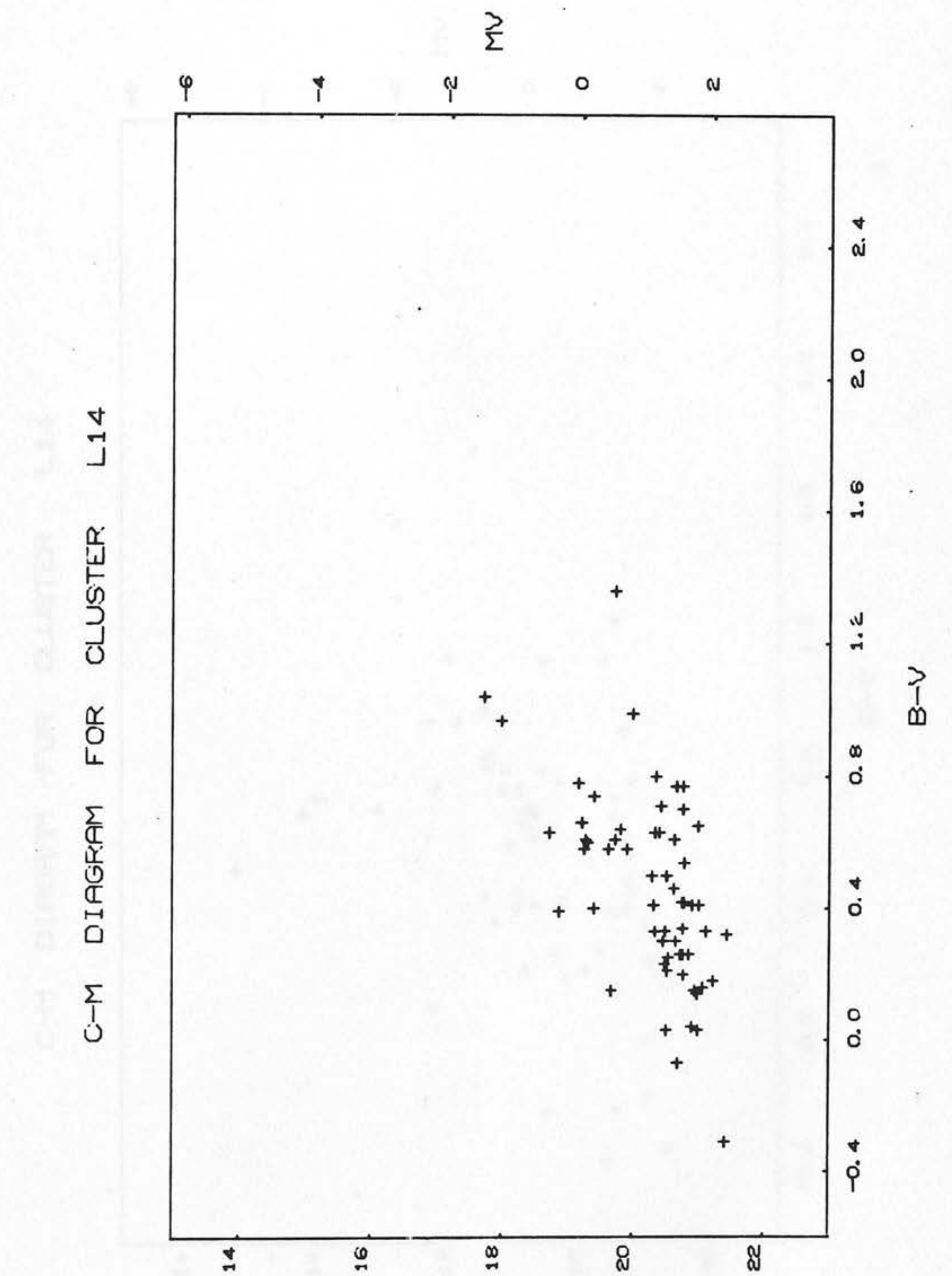
C-M DIAGRAM FOR CLUSTER L14
REGION 2
V
MV
B-V
14
16
18
20
22
-6
-4
-2
0
2
-0.4
0.0
0.4
0.8
1.2
1.6
2.0
2.4

Fig. 51.

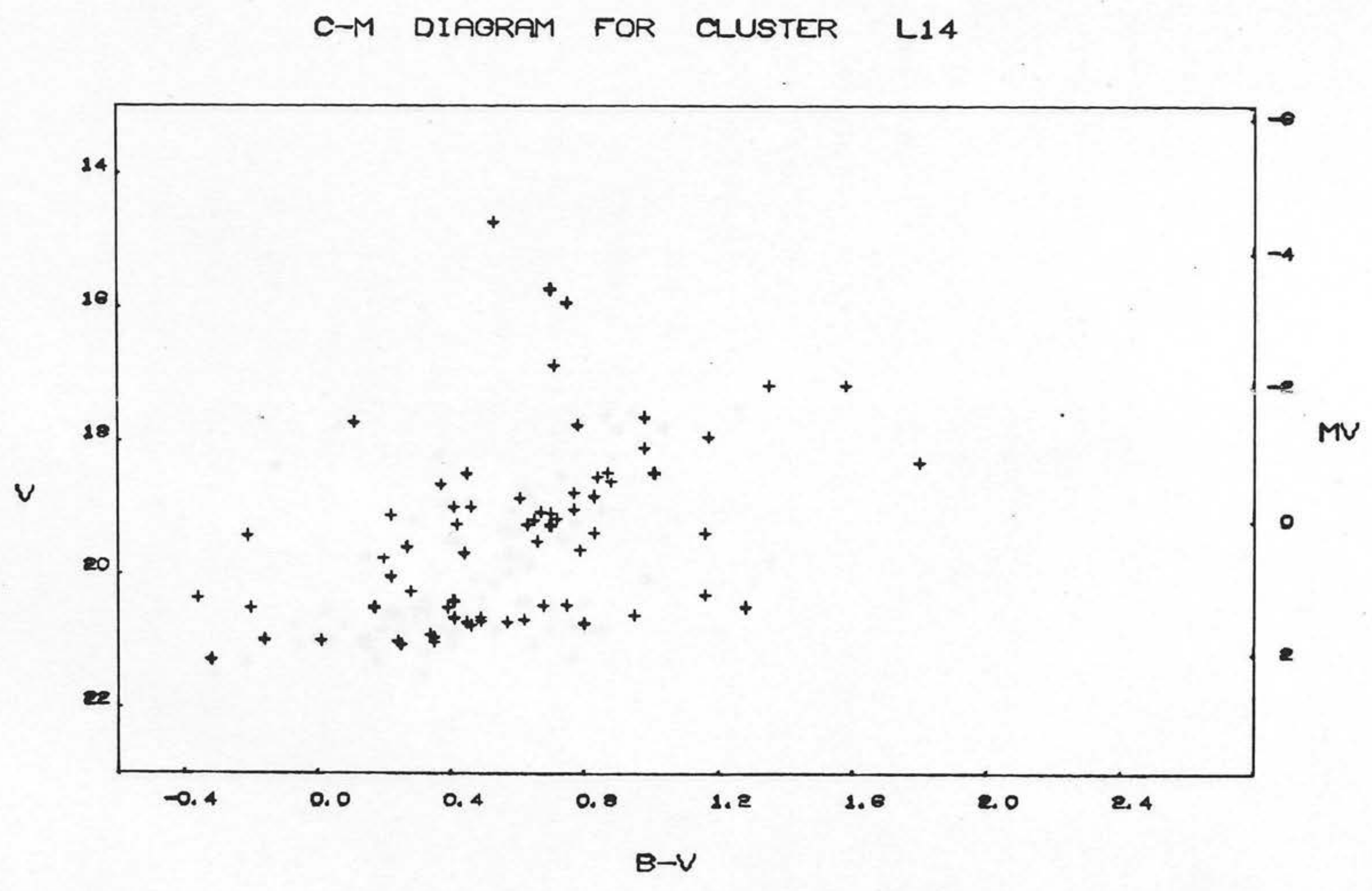

REGION 3

Fig. 52.

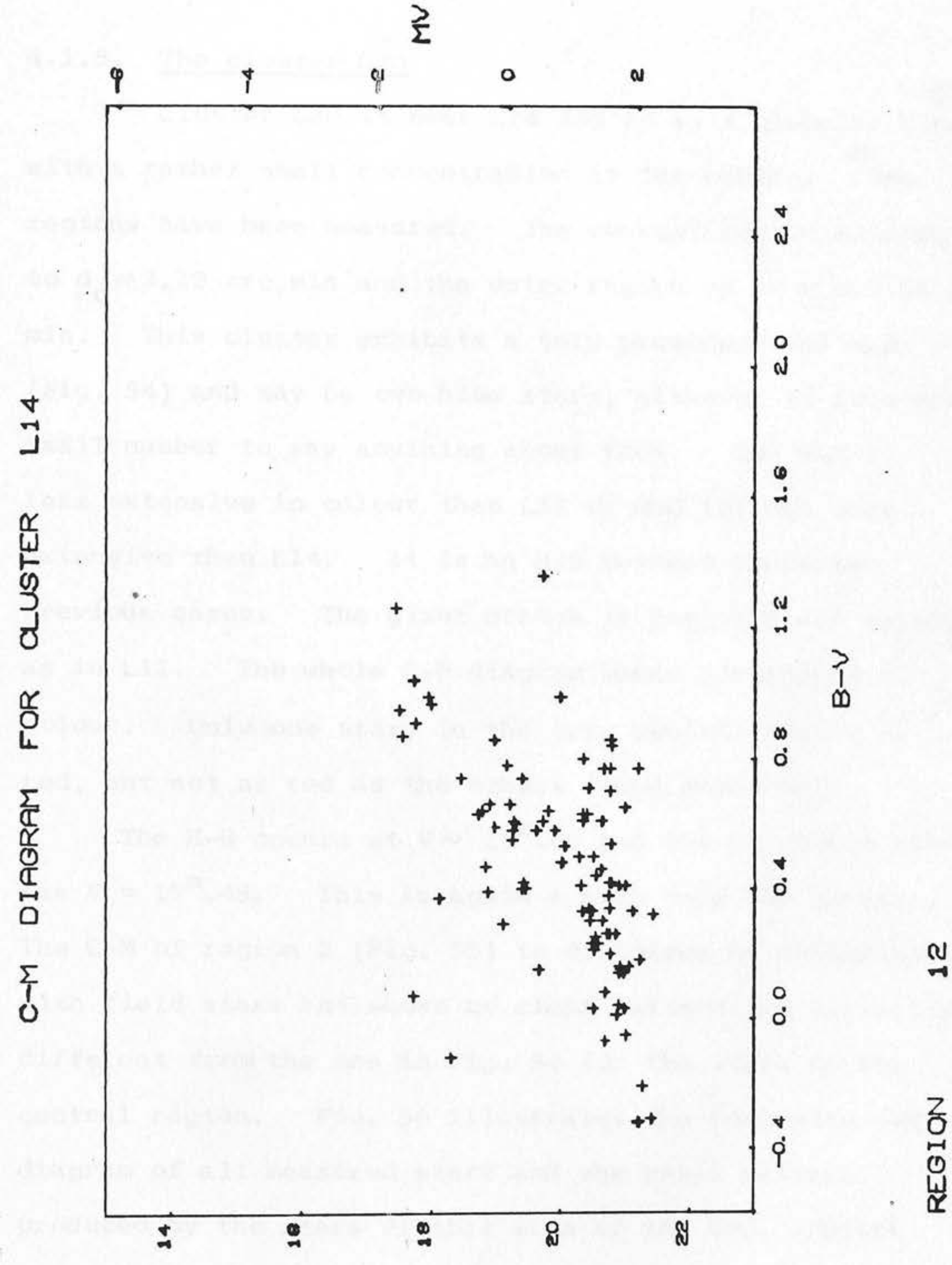
C-M DIAGRAM FOR CLUSTER L14
REGION 12
MV
-6
-4
-2
0
2
V
14
16
18
20
22
B-V
-0.4
0.0
0.4
0.8
1.2
1.6
2.0
2.4

Fig. 53.

The field's (Fig. 52) C-M diagram has a more extended and redder giant branch that could indicate an age difference between the cluster and the field stars.

4.1.5. <u>The cluster L20</u>

Cluster L20 is near L14 and it is a globular cluster with a rather small concentration in the centre. Two regions have been measured. The central region extends up to $d_c \sim 2.12$ arc min and the outer region up to $d_c \sim 3.06$ arc min. This cluster exhibits a very prominent red H-B (Fig. 54) and may be two blue stars, although it is a very small number to say anything about them. The H-B is less extensive in colour than L11 or NGC 121 but more extensive than L14. It is an H-B between these two previous cases. The giant branch is poor and not extended as in L11. The whole C-M diagram seems compressed in colour. Only one star, in the very central region is red, but not as red as the others found previously.

The H-B occurs at $V \sim 19^m.00$ and the brightest star has $V = 17^m.48$. This is again a halo type SMC cluster. The C-M of region 2 (Fig. 55) is distorted by contamination with field stars and shows no clear pattern and certainly different from the one in Fig. 54 for the stars of the central region. Fig. 56 illustrates the composite C-M diagram of all measured stars and the usual pattern, produced by the stars of this area of the SMC, appears again.

The age of this cluster is probably between that of L11 and L15. This result came out on the basis of the H-B

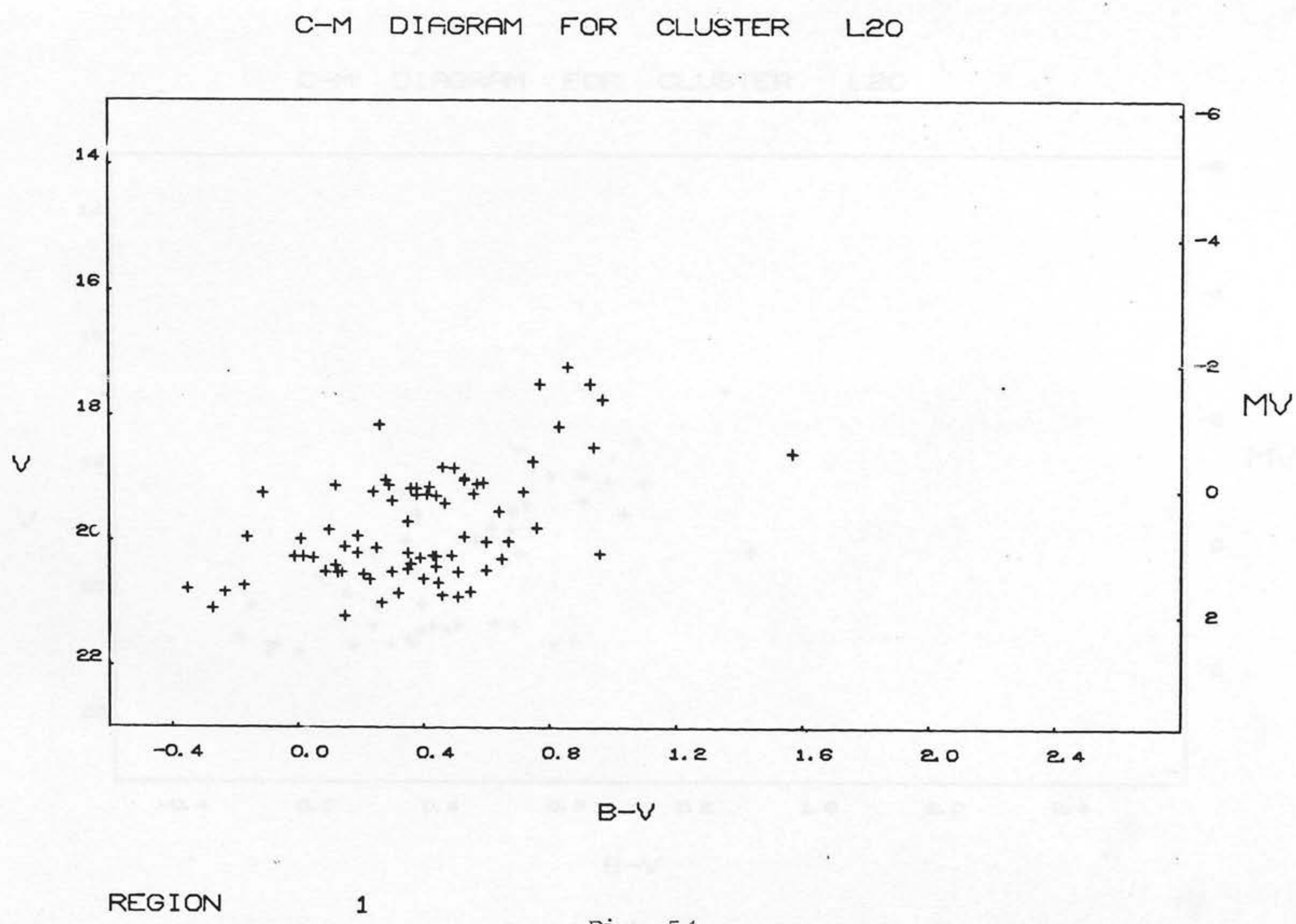
C-M DIAGRAM FOR CLUSTER L20
V
14
16
18
20
22
MV
-6
-4
-2
0
2
-0.4
0.0
0.4
0.8
1.2
1.6
2.0
2.4
B-V
REGION 1

Fig. 54.

C-M DIAGRAM FOR CLUSTER L20

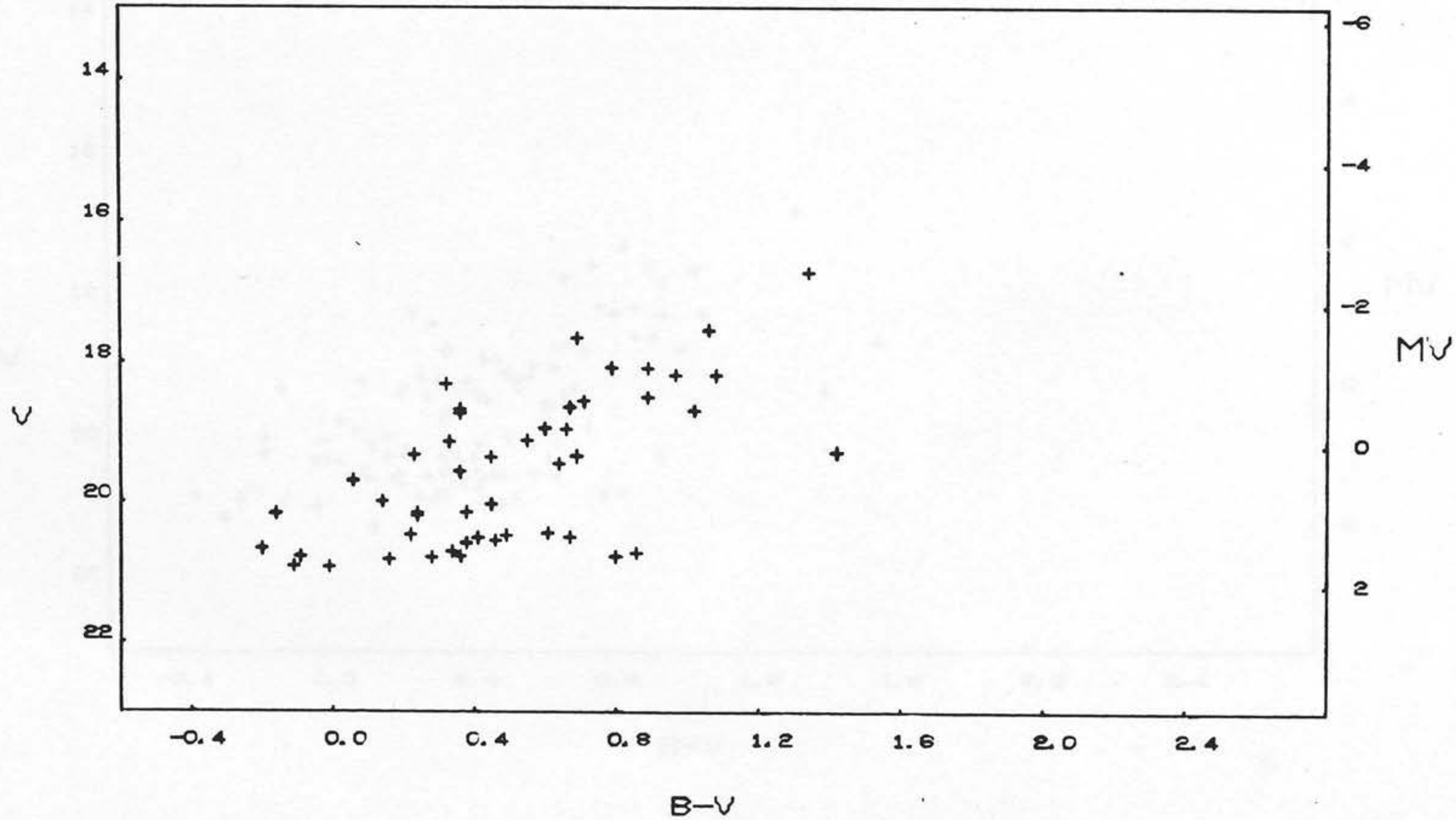

REGION 2

Fig. 55.

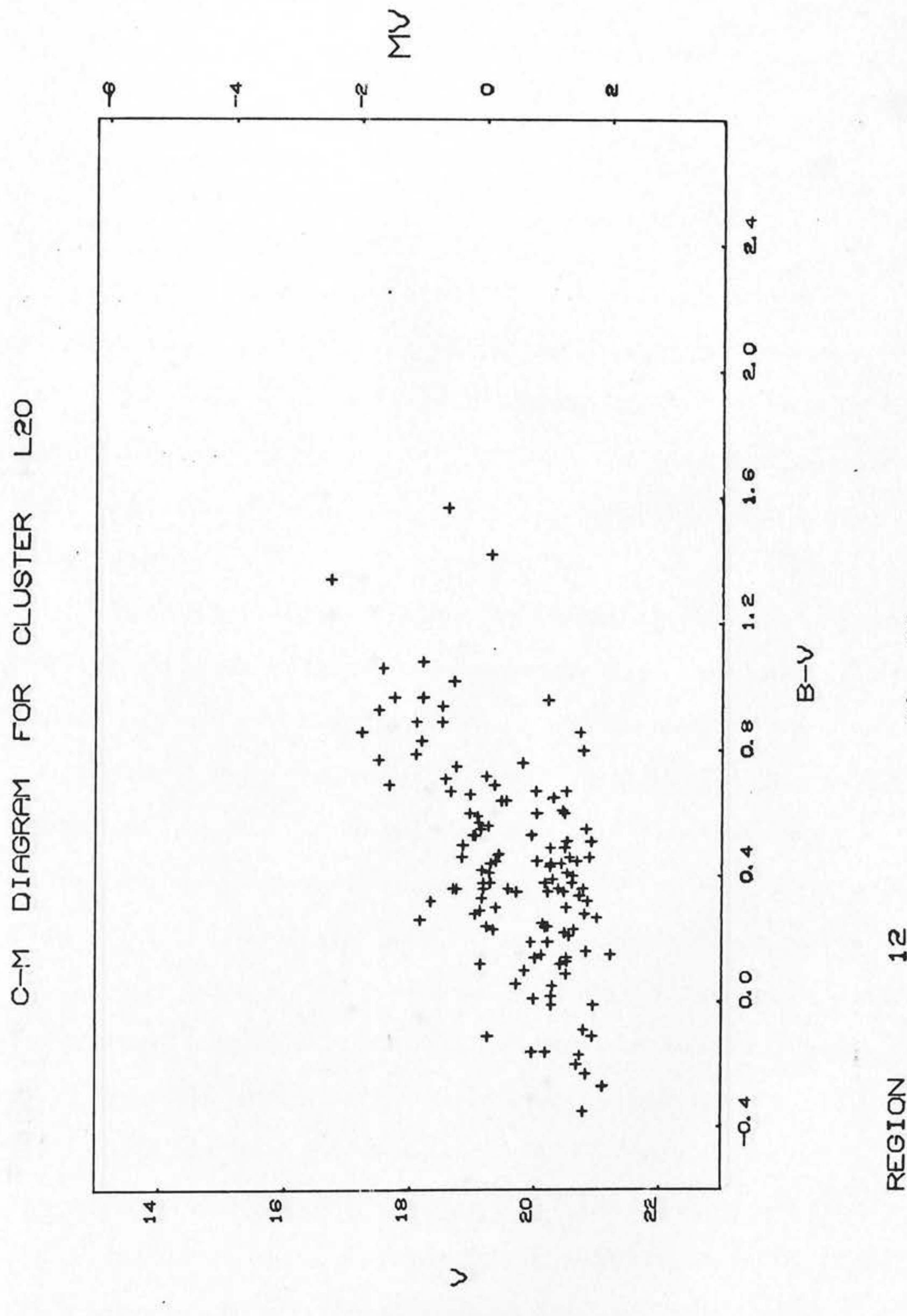
C-M DIAGRAM FOR CLUSTER L20
REGION 12
V
14
16
18
20
22
MV
-6
-4
-2
0
2
B-V
-0.4
0.0
0.4
0.8
1.2
1.6
2.0
2.4

Fig. 56.

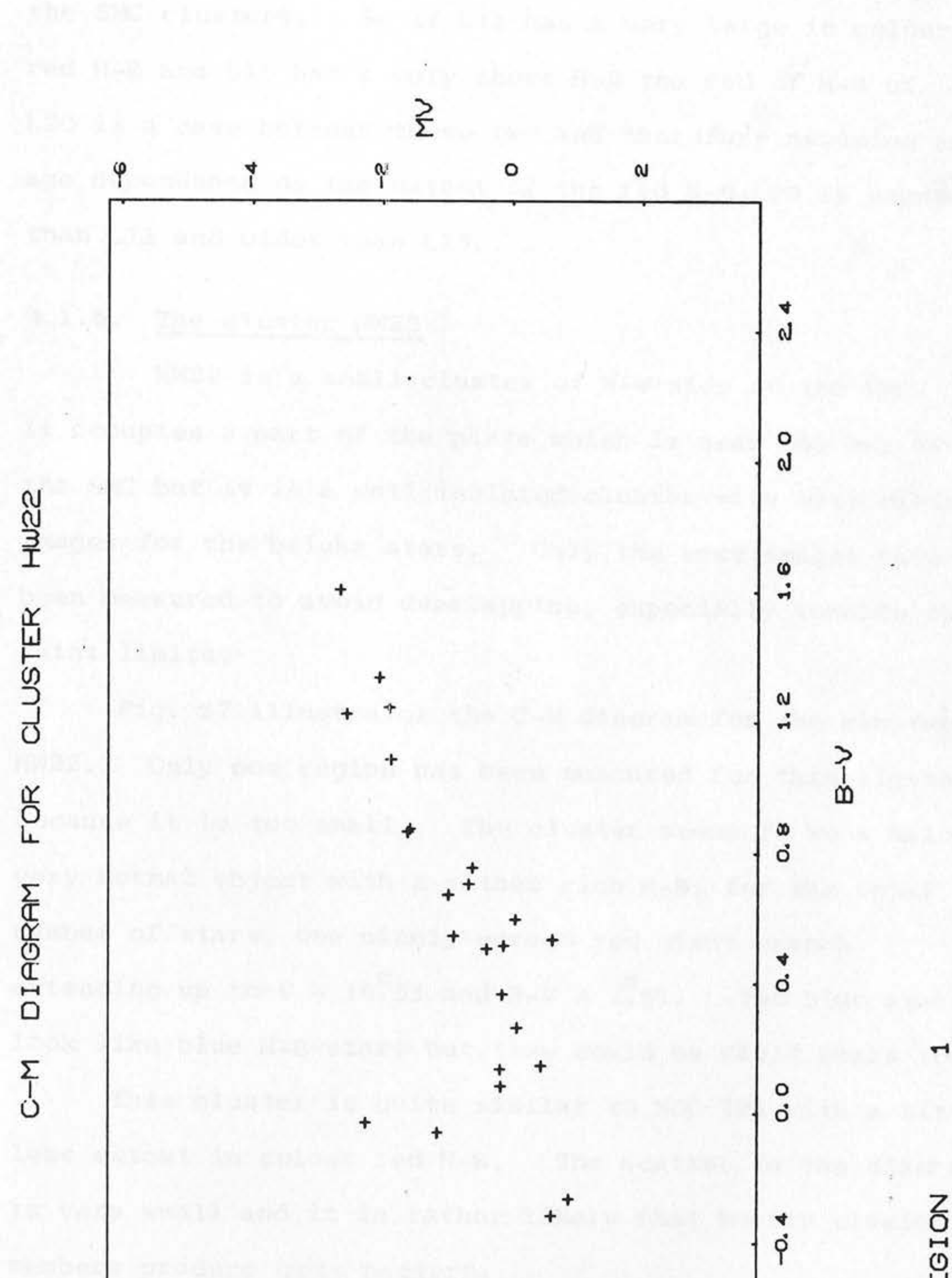
C-M DIAGRAM FOR CLUSTER HW22
REGION 1
V
MV
B-V
14
16
18
20
22
-6
-4
-2
0
2
-0.4
0.0
0.4
0.8
1.2
1.6
2.0
2.4

Fig. 57.

morphology, which so far is the main varying character in the SMC clusters. So if L11 has a very large in colour red H-B and L15 has a very short H-B the red of H-B of L20 is a case between these two and therefore assuming an age dependence on the extent of the red H-B,L20 is younger than L11 and older than L15.

4.1.6. <u>The cluster HW22</u>

HW22 is a small cluster of N-W side of the SMC. It occupies a part of the plate which is near the bar of the SMC but it is a well isolated cluster with very clear images for the bright stars. Only the best images have been measured to avoid overlapping, especially towards the faint limits.

Fig. 57 illustrates the C-M diagram for the cluster HW22. Only one region has been measured for this cluster because it is too small. The cluster seems to be a halo very normal object with a rather rich H-B, for the total number of stars, one nicely curved red giant branch extending up to $V = 16^{m}.55$ and $B-V = 1^{m}.61$. Two blue stars look like blue H-B stars but they could be field stars too.

This cluster is quite similar to NGC 121 with a little less extent in colour red H-B. The scatter in the diagram is very small and it is rather likely that mostly cluster members produce this pattern.

Consequently the cluster HW22 is another halo type SMC cluster. It is interesting though to know if it is an intermediate age type cluster younger than the western halo clusters. The study of the faint stars below

$V \sim 20^m.00$ would complete the diagram and the age question.

4.1.7. The cluster L48

The cluster L48 is a small cluster of the northern part of the SMC with a very compact nucleus and many faint stars around. The area has been divided into two regions. The central and the outer one.

Region 1 has a diameter $d_c \sim 2.3$ arc min whereas region 2 extend up to $d_{out} \sim 3.0$ arc min.

The cluster members are contaminated with the field stars and the investigation becomes difficult as always in the Cloud. Young stars of the central region of the Cloud are present and they are responsible for the distortion of the C-M diagrams for this cluster. Fig. 58 for the stars of the region 1, has a red giant branch, main sequence stars and faint blue stars.

This cluster is probably a halo type cluster with a poor red giant branch and probably the small clump at $V \sim 19^m.00$ is the red H-B, whereas the main sequence stars, are field stars. The C-M diagram (Fig. 59) of the outer region is much more scattered (because of blending) where all sorts of stars must be present, like cluster stars, some halo foreground stars and some bar-like background stars. The same population must be also in the region 1, but the proportion of cluster members is expected to be larger. But still it cannot be certain if some of the blue faint stars are blue H-B stars of the cluster.

One very red star in the central region has M_V = -0.12 and B-V = +2.11 which is very faint indeed.

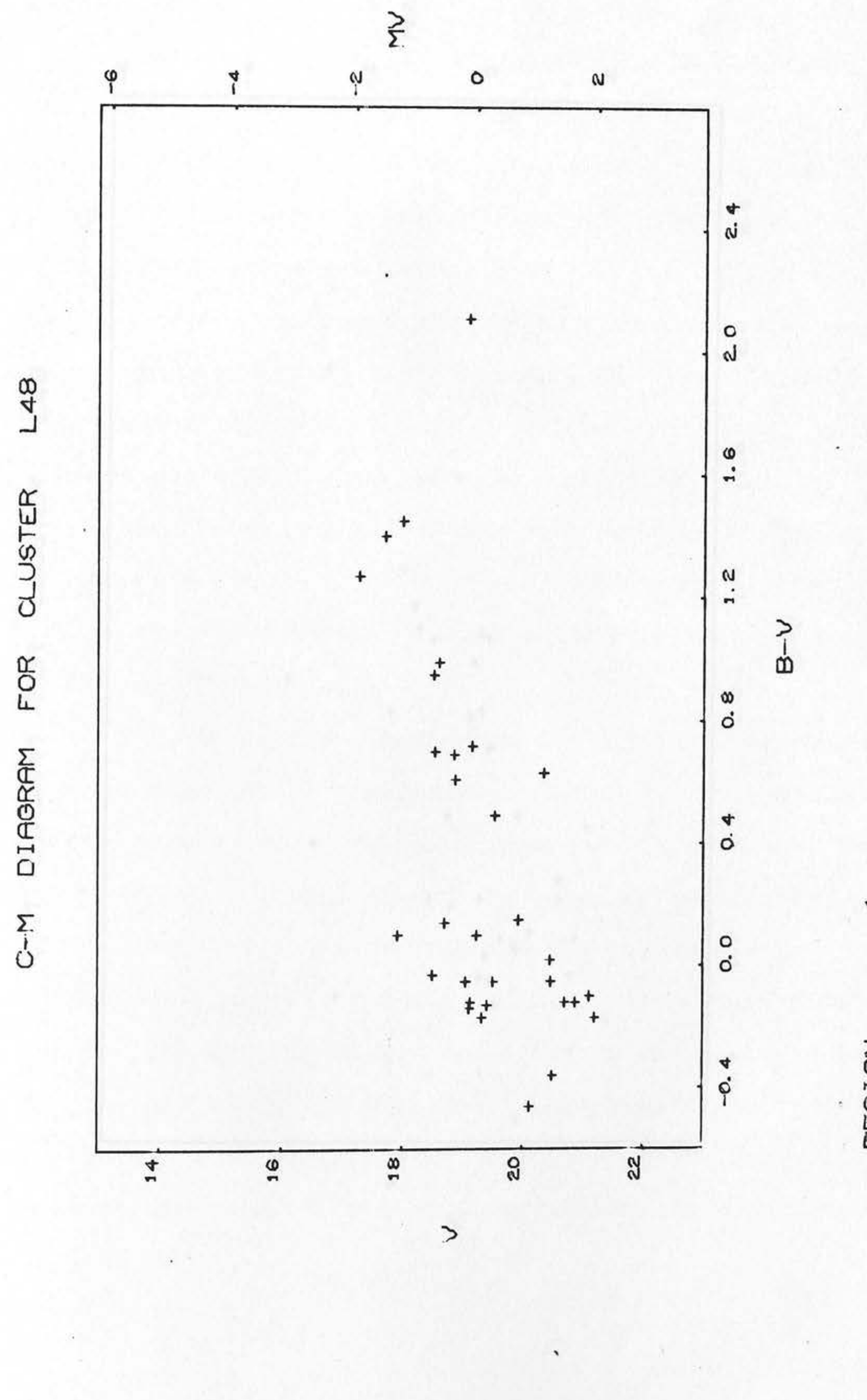
C-M DIAGRAM FOR CLUSTER L48
REGION 1
B-V
V
MV
-0.4
0.0
0.4
0.8
1.2
1.6
2.0
2.4
14
16
18
20
22
-6
-4
-2
0
2

Fig. 58.

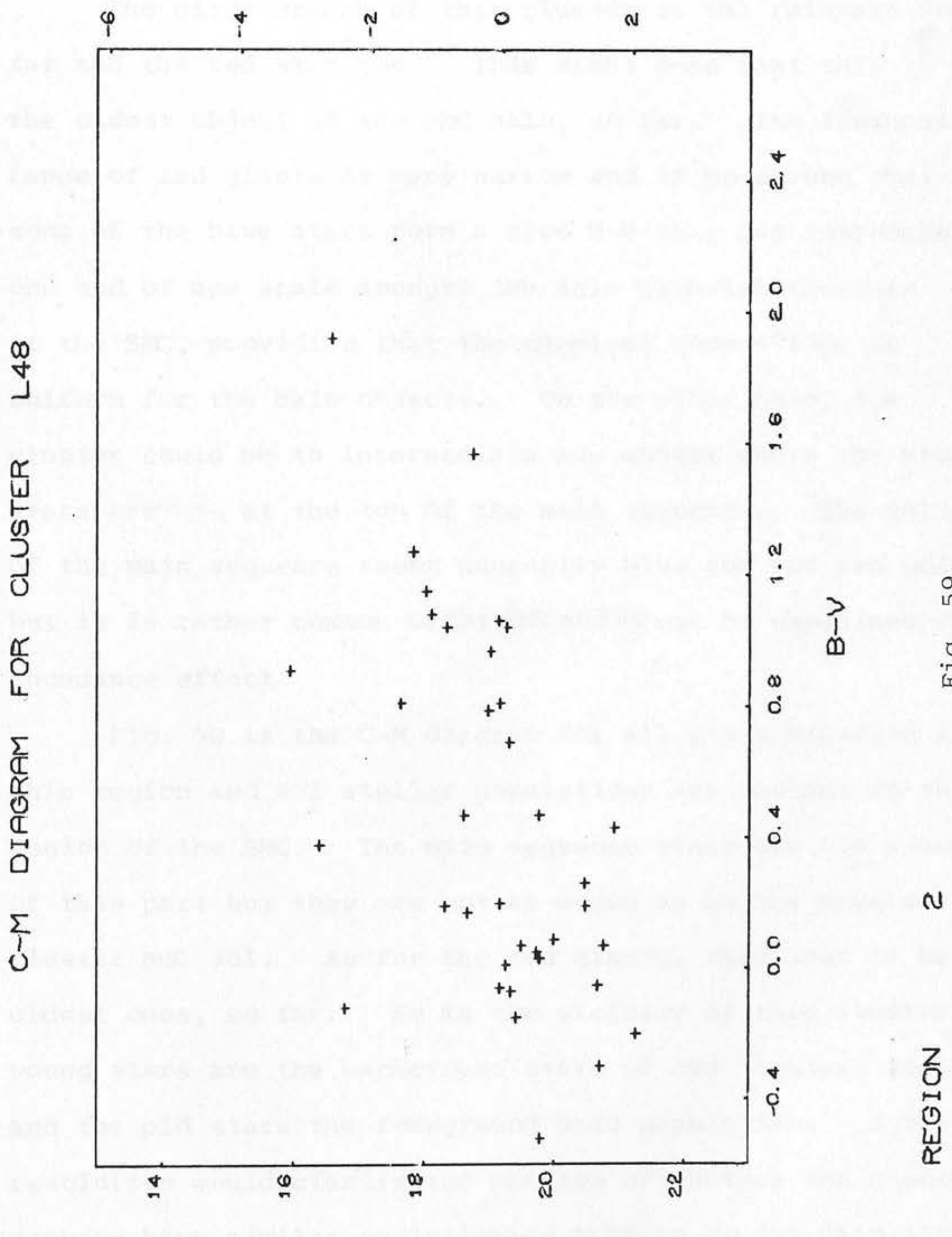
C-M DIAGRAM FOR CLUSTER L48
REGION 2
V
MV
B-V
14
16
18
20
22
-6
-4
-2
0
2
-0.4
0.0
0.4
0.8
1.2
1.6
2.0
2.4

Fig. 59.

Another red star is present at the second region but very near the limit of region 1. It is less red than the latter one but brighter, it has $M_V = -2^m.61$ and $B\text{-}V = +1^m.92$.

The giant branch of this cluster is the faintest so far and the red star too. This might mean that this is the oldest object of the SMC halo, so far. The luminosity range of red giants is very narrow and if we assume that some of the blue stars form a blue H-B this can introduce one end of age scale amongst the halo globular clusters of the SMC, providing that the chemical composition is uniform for the halo objects. On the other hand, the cluster could be an intermediate age object where the blue stars are the at the top of the main sequence. The colour of the main sequence seems unusually blue for our own Galaxy but it is rather common in the SMC and it can be explained as abundance effect.

Fig. 60 is the C-M diagram for all stars measured in this region and all stellar populations are present in this region of the SMC. The main sequence stars are the youngest of this part but they are not as young as at the area of the cluster NGC 361. As for the red giants, they seem to be the oldest ones, so far. So in the vicinity of this cluster the young stars are the background stars of the "central region" and the old stars the foreground halo population. A better resolution would clarify the problem of whether the cluster members have similar evolutionary history to the halo stars or not.

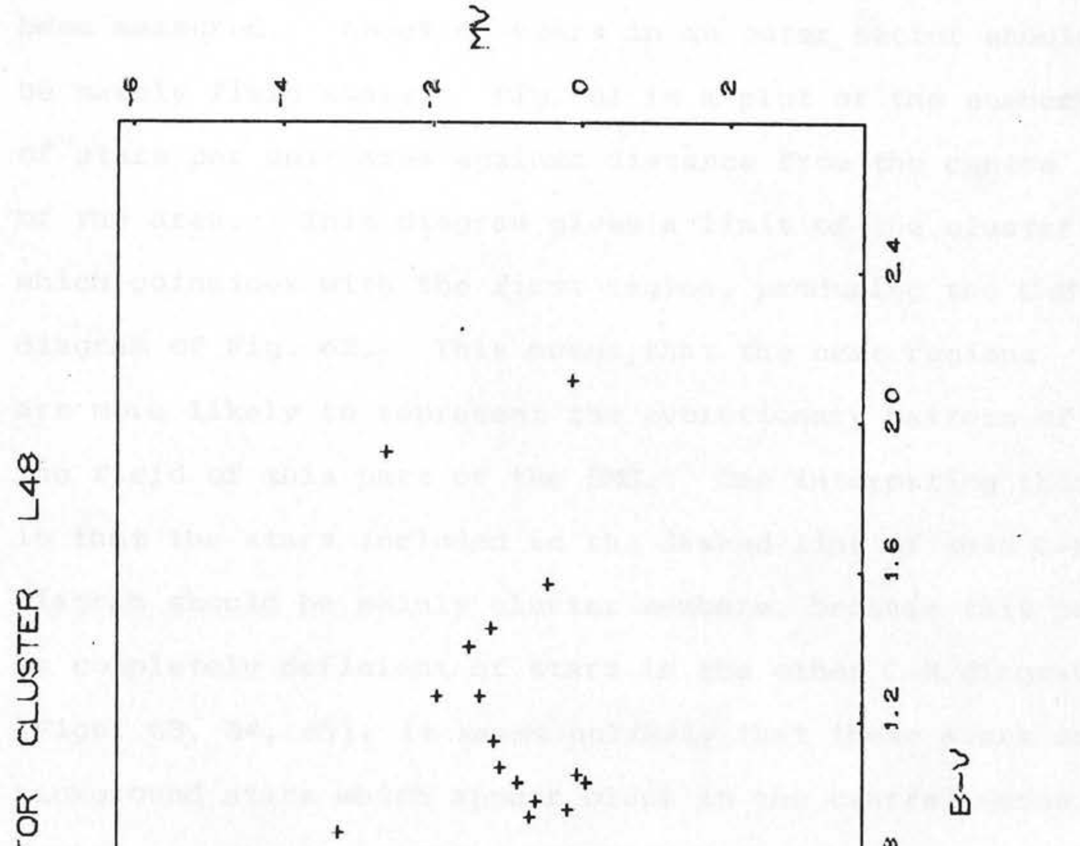
C-M DIAGRAM FOR CLUSTER L48
REGION 12
V
MV
B-V
14
16
18
20
22
-6
-4
-2
0
2
-0.4
0.0
0.4
0.8
1.2
1.6
2.0
2.4

Fig. 60.

4.1.8. The cluster L13

The cluster L13 is one of the western parts of the SMC. Stars from three regions around the clusters have been measured. About 60 stars in an outer sector should be mainly field stars. Fig. 61 is a plot of the number of stars per unit area against distance from the centre of the area. This diagram gives a limit of the cluster which coincides with the first region, producing the C-M diagram of Fig. 62. This means that the next regions are more likely to represent the evolutionary pattern of the field of this part of the SMC. One interesting thing is that the stars included in the dashed line of this C-M diagram should be mainly cluster members, because this part is completely deficient of stars in the other C-M diagrams (Figs. 63, 64, 65). It seems unlikely that these stars are background stars which appear bluer in the central dense regions. The rest of the C-M diagram is very consistent in the other diagrams and no such case has been found in another cluster. Therefore the stars between $V \sim 18^m.60$ to $V \sim 20^m.0$ and $B-V \sim -0.35$ to $B-V \sim 0.0$ can be a blue H-B not often found as clear as that in the SMC so far. Some of the blue stars in L48 falling in the same range of colour and luminosity may be of the same kind but we cannot so easily distinguish them from the field. The red H-B occurs at about $V \sim 19^m.50$ and the giant branch is very poor in star number but it has a good range of luminosity and colour. Four red giants in a clump exactly above the red H-B might be a post-H-B if it is not a random formation.

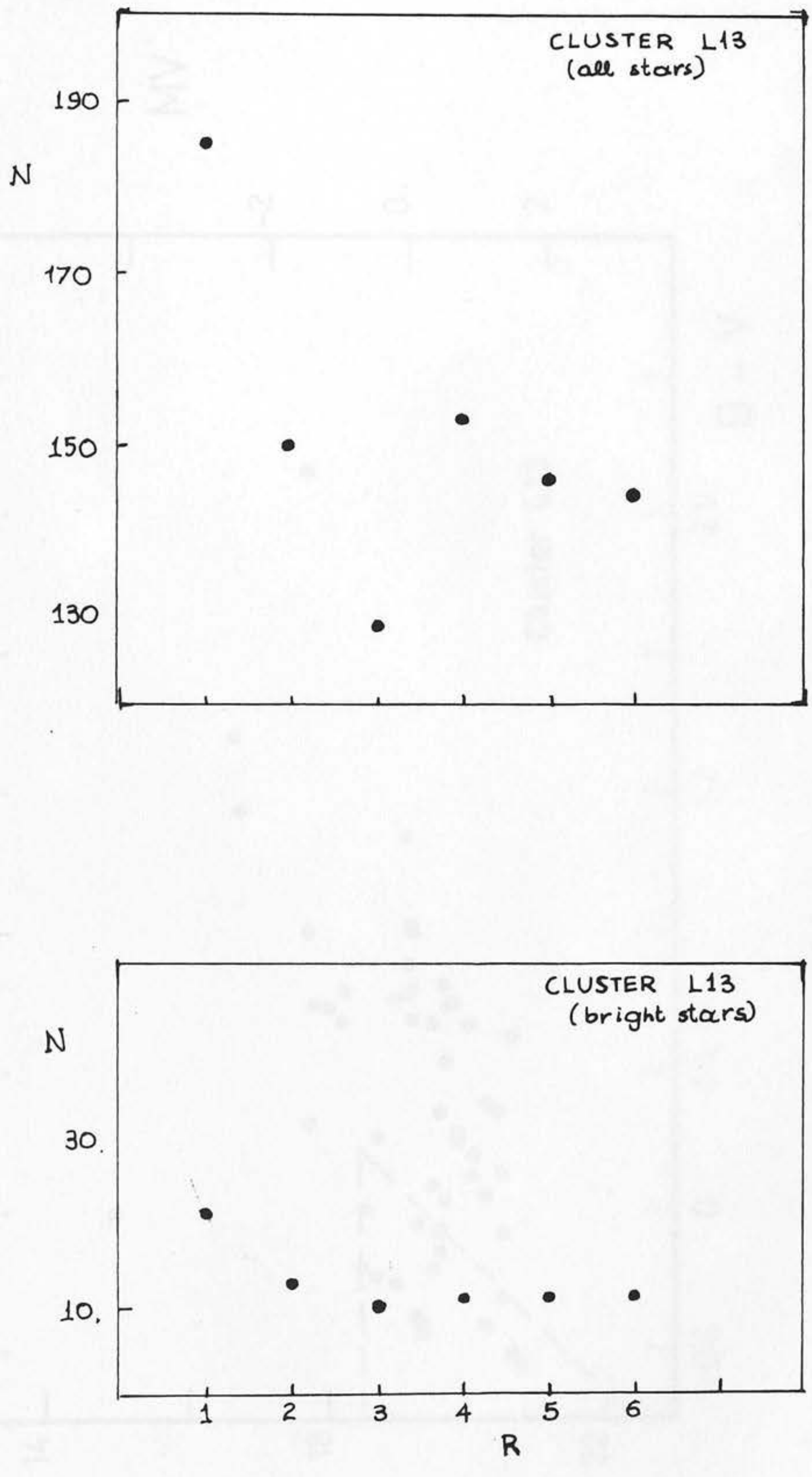

Fig. 61. Number of stars in equal areas around the centre of the cluster.

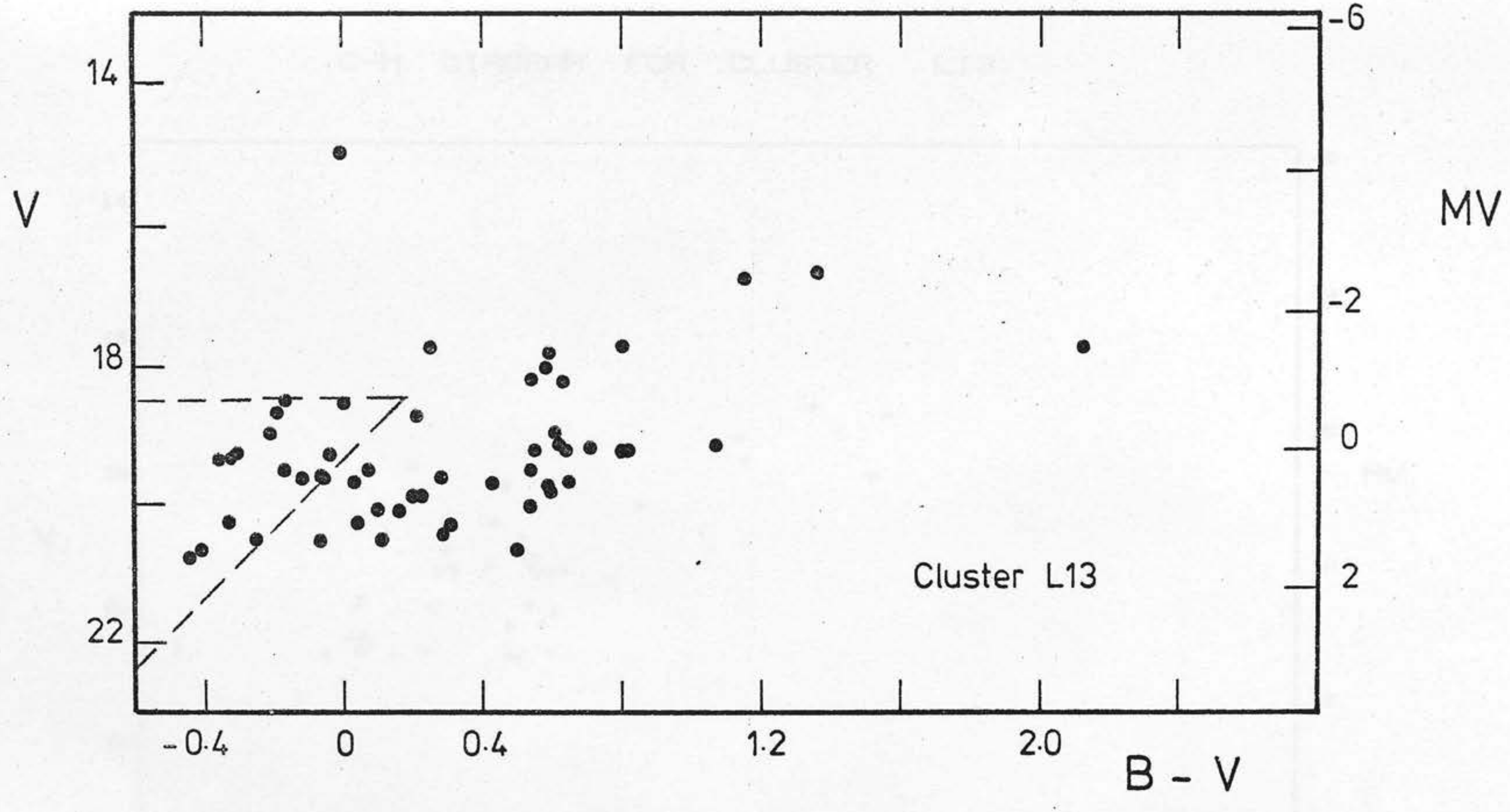

Fig. 62. C-M diagram for stars of cluster L13. The area which is included in the dashed line contains stars only of the central region of the cluster.

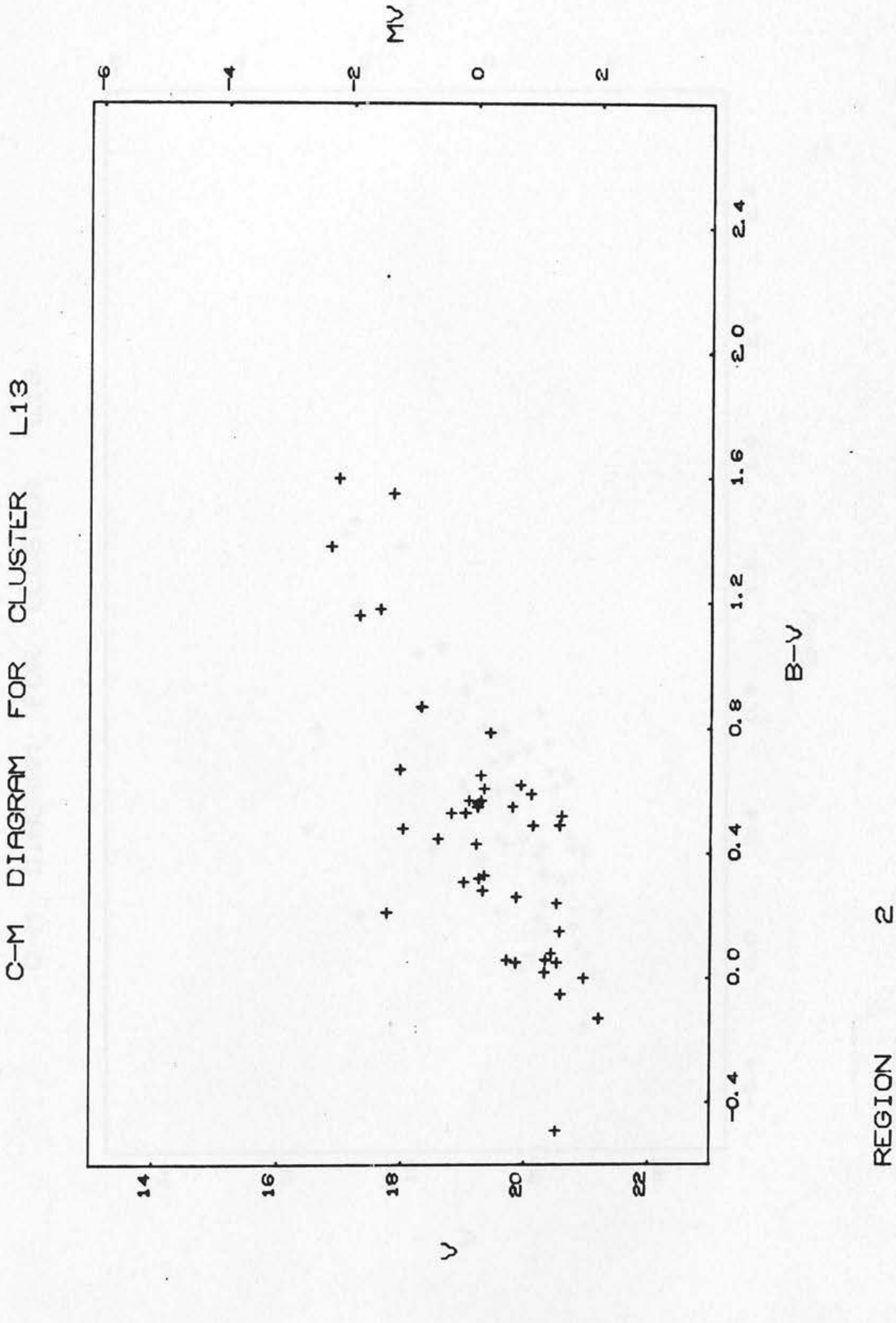
C-M DIAGRAM FOR CLUSTER L13
MV
-6
-4
-2
0
2
V
14
16
18
20
22
-0.4
0.0
0.4
0.8
1.2
1.6
2.0
2.4
B-V
REGION 2

Fig. 63.

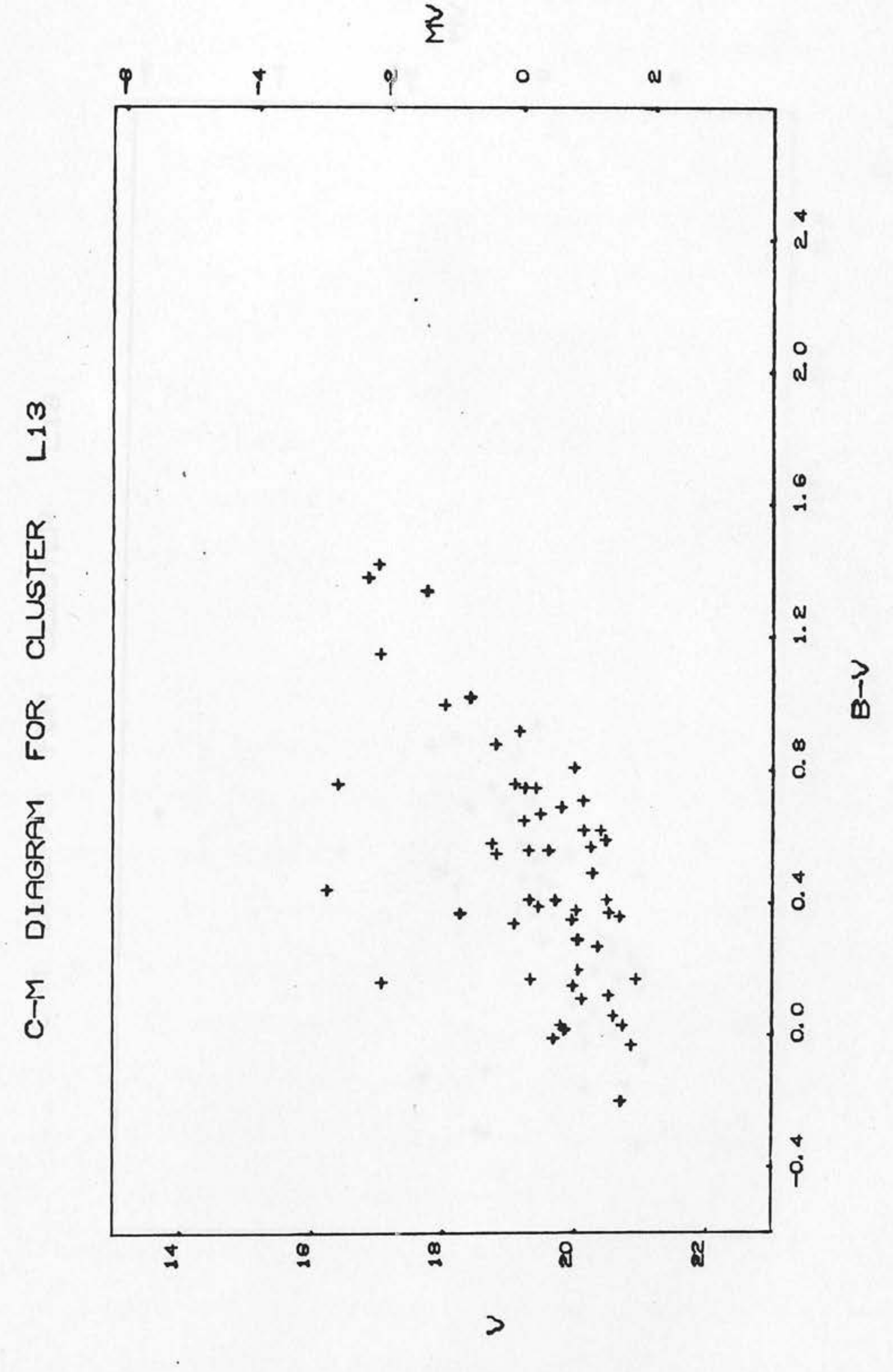
C-M DIAGRAM FOR CLUSTER L13
MV
-8
-4
-2
0
2
V
14
16
18
20
22
-0.4
0.0
0.4
0.8
1.2
1.6
2.0
2.4
B-V
REGION 3

Fig. 64.

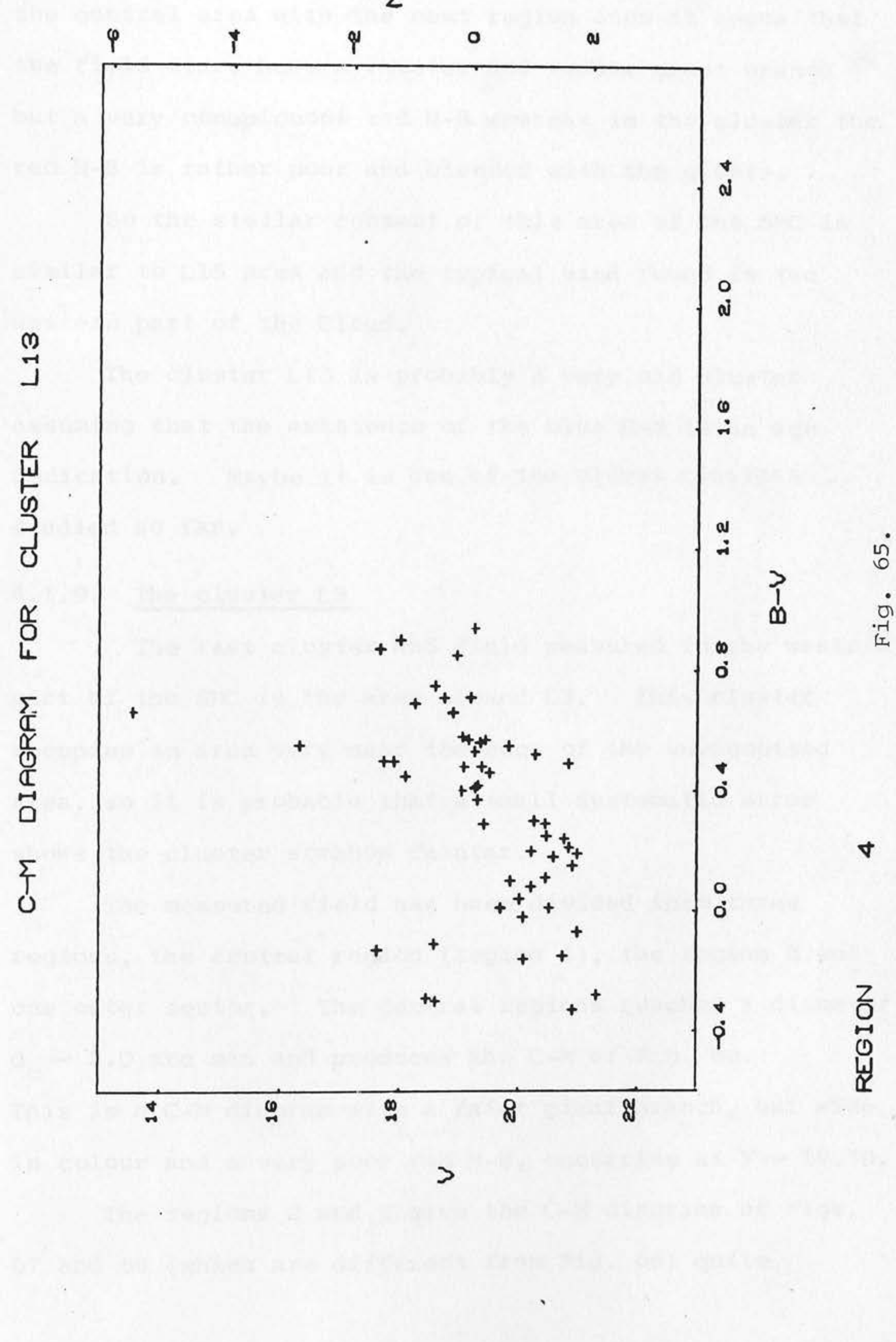
C-M DIAGRAM FOR CLUSTER L13
MV
-6
-4
-2
0
2
V
14
16
18
20
22
B-V
-0.4
0.0
0.4
0.8
1.2
1.6
2.0
2.4
REGION 4

Fig. 65.

One very red star is present in the central region with $M_V = -1.48$ and $B-V = 2.25$ and makes it a typical phenomenon of the halo type clusters. Comparing the C-M diagram of the central area with the next region ones it seems that the field stars have a fainter and redder giant branch but a very conspicuous red H-B whereas in the cluster the red H-B is rather poor and blended with the giants.

So the stellar content of this area of the SMC is similar to L15 area and the typical kind found in the western part of the Cloud.

The cluster L13 is probably a very old cluster assuming that the existence of the blue H-B is an age indication. Maybe it is one of the oldest clusters studied so far.

4.1.9. The cluster L3

The last cluster and field measured in the western part of the SMC is the area around L3. This cluster occupies an area very near the edge of the unvignetted area, so it is probable that a small systematic error shows the cluster somehow fainter.

The measured field has been divided into three regions, the central region (region 1), the region 2 and one outer sector. The central regions reaches a diameter $d_c \sim 2.0$ arc min and produces the C-M of Fig. 66. This is a C-M diagram with a faint giant branch, but wide in colour and a very poor red H-B, occurring at $V \sim 19.50$.

The regions 2 and 3 give the C-M diagrams of Figs. 67 and 68 (which are different from Fig. 66) quite

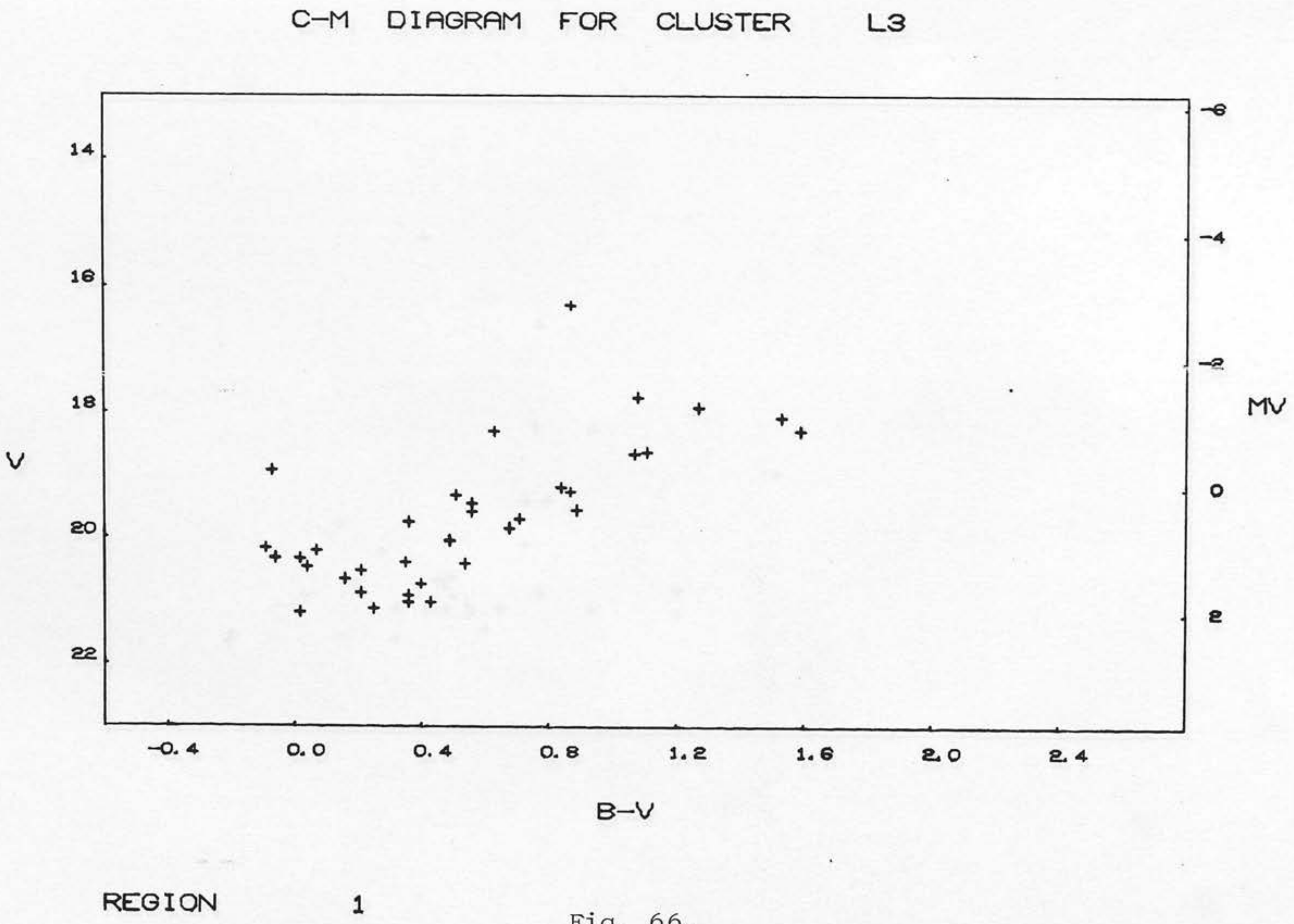
C-M DIAGRAM FOR CLUSTER L3
V
14
16
18
20
22
MV
-6
-4
-2
0
2
-0.4
0.0
0.4
0.8
1.2
1.6
2.0
2.4
B-V
REGION 1

Fig. 66.

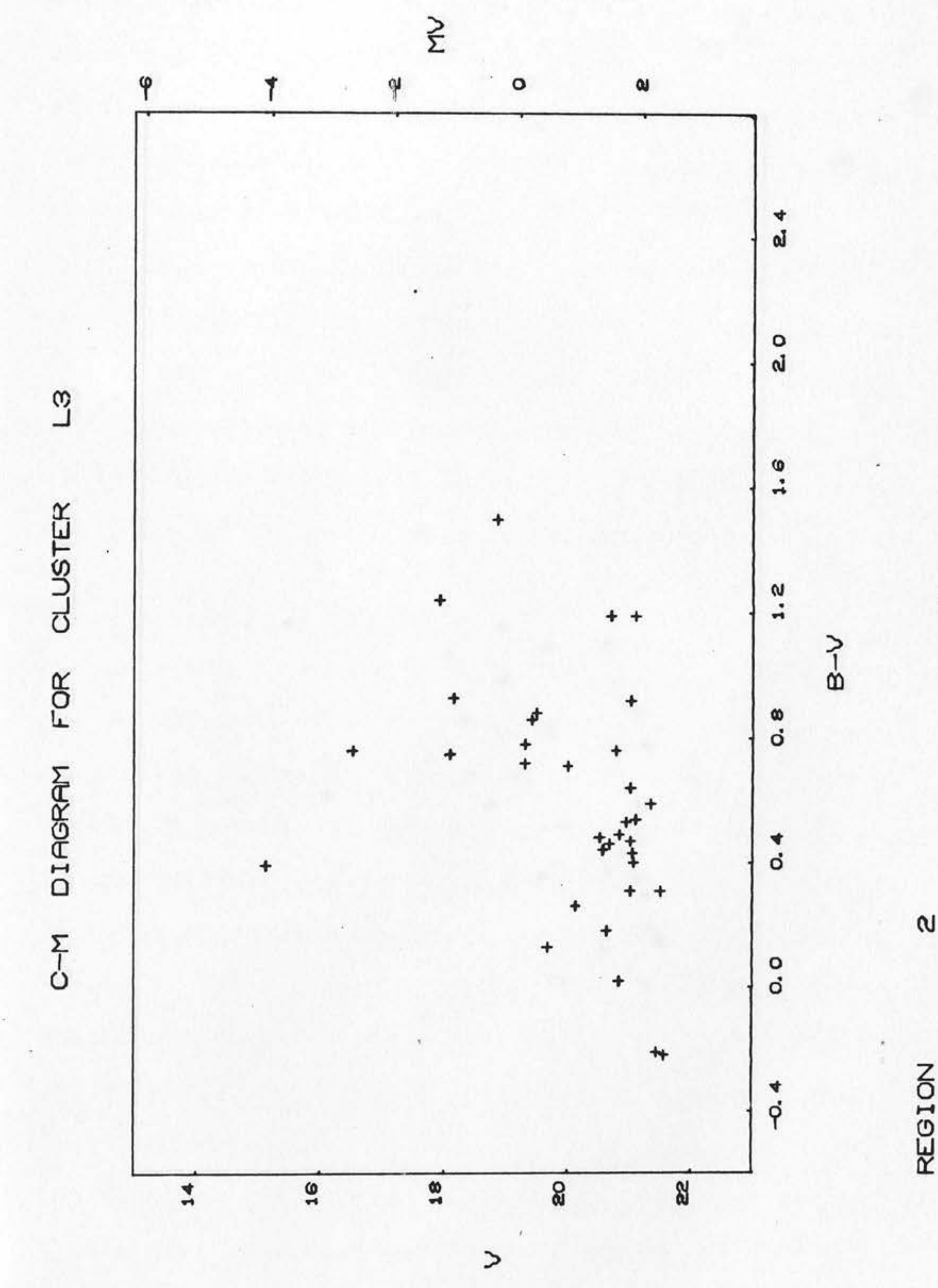
C-M DIAGRAM FOR CLUSTER L3
REGION 2
V
MV
B-V
14
16
18
20
22
-0.4
0.0
0.4
0.8
1.2
1.6
2.0
2.4
6
4
2
0
2

Fig. 67.

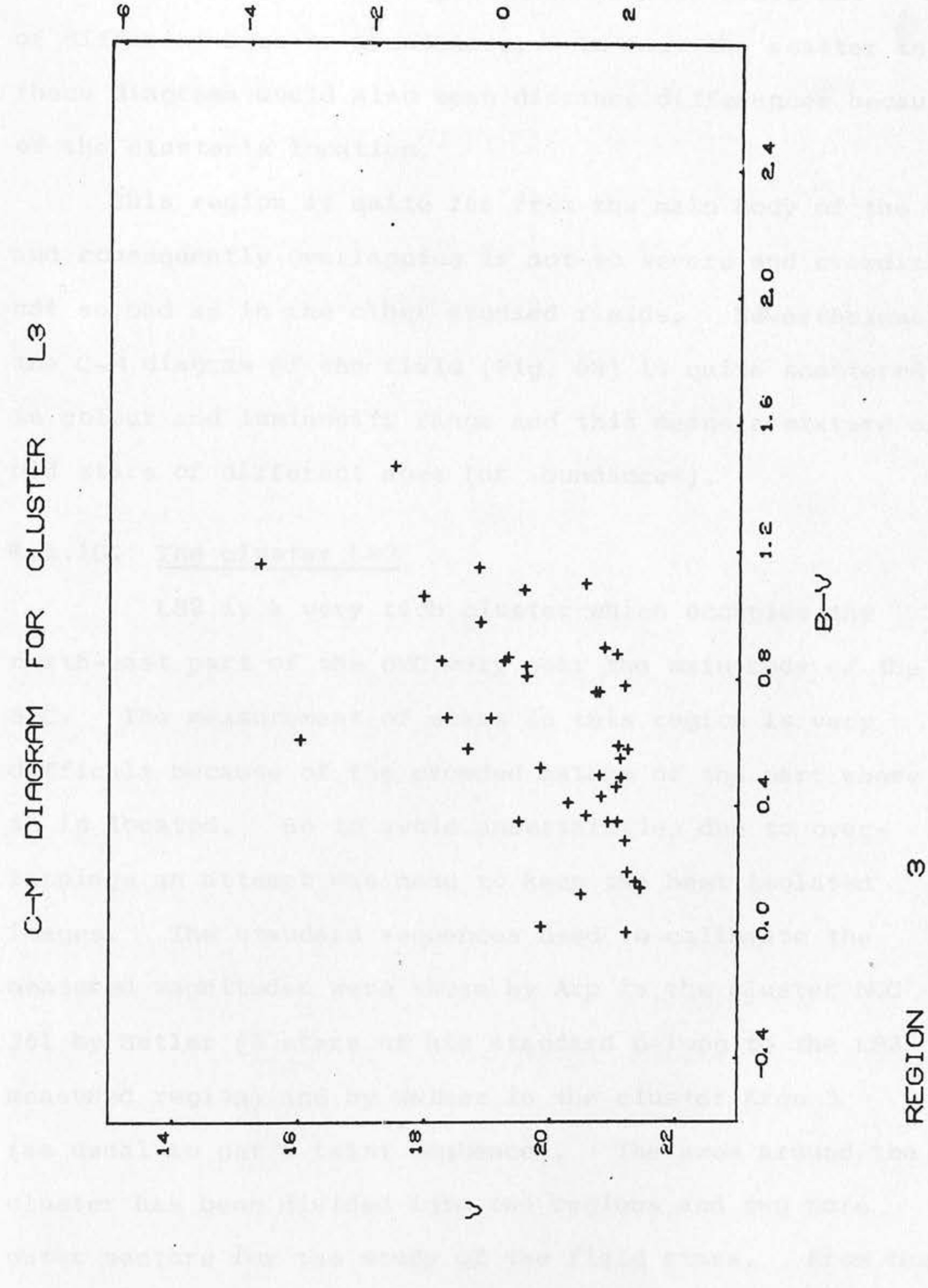
C-M DIAGRAM FOR CLUSTER L3
MV
-6
-4
-2
0
2
V
14
16
18
20
22
B-V
-0.4
0.0
0.4
0.8
1.2
1.6
2.0
2.4
REGION 3

Fig. 68.

distorted by field stars and very scattered. So Fig. 66 is the characteristic diagram for the stars of the clusters whereas the next regions have mostly field stars which according to their C-M diagram are old halo stars but of different ages or abundances. In fact the scatter in these diagrams would also mean distance differences because of the cluster's location.

This region is quite far from the main body of the SMC and consequently overlapping is not so severe and crowding not so bad as in the other studied fields. Nevertheless the C-M diagram of the field (Fig. 68) is quite scattered in colour and luminosity range and this means a mixture of old stars of different ages (or abundances).

4.1.10. <u>The cluster L82</u>

L82 is a very rich cluster which occupies the north-east part of the SMC very near the main body of the SMC. The measurement of stars in this region is very difficult because of the crowded nature of the part where it is located. So to avoid uncertainties due to overlappings an attempt was made to keep the best isolated images. The standard sequences used to calibrate the measured magnitudes were those by Arp in the cluster NGC 361 by Butler (3 stars of his standard belong to the L82 measured region) and by Walker in the cluster Kron 3 (as usual to get a faint sequence). The area around the cluster has been divided into two regions and two more outer sectors for the study of the field stars. From the central area contamination makes it almost impossible to discuss anything conclusive about the cluster members. According to Brück's (1976) classification the cluster is a red globular cluster and the C-M diagram of the central region proves this (Fig. 69). The crosses represent stars very near the cluster centre (region a) and the open circles stars from a ring next to region a (region b). There are no blue giants in this diagram but a great deal of faint blue stars. There is a poor giant branch extended in colour up to B-V ~ 1.6. It must also be taken into account that about 50% of the measured stars, mostly bright stars, have been rejected because of overlappings so the investigation of the actual cluster members is more difficult.

Three different star populations must contribute to these C-M diagrams: the cluster members, the halo's old stars and the bar's main sequence stars. In Fig. 70 the regions 1a and 1b are plotted and the two different populations are marked. The solid line includes the typical L15 C-M diagram whereas the dashed line represents the diagram for stars of the cluster M11, which is an open cluster of our own Galaxy with main sequence stars and some Helium burning stars. These two seem to cover the stellar content of this diagram. Figs. 71, 72 and 73 illustrate diagrams of the regions further out and it is interesting to see that the part of the M11 locus (where the evolved stars should be) is filled by stars from the outer regions. So it is more likely that this area of the SMC near the bar comprises young stars and some core Helium burning ones whereas the halo stars are old halo type with the typical

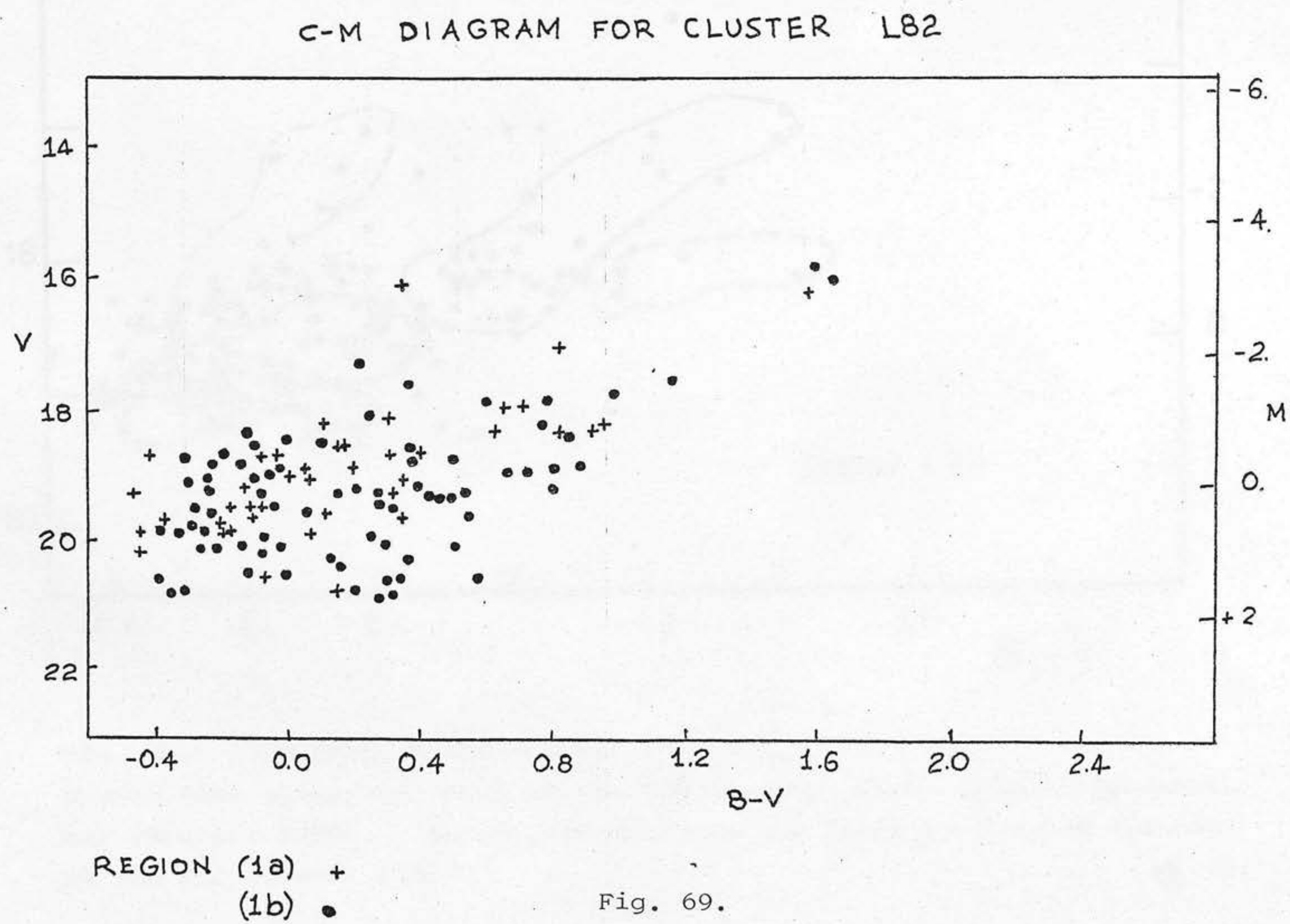
C-M DIAGRAM FOR CLUSTER L82
V
14
16
18
20
22
MV
-6.
-4.
-2.
0.
+2
-0.4
0.0
0.4
0.8
1.2
1.6
2.0
2.4
B-V
REGION (1a) +
(1b) ●

Fig. 69.

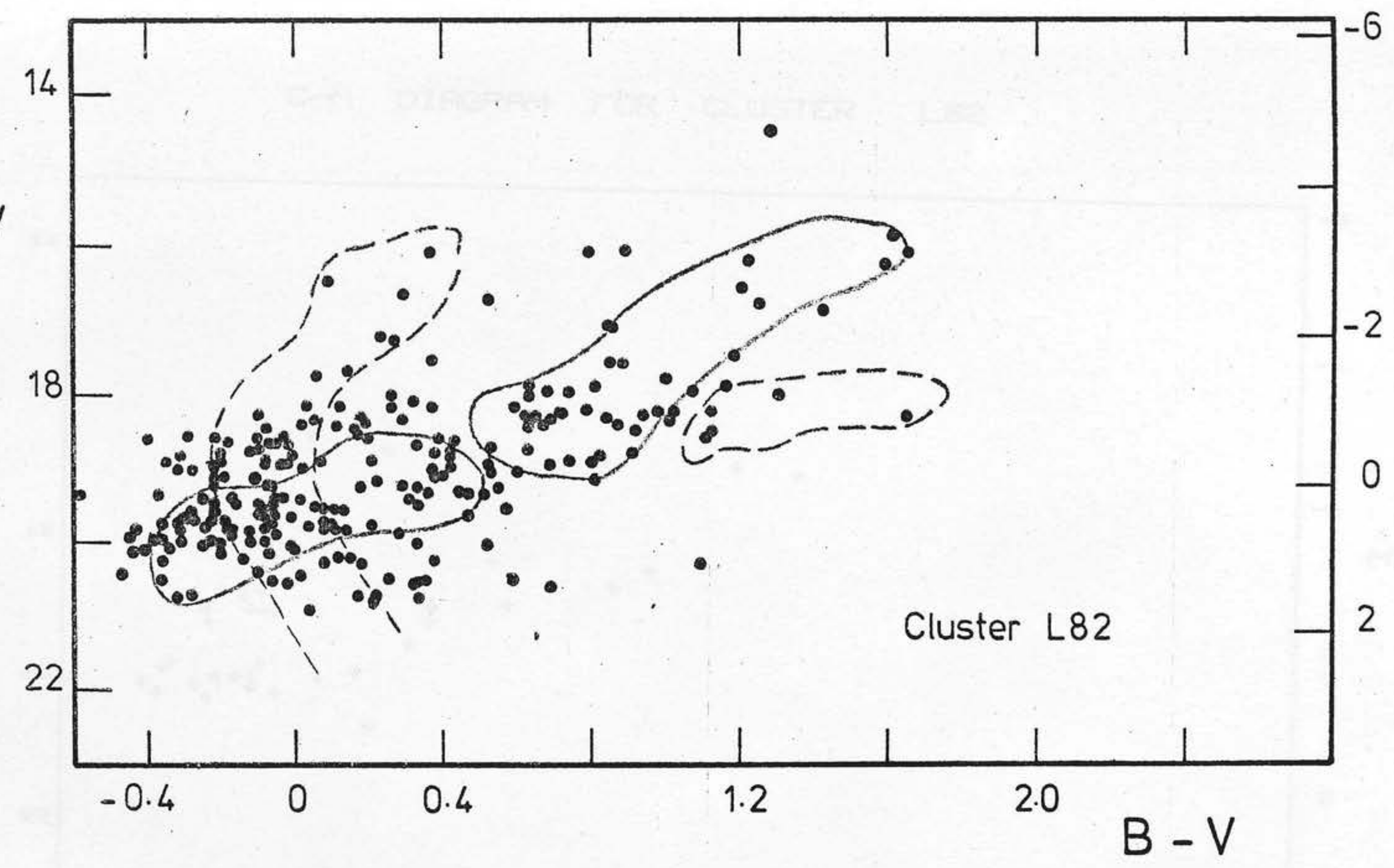

Fig. 70. C-M diagram for cluster L82 (region 1a & 1b). Dashed line gives the locus of the C-M diagram of the galactic cluster M11 (Meurers 1953). Solid line includes the locus of the C-M diagram of the SMC cluster L15.

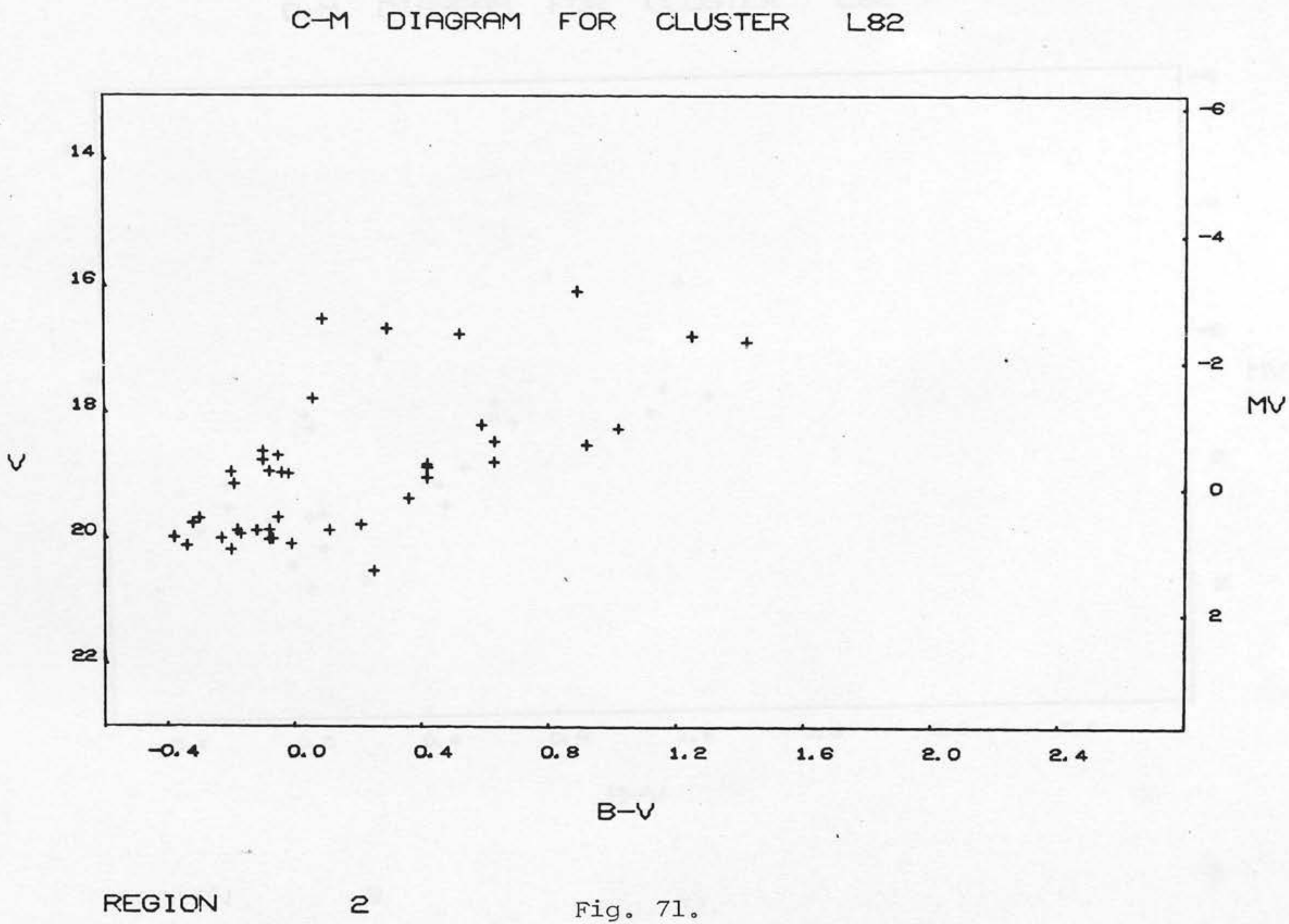
C–M DIAGRAM FOR CLUSTER L82
V
14
16
18
20
22
MV
-6
-4
-2
0
2
-0.4
0.0
0.4
0.8
1.2
1.6
2.0
2.4
B–V
REGION 2

Fig. 71.

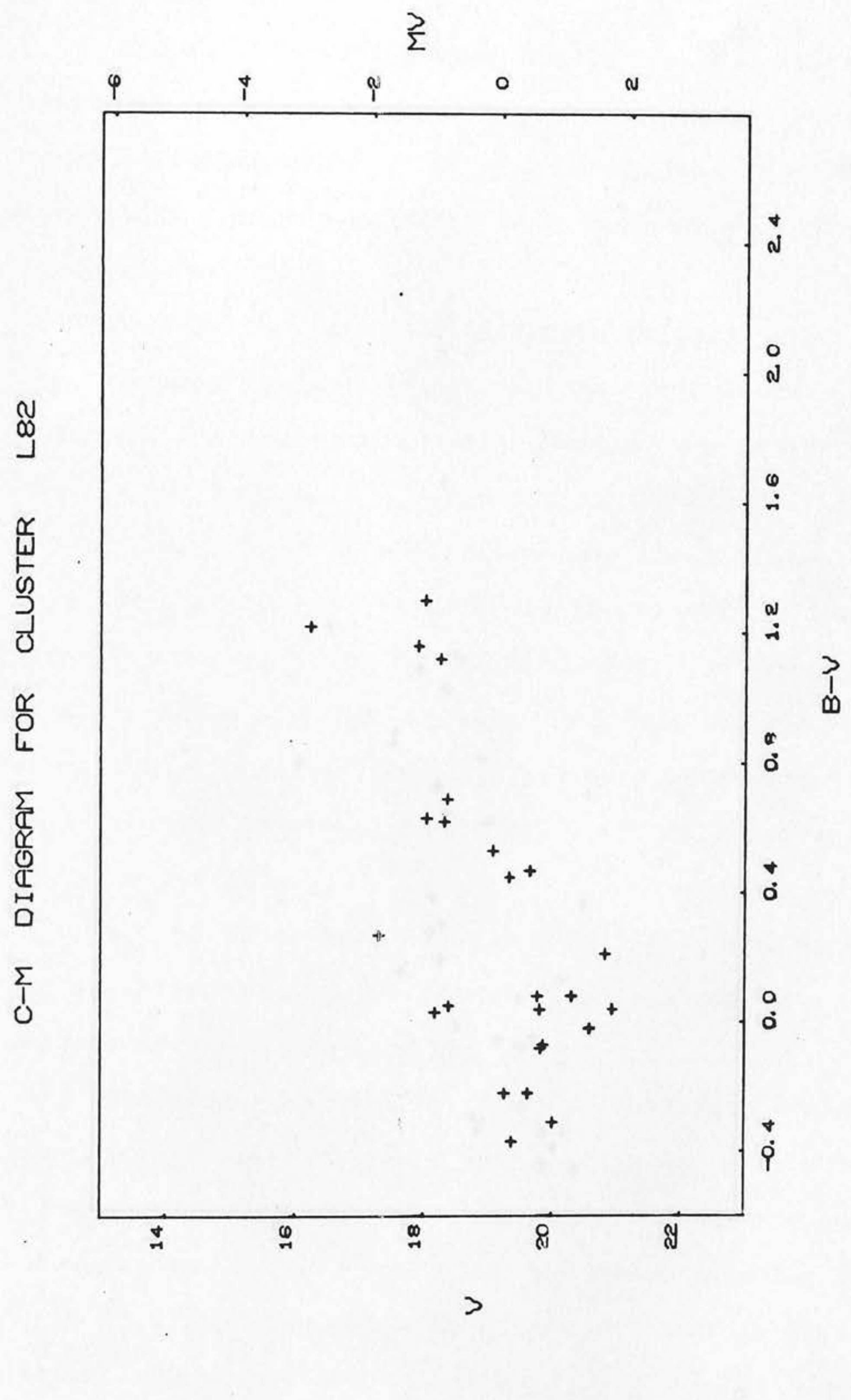
C-M DIAGRAM FOR CLUSTER L82
REGION 3
V
MV
B-V
14
16
18
20
22
-6
-4
-2
0
2
-0.4
0.0
0.4
0.8
1.2
1.6
2.0
2.4

Fig. 72.

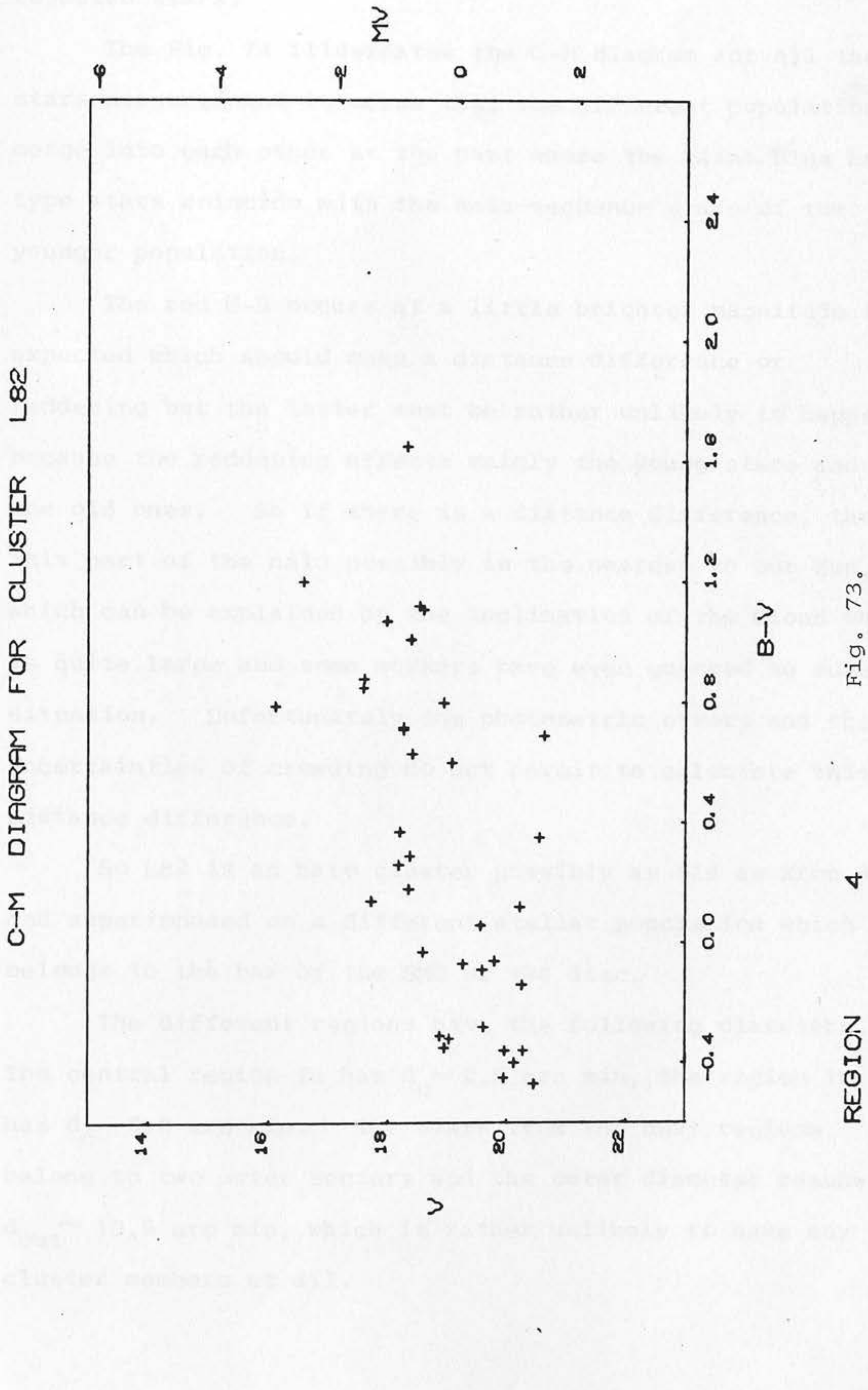
C-M DIAGRAM FOR CLUSTER L82
REGION 4
MV
-6
-4
-2
0
2
V
14
16
18
20
22
B-V
-0.4
0.0
0.4
0.8
1.2
1.6
2.0
2.4

Fig. 73.

red H-B and probably a blue H-B too. The discontinuities in the red giant branch do not mean much because of the rejected stars.

The Fig. 74 illustrates the C-M diagram for all the stars measured and it seems that the different populations merge into each other at the part where the faint blue halo type stars coincide with the main sequence stars of the younger population.

The red H-B occurs at a little brighter magnitude than expected which should mean a distance difference or reddening but the latter must be rather unlikely to happen, because the reddening affects mainly the young stars and not the old ones. So if there is a distance difference, then this part of the halo possibly is the nearest to our Sun, which can be explained by the inclination of the Cloud which is quite large and some workers have even guessed an edge-on situation. Unfortunately the photometric errors and the uncertainties of crowding do not permit to calculate this distance difference.

So L82 is an halo cluster possibly as old as Kron 3 and superimposed on a different stellar population which belongs to the bar of the SMC or the disc.

The different regions have the following diameters. The central region 1a has $d_c \sim 2.5$ arc min, the region 1b has $d_c \sim 3.8$ arc min. The stars from the next regions belong to two outer sectors and the outer diameter reaches $d_{out} \sim 10.8$ arc min, which is rather unlikely to have any cluster members at all.

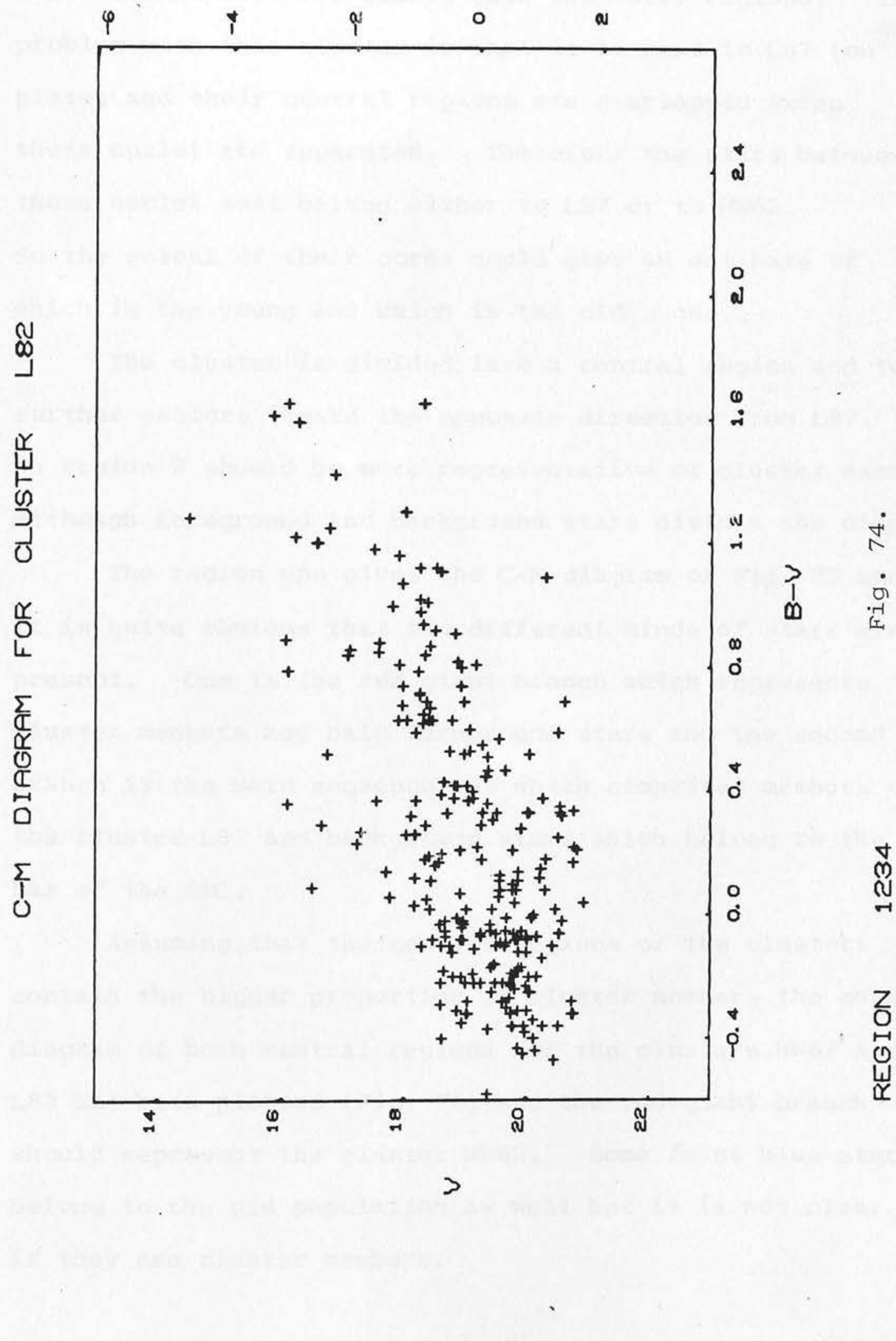
C-M DIAGRAM FOR CLUSTER L82
REGION 1234
V
14
16
18
20
22
B-V
-0.4
0.0
0.4
0.8
1.2
1.6
2.0
2.4
MV
-6
-4
-2
0
2

Fig. 74.

4.1.11. The cluster HW62

This is a cluster of the northern side of the SMC. Its core is rather elliptical and the central regions contain much more red giants than the outer regions. The problem with this cluster is that it is next to L87 (on the plate) and their central regions are overlapped except their nuclei are separated. Therefore the stars between these nuclei must belong either to L87 or to HW62. So the colour of their cores could give an estimate of which is the young and which is the old one.

The cluster is divided into a central region and two further sectors toward the opposite direction from L87. So region 2 should be more representative of cluster members although foreground and background stars distort the diagram.

The region one gives the C-M diagram of Fig. 75 and it is quite obvious that two different kinds of stars are present. One is the red giant branch which represents cluster members and halo foreground stars and the second branch is the main sequence one which comprises members of the cluster L87 and background stars which belong to the bar of the SMC.

Assuming that the central regions of the clusters contain the bigger proportion of cluster members the composite diagram of both central regions for the clusters HW62 and L82 has been plotted (Fig. 76) and the red giant branch should represent the cluster HW62. Some faint blue stars belong to the old population as well but it is not clear if they are cluster members.

C-M DIAGRAM FOR CLUSTER HW62

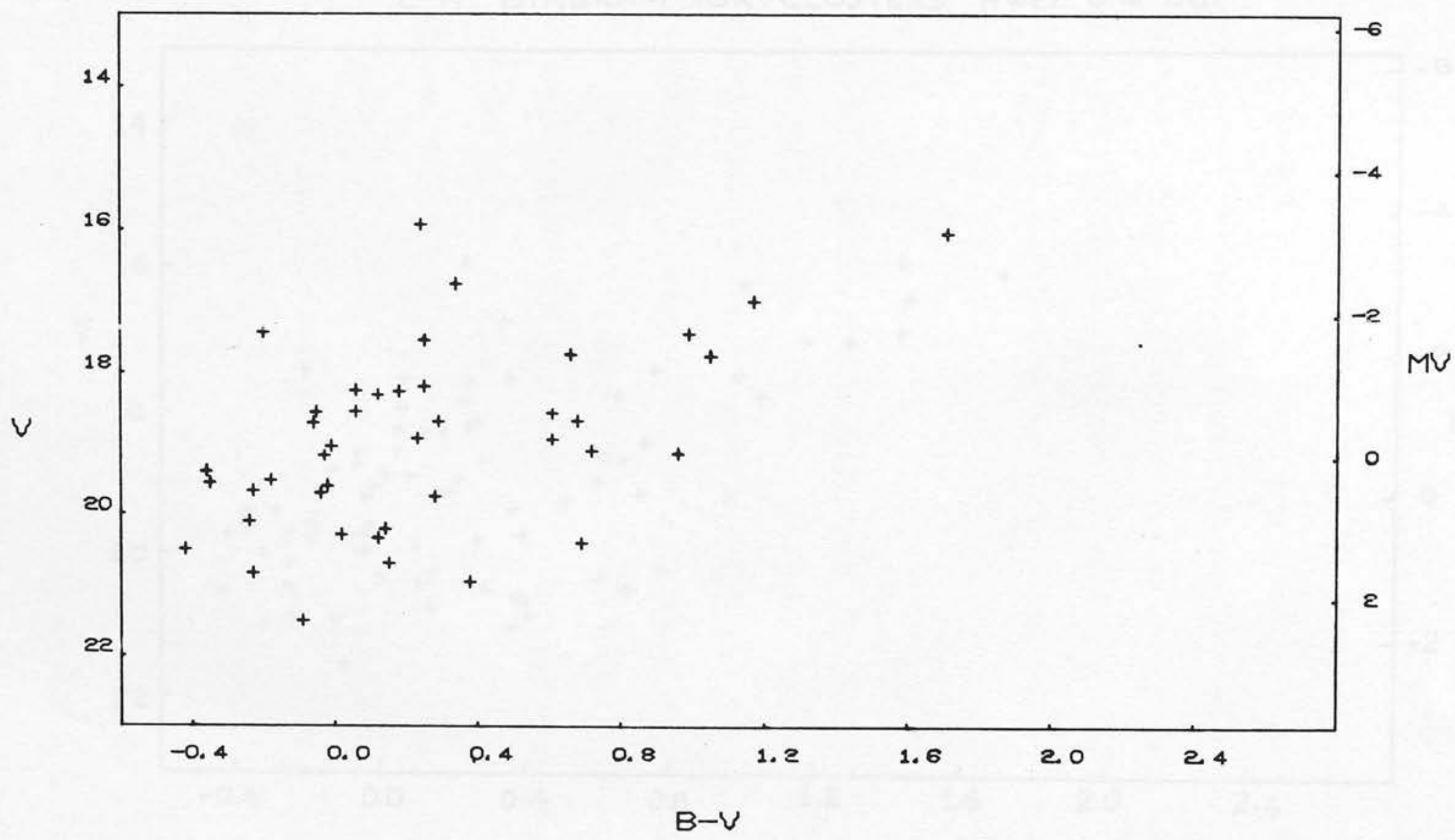

REGION 1

Fig. 75.

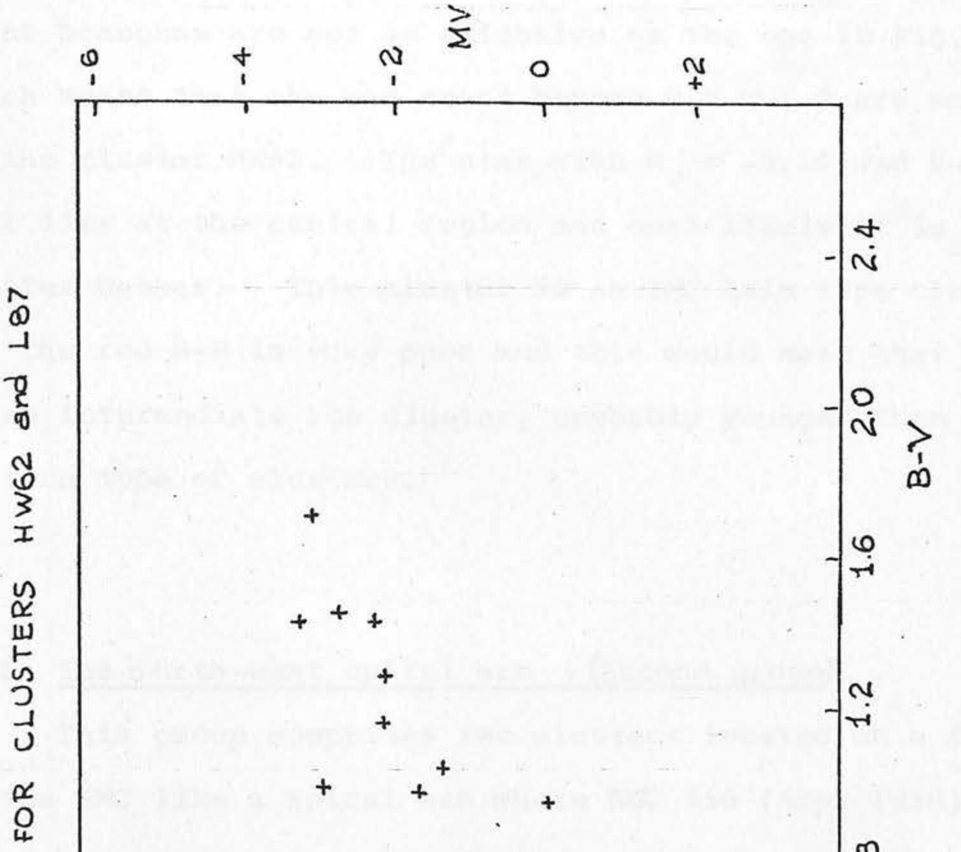
C-M DIAGRAM FOR CLUSTERS HW62 and L87
CENTRAL REGIONS
V
14
16
18
20
22
B-V
-0.4
0.0
0.4
0.8
1.2
1.6
2.0
2.4
MV
-6
-4
-2
0
+2

Fig. 76.

Figs. 77 and 78 for the regions 2 and 3 have stars from both populations and mostly blue faint stars. Their red giant branches are not as extensive as the one in Fig. 51 which means that the red stars beyond B-V ~ 1.2 are members of the cluster HW62. The star with M_V = -3.15 and B-V = 1.71 lies at the central region and most likely it is a cluster member. This cluster is an SMC halo type cluster but the red H-B is very poor and this would mean that it is an intermediate age cluster, probably younger than the western type of clusters.

4.2. The north-west spiral arm - (second group)

This group comprises two clusters located on a feature of the SMC like a spiral arm where NGC 458 (Arp, 1958) is found as well. Standard stars from NGC 458 photoelectric sequence combined with those in Kron 3 and 47 TUC were used for the calibration of the photographic photometry in order to reach the faint limits.

These two clusters are HW64 and L90. Each cluster was divided into equal areas around their centre and the separate C-M diagrams and the composite ones have been produced. All these areas give C-M diagrams which show two clearly distinguished branches. One is the red giant branch and the other is the main sequence, both in the same range of absolute magnitude. An attempt was made to find clusters in our Galaxy which would produce the same sort of evolutionary track. In Fig. 79 the galactic

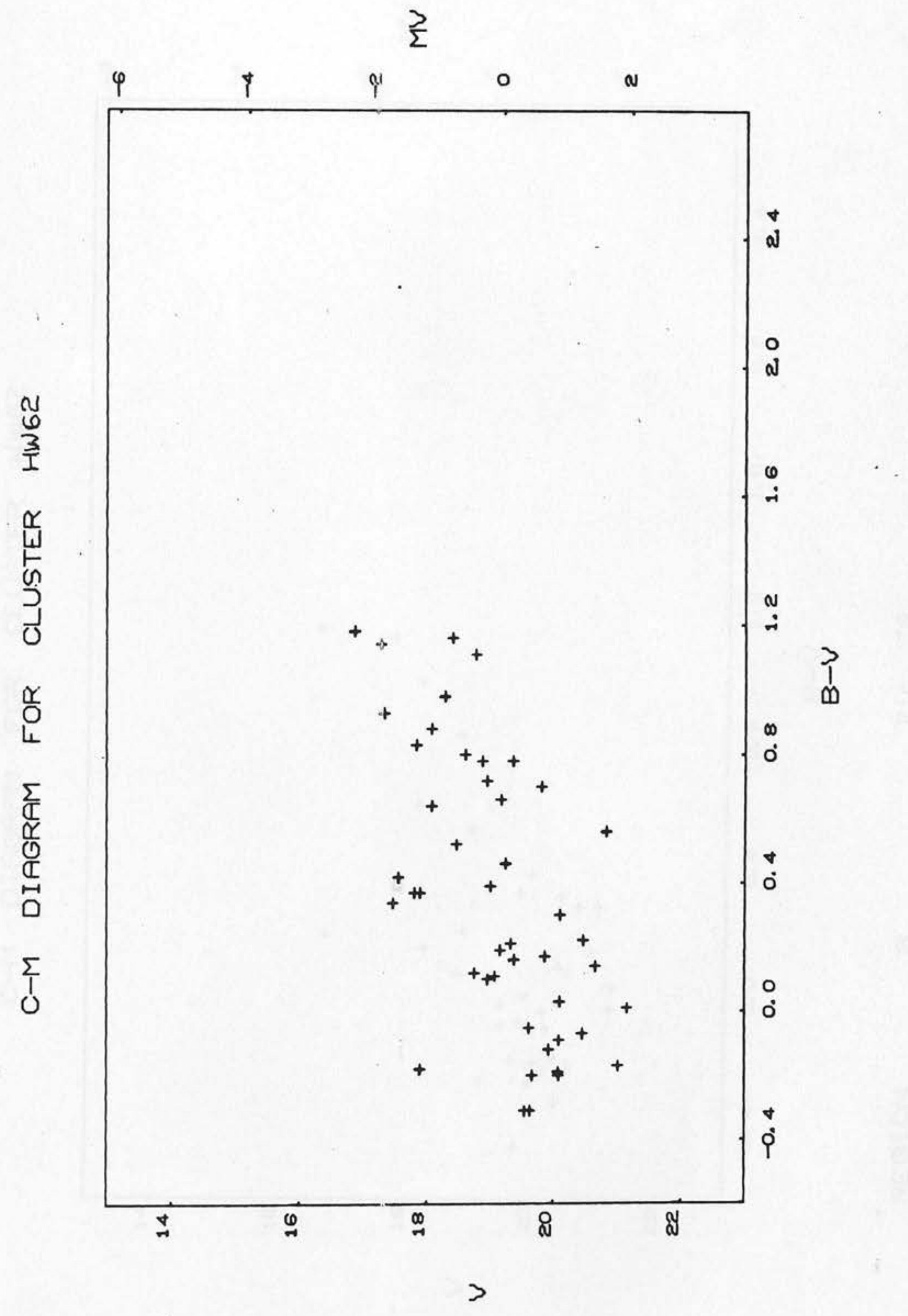
C-M DIAGRAM FOR CLUSTER HW62
V
14
16
18
20
22
MV
-6
-4
-2
0
2
-0.4
0.0
0.4
0.8
1.2
1.6
2.0
2.4
B-V
REGION 2

Fig. 77.

C-M DIAGRAM FOR CLUSTER HW62

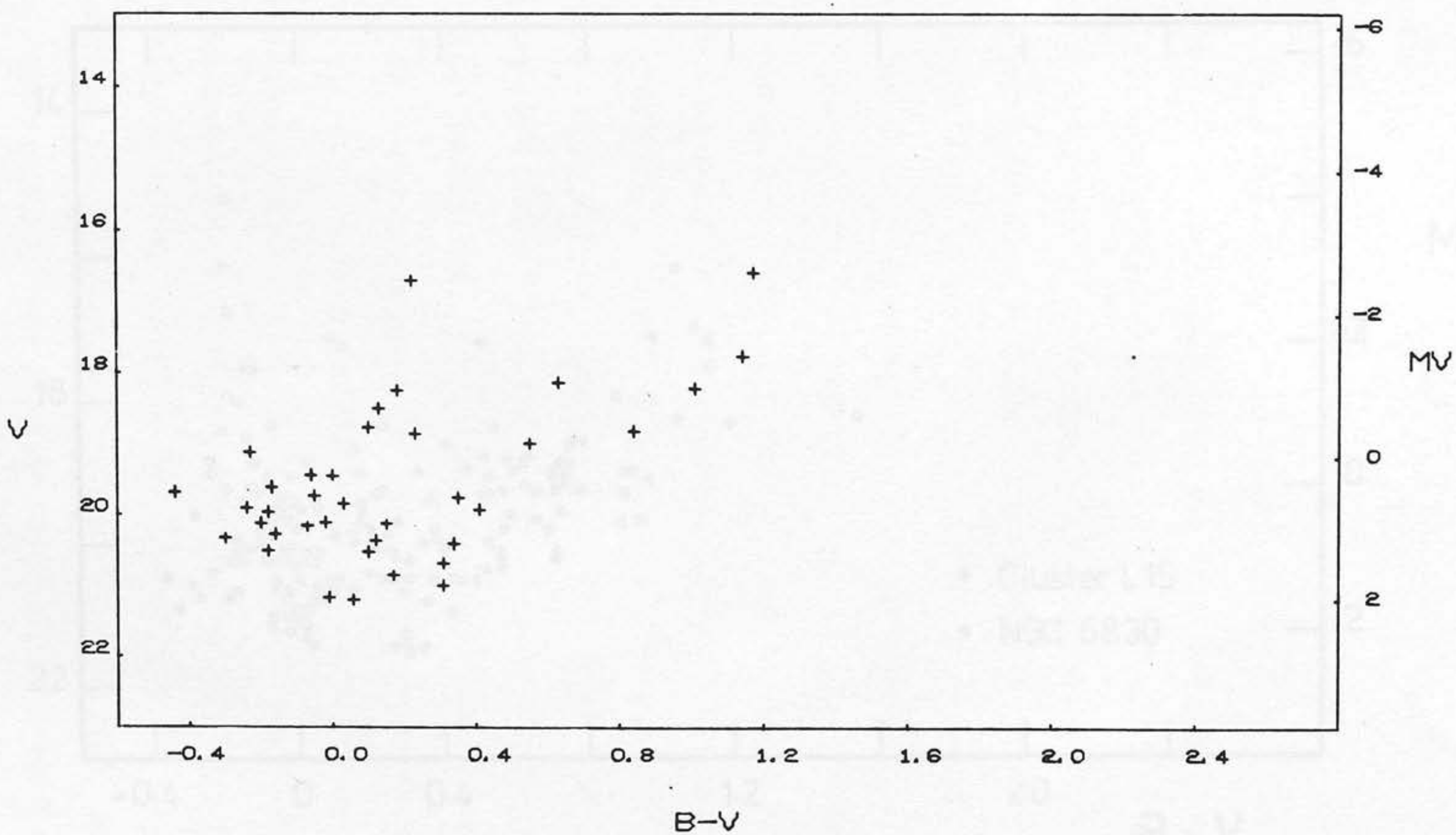

REGION 3

Fig. 78.

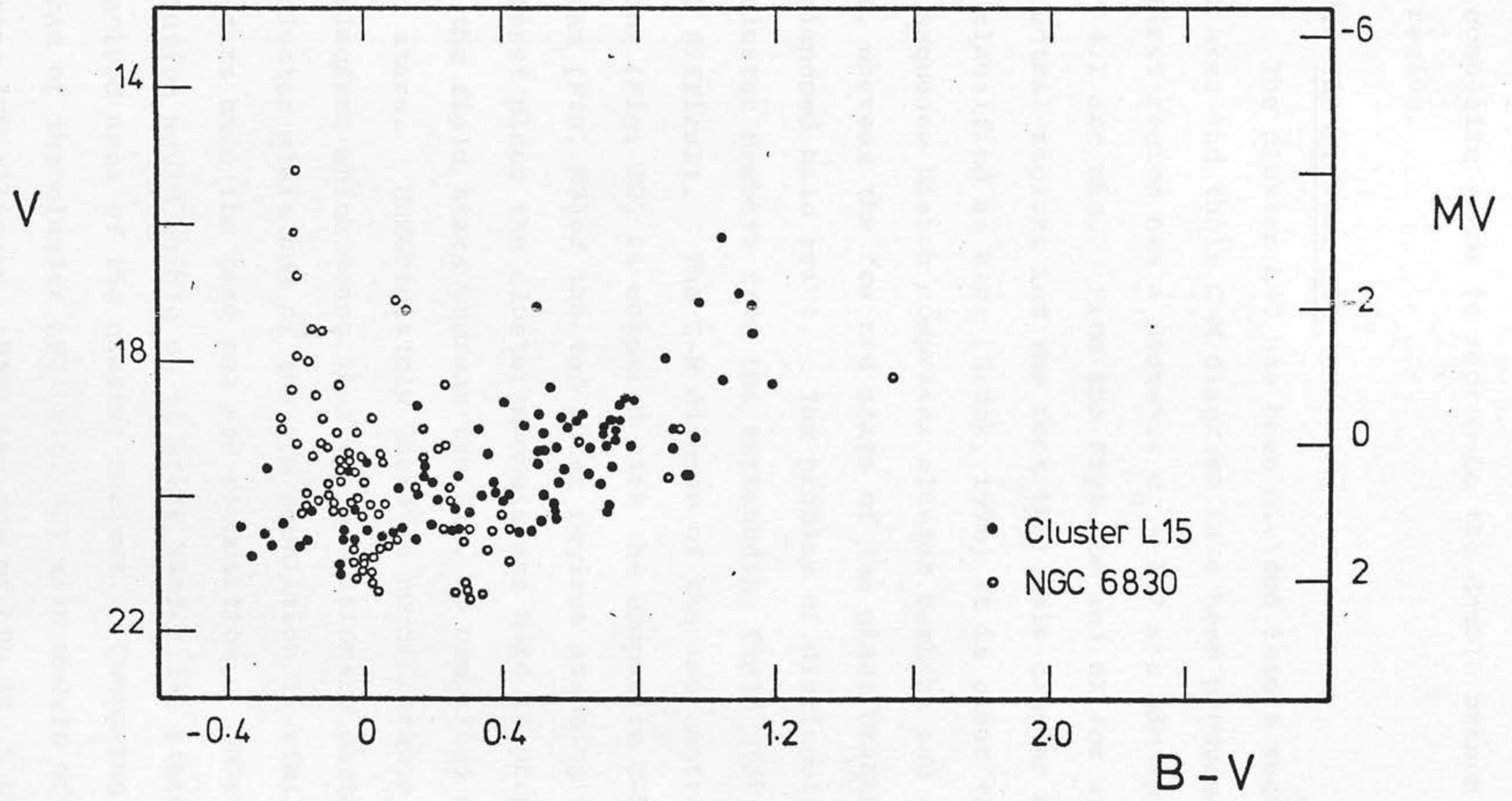

Fig. 79. Composite C-M for the clusters L15 (SMC) and the galactic cluster NGC 6830 (Johnson et al. 1961).

cluster NGC 6830 (Johnson et al. 1961) is combined with L15 of the SMC which represent the halo population and this composite seems to reproduce the double branch of this region.

4.2.1. The cluster L90

The cluster L90 has been divided into 6 regions of equal area and their C-M diagrams have been produced. The first region has a diameter $d_c \sim 1.7$ arc min and $d_{out} \sim 4.1$ arc min. From the Figs. 80 and 81 for stars of the central regions and the fact that this cluster has been classified as blue (Brück, 1976) it is clear that the main sequence branch comprises cluster members and field stars, whereas the few red stars of the giant branch are superimposed halo stars. The problem of distinguishing the cluster members from the surrounding field stars is still difficult. The C-M diagram of the two central regions (Fig. 82) is compared with the composite C-M diagram (Fig. 83)of the two outer regions assuming that in the first place the cluster members are more in proportion than the field stars whereas the Fig. 83 comprises mainly field stars. Unfortunately there is no difference in these two diagrams which means that the evolutionary pattern of the cluster stars and of the arm population is similar, and the stars have the same age and composition. Only better resolution would enable us to study better the stars in the unresolved area of the cluster nucleus. Comparing the C-M diagram of the cluster L90 (Fig. 82) with models of galactic clusters (Shleisinger, 1969) the age of L90 is 5×10^7 years .

C-M DIAGRAM FOR CLUSTER L90

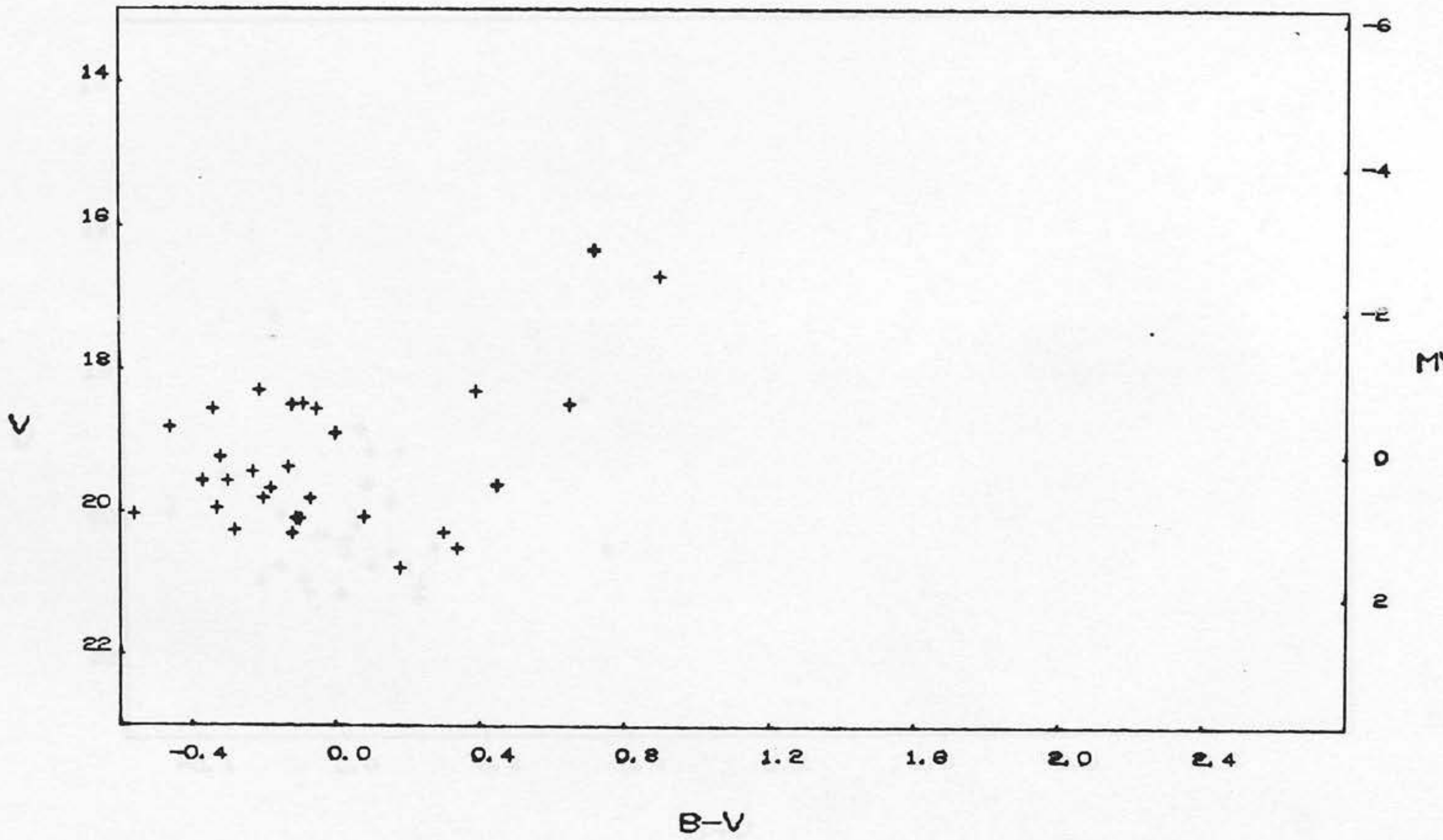

REGION 1

Fig. 80.

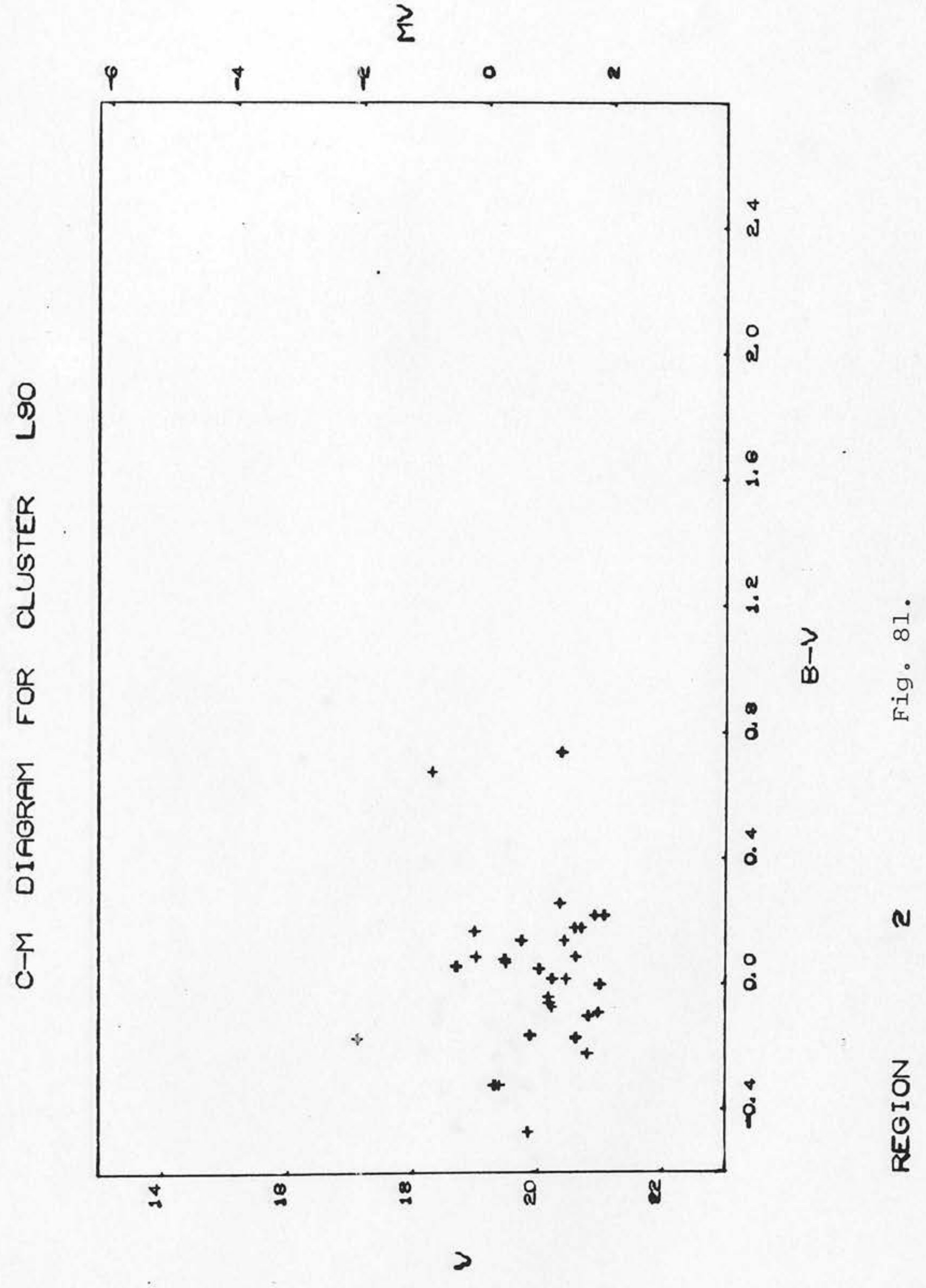
C-M DIAGRAM FOR CLUSTER L90
MV
-6
-4
-2
0
2
V
14
16
18
20
22
B-V
-0.4
0.0
0.4
0.8
1.2
1.6
2.0
2.4
REGION 2

Fig. 81.

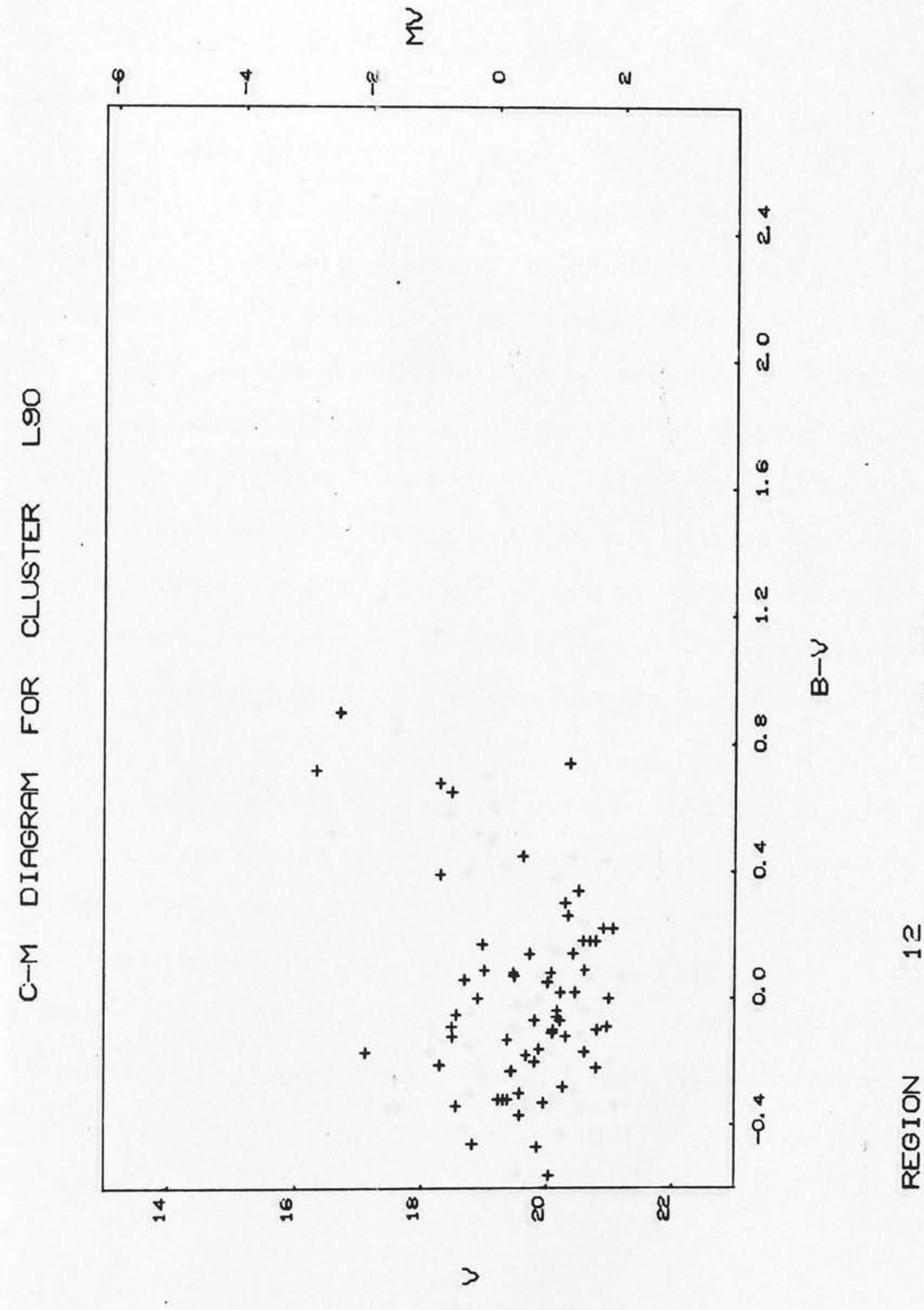
C-M DIAGRAM FOR CLUSTER L90
REGION 12
V
MV
B-V
14
16
18
20
22
-6
-4
-2
0
2
-0.4
0.0
0.4
0.8
1.2
1.6
2.0
2.4

Fig. 82.

C-M DIAGRAM FOR CLUSTER L90

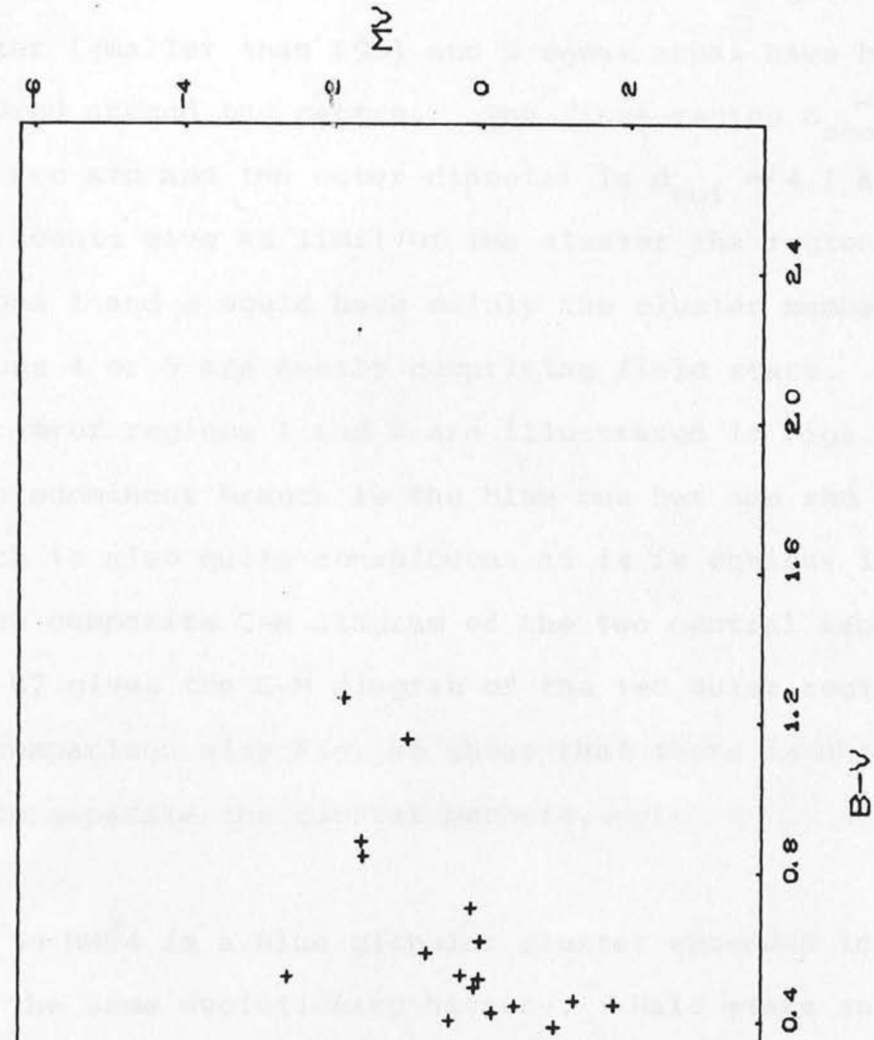

REGION 56

Fig. 83.

4.2.2. <u>The cluster HW64</u>

The cluster HW64 is located near the cluster L90 and both on the same arm. This cluster is a globular-like cluster (smaller than L90) and 5 equal areas have been measured around the centre. The first region $d_{centr} \sim 1.9$ arc min and the outer diameter is $d_{out} \sim 4.1$ arc min. Star counts give as limit of the cluster the region 2, so regions 1 and 2 would have mainly the cluster members whereas regions 4 or 5 are mostly comprising field stars. The C-M diagrams of regions 1 and 2 are illustrated in Figs. 84 and 85. The predominent branch is the blue one but one red giant branch is also quite conspicuous as it is obvious in Fig. 86, the composite C-M diagram of the two central regions. Fig. 87 gives the C-M diagram of the two outer regions and comparison with Fig. 86 shows that there is not any way to separate the cluster members.

So HW54 is a blue globular cluster embedded in a field with the same evolutionary history. Halo stars superimposed on this field give the typical C-M diagram of the SMC for the population II stars. One very red star with $M_V = 1.12$ and B-V = 2.01 is at the central region of the cluster but it is rather an halo object superimposed on this region. The age of HW64 is also $\sim 7 \times 10^7$ years like L90 (see 4.1.2.).

C-M DIAGRAM FOR CLUSTER HW64

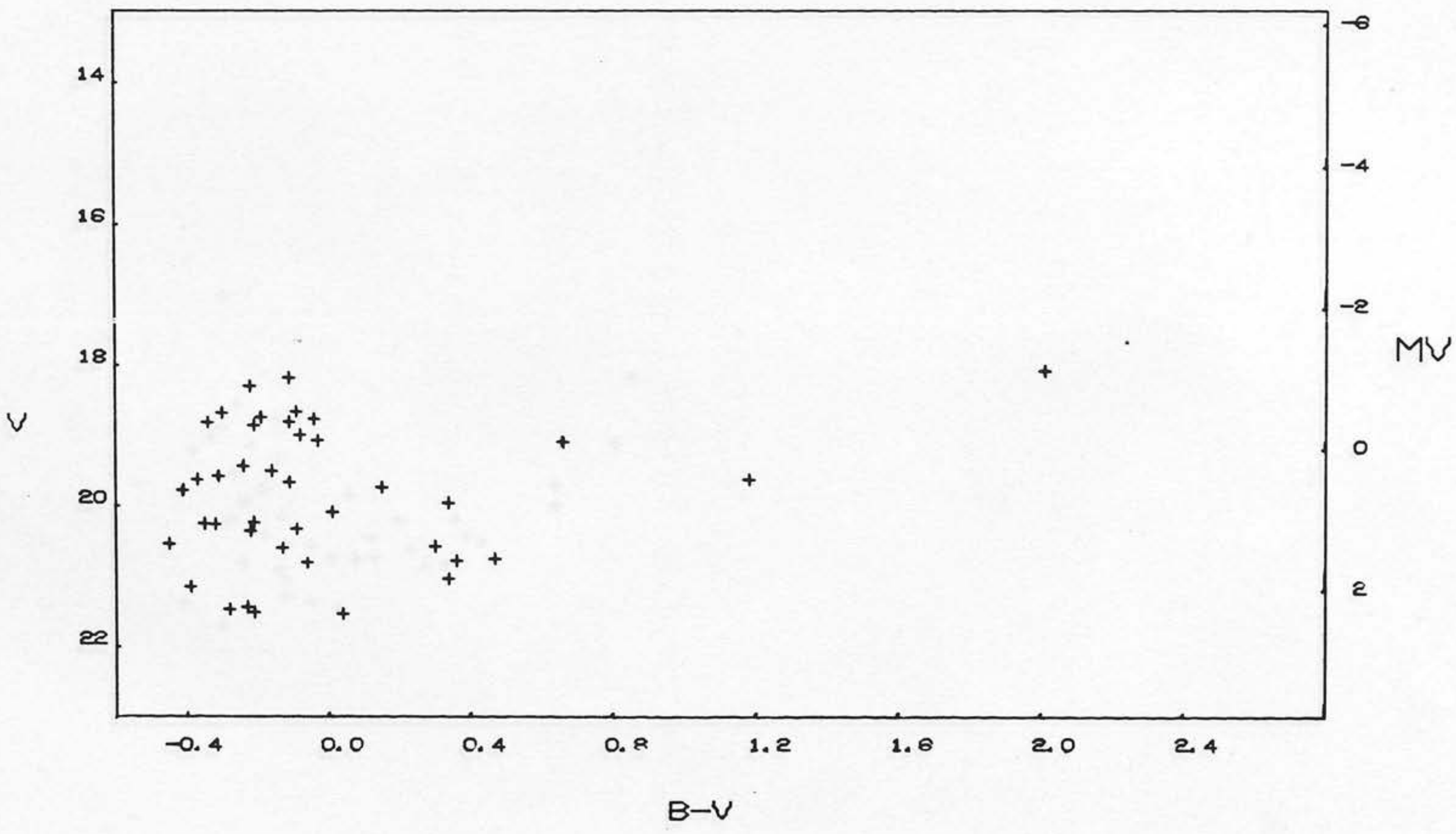

REGION 1

Fig. 84.

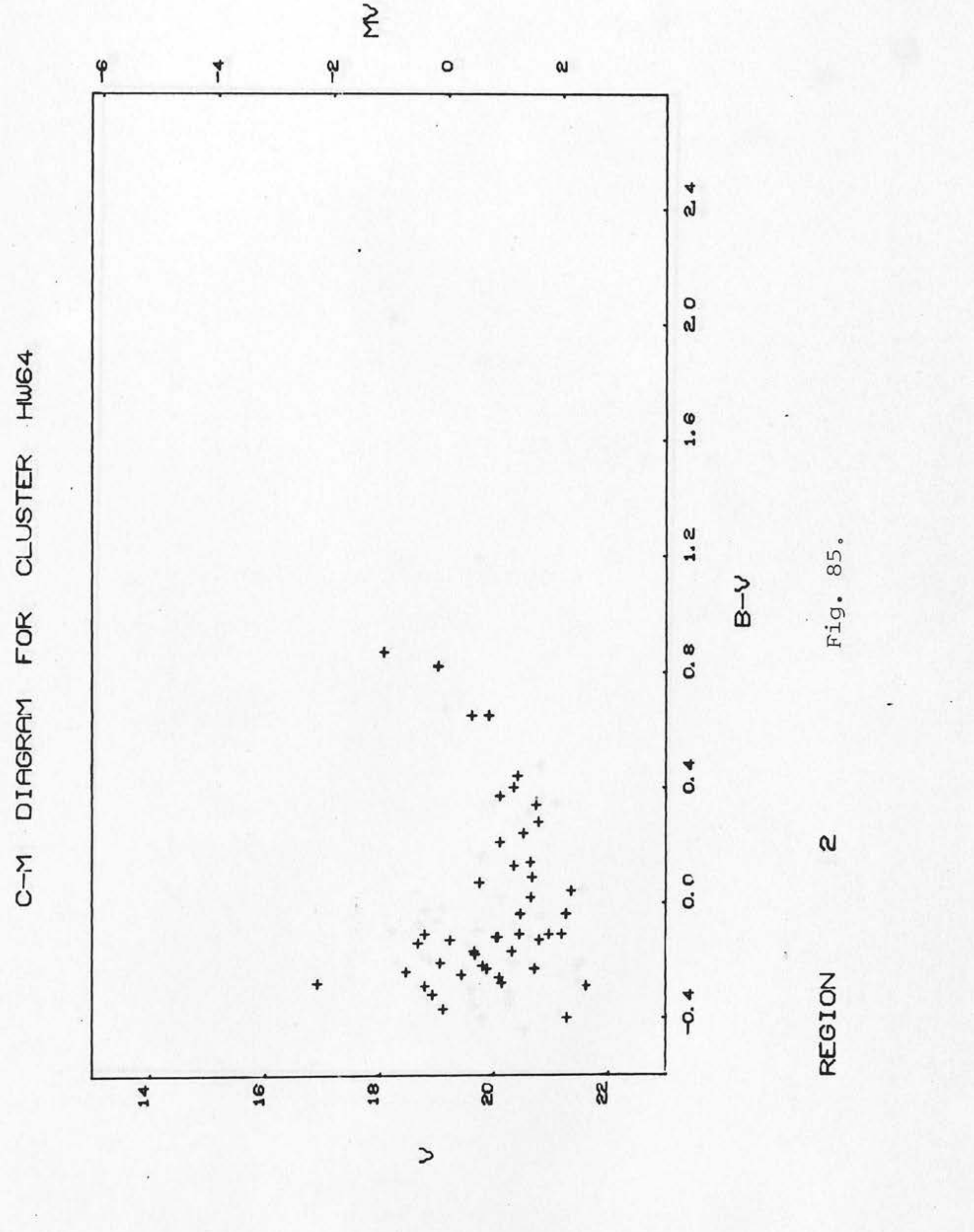

C-M DIAGRAM FOR CLUSTER HW64
REGION 2
V
14
16
18
20
22
MV
-6
-4
-2
0
2
B-V
-0.4
0.0
0.4
0.8
1.2
1.6
2.0
2.4

Fig. 85.

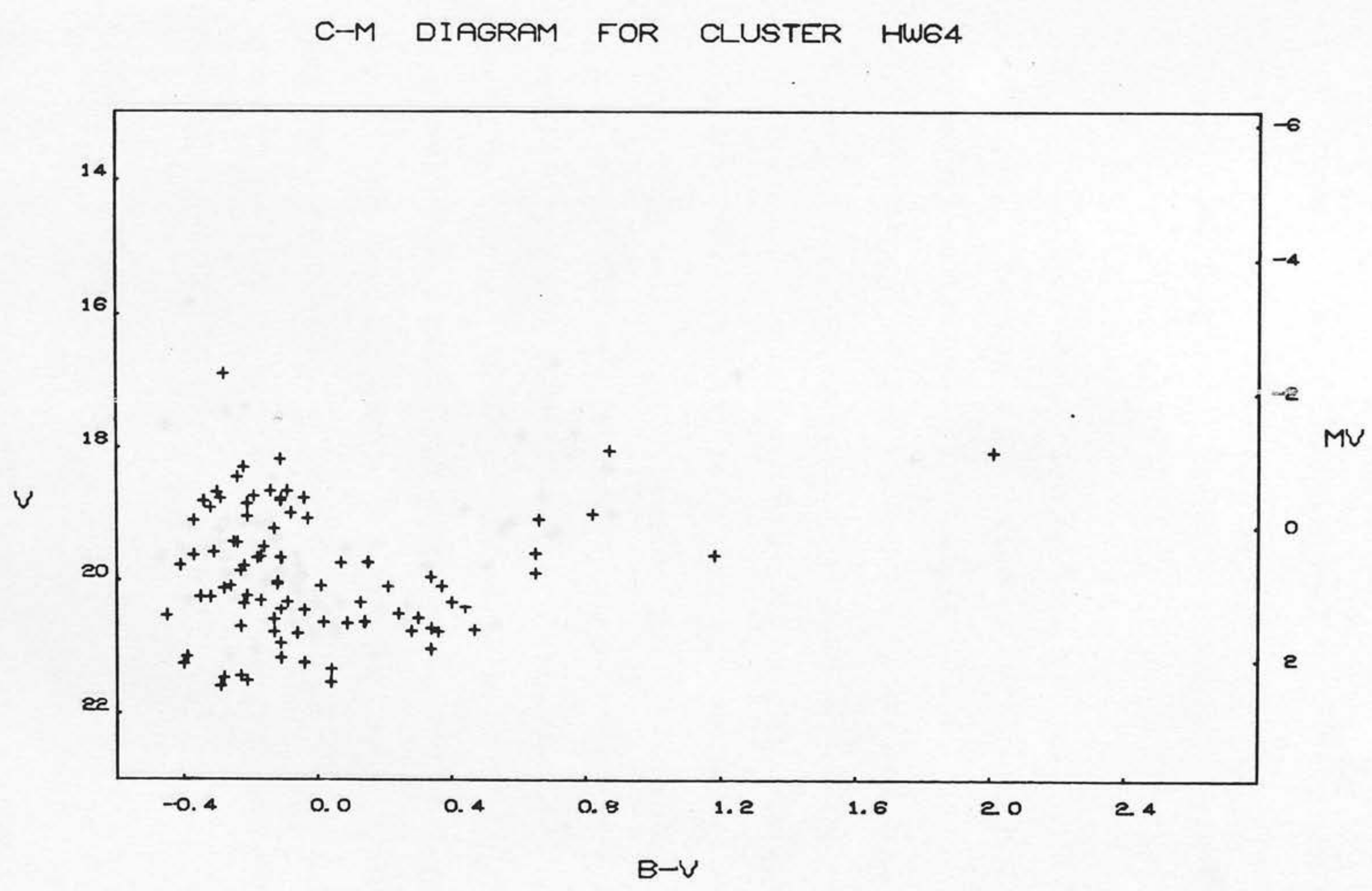

REGION 12

Fig. 86.

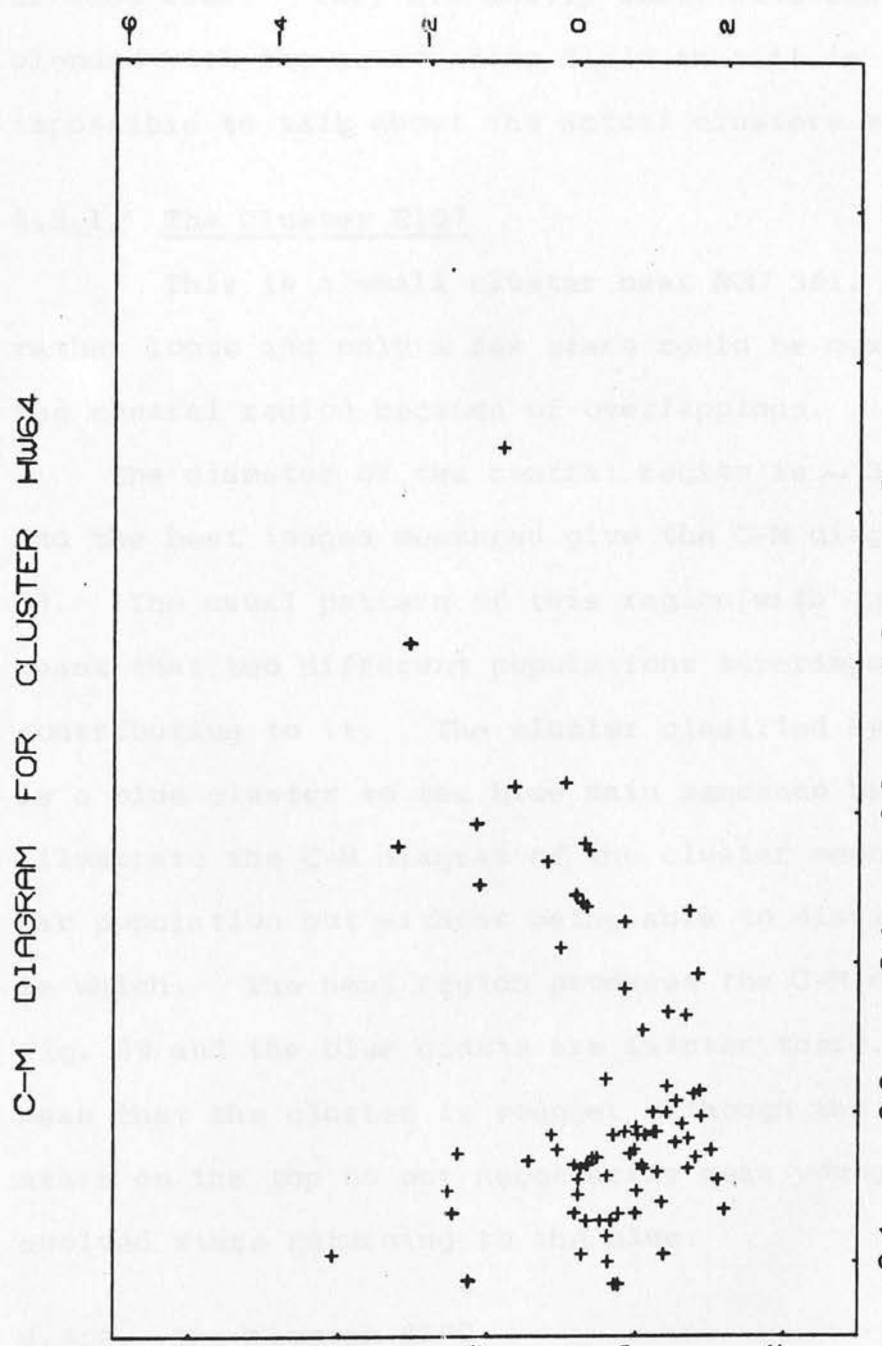
C-M DIAGRAM FOR CLUSTER HW64
MV
-6
-4
-2
0
2
-0.4
0.0
0.4
0.8
1.2
1.6
2.0
2.4
B-V
14
16
18
20
22
V
REGION 45

Fig. 87.

4.3. Third group

The last group comprises clusters of the north part of the SMC near the cluster NGC 361 which is in a crowded area. They are mostly small clusters and so blended with the surrounding field that it is almost impossible to talk about the actual clusters separately.

4.3.1. The cluster E107

This is a small cluster near NGC 361. It is rather loose and only a few stars could be measured in the central region because of overlappings.

The diameter of the central region is $\sim$ 3.8 arc min and the best images measured give the C-M diagram of Fig. 88. The usual pattern of this region(with two branches) means that two different populations superimposed are contributing to it. The cluster clasified by Brück (1976) is a blue cluster so the blue main sequence branch must illustrate the C-M diagram of the cluster members and of the bar population but without being able to distinguish which is which. The next region produces the C-M diagram of Fig. 89 and the blue giants are fainter there. This might mean that the cluster is younger although the blue bright stars on the top do not necessarily mean younger age, but evolved stars returning to the blue.

4.3.2. The cluster E102

This is another small blue cluster near the cluster NGC 361. The crowding makes difficulties as always in this area. Stars in three regions around the cluster have

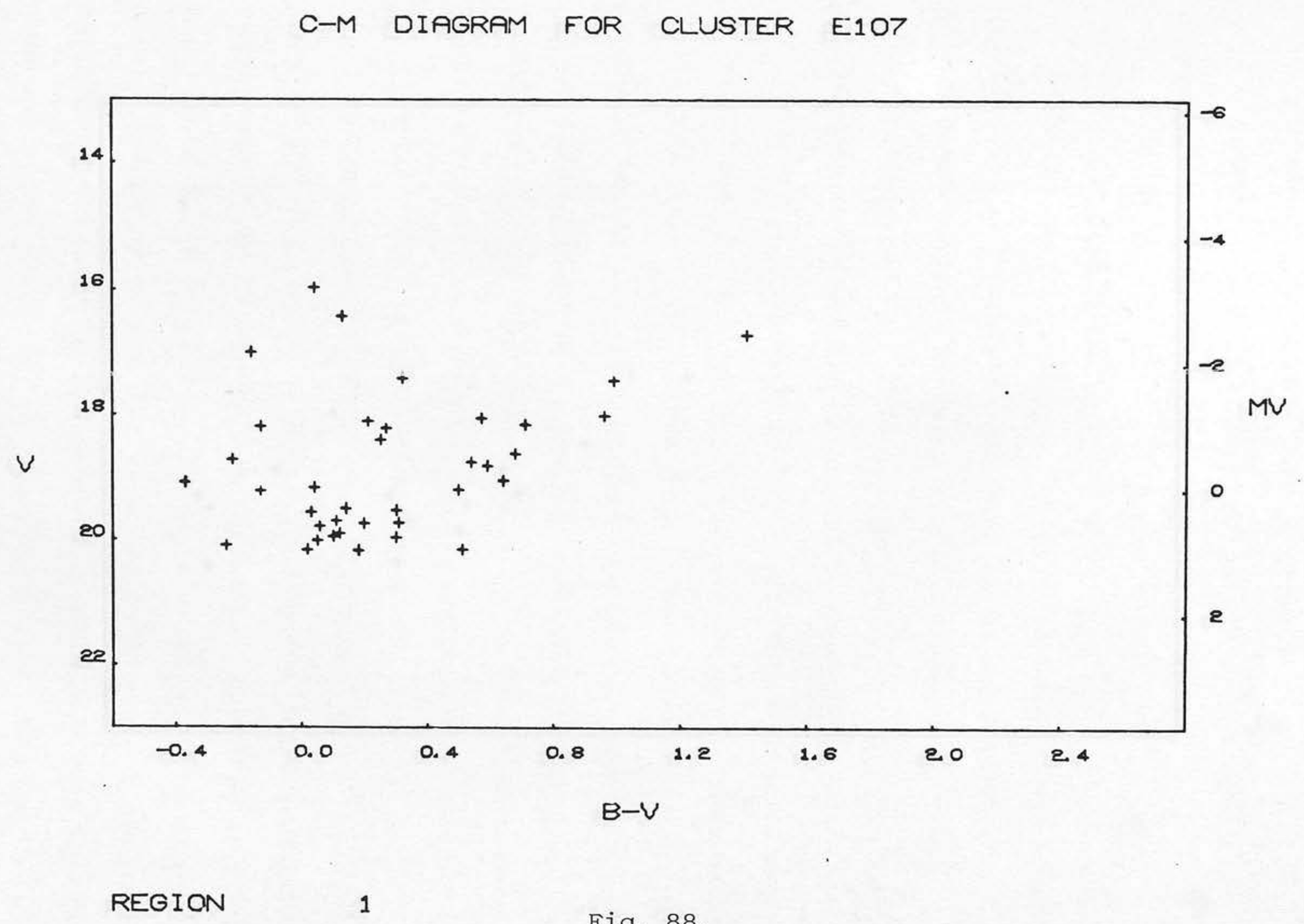
C–M DIAGRAM FOR CLUSTER E107
V
14
16
18
20
22
−0.4
0.0
0.4
0.8
1.2
1.6
2.0
2.4
B–V
MV
−6
−4
−2
0
2
REGION 1

Fig. 88.

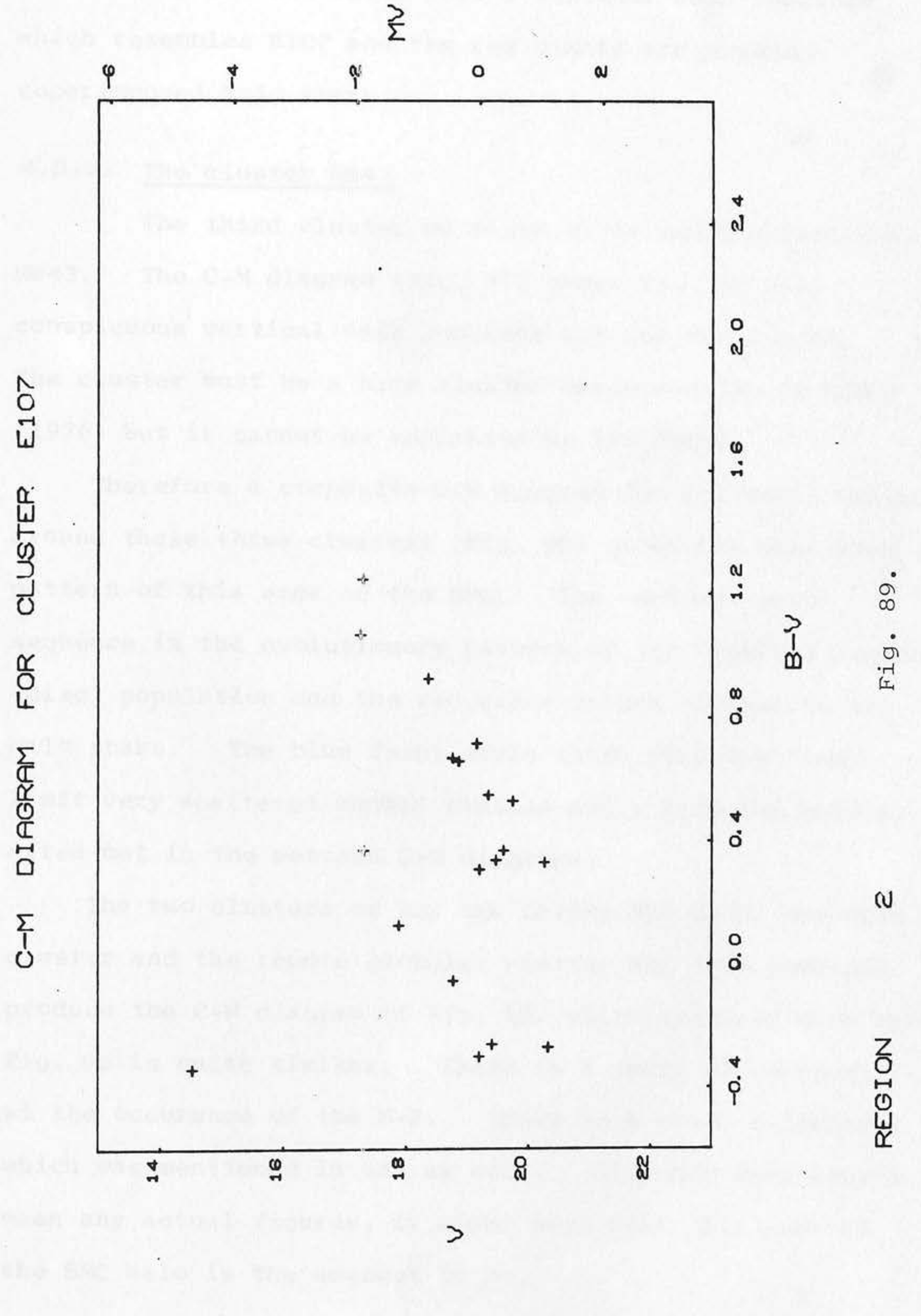
C-M DIAGRAM FOR CLUSTER E107
REGION 2
MV
-6
-4
-2
0
2
V
14
16
18
20
22
B-V
-0.4
0.0
0.4
0.8
1.2
1.6
2.0
2.4

Fig. 89.

been measured and the diameter of the central region is $d_{centr} \sim 1.6$ arc min, which gives the C-M diagram of Fig. 90. The cluster and its field form a vertical main sequence which resembles E107 and the red giants are probably superimposed halo stars.

4.3.3. The cluster HW43

The third cluster of these three small clusters is HW43. The C-M diagram (Fig. 91) comprises one very conspicuous vertical main sequence and one red branch. The cluster must be a blue cluster one, according to Brück (1976) but it cannot be separated by its field.

Therefore a composite C-M diagram for all stars measured around these three clusters (Fig. 92) gives the characteristic pattern of this area of the SMC. The vertical main sequence is the evolutionary pattern of the "central region" (disc) population and the red giant branch represents the halo stars. The blue faint stars which make the faint limit very scattered should include stars from the halo so often met in the western C-M diagrams.

The two clusters of our own Galaxy NGC 6830, one open cluster and the remote globular cluster NGC 7006 combined produce the C-M diagram of Fig. 93 which compared with that of Fig. 92 is quite similar. There is a small difference at the occurance of the H-B. There is a small difference which was mentioned in L82 as well. Although this cannot mean any actual figures, it might mean that this part of the SMC halo is the nearest to us.

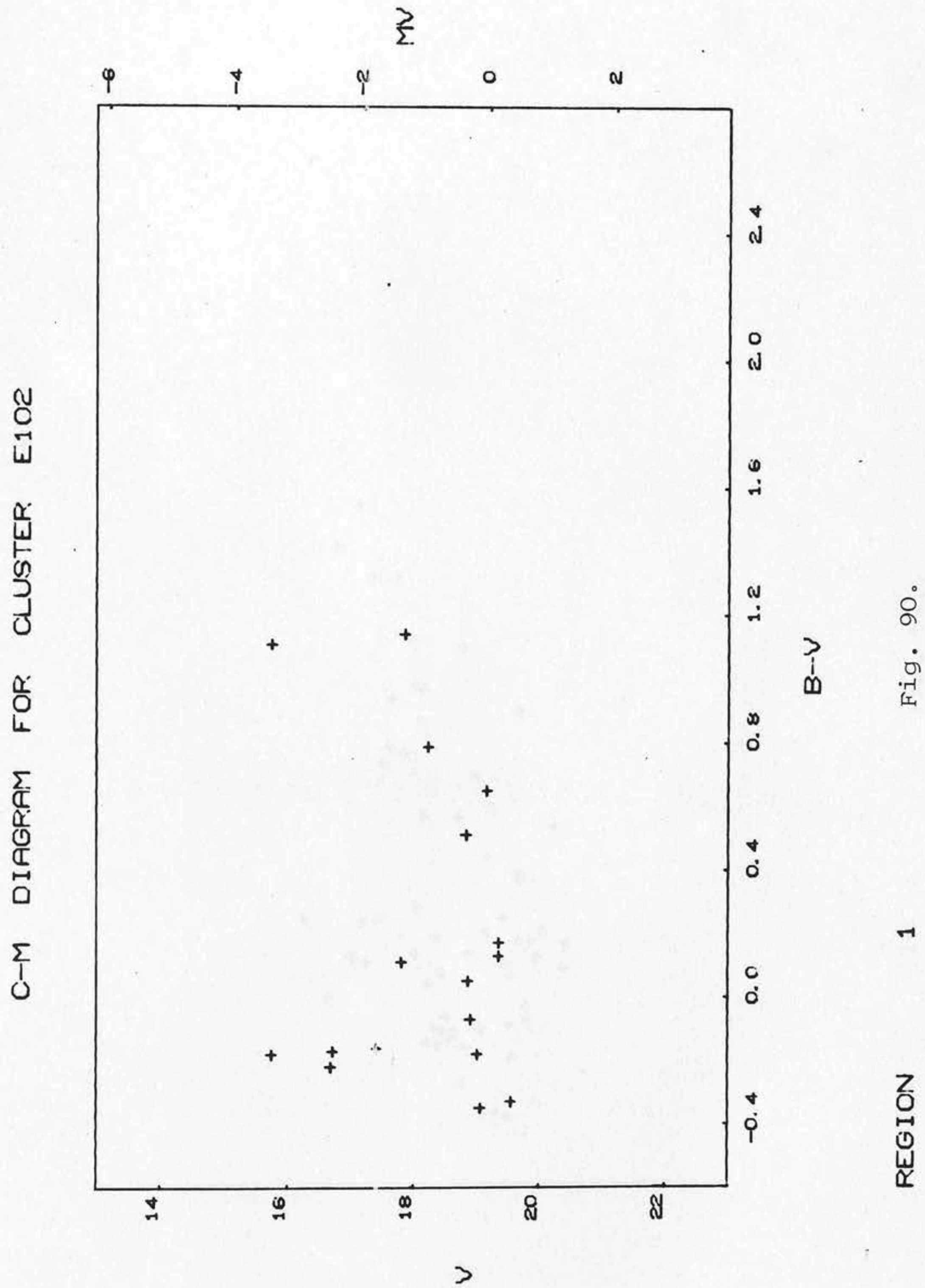
C-M DIAGRAM FOR CLUSTER E102
MV
-6
-4
-2
0
2
V
14
16
18
20
22
B-V
-0.4
0.0
0.4
0.8
1.2
1.6
2.0
2.4
REGION 1

Fig. 90.

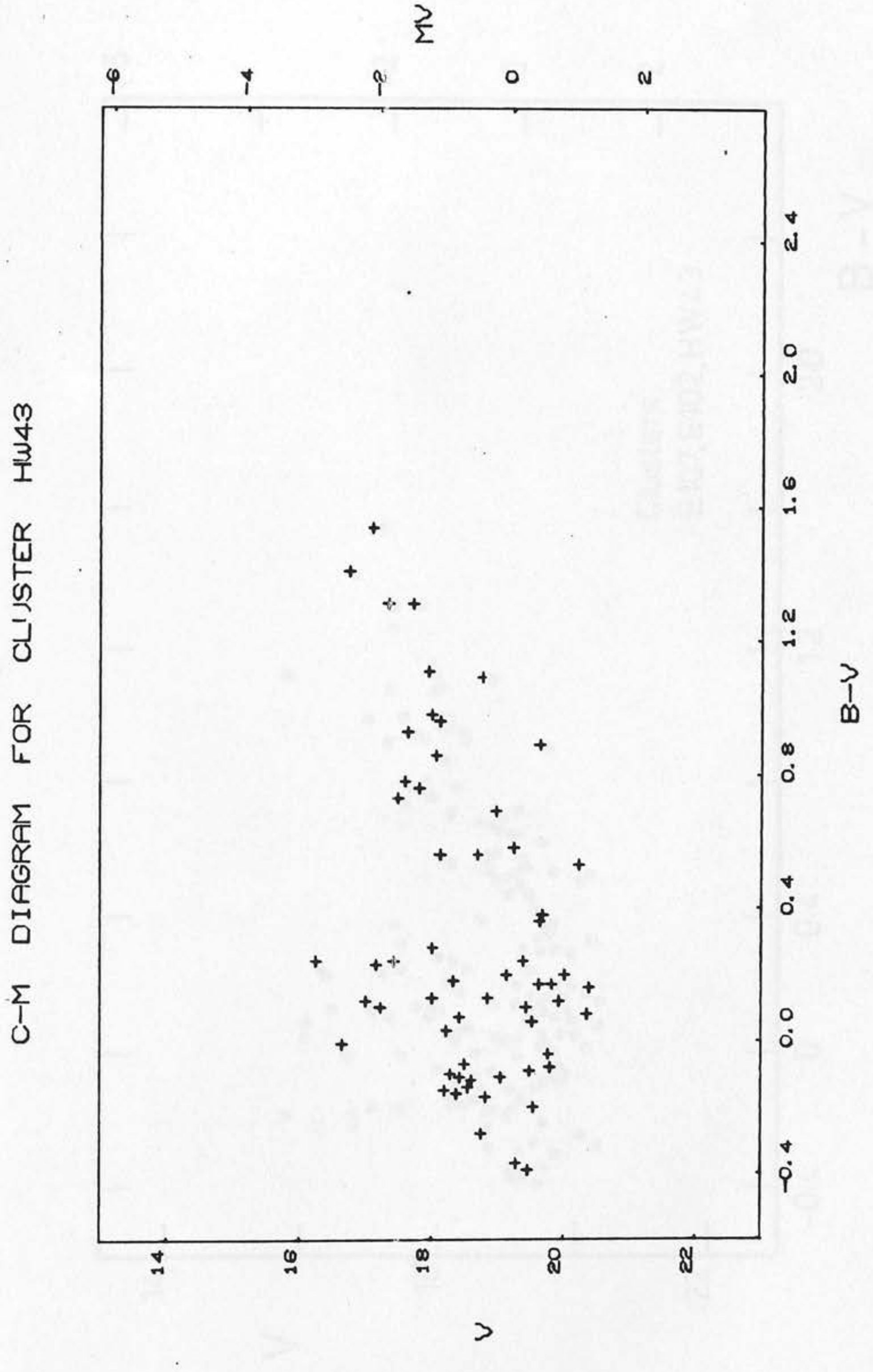

REGION 12

Fig. 91.

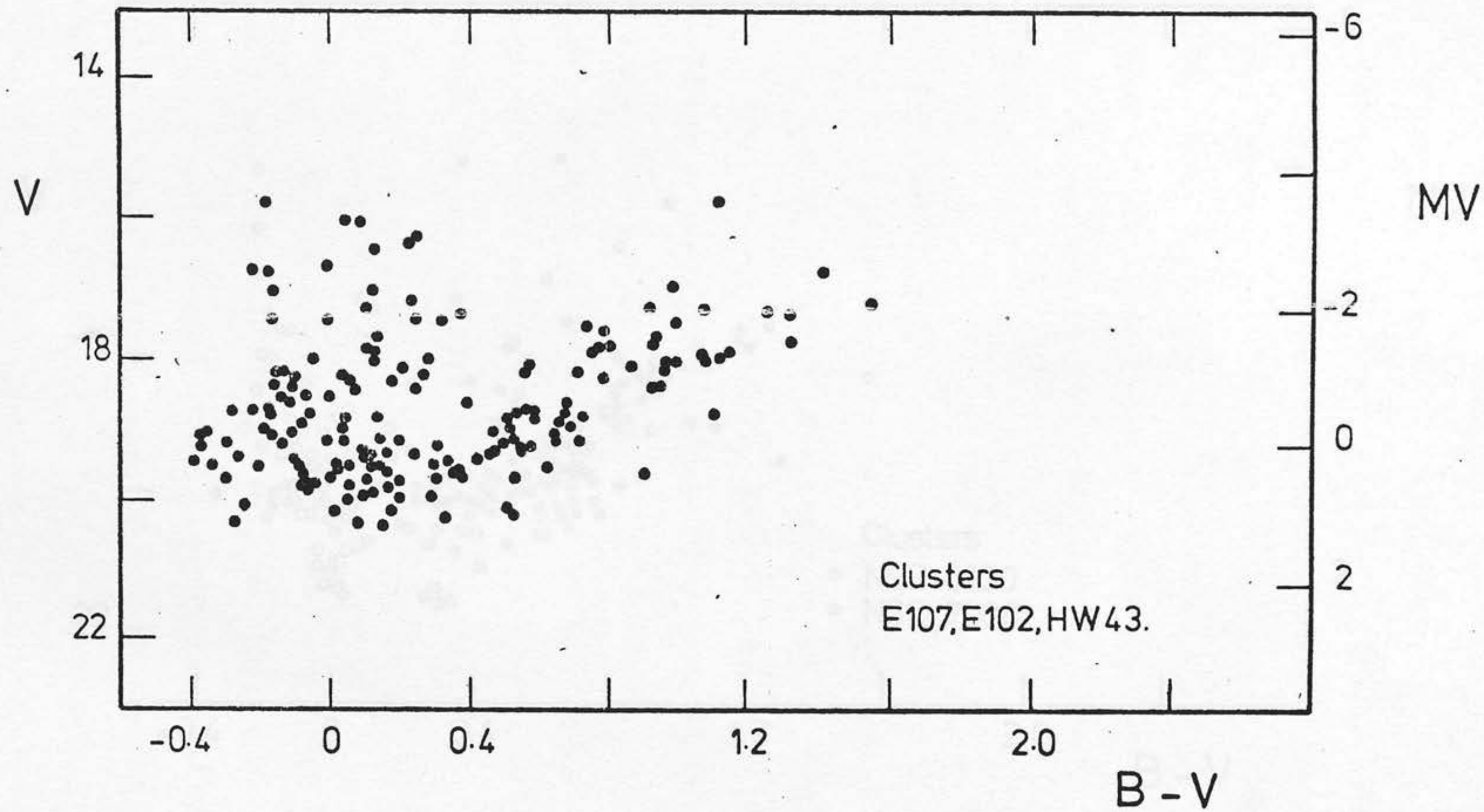

Fig. 92. Composite C-M diagram for clusters E107, E102, HW43.

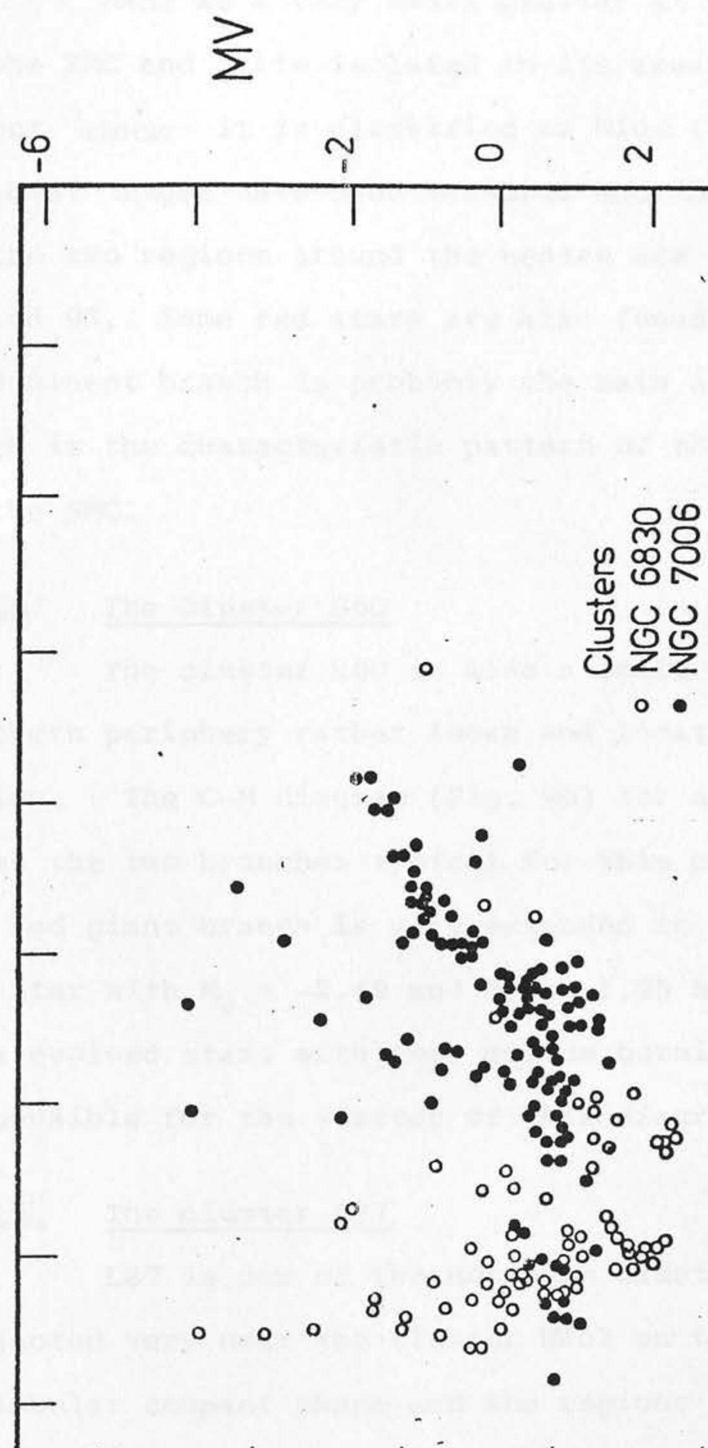

Fig. 93. Composite C-M diagram for the galactic clusters NGC 6830 (Johnson et al. 1961) and NGC 7006 (Sandage, 1967).

4.3.4. The cluster HW32

HW32 is a very small cluster at the northern side of the SMC and quite isolated in its area. It is a young object since it is classified as blue (Brück, 1976). The best images have been measured and the C-M diagrams of the two regions around the centre are given in Figs. 94 and 95. Some red stars are also found but the predominent branch is probably the main sequence one, which is the characteristic pattern of the "central region" of the SMC.

4.3.5 The cluster E60

The cluster E60 is also a small cluster of the northern periphery rather loose and located in a very dense region. The C-M diagram (Fig. 96) for all stars measured shows the two branches typical for this part of the SMC. The red giant branch is very extended in colour and one red star with M_V = -2.69 and B-V = 1.93 has been found. Some evolved stars with core Helium burning might be also responsible for the scatter of this diagram.

4.3.6. The cluster L87

L87 is one of the northern clusters which is projected very near the cluster HW62 on the plate. It has a globular compact shape and the regions measured have been divided into three sectors starting from the centre and towards the opposite direction of HW62 (Fig. 97).

This cluster is very near the bar of the SMC and the "mixing" of different populations is very severe for the investigation of the stellar content of this field.

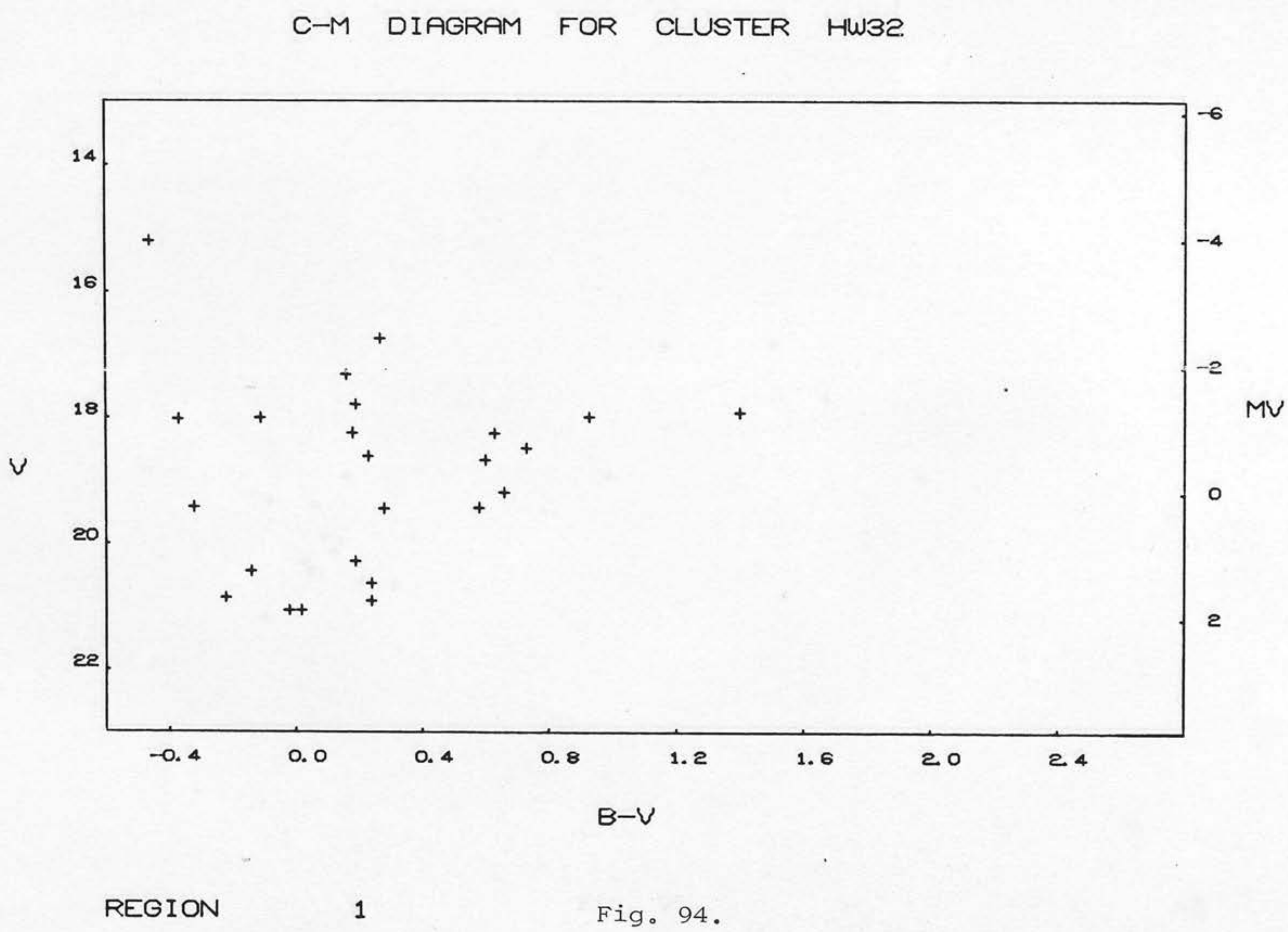
C-M DIAGRAM FOR CLUSTER HW32
14
16
18
20
22
V
-6
-4
-2
0
2
MV
-0.4
0.0
0.4
0.8
1.2
1.6
2.0
2.4
B-V
REGION 1

Fig. 94.

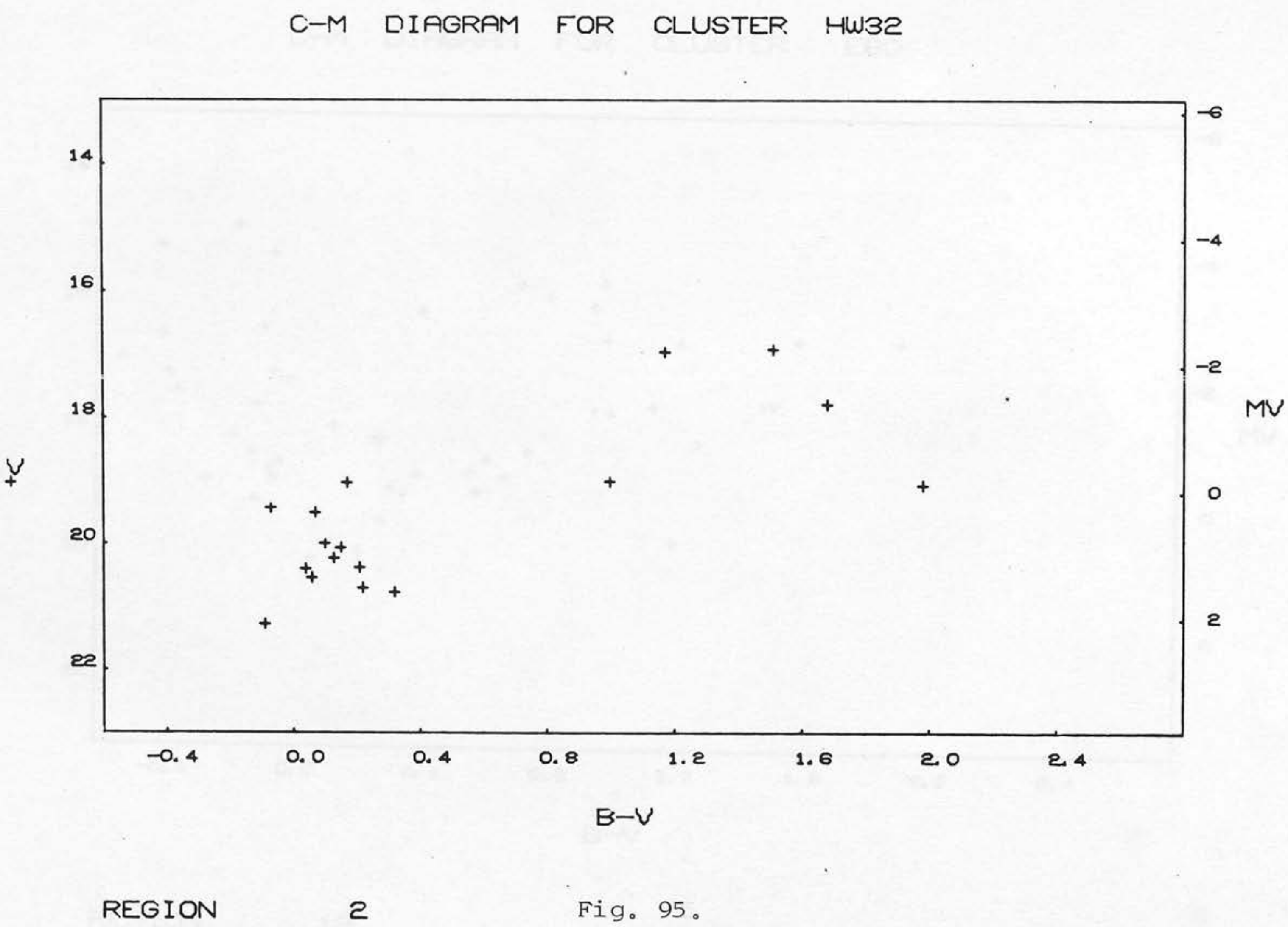
C-M DIAGRAM FOR CLUSTER HW32
V
MV
B-V
14
16
18
20
22
-6
-4
-2
0
2
-0.4
0.0
0.4
0.8
1.2
1.6
2.0
2.4
REGION 2

Fig. 95.

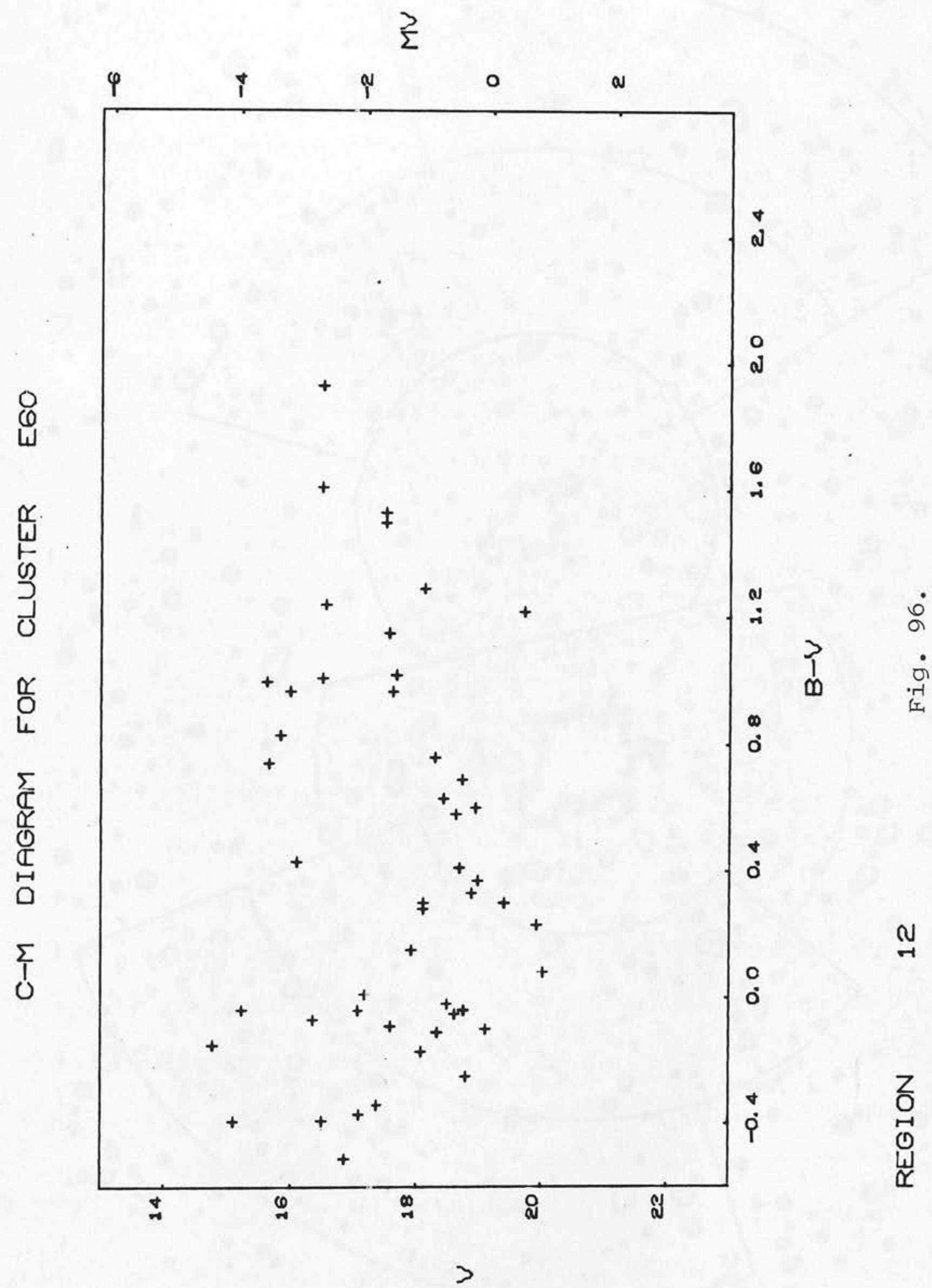
C-M DIAGRAM FOR CLUSTER E60
REGION 12
V
MV
B-V
14
16
18
20
22
-6
-4
-2
0
2
-0.4
0.0
0.4
0.8
1.2
1.6
2.0
2.4

Fig. 96.

Fig. 97. Charts of clusters HW62 and L87.

The C-M diagram of Fig. 98 comprises stars of the halo with stars from the "central region" of the SMC, members of the cluster HW62 and members of the cluster L87. Apart from that, overlapping of images was another difficulty and about 50% of stars were rejected.

The central region has a diameter d ~ 2.0 arc min and the Fig. 98 exhibits one red giant branch bright and extended in colour, up to B-V = 1.71, with faint blue stars as well, very typical for the halo population of the SMC. The same giant branch is present in Fig. 100(of the third region)whereas in Fig. 99(of the second region)it is poor. Kron (1956) and Brück (1976) have classified L87 as predominently blue, so the blue giant branch is characterising the cluster but again we cannot separate it by its surrounding field. From Fig. 99 the main sequence, according to Shleisinger (1969) models,should give an age of 7 x 10^7 years which is probably the age of the "central region" stars around the cluster L87.

For the actual clusters some assumptions can be made. In Fig. 101, an hypothetical C-M diagram might be the representative of L87. In fact it is a composite diagram produced by Fig. 98, the blue branch of Fig. 75 (which is the C-M diagram of the central region of the cluster HW62). This is the C-M diagram of young stars of the "central region" including some cluster members and it is more likely that the bright blue stars are stars of the cluster L87, which in this case is a blue globular cluster (may be not as young as L90 or HW64). Some of the bright blue stars

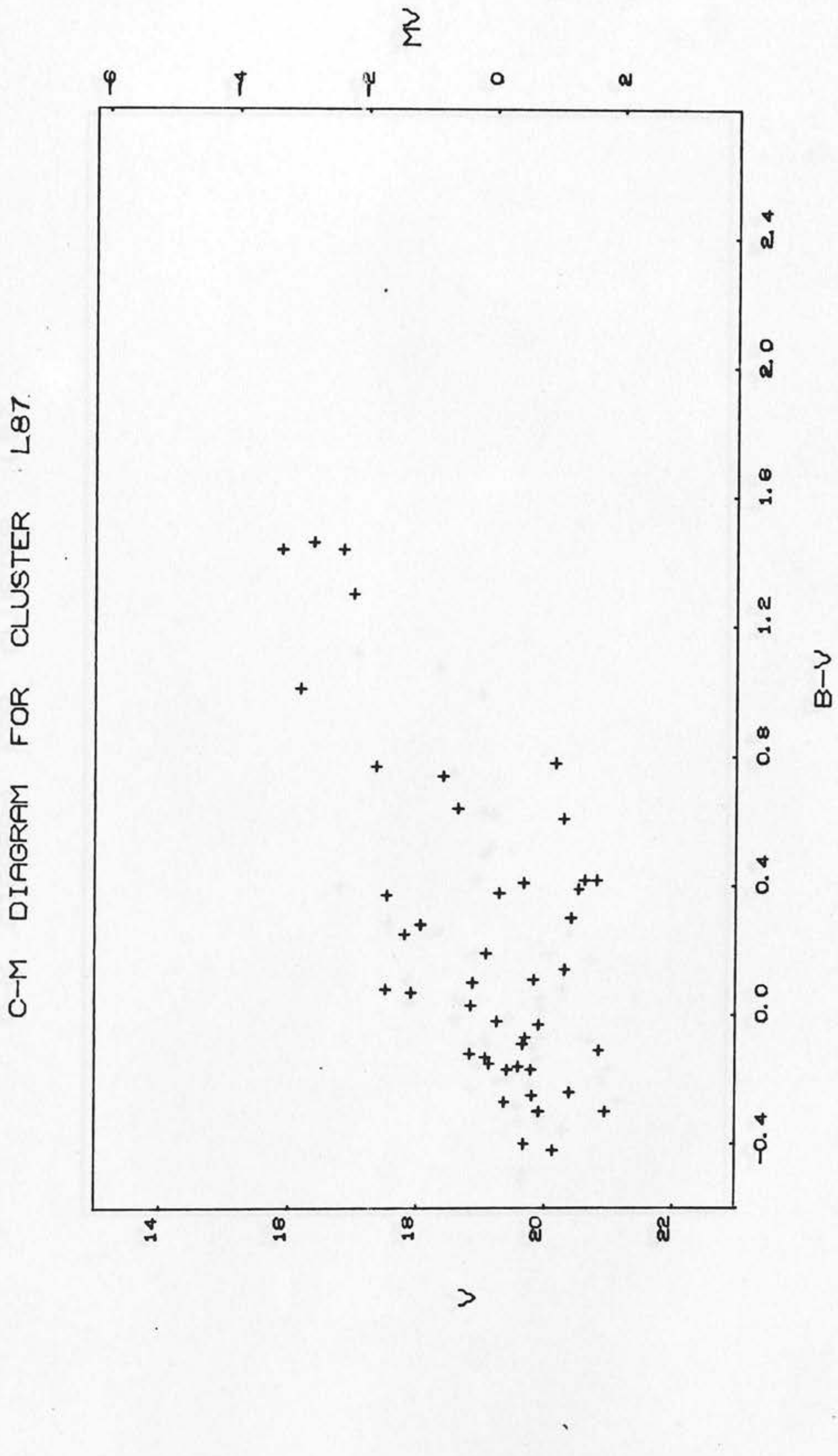

REGION 1

Fig. 98.

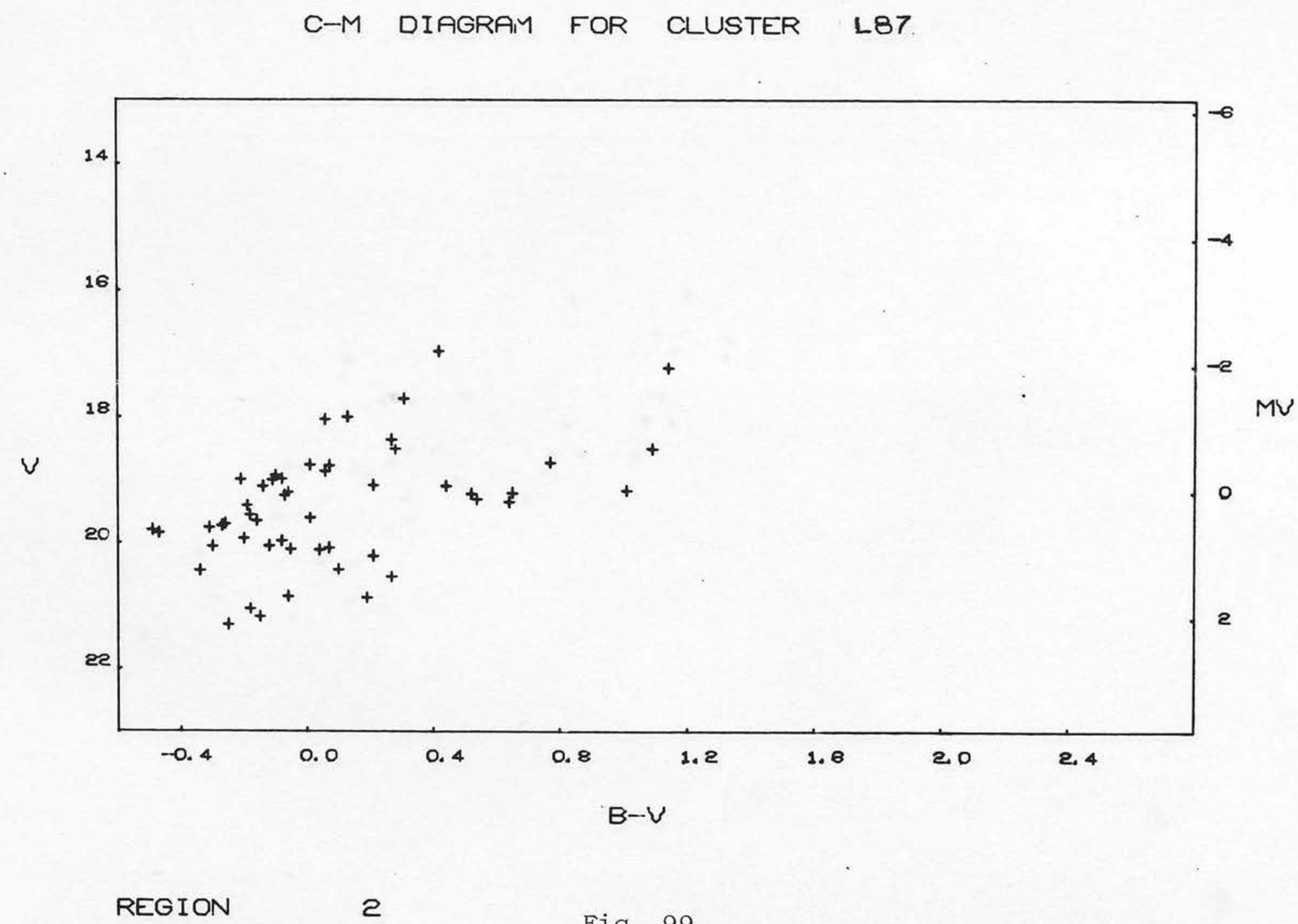
C–M DIAGRAM FOR CLUSTER L87
V
14
16
18
20
22
MV
-6
-4
-2
0
2
-0.4
0.0
0.4
0.8
1.2
1.6
2.0
2.4
B–V
REGION 2

Fig. 99.

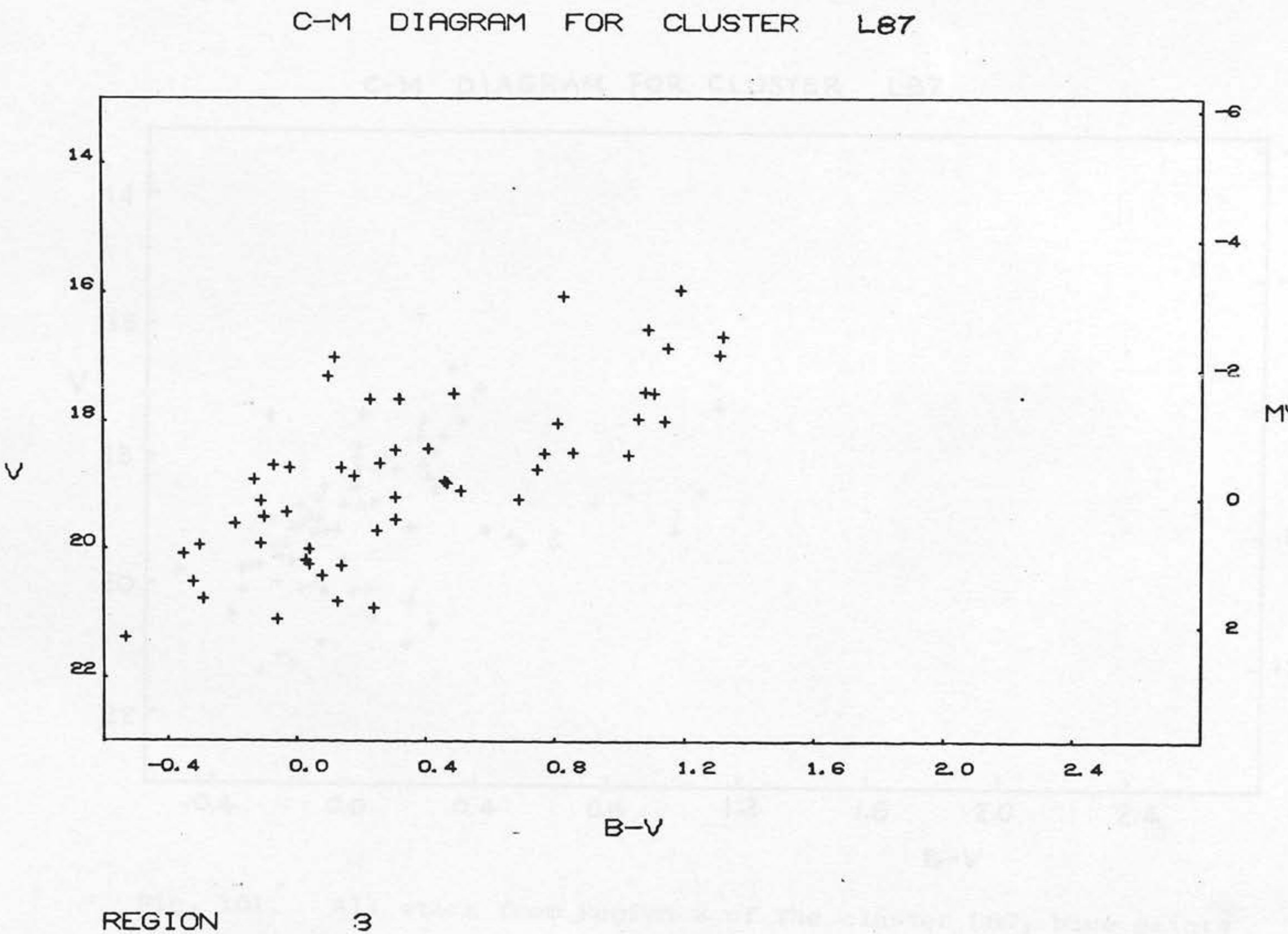
C-M DIAGRAM FOR CLUSTER L87
14
16
18
20
22
V
-6
-4
-2
0
2
MV
-0.4
0.0
0.4
0.8
1.2
1.6
2.0
2.4
B-V
REGION 3

Fig. 100.

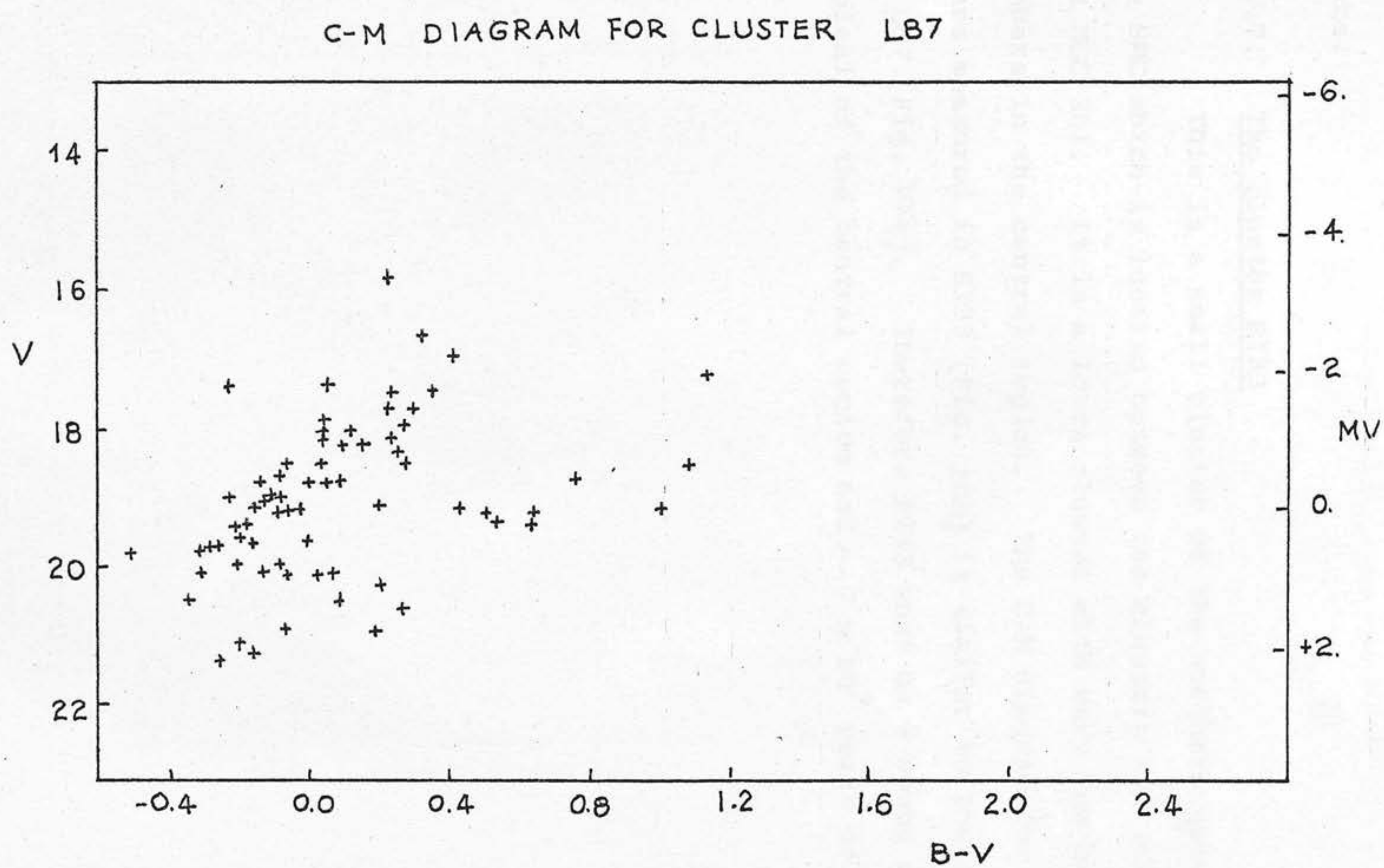

Fig. 101. All stars from Region 2 of the cluster L87, blue gaints from Region 1 of L87 and blue giants from Region 1 of HW62 (Fig. 75).

look like being already evolved core Helium burning stars and therefore their age should be of the order of 7×10^7 years.

4.3.7. <u>The cluster E133</u>

This is a small cluster of the northern side of the SMC which is located between the clusters NGC 362, HW64 and NGC 361. It is a loose cluster with very few bright members in the central region. The C-M diagram for all stars measured in E133 (Fig. 102) is similar to the field of L87 (Fig. 103). Therefore E133 must be a young cluster typical of the central region and $\sim 7 \times 10^7$ years of age.

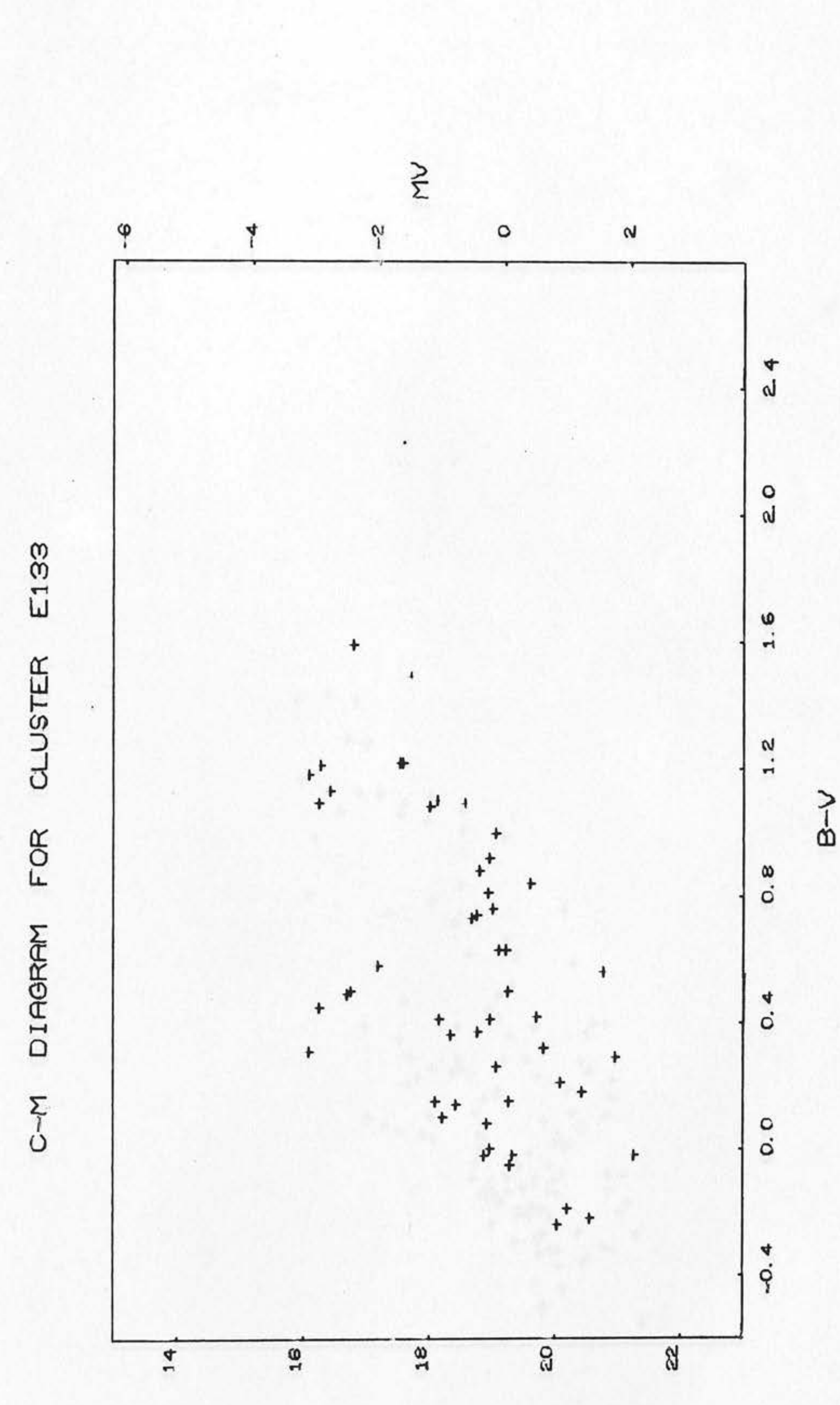

REGION 123

Fig. 102.

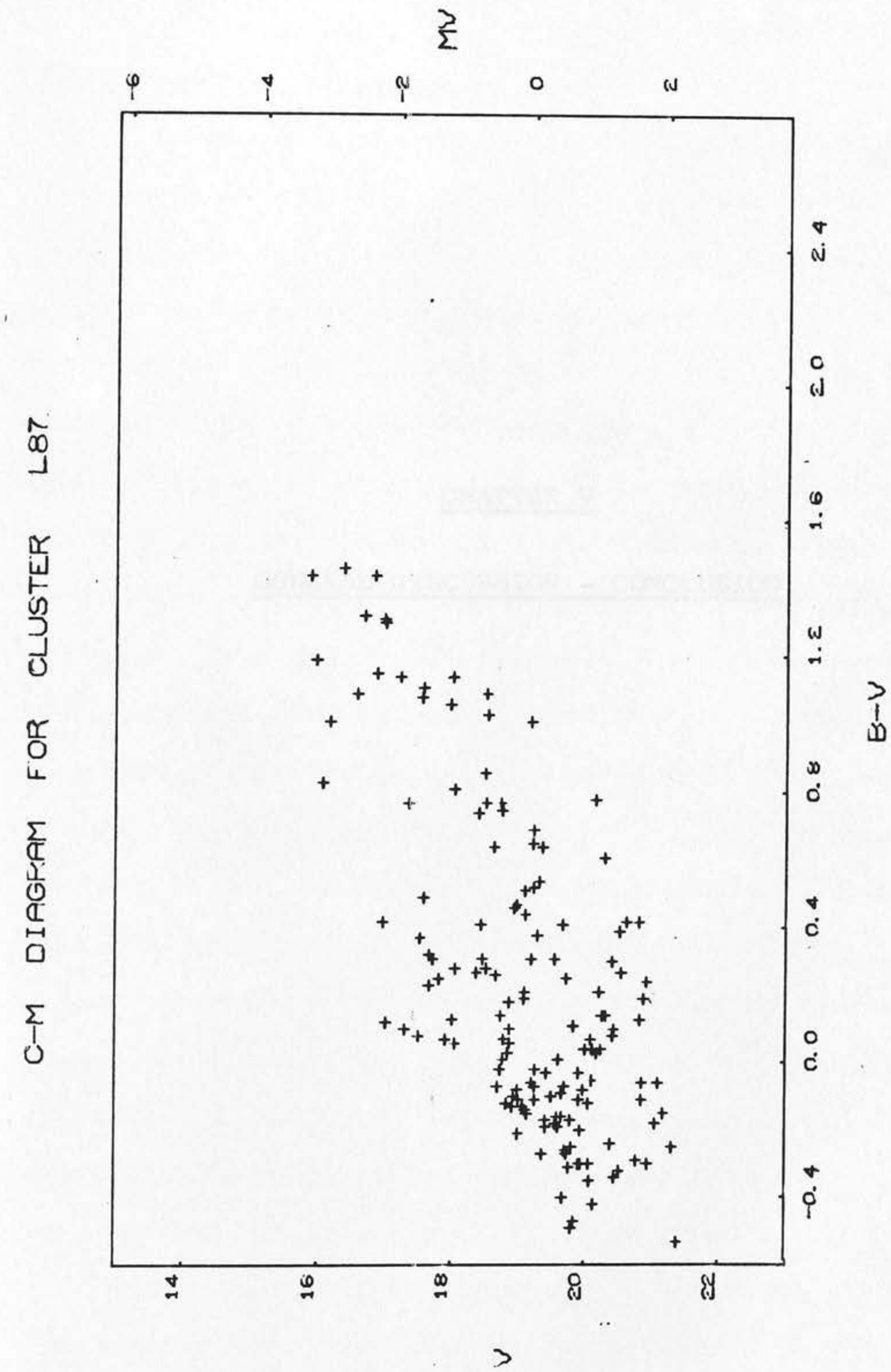
C-M DIAGRAM FOR CLUSTER L87
V
14
16
18
20
22
MV
-6
-4
-2
0
2
B-V
-0.4
0.0
0.4
0.8
1.2
1.6
2.0
2.4
REGION 123

Fig. 103.

CHAPTER V

GENERAL DISCUSSION - CONCLUSION

5.1. In this Chapter the main results are summarised and a detailed discussion is given for the two main groups of clusters and the field stars of the SMC.

5.1.1. Group of old clusters

The old clusters for which the C-M diagrams have been produced are 18. Eleven clusters were studied on the U.K. Schmidt plates in the course of the present project and six more were already known by previous workers. They are spread in all regions of the SMC but the western part seems to be the ideal place to study the old clusters because there is no contamination by young objects. The C-M diagrams consist of a giant branch, a horizontal branch and an unusually large number of blue faint stars scattered from B-V = $-0^m.4$ to B-V = $-0^m.8$. If we produce the composite C-M diagram of some characteristic globular clusters of our own Galaxy including the reddest and bluest tracks then the diagram of Fig. 104a gives the general pattern in our own Galaxy (for the clusters 47 TUC, NGC 362, NGC 288, NGC 4147, NGC 483, NGC 5024, NGC 5897 and NGC 6656). A similar diagram for the SMC is illustrated in Fig. 104b where the stars of the central areas of the clusters L11, L3, L20, L14, L13, L15 and HW22 have been taken. The C-M diagrams of the galactic globulars have been taken by the Atlas of Globular Clusters by Alcaino (1973).

Comparing Figs. 104a and 104b one can see quite a few main differences which can be explained by the evolutionary differences in the two galaxies. First of

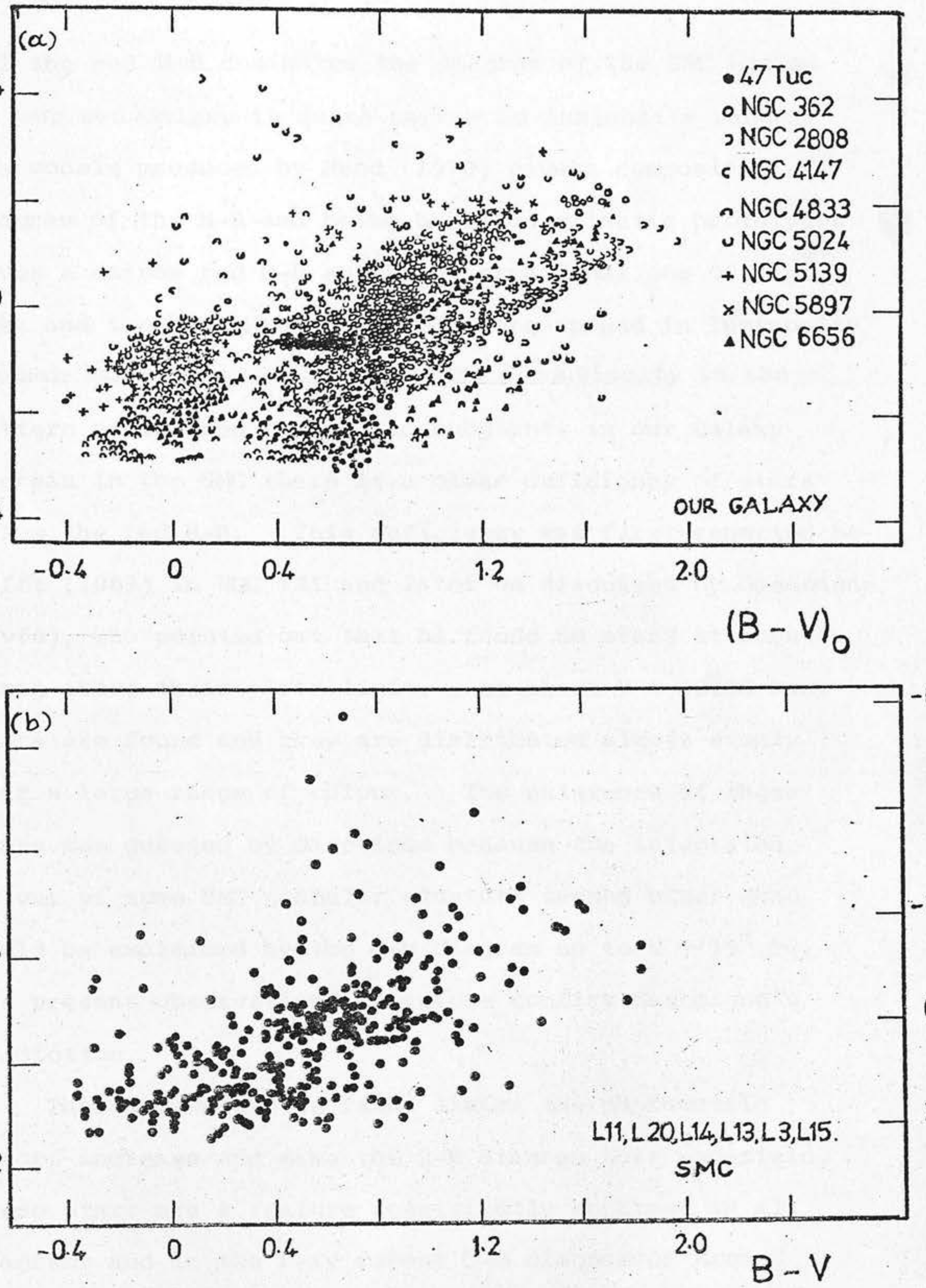

Fig. 104. (a) Composite C-M diagram of galactic globular clusters (Alcaino, 1973).

(b) Composite C-M diagram of the central region of 6 clusters of the western part of the SMC.

all the red H-B dominates the diagram of the SMC but as in our own Galaxy is quite narrow in luminosity range. The models produced by Rood (1970) give a composite C-M diagram of the H-B and being based on galactic prototypes gives a narrow red H-B as the observational one of Fig. 104a and the blue H-B four times more spread in luminosity, rather like Fig. 104a. There is a continuity in the pattern of the red giants and subgiants in our Galaxy whereas in the SMC there is a clear deficiency of stars below the red H-B. This deficiency was first reported by Tifft (1963) in NGC 121 and later on discussed by Gascoigne (1966), who pointed out that he found no stars at about 1 mag above their plate limit. At about $V = 20^{m}.50$ many stars are found and they are distributed almost evenly over a large range of colour. The existence of these stars was guessed by Gascoigne because the integrated colour of some SMC globular clusters seemed bluer than could be explained by the C-M diagram up to $V \sim 19^{m}.50$. The present observations therefore confirm Gascoigne's prediction.

Though towards the faint limits the photometric errors increase and make the C-M diagram more uncertain, these stars are a feature consistently apparent in all diagrams and in the very recent C-M diagram of Kron 3 (Gascoigne, 1976) obtained from the Anglo-Australian Telescope plates as well. The clear gap found in galactic globular clusters between the blue H-B stars and the subgiant branch does not exist in the SMC.

A very conspicuous red H-B seems to be characteristic of the anomalous clusters of our Galaxy or the Draco system Fig. (35) and seems to violate the correlation between the metal abundance and the morphology of the H-B. The SMC has been found metal deficient for many indirect and some direct cases (Chapter III). Consequently two possibilities can be supported.

(a) the halo clusters are metal deficient and form a red H-B which implies that a third parameter is needed apart from z and age to explain the behaviour of the H-B. The Nitrogen was proposed as a parameter and it seems that the SMC is deficient in Nitrogen, or

(b) the activity of a nucleus of a galaxy may be responsible for the formation of heavy elements and this activity seems rather slow in galaxies with no dense nuclei (van den Bergh, 1974). So the unusual H-B could be a matter of age and the clusters can be younger in age than their galactic counterparts but metal deficient.

One fact supporting the idea of a younger age is the existence of very red stars which have been found in three clusters (Feast and Evans 1973) to be carbon stars. In our own Galaxy there are no carbon stars observed in the old globular clusters though they have been found in some intermediate age clusters.

The faint blue stars also require explanation. Some of the blue faint stars can be blue H-B stars and probably field stars mainly because in very few cases there is a clear evidence of a blue H-B in individual clusters.

This is consistent with the fact that Graham (1975) found a big proportion of RR Lyrae stars in the field around the cluster NGC 121 and the north part of the SMC near the cluster NGC 361. He reported that there are 10 times as many RR Lyrae stars in the SMC as in our own Galaxy. So a considerable number of population II stars must exist in the field of the SMC. This however does not explain the stars which fall in the gap between the blue H-B and the subgiant region.

There is a possibility also, that some of these stars are "blue stragglers". In NGC 188 (Cannon 1968) and M71 (Arp and Hartwick, 1971) (both intermediate age objects) have reported that the number of blue stragglers is approximately the same as the number of subgiants in the same range of luminosity. Some of these stars are displaced from their proper locus on the C-M diagram because they are close binaries and some mass exchange takes place which make the stars look bluer, thus forming a pseudo-horizontal branch. Stellar rotation can also displace the stars on the C-M diagram. Fast rotating stars appear displaced to the right of the zero age main sequence (Golay, 1974) towards higher or lower luminosity. Feast in 1974 has reported that the fast rotating stars are quite numerous in the SMC, which could explain some of these faint stars.

So these characteristics would imply that the age of the globular clusters in the SMC is somehow younger than in our own Galaxy and they possibly are 10^9 - 5×10^9 years old.

To summarise the results for the old group of clusters the table 4 is giving the main characteristics of each cluster studied in the present work or previously.

In table 4 it is obvious that the red H-B is the main conspicuous feature of the old globular clusters except in the case of L13 which is found to have a blue H-B as well. It would be very interesting to re-examine L13 with a high resolution telescope to confirm this result. For the red clusters of the northern part it is not easy to make sure if there are blue H-B stars because there is contamination with the young population of the bar and the central system of the SMC. But there is not any strong evidence for the existence of blue H-B in those clusters.

One last and very important remark is that all clusters seem to be embedded in a field of the same evolutionary history which implies that mixing has not occurred in the SMC halo.

The clusters found to be old objects and for which the C-M diagram is produced are 18 so far, as it is seen in column 1. The different parameters of the columns 2-8 are read off the C-M diagrams.

Column 2 gives the name of each cluster and especially its number in the catalogue it first appeared. In columns 3 and 4 a description of the H-B is given as far as the colour is concerned. The description red means that almost all stars of the horizontal branch occupy the red side of the variable stars strip.

The actual limits of column 4 are not very reliable

TABLE 4

Old clusters of the SMC with known C-M diagrams

		H-B			Red Giant Branch		Very Red Stars		
No.	Cluster Name	Description	Colour extent from	to	Bright Limit V	(B-V)max	M_V	B-V	Remarks
1	NGC 121	red	+0.2	+0.8	16.50	+1.70 V	-2.60	+1.90	Studied by Tifft(1963)
2	L11	red	+0.45	+1.0	16.50	+1.60	-2.65	+2.54	
3	HW40	red	+0.5	+1.0	17.50	+1.40	-2.59	+2.80	
4	L20	red	+0.2	+0.60	17.00	+1.60 V	-	-	
5	HW22	red	+0.1	+0.50	16.50	+1.70 V	-	-	
6	NGC 419	red	+0.4	0.80	16.00	+1.70	-3.0	+2.20	Arp(1958)
7	L14	red	+0.3	0.50	17.00	+1.30	-	-	
8	L15	red	+0.45	+0.75	16.50	+1.40	-1.0	+2.25	
9	L82	red	+0.60	+0.90	15.50	+1.30	-	-	
10	Kron 3	red	+0.70	+0.90	16.00	+1.75	-2.50	+2.37	Walker(1970) Gascoigne (1976)
11	HW62	red-blue	+0.50	+0.80	15.50	+1.70	-	-	not proved to be red globulars.
12	L48	red-blue	+0.60	+0.70	17.20	+1.40	-2.61 -0.12	+1.92 +2.11	not proved to be red globulars
13	L3	red	+0.5	+0.60	17.50	+1.60	-	-	
14	L13	blue			17.00	+1.40	-1.48	+2.25	
15	NGC 361				16.00	+1.60	-3.0	+2.20	Arp(1959)
16	NGC 339	red	+0.5	+0.8	16.00	+1.50	-2.90	+2.20	Gascoinge (1966)
17	L1	red	+0.5	+0.8	16.00	+1.70	-3.10	+2.50	Gascoigne (1966)
18	Kron 3	red	not clear		-	-	-	-	Gascoigne (1966)

in terms of absolute values but it was intended to illustrate the differences between the clusters themselves.

In columns 5 and 6 some characteristics of the giant branches are given, although the problem of contamination with the field stars make the limits not very certain.

In the last two columns, the absolute magnitude and colour of the very red stars are written wherever they are found.

5.1.2. Group of young clusters

The study of the young clusters is more difficult in the SMC. They seem to be concentrated on the northern part of the Cloud and they are severely contaminated with the superimposed halo population II stars. In spite of that nine clusters have been studied. Two of them occupy the north east arm (de Vaucouleurs, 1973) and the other arms are on the north part of the Cloud near the cluster NGC 361.

The clusters HW64 and L90 are blue clusters with a very wide (in colour) main sequence branch and their age is estimated 5×10^7 years. As in the case of the old clusters the young clusters seem to be of the same kind as their field, therefore this age can be ascribed to the arm population as well. The main sequence is bluer than expected for clusters of the age of Pleiades and this can be explained if the stars are metal deficient.

L90 also is a "bluer globular", which was found to be unusual for our Galaxy. The study of these clusters started in the Large Magellanic Cloud and Freeman in 1974 tried to apply dynamical theories known to explain the old galactic globular clusters. He proved that they are dynamically globulars and they fit to the relevant models (King 1966).

The mechanism of the formation of these clusters is not so clear. One explanation (Graham, 1975) is that the Magellanic Clouds passed within 20 Kp of the galactic centre about 5 x 10^8 years ago and it may be, that we are seeing a burst of cluster formation associated with this event. Other low mass galaxies as M33 have been found to have the same sort of young clusters (Freeman, 1974).

The seven young clusters studied in the north part of the SMC make the number of known C-M diagrams for young objects 18 altogether. The age was estimated comparing to Galactic prototypes and they all seem to have ages between 10^6 to 7 x 10^7 years. The bar and the wing seem to be the loci of the youngest population of the SMC which have been found to be active parts containing mainly HII regions, or young population objects.

In table 5 all these results and age estimates are given for all the young objects with known C-M diagrams.

In column 2 the name of the cluster is given as described before, whereas columns 3 and 4 are characteristic of the main sequence read off the C-M diagrams.

An estimate of age is given in the column 5, as it arises by comparison with galactic clusters, or models.

TABLE 5

Young clusters of the SMC with known C-M diagrams

No.	Cluster Name	M_V max(main sequence) Brightest members	Colour extent (main sequence)	Age Estimate	Remarks
1	L90	- 1.0	-0.10, 0.0	5×10^7	blue globular?
2	HW64	- 1.0	-0.40, 0.0	5×10^7	
3	E107	- 3.0	-0.2, 0.2	$10^6 - 10^7$	
4	E102	- 3.0	-0.4, 0.1	$10^6 - 10^7$	
5	HW43	- 3.0	-0.2, 0.2	$10^6 - 10^7$	
6	HW32	- 3.0	-0.4, 0.2	$10^6 - 10^7$	
7	E60	- 4.0	-0.4, 0.2	$10^6 - 10^7$	
8	L87	- 3.0	-0.2, 0.4	7×10^7	blue globular?
9	E133	- 3.0	0.0 - 0.6	$10^6 - 10^7$	
10	NGC 330	- 5.0	-0.25, 0.1	5×10^6	it contains very bright evolved stars. Arp, 1958 Robertson, 1974.
11	C1	- 4.0	-0.2, 0.2	10^6	
12	C2	- 4.0	-0.2, 0.2	10^6	Andrews, 1971.
13	C3	- 4.0	-0.2, 0.2	10^6	
14	NGC 456	- 5.0	-0.4, 0.2	$10^6 - 10^7$	
15	NGC 465	- 5.0	-0.4, 0.2	$10^6 - 10^7$	
16	NGC 460a	- 5.0	-0.4, 0.2	$10^6 - 10^7$	Westerlund, 1964
17	NGC 460b	- 5.0	-0.4, 0.2	$10^6 - 10^7$	
18	NGC 458	- 4.0		7×10^7	Arp, 1959

5.1.3. Field stars of the SMC

In performing the photometry of the clusters, extensive areas surrounding most of them have also been measured for comparison as described in Chapter IV. Thus information is also provided regarding the field stars themselves, which is immediately useful for analysis since all stars are at the same distance.

a. Western halo field

The field stars have also been divided into two main categories. The old group and the young group. The old group is again better represented by stars of the western part where no young stars exist. In Fig. 49 the C-M diagram contains stars of the outer regions of the studied clusters. The pattern is the same as Fig. 104b, again a conspicuous red H-B and many faint blue stars. There is also a deficiency of stars at the subgiant region below the H-B.

As it has already been discussed the faint blue stars are population II stars, possibly explained by the high proportion of RR Lyrae stars reported by Graham (1975). Two very red stars have also been found in the field. Feast (1974) reported that many carbon stars have been found in the SMC fields which might mean a younger age than the galactic halo. It has also been reported by Webster (Chapter III) a Nitrogen deficiency in the planetary nebulae of the SMC. All these facts could lead to the result that the age of the SMC halo is younger than our own Galaxy.

Vigroux et al (1976) have discussed the role of isotopes of C, N and O in the chemical evolution of galaxies. They produced models of the abundance determinations of ^{12}C, ^{13}C and ^{14}N in the solar neighbourhood which might be applied to the situation in the SMC. They assumed a certain initial Hydrogen and Helium abundance at time t = 0 and they calculated the production of the elements through time (Fig. 105). It comes out that at the time between 10^9 - 5 x 10^9 years the Nitrogen is deficient compared with ^{12}C whereas later the abundances approach each other. Assuming that the SMC can be fitted to a similar model then it seems that the elements agree qualitatively and therefore the SMC old component would have an age of 10^9 - 5 x 10^9 years.

It is also worth noting that the cluster stars seem to be embedded in a field of the same evolutionary history. It seems that the halo is not comprising a mixture of different stars but an old component that is the same whether we are examining the clusters or the field. So for some reason the halo is not well mixed which is not easy to explain, with our present knowledge about the dynamics of the SMC.

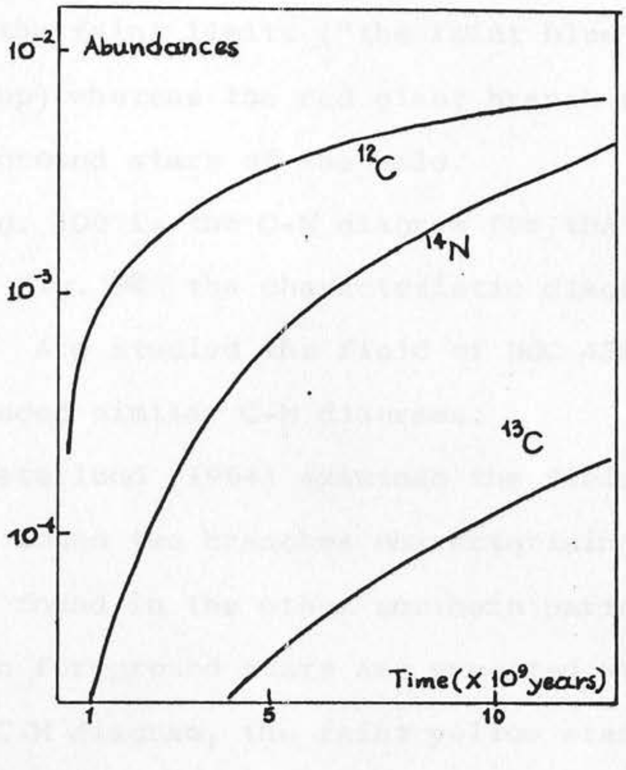

Fig. 105. Evolution with time of the ^{12}C, ^{13}C and ^{14}N abundances (in mass) in the solar neighbourhood without instant recycling. (After Vigroux et al., 1976).

b. Northern field.

The field stars on the north side produce a C-M diagram of Figs. 106 and 92. Two stellar components seem to be superimposed on this part of the SMC, the halo stars and the disc stars which are old and young objects respectively.

The main sequence branch which is very scattered may consist of young disc objects and old population II stars toward the faint limits ("the faint blue" component of the old group) whereas the red giant branch and red H-B consist of foreground stars of the halo.

Fig. 106 is the C-M diagram for the northern spiral arm and Fig. 92 the characteristic diagram of the northern field. Arp studied the field of NGC 458 and NGC 361 and he produced similar C-M diagrams.

Westerlund (1964) examined the field of the wing; he also found two branches characterising the C-M diagram exactly found in the other northern parts. While many galactic foreground stars are expected at the yellow part of the C-M diagram, the faint yellow stars and the red giants have been interpreted as halo SMC stars but no members of the wing are in that range of colours. Therefore the main sequence branch stars have been accepted as the field stars of the wing. It is worth noting that Westerlund's C-M diagram is very similar to Fig. 92.

Therefore in all cases the red giant component has been interpreted as the C-M diagram of the halo stars. Comparing the giant branch of the northern halo with the western halo (Fig. 49) it is evident that the red H-B is different. The western halo has a much more conspicuous red H-B than the northern halo and the giant branch is bluer and less scattered in colour range. The C-M diagram of the northern halo resembles the diagrams for the clusters L15 and L13. This fact could mean an

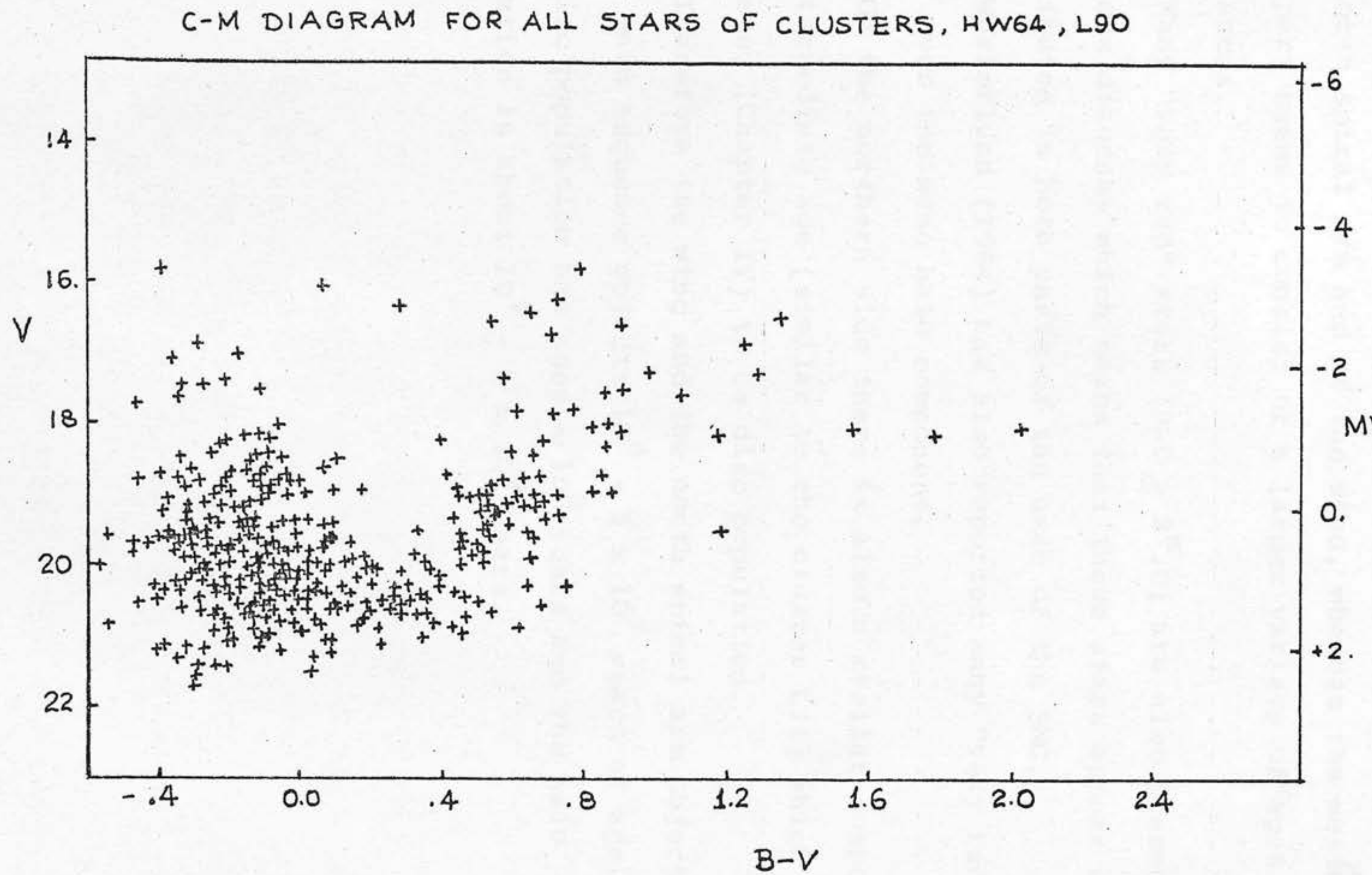

Fig. 106. Typical C-M diagram of the north-east arm stellar content.

asymmetric distribution of the halo stars from one end to the other as far as the age is concerned. The northern part would appear to comprise old stars of a certain age and it is consistent and characteristic of the halo over the north spiral arm and of the wing, whereas the western halo part seems to consist of a larger variety of ages or abundances.

Many "very red" stars ($B-V > 2^{m}.0$) are also present in these diagrams which means that these stars appear evenly distributed in both parts of the halo of the SMC.

Westerlund (1964) has also reported many "very red" stars over the wing halo component.

On the northern side there is also a stellar component of intermediate age (similar to the cluster L11) which was suggested (Chapter IV) to be disc population.

Therefore the wing and the north spiral arm objects are young main sequence objects $10^6 - 5 \times 10^7$ years of age. The disc population has ages $\sim 10^8$ years and the halo population is about $10^9 - 5 \times 10^9$ years.

5.2. Conclusion

From the study of the C-M diagrams of different regions in the SMC and especially in the W-N-E periphery the following points are the most important.

i) There is a variety of old globular clusters in the SMC halo with different horizontal branch morphology and with a preference of a conspicuous red H-B. The fact that the red part of the variable stars strip seems to be quite populous whereas the blue part almost non-existent, does not necessarily mean high metallicity as in our own Galaxy. The deficiency in Nitrogen found for the planetary nebulae of the Cloud, might be an important parameter for the explanation of the structure of the H-B in the SMC as it is suggested for the anomalous clusters of our Galaxy.

These old objects are found all over the whole studied area of the SMC, although in the north part the cluster members suffer severe contamination with the bar of arm's stellar content.

Another characteristic of these clusters is the existence of very red stars found in their central area which could be carbon stars.

Many faint blue stars are also an unusual feature of these clusters and many of them can be explained as being "blue stragglers".

These characteristics like the conspicuous red H-B, the very red stars and the "blue faint" ones would support the argument that the old SMC clusters are younger than their galactic counterparts.

The resemblance of these C-M diagrams with some diagrams of remote globular clusters of our own Galaxy and some dwarf galaxies and also the conclusion of Graham who found a similarity in the distribution of the RR Lyrae stars between the SMC and some dwarf galaxies might mean that galaxies like the SMC with very little activity in their nucleus have different evolutonary history and lower metal content because of a slower metal production in their nucleus. The age of these objects cannot be estimated accurately, but only on the basis of galactic prototypes it is $\sim 10^9 - 5 \times 10^9$ years.

ii) The young clusters are found only on the bar and the north-east part of the SMC showing age variations according to the subsystem in which they are found.

(a) Two clusters on the north-east spiral arm produce C-M diagrams which represent quite well the stellar content of this feature and give an age estimate 5×10^7 years according to Galactic models.

(b) One group of northern young clusters shows that the central region which is an extension of the bar contains young objects and probably younger than the ones of type (i).

The blueness of the young clusters compared with those of our own Galaxy is also another indication of the low metallicity of the SMC.

iii) One result which applies to all categories of the different areas studied is that the clusters seem to be mixed up with their surrounding fields and that they show the same evolutionary history as the cluster members.

The western part was found to contain the oldest objects and only old population whereas the north east part contains both old and young objects superimposed. If the inclination of the Cloud is as large as 70^{o} or more and if there are features like the north east arm, symmetric in the opposite side, they must be hidden by the bar, not visible to us, and consequently leaving the western part comprising purely the older population.

5.3. Suggestions for future work

The study of more clusters is needed, in order to get a larger sample of C-M diagrams of the SMC and compare their behaviour with our Galaxy or other galaxies.

The clusters of the southern part of the Cloud should be studied and except Kron 37 and NGC 339 (Gascoigne, 1966) no other C-M diagrams exist, therefore the southern halo objects are almost unknown.

The same plates which have been used for this work would also be very useful for further work. The field stars distribution can be studied and in particular star counts by "COSMOS" (already begun) will give important answers as the extension and shape of the halo and the arms. The N-E young field would also be very interesting to study and compare with the S-W field component.

The difficulty of the contamination of the field stars with the cluster members can be partly solved by taking plates of individual clusters with higher resolution telescopes. Therefore the dynamical behaviour of the "blue" globular clusters can be studied as well.

Individual clusters with a particular interest should be re-examined with the larger telescopes. The cluster L13 is one of those because it appears to have blue H-B and it will be very useful to have more cluster stars with a higher resolution.

The two globular clusters L90 and L87 would be a good sample to apply Freeman's suggestions (1974) about their dynamical behaviour and more accurate C-M diagrams are needed.

The clusters L17, L7, L3 and L12 are clusters of the S-W area of the SMC on circle which has been suggested to be an expanding shell (Westerlund, 1974). The study of the field stars and clusters on this area would give useful information on the existence of these shells.

Good sets of photoelectric sequences in the different areas of the SMC are urgently needed which must reach $V \sim 22^m.0$. Electronographic magnitudes have been shown to be a good solution to the problem of standard stars.

Spectroscopy of the very red stars found in the different clusters or their field would prove whether these are in fact carbon stars as in the case of NGC 419, NGC 121 and Kron 3 (Feast, 1974).

Spectroscopy of the giants of the clusters would also be suggested (as it has already been said in the latest I.A.U. report for the future of star cluster study) in order to define the metallicity of the different populations in the SMC and compare them with other galaxies.

APPENDIX

The charts of the individual clusters are given followed by the lists of stars which were selected amongst the measured stars.

The lists are the computer output and give the number of cluster and name of the region as they are found in the charts.

Column 1 of the list gives the name of the star, column 2 the visual magnitude, column 4, the absolute magnitude of each star (assuming that the distance modulus of the Small Magellanic Cloud is m-M = 19.20, Westerlund 1972) and the last column gives the colour index B-V.

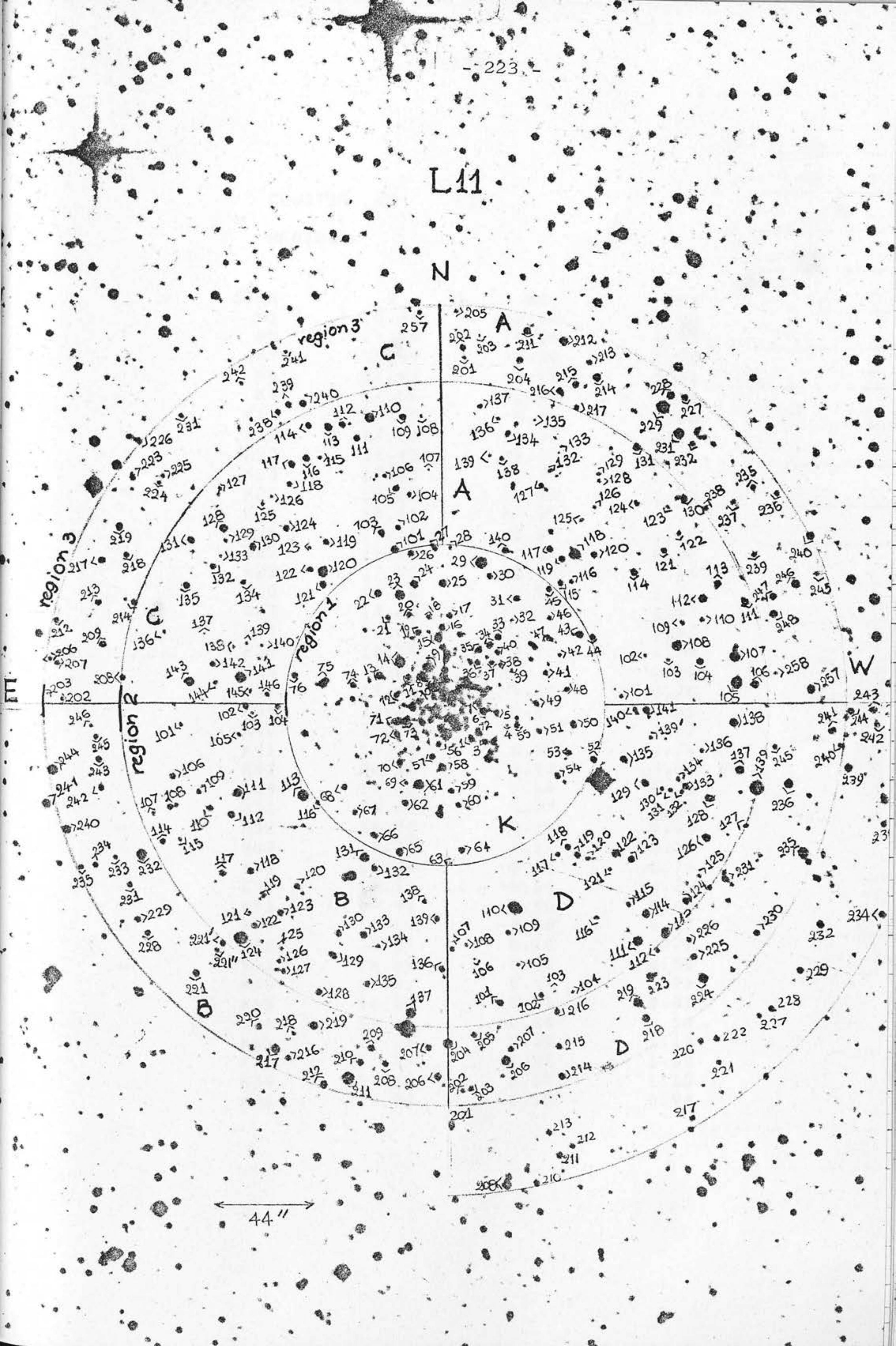
L11
N
E
W
region 1
region 2
region 3
A
B
C
D
K
44″

CLUSTER NO L11

REGION 1

STAR	V	MV	B-V
K1	18.37	-0.83	0.52
K5	19.06	-0.14	0.45
K7	18.44	-0.76	0.08
K8	17.67	-1,53	0,41
K9	17.58	-1.62	0.42
K14	16.81	-2.39	1.28
K15	17.60	-1.60	0.67
K22	18,45	-0.75	1.18
K23	17.43	-1.77	1.04
K25	18,21	-0.99	1.14
K26	18.21	-0.99	1.14
K26	19.15	-0.05	0.86
K27	19.27	0.07	0.87
K29	17.25	-1.95	0.68
K30	19.20	0.00	0.76
K33	18.82	-0.38	0.87
K34	18.80	-0.40	0.63
K35	18.94	-0.26	0.59
K36	18.84	-0.36	0.57
K37	19.49	0.29	0.30
K39	20.37	1.17	0.51
K40	19.33	0.13	0.47
K41	19.73	0.53	0.39
K42	20.33	1.13	0.55
K44	19.36	0.16	1.20
K51	19.47	0.27	0.59
K52	18.92	-0.28	1.03
K53	19.37	0.17	0.74
K55	19.16	-0.04	0.74
K57	19.11	-0.09	0.22
K58	18.40	-0.80	0.62
K59	19.12	-0.08	0.37
K60	19.36	0.16	0.79
K62	19.21	0.01	0.58
K64	19.32	0.12	0.79
K65	18.59	-0.61	0.81
K66	19.16	-0.04	0.59
K68	19.50	0.30	1.10
K73	17.29	-1.91	1.00
K74	19.22	0.02	1.10
K76	19.38	0.18	0.94

CLUSTER NO L11

REGION 2

STAR	V	MV	B-V
A01	18.96	-0.24	0.92
A02	19.45	0.25	0.96
A03	21.15	1.95	0.12
A07	19.57	0.37	0.99
A09	19.39	0.19	1.32
A10	16.69	-2.51	0.80
A11	17.99	-1.21	1.07
A13	18.55	-0.65	1.10
A16	20.98	1.78	0.03
A18	19.64	0.44	0.63
A20	19.73	0.53	1.24
A22	19.30	0.10	0.92
A23	19.37	0.17	0.97
A24	19.52	0.32	0.92
A25	20.91	1.71	0.12
A26	18.79	-0.41	1.01
A27	20.85	1.65	0.39
A28	19.03	-0.17	0.69
A29	19.11	-0.09	1.04
A30	19.72	0.52	0.93
A31	19.74	0.54	0.79
A33	19.08	-0.12	1.04
A35	18.99	-0.21	1.32
A36	20.57	1.37	0.40
A37	18.60	-0.60	1.21
A39	16.50	-2.70	0.77
A40	20.26	1.06	0.48
B04	19.43	0.23	0.73
B05	17.25	-1.95	1.32
B06	19.32	0.12	0.96
B07	17.31	-1.89	1.47
B08	17.86	-1.34	1.15
B10	21.04	1.84	0.02
B11	19.31	0.11	1.06
B14	19.36	0.16	0.74
B17	19.29	0.09	1.01
B18	17.22	-1.98	1.31
B19	19.36	0.16	0.88
B20	19.50	0.30	0.79
B21	20.24	1.04	0.94
B25	20.38	1.18	0.80
B27	20.01	0.81	1.11
B29	20.53	1.33	0.58
B31	19.48	0.28	0.79
B34	19.67	0.47	0.79

CLUSTER NO L11

REGION 2

C01	18.30	-0.90	1.33
C03	19.99	0.79	0.97
C05	19.40	0.20	0.68
C09	19.53	0.33	0.93
C10	17.73	-1.47	1.44
C12	19.25	0.05	1.09
C13	18.71	-0.49	1.04
C14	19.53	0.33	0.67
C19	19.30	0.10	1.17
C20	17.40	-1.80	0.89
C21	19.03	-0.17	0.76
C22	19.35	0.15	0.77
C24	19.41	0.21	0.83
C28	18.52	-0.68	1.26
C30	19.29	0.09	0.97
C33	21.00	1.80	0.00
C37	20.86	1.66	0.31
C38	21.01	1.81	0.15
C39	20.64	1.44	0.36
C41	16.81	-2.39	1.21
C43	17.28	-1.92	1.51
C44	20.58	1.38	-0.04
D02	19.32	0.12	0.63
D04	19.32	0.12	1.00
D10	19.36	0.16	0.94
D11	16.75	-2.45	2.54
D13	16.49	-2.71	1.82
D18	18.96	-0.24	1.19
D19	19.67	0.47	0.81
D24	16.28	-2.92	0.82
D30	19.56	0.36	0.66
D31	17.80	-1.40	1.29
D32	19.41	0.21	0.75
D36	19.09	-0.11	0.91

CLUSTER NO L11

REGION 3

STAR	V	MV	B-V
A04	17.87	-1.33	0.82
A06	17.51	-1.69	1.50
A07	19.36	0.16	0.77
A19	18.33	-0.87	1.36
A24	17.83	-1.37	1.80
A25	19.51	0.31	0.01
A35	17.57	-1.63	1.51
A41	20.04	0.84	0.70
B29	16.91	-2.29	0.94
B48	19.07	-0.13	1.06
B57	19.28	0.08	0.93
C07	19.48	0.28	0.71
C14	19.35	0.15	0.84
C17	19.46	0.26	0.63
C18	19.37	0.17	1.16
C21	19.97	0.77	0.80
C38	20.11	0.91	-0.02
C39	19.60	0.40	0.94
D08	18.89	-0.31	1.76
D09	19.14	-0.06	1.01
D10	19.19	-0.01	0.91
D11	16.99	-2.21	0.45
D12	18.50	-0.70	1.30
D18	19.96	0.76	0.89
D19	18.23	-0.97	1.31
D20	19.22	0.02	0.94
D21	18.89	-0.31	0.82
D21''	19.49	0.29	0.42
D29	19.57	0.37	0.77
D31	19.50	0.30	0.89
D32	17.09	-2.11	1.57
D34	19.29	0.09	1.11
D40	17.90	-1.30	1.25
D44	16.96	-2.24	1.31
D43	19.17	-0.03	1.02
D45	19.62	0.42	1.11

END

&RUN;

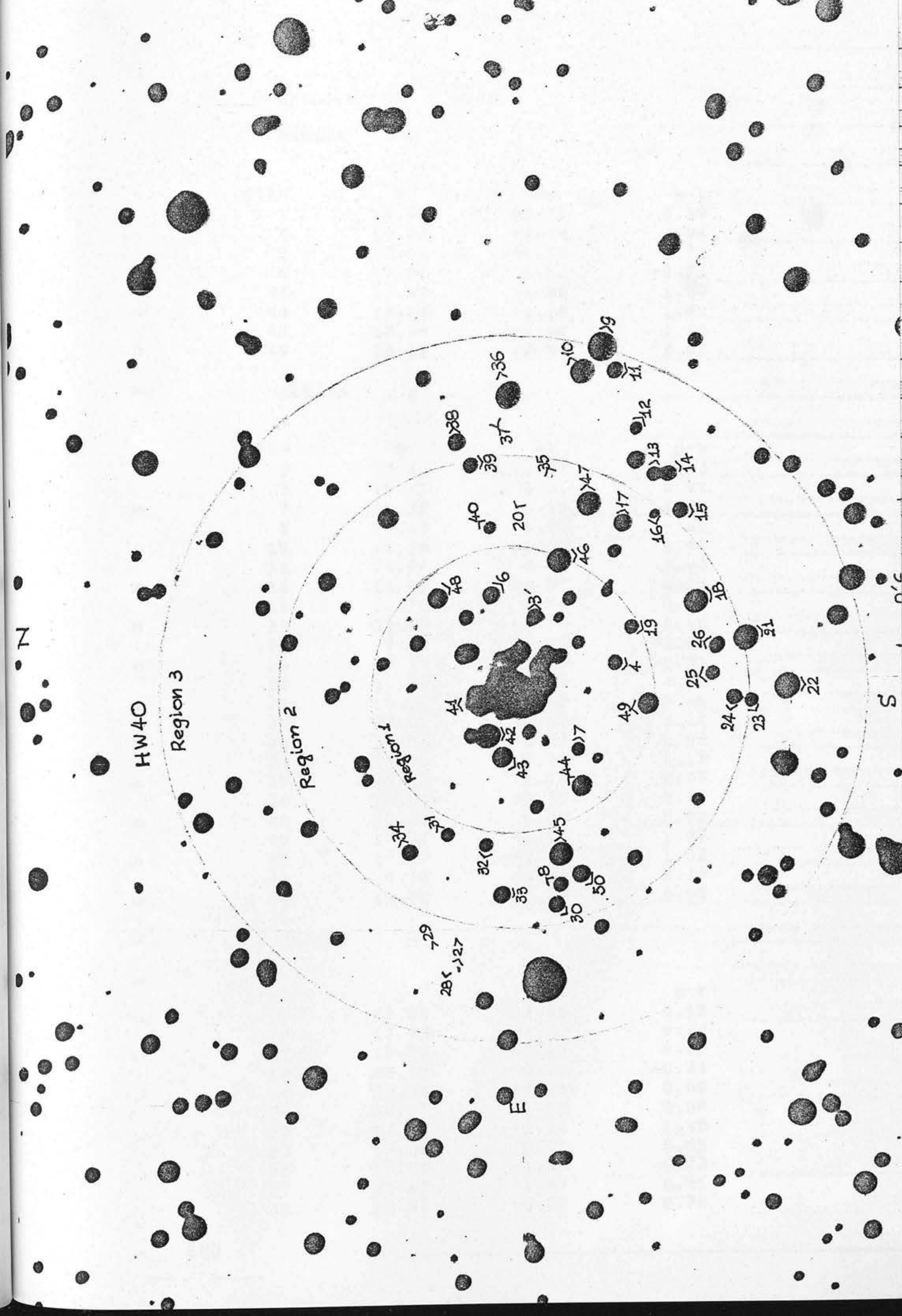
HW40
Region 3
Region 2
Region 1
N
E
S

CLUSTER NO HW40

REGION 1

STAR	V	MV	B-V
1	18.49	-0.71	0.39
4	19.06	-0.14	0.94
5	19.02	-0.18	0.71
6	19.61	0.41	-0.26
41	17.40	-1.80	1.09
44	18.04	-1.16	1.40
48	18.30	-0.90	1.23
49	16.61	-2.59	2.80

REGION 2

STAR	V	MV	B-V
2	19.13	-0.07	0.63
3	19.21	0.01	0.91
7	19.32	0.12	0.45
8	19.18	-0.02	0.61
15	19.06	-0.14	0.88
16	19.96	0.76	0.03
18	18.53	-0.67	0.08
19	19.76	0.56	0.14
20	20.93	1.73	0.14
24	19.69	0.49	-0.09
25	19.39	0.19	0.81
26	19.54	0.34	0.22
31	19.20	0.00	0.86
32	19.87	0.67	0.01
33	18.98	-0.22	0.63
34	19.50	0.30	0.17
35	20.38	1.18	0.33
39	19.01	-0.19	0.78
40	19.48	0.28	0.52
45	17.70	-1.50	1.27
46	17.75	-1.45	1.03
47	18.33	-0.87	0.39
50	18.91	-0.29	0.55

REGION 3

STAR	V	MV	B-V
9	17.54	-1.66	0.15
10	17.93	-1.27	0.74
11	19.01	-0.19	0.62
12	20.15	0.95	0.34
14	18.94	-0.26	0.60
21	18.17	-1.03	0.08
22	17.10	-2.10	1.45
23	19.31	0.11	0.85
36	17.51	-1.69	0.73
37	20.67	1.47	0.41
38	18.97	-0.23	0.76

END

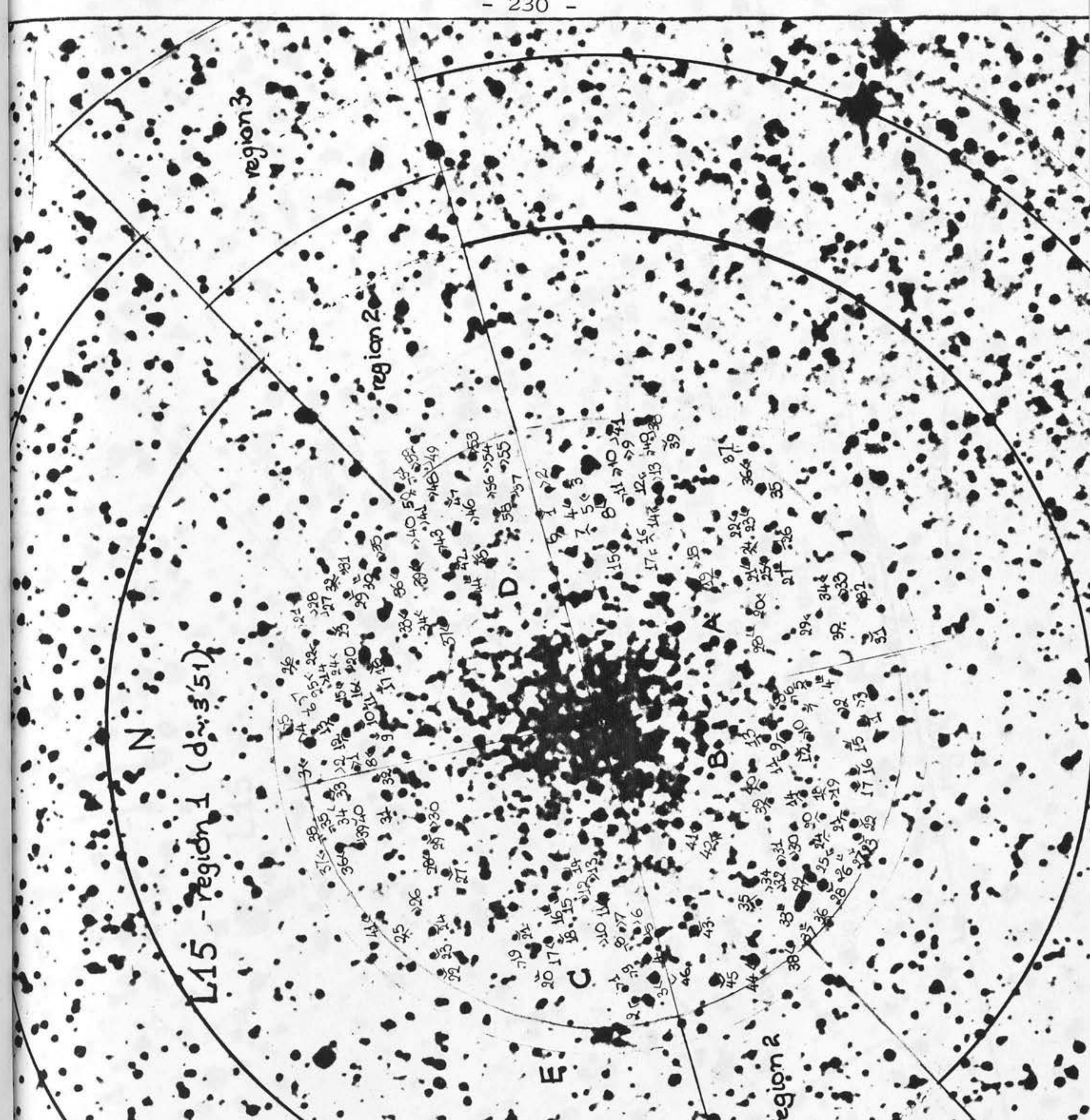
L15 - region 1 (d~3'51)
region 2
region 2
region 3
region 3
N
E
E
A
B
C
D

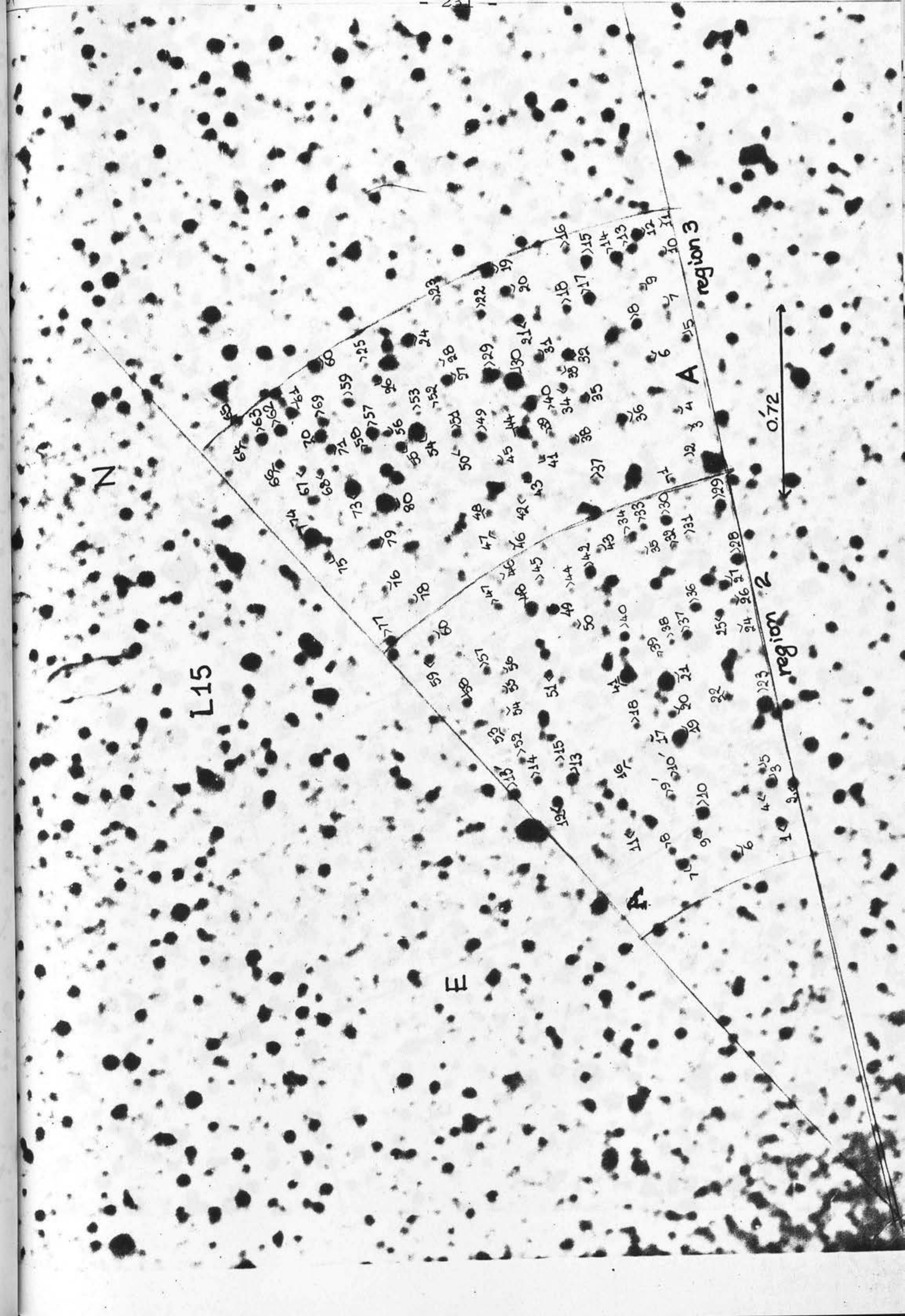
N
E
L15
A
region 3
region 2
0.'72

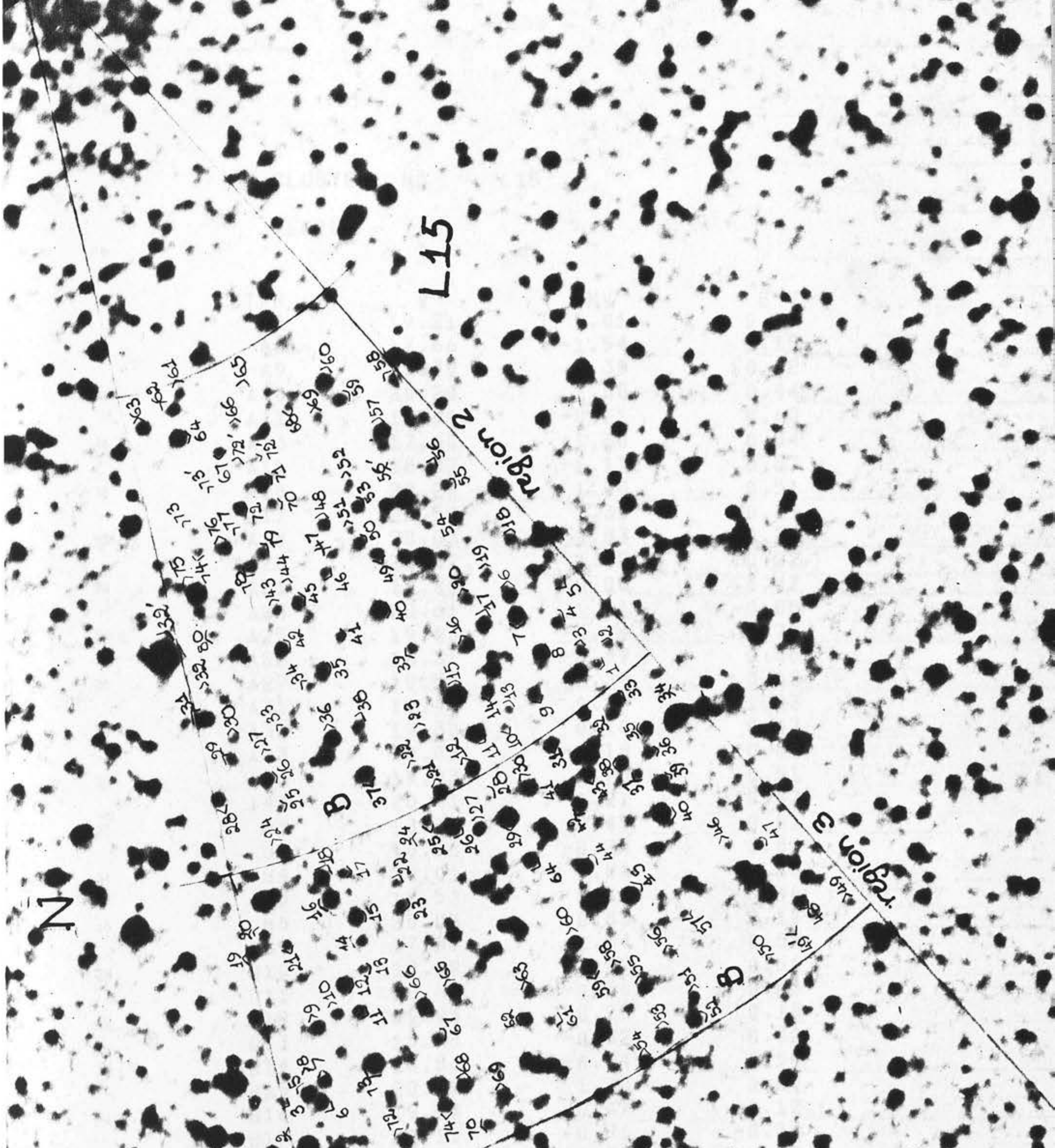
L15
N
E
region 2
region 3

CLUSTER NO L15

REGION 1

STAR	V	MV	B-V
A6	19.21	0.01	0.66
A8	17.66	-1.54	1.15
A9	20.59	1.39	0.22
A10	20.20	1.00	0.44
A11	18.99	-0.21	0.60
A13	17.60	-1.60	0.54
A15	18.03	-1.17	0.67
A16	20.20	1.00	0.51
A17	20.53	1.33	0.25
A18	20.03	0.83	0.29
A20	20.32	1.12	0.22
A21	19.26	0.06	0.47
A24	20.61	1.41	-0.08
A25	19.16	-0.04	0.72
A26	18.31	-0.89	0.66
A27	19.59	0.39	0.62
A31	19.44	0.24	1.03
A32	19.30	0.10	0.47
A33	19.02	-0.18	0.64
A36	19.93	0.73	0.51
A43	20.41	1.21	0.37
B1	18.73	-0.47	0.91
B2	18.96	-0.24	0.81
B4	20.01	0.81	-0.10
B5	19.53	0.33	0.46
B6	20.03	0.83	0.17
B9	17.56	-1.64	0.62
B10	19.29	0.09	0.51
B11	18.64	-0.56	0.63
B12	19.95	0.75	0.18
B13	18.58	-0.62	0.32
B14	18.86	-0.34	0.54
B15	20.20	1.00	0.10
B16	19.67	0.47	-0.12
B17	20.11	0.91	-0.31
B19	19.54	0.34	0.59
B20	19.45	0.25	0.52
B22	18.70	-0.50	0.22
B23	18.61	-0.59	0.91
B28	17.28	-1.92	0.82
B29	17.20	-2.00	0.82
B30	19.59	0.39	0.63
B31	18.67	-0.53	1.25
B33	19.98	0.78	0.20
B35	19.22	0.02	0.96

CLUSTER NO L15

REGION 1

STAR	V	MV	B-V
B37	20.19	0.99	0.41
B38	18.87	-0.33	0.94
B40	18.97	-0.23	0.87
B43	17.62	-1.58	0.84
B44	18.08	-1.12	0.67
B45	19.74	0.54	0.58
B46	20.33	1.13	0.35
B49	20.28	1.08	-0.21
C1	19.80	0.60	0.22
C2	18.82	-0.38	0.71
C3	17.45	-1.75	0.81
C4	18.71	-0.49	0.51
C5	18.61	-0.59	0.75
C6	19.09	-0.11	0.47
C8	20.64	1.44	-0.13
C10	20.22	1.02	0.67
C11	17.79	-1.41	0.94
C12	19.98	0.78	0.45
C14	17.99	-1.21	0.80
C15	18.95	-0.25	0.13
C16	19.44	0.24	0.29
C20	20.71	1.51	-0.03
C22	19.36	0.16	0.57
C24	19.43	0.23	-0.26
C25	20.68	1.48	0.02
C26	19.61	0.41	0.66
C27	18.82	-0.38	1.33
C28	19.43	0.23	0.52
C30	19.09	-0.11	0.17
C32	19.28	0.08	0.80
C33	18.93	-0.27	0.61
C36	18.31	-0.89	0.76
C38	20.35	1.15	0.04
C39	19.18	-0.02	0.45
C42	20.41	1.21	0.29
C44	20.21	1.01	0.40
C45	20.61	1.41	0.35

CLUSTER NO L15

REGION 1

STAR	V	MV	B-V
D1	19.51	0.31	0.63
D3	19.71	0.51	0.66
D4	17.34	-1.86	1.09
D5	19.13	-0.07	0.40
D7	21.06	1.86	-0.06
D8	19.33	0.13	0.62
D10	18.86	-0.34	0.64
D11	18.20	-1.00	2.25
D12	18.94	-0.26	0.70
D13	18.84	-0.36	0.70
D15	19.58	0.38	0.74
D17	20.03	0.83	0.39
D19	16.41	-2.79	1.43
D21	19.64	0.44	0.21
D22	19.75	0.55	0.23
D23	20.28	1.08	0.25
D24	20.66	1.46	-0.06
D26	19.95	0.75	0.69
D27	20.93	1.73	0.27
D32	20.82	1.62	0.08
D33	19.61	0.41	0.37
D35	19.13	-0.07	0.87
D37	18.46	-0.74	0.71
D39	18.55	-0.65	1.06
D40	20.35	1.15	0.19
D42	18.77	-0.43	0.75
D44	19.62	0.42	0.74
D45	18.42	-0.78	0.62
D46	19.92	0.72	0.16
D49	20.50	1.30	0.24
D53	18.73	-0.47	0.87
D54	20.30	1.10	0.42
D56	20.64	1.44	0.03
D56	20.70	1.50	-0.13
D58	18.99	-0.21	0.11

CLUSTER NO L15

REGION 2

STAR	V	MV	B-V
A1	19.35	0.15	0.71
A2	19.07	-0.13	0.96
A3	19.32	0.12	0.66
A10	19.30	0.10	-0.13
A13	19.26	0.06	0.82
A15	21.02	1.82	0.02
A16	20.80	1.60	0.28
A17	20.62	1.42	0.15
A19	17.91	-1.29	0.71
A20	19.96	0.76	0.21
A21	16.62	-2.58	0.30
A23	17.79	-1.41	-0.07
A24	20.47	1.27	0.37
A26	19.98	0.78	0.43
A27	19.56	0.36	0.31
A28	19.58	0.38	0.02
A29	19.08	-0.12	0.61
A31	20.55	1.35	0.50
A33	20.35	1.15	0.07
A34	19.77	0.57	0.70
A36	19.95	0.75	0.01
A37	20.03	0.83	0.37
A38	20.08	0.88	0.47
A39	20.60	1.40	0.01
A60	19.47	0.27	0.62
A41	17.79	-1.41	0.96
A42	19.25	0.05	0.77
A44	21.01	1.81	0.35
A45	21.23	2.03	-0.28
A48	18.90	-0.30	0.84
A49	19.26	0.06	0.60
A52	21.03	1.83	-0.34
A57	20.74	1.54	-0.23
A60	20.64	1.44	-0.02
A61	19.35	0.15	0.53

CLUSTER NO L15

REGION 2

STAR	V	MV	B-V
B32'	14.62	-4.58	0.55
B2	20.34	1.14	0.34
B3	20.01	0.81	0.39
B6	18.98	-0.22	0.71
B7	18.47	-0.73	0.65
B8	18.88	-0.32	0.47
B9	19.87	0.67	0.33
B10	20.61	1.41	0.02
B11	18.21	-0.99	0.93
B12	18.97	-0.23	0.82
B13	20.71	1.51	-0.05
B15	17.15	-2.05	0.09
B16	19.66	0.46	0.30
B17	18.84	-0.36	0.51
B18	20.15	0.95	0.13
B23	20.07	0.87	0.36
B24	19.18	-0.02	0.52
B25	20.49	1.29	0.21
B26	19.04	-0.16	0.69
B29	20.19	0.99	0.06
B30	20.49	1.29	0.48
B31	18.68	-0.52	0.56
B33	20.30	1.10	0.61
B35	19.57	0.37	0.15
B36	18.27	-0.93	0.92
B37	18.74	-0.46	0.52
B38	20.10	0.90	0.00
B40	18.50	-0.70	0.65
B41	20.65	1.45	-0.01
B49	19.80	0.60	0.01
B50	19.55	0.35	0.44
B53	19.41	0.21	0.70
B57	19.11	-0.09	-0.13
B58	19.90	0.70	-0.11
B59	19.15	-0.05	0.70
B61	20.10	0.90	0.03
B62	18.92	-0.28	0.69
B63	18.53	-0.67	0.99
B64	17.67	-1.53	0.98
B67	20.03	0.83	0.20
B71	18.69	-0.51	0.56
B72	19.22	0.02	0.52
B74	20.26	1.06	0.23
B77	20.21	1.01	0.38
B78	19.21	0.01	0.51
B79	20.06	0.86	0.11
B80	19.99	0.79	0.55
B56'	20.45	1.25	0.32
B72'	20.29	1.09	0.36
B73'	20.61	1.41	0.26

CLUSTER NO L15

REGION 3

STAR	V	MV	B-V
A2	21.10	1.90	-0.07
A4	21.10	1.90	0.01
A5	20.13	0.93	0.40
A7	20.57	1.37	0.11
A8	19.38	0.18	0.89
A9	20.57	1.37	0.31
A11	19.79	0.59	0.65
A12	18.99	-0.21	0.61
A15	19.09	-0.11	0.90
A17	18.97	-0.23	0.70
A18	20.67	1.47	-0.29
A20	19.66	0.46	0.72
A21	19.23	0.03	0.96
A22	20.04	0.84	0.38
A23	20.79	1.59	0.05
A24	18.44	-0.76	1.18
A25	20.61	1.41	0.45
A26	20.24	1.04	-0.04
A30	17.13	-2.07	1.08
A32	19.13	-0.07	0.69
A33	20.62	1.42	0.48
A34	20.62	1.42	-0.06
A36	19.37	0.17	0.77
A39	20.57	1.37	0.24
A42	20.55	1.35	0.27
A46	21.27	2.07	-0.07
A47	20.66	1.46	0.06
A51	19.82	0.62	0.94
A52	20.63	1.43	0.09
A53	20.68	1.48	0.05
A54	17.24	-1.96	0.96
A55	19.89	0.69	0.19
A56	20.08	0.88	0.52
A57	19.03	-0.27	0.73
A59	20.07	0.87	0.41
A60	19.61	0.41	0.00
A61	19.38	0.18	0.53
A62	19.23	0.03	0.72
A63	19.34	0.14	0.70
A65	19.72	0.52	0.57
A68	20.29	1.09	0.70
A70	19.38	0.18	0.55
A71	19.87	0.67	0.56
A73	18.08	-1.12	0.87
A74	17.31	-1.89	1.10
A75	20.28	1.08	0.55
A76	20.95	1.75	-0.33
A77	19.46	0.26	0.50
A78	20.76	1.56	-0.18
A80	17.35	-1.85	0.50

CLUSTER NO L15

REGION 3

STAR	V	MV	B-V
B49'	20.73	1.53	0.15
B2	20.36	1.16	0.40
B3	20.45	1.25	0.51
B5	18.81	-0.39	0.15
B10	20.00	0.80	0.10
B11	18.73	-0.47	0.40
B12	18.88	-0.32	0.63
B15	19.48	0.28	0.36
B16	18.48	-0.72	0.54
B19	19.09	-0.11	0.33
B20	20.32	1.12	-0.16
B21	20.25	1.05	0.26
B22	20.81	1.61	-0.27
B23	19.91	0.71	0.68
B24	20.37	1.17	0.55
B25	20.53	1.33	-0.24
B27	19.71	0.51	-0.05
B28	20.16	0.96	0.55
B29	17.31	-1.89	1.11
B30	18.97	-0.23	0.57
B31	19.21	0.01	0.73
B32	19.83	0.63	0.27
B33	19.17	-0.03	0.52
B35	19.81	0.61	0.17
B36	20.06	0.86	0.15
B38	19.59	0.39	0.50
B39	18.91	-0.29	0.50
B40	17.69	-1.51	1.12
B42	19.70	0.50	-0.29
B44	18.75	-0.45	0.74
B45	18.36	-0.84	1.02
B47	20.14	0.94	0.21
B49	20.52	1.32	0.19
B50	20.82	1.62	-0.19
B53	19.07	-0.13	0.69
B55	19.71	0.51	0.17
B56	20.70	1.50	-0.03
B57	20.59	1.39	0.00
B58	20.70	1.50	-0.06
B59	18.66	-0.54	0.75
B60	19.07	-0.13	0.72
B61	20.31	1.11	0.30
B62	19.37	0.17	0.65
B63	19.89	0.69	0.37
B64	19.07	-0.13	0.59
B65	18.97	-0.23	0.73
B66	18.70	-0.50	0.78
B70	20.08	0.88	0.34
B71	20.59	1.39	-0.36
B73	16.34	-2.86	1.03
B74	19.04	-0.16	0.47

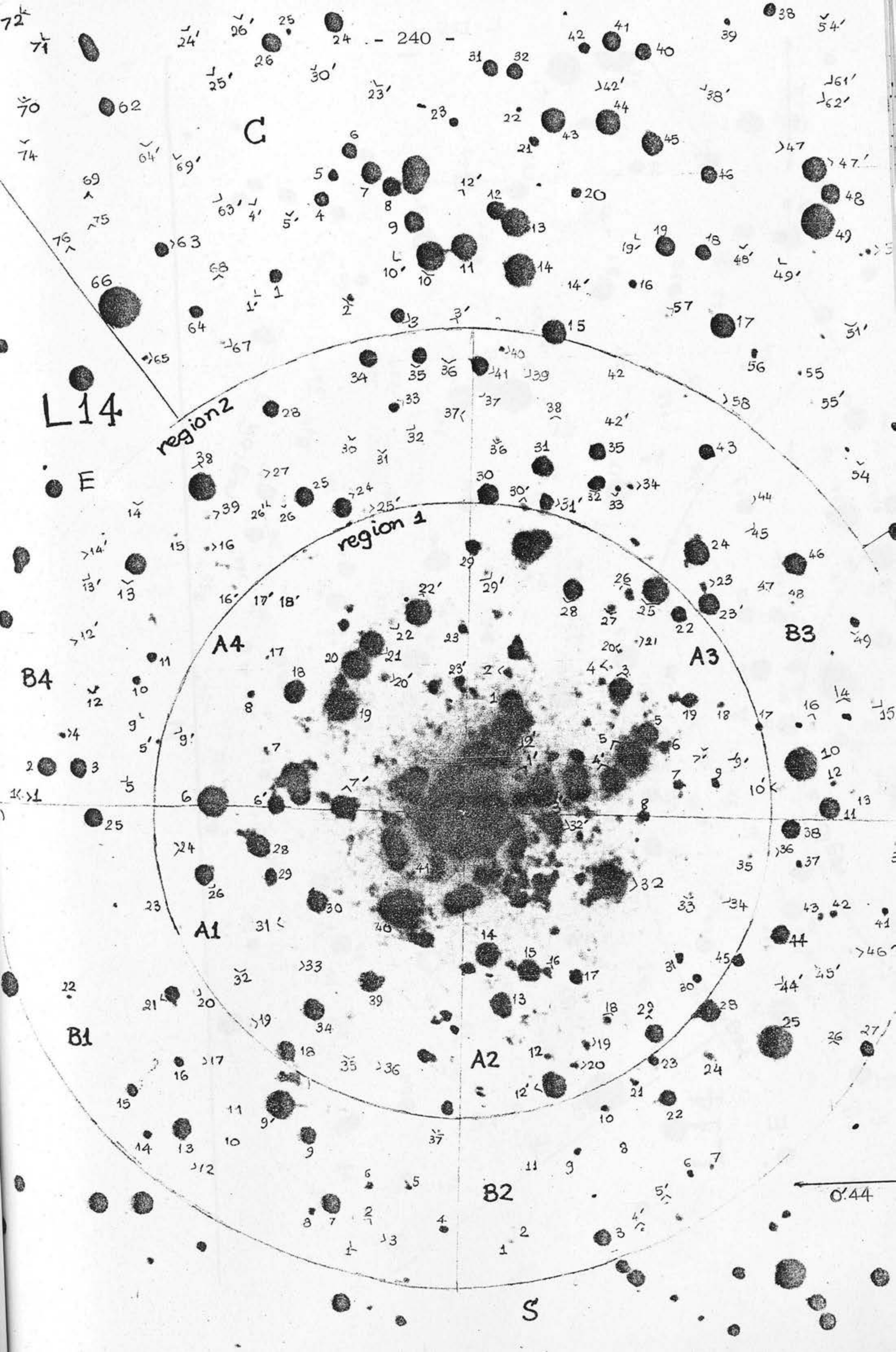
L14
C
E
S
region 1
region 2
A1
A2
A3
A4
B1
B2
B3
B4
0.'44

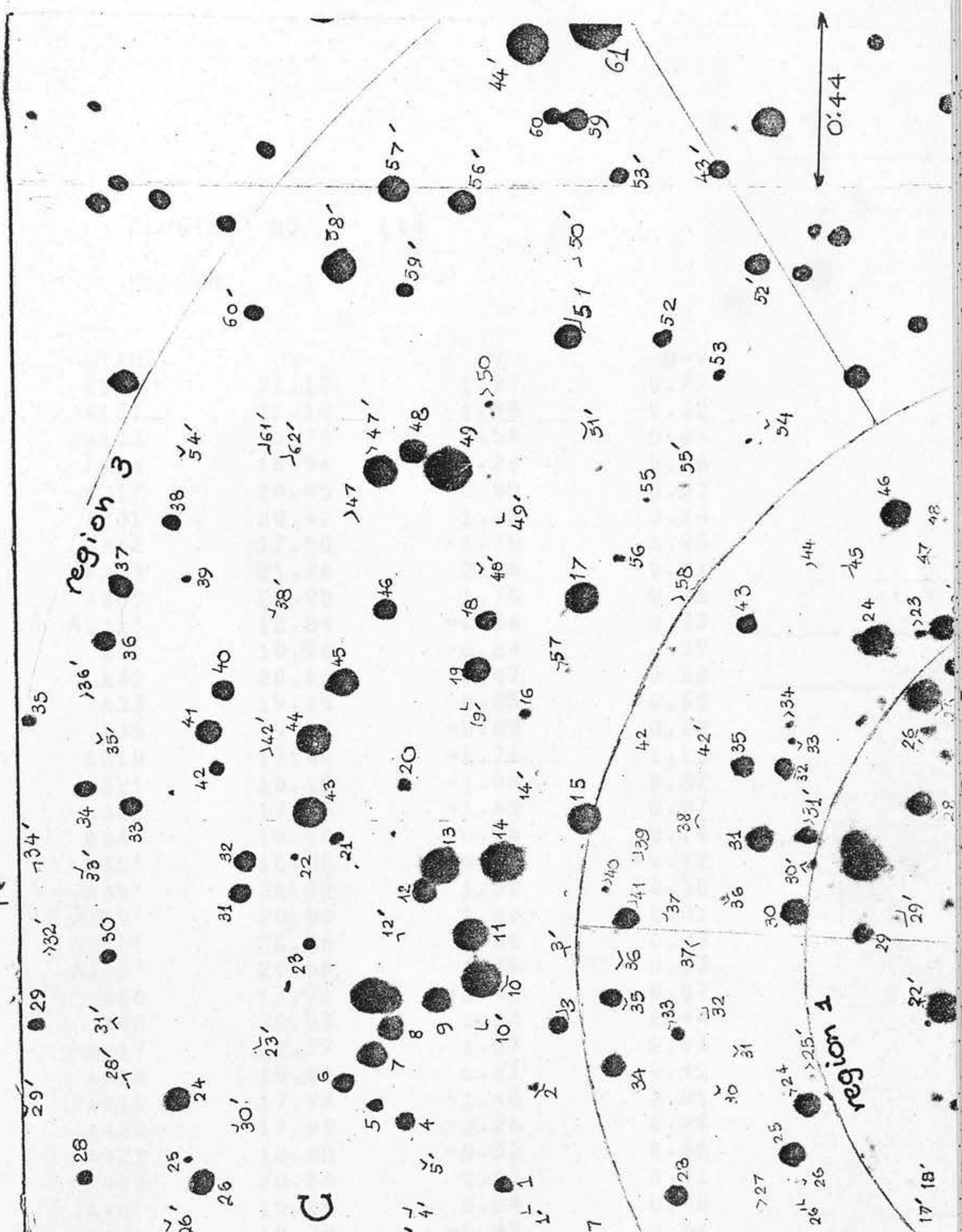
N
E
L14
region 3
region 2
region 1
0'.44

CLUSTER NO L14

REGION 1

STAR	V	MV	B-V
A127	21.17	1.97	0.77
A131	21.18	1.98	-0.32
A133	20.76	1.56	0.86
A114	18.96	-0.24	0.86
A217	20.05	0.85	0.53
A231	20.42	1.22	0.34
A232	17.50	-1.70	0.95
A234	21.26	2.06	-0.21
A235	20.90	1.70	0.16
A232'	18.84	-0.36	0.47
A31	18.96	-0.24	0.59
A32	20.67	1.47	0.08
A33	19.25	0.05	0.55
A35	19.11	-0.09	0.29
A310	17.44	-1.76	1.26
A32'	18.12	-1.08	0.37
A33'	17.55	-1.65	0.87
A34'	18.44	-0.76	0.74
A35'	18.30	-0.90	-0.12
A39'	20.72	1.52	0.38
A329'	20.86	1.66	0.01
A330'	20.56	1.36	0.23
A330'	20.56	1.36	0.23
A46	17.71	-1.49	0.07
A48	20.53	1.33	0.44
A417	20.77	1.57	0.84
A418	19.41	0.21	0.42
A419	17.74	-1.46	0.91
A420	17.94	-1.26	0.99
A421	18.88	-0.32	0.66
A423	20.33	1.13	0.61
A46'	19.44	0.24	0.40
A47'	18.78	-0.42	0.64
A418'	21.00	1.80	-0.05
A420'	20.88	1.68	0.14
A423'	20.01	0.81	0.48

CLUSTER NO L14

REGION 2

STAR	V	MV	B-V
B19'	17.70	-1.50	1.04
B11	20.61	1.41	0.46
B12	20.73	1.53	0.42
B14	20.77	1.57	0.42
B17	19.97	0.77	0.99
B110	20.97	1.77	0.65
B111	21.41	2.21	0.32
B113	19.30	0.10	0.60
B115	19.80	0.60	0.64
B116	20.44	1.24	0.30
B120	20.70	1.50	0.26
B125	19.27	0.07	0.61
B21	20.50	1.30	0.50
B23	19.62	0.42	0.58
B25	20.28	1.08	0.50
B210	20.63	1.43	0.30
B223	20.31	1.11	0.41
B227	19.89	0.69	0.58
B237	20.47	1.27	0.23
B239	20.88	1.68	0.04
B245	20.33	1.13	0.63
B246	20.96	1.76	0.14
B24'	20.77	1.57	0.54
B25'	20.84	1.64	0.26
B311	19.15	-0.05	0.78
B312	20.34	1.14	0.80
B314	21.39	2.19	-0.31
B315	21.05	1.85	0.16
B316	20.92	1.72	0.15
B323	20.74	1.54	0.26
B324	18.71	-0.49	0.63
B325	18.87	-0.33	0.39
B326	20.51	1.31	0.21
B338	20.64	1.44	0.77
B345	20.62	1.42	0.61
B348	19.71	0.51	1.36
B349	20.49	1.29	0.03
B323'	19.39	0.19	0.40
B42	19.25	0.05	0.58
B43	19.65	0.45	0.15
B45	21.20	2.00	0.18
B49	20.67	1.47	-0.07
B410	20.33	1.13	0.33
B412	20.97	1.77	0.03
B413	19.20	0.00	0.66
B415	20.47	1.27	0.33
B424	19.39	0.19	0.74
B427	20.74	1.54	0.34
B429	20.88	1.68	0.41
B431	21.10	1.90	0.33
B432	20.98	1.78	0.41
B433	20.76	1.56	0.20
B435	19.71	0.51	0.61
B438	17.98	-1.22	0.97
B439	20.74	1.54	0.70
B45'	20.41	1.21	0.71
B414'	20.53	1.33	0.25
B416'	20.38	1.18	0.63
B424'	20.74	1.54	0.77

CLUSTER NO L14

REGION 3

STAR	V	MV	B-V
C1	19.62	0.42	0.79
C4	20.35	1.15	-0.36
C5	20.50	1.30	-0.20
C7	18.86	-0.34	0.61
C8	18.98	-0.22	0.46
C9	19.24	0.04	0.42
C10	17.63	-1.57	0.98
C11	18.10	-1.10	0.98
C12	19.15	-0.05	0.72
C13	17.71	-1.49	0.11
C14	17.16	-2.04	1.35
C15	19.11	-0.09	0.22
C17	18.46	-0.74	0.87
C19	19.75	0.55	0.20
C21	20.24	1.04	0.28
C26	18.98	-0.22	0.41
C27	17.16	-2.04	1.58
C28	19.49	0.29	0.66
C30	19.37	0.17	1.16
C31	19.06	-0.14	0.67
C32	19.25	0.05	0.63
C34	19.08	-0.12	0.70
C36	19.02	-0.18	0.77
C37	18.60	-0.60	0.88
C38	19.37	0.17	0.83
C40	19.17	-0.03	0.65
C41	18.54	-0.66	0.84
C43	18.32	-0.88	1.80
C44	17.93	-1.27	1.17
C45	19.40	0.20	-0.21
C48	18.82	-0.38	0.83
C49	16.87	-2.33	0.71
C51	18.77	-0.43	0.77
C56	20.29	1.09	1.16
C58	20.68	1.48	0.49
C59	18.64	-0.56	0.37
C61	14.72	-4.48	0.53
C62	19.24	0.04	0.70
C66	15.72	-3.48	0.70
C67	20.47	1.27	0.17
C70	20.92	1.72	0.35
C71	21.27	2.07	-0.32
C75	20.38	1.18	0.41
C3'	20.96	1.76	-0.16
C5'	20.70	1.50	0.45
C10'	20.48	1.28	0.39
C12'	20.63	1.43	0.49

CLUSTER NO L14

REGION 3

STAR	V	MV	B-V
C19'	20.44	1.24	0.75
C23'	20.75	1.55	0.46
C25'	20.71	1.51	0.80
C26'	20.45	1.25	0.68
C27'	20.66	1.46	0.62
C31'	20.03	0.83	0.22
C32'	20.89	1.69	0.34
C33'	20.70	1.50	0.57
C36'	21.00	1.80	0.24
C38'	21.01	1.81	0.35
C42'	20.60	1.40	0.95
C44'	15.93	-3.27	0.75
C47'	18.47	-0.73	0.45
C48'	21.04	1.84	0.25
C49'	20.46	1.26	1.28
C54'	20.63	1.43	0.41
C55'	20.97	1.77	0.01
C56'	18.46	-0.74	1.01
C58'	17.76	-1.44	0.78
C59'	19.66	0.46	0.44
C60'	19.58	0.38	0.27

END

&RUN;

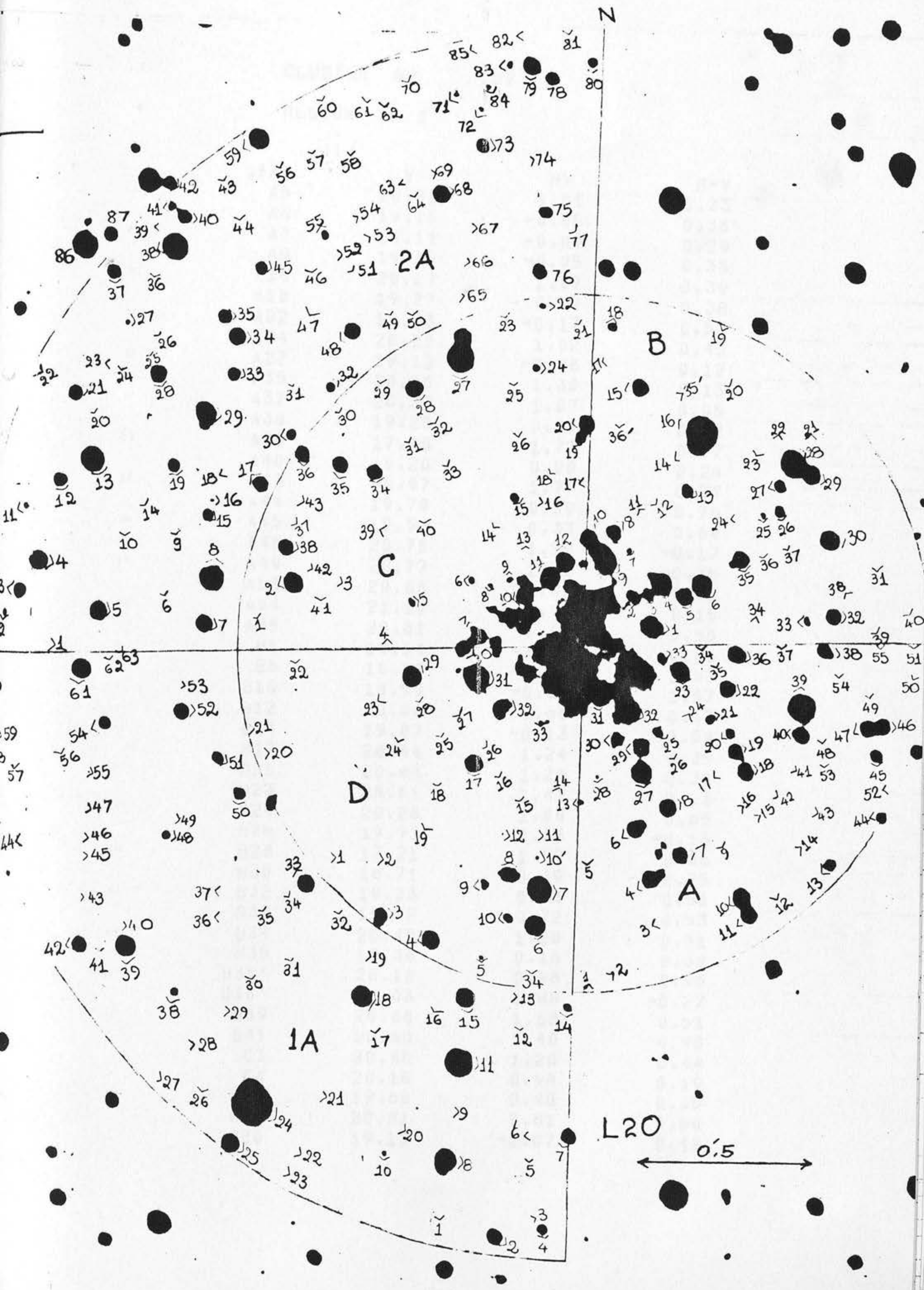
N
2A
B
C
D
A
1A
L20
0'5

CLUSTER NO L20

REGION 1

STAR	V	MV	B-V
A5	20.81	1.61	-0.23
A6	19.15	-0.05	0.36
A7	19.11	-0.09	0.29
A8	19.15	-0.05	0.38
A16	20.27	1.07	0.39
A18	19.27	0.07	0.38
A22	19.03	-0.17	0.53
A24	20.22	1.02	0.43
A27	19.12	-0.08	0.12
A35	20.50	1.30	0.13
A37	20.27	1.07	0.05
A38	19.20	0.00	0.72
A39	17.48	-1.72	0.77
A40	19.20	0.00	0.24
A43	20.97	1.77	0.27
A44	19.79	0.59	0.76
A45	19.53	0.33	0.64
A48	20.70	1.50	-0.17
A49	20.77	1.57	-0.35
A53	20.86	1.66	0.46
A54	21.19	1.99	0.15
A55	20.81	1.61	0.55
B1	18.14	-1.06	0.26
B6	18.16	-1.04	0.83
B10	18.59	-0.61	1.57
B12	20.00	0.80	0.67
B15	19.07	-0.13	0.59
B17	20.44	1.24	0.35
B20	20.48	1.28	0.30
B23	20.61	1.41	0.23
B24	20.28	1.08	0.65
B26	19.93	0.73	-0.16
B28	17.21	-1.99	0.86
B30	18.71	-0.49	0.75
B32	19.23	0.03	0.56
B33	19.92	0.72	0.53
B34	20.48	1.28	0.51
B35	19.36	0.16	0.30
B35'	20.18	0.98	0.96
B36'	21.08	1.88	-0.27
B39	20.88	1.68	0.51
B41	20.60	1.40	0.40
C3	20.40	1.20	0.44
C4	20.18	0.98	0.19
C14	19.68	0.48	0.35
C17	20.01	0.81	0.60
C20	19.13	-0.07	0.42

CLUSTER NO L20

REGION 1

STAR	V	MV	B-V
C24	19.91	0.71	0.19
C2]	19.28	0.08	0.44
C29	20.18	0.98	0.35
C34	19.39	0.19	0.47
C35	19.09	-0.11	0.57
C36	18.99	-0.21	0.53
C38	19.26	0.06	0.41
C39	20.11	0.91	0.25
D5	20.22	1.02	0.49
D6	18.82	-0.38	0.46
D7	17.73	-1.47	0.97
D8	18.83	-0.37	0.50
D9	20.24	1.04	-0.01
D101	19.82	0.62	0.10
D11	20.23	1.03	0.44
D12	20.38	1.18	0.12
D13	20.09	0.89	0.15
D14	19.96	0.76	0.01
D16	20.24	1.04	0.02
D17	19.03	-0.17	0.28
D19	20.48	1.28	0.14
D22	20.53	1.33	0.21
D23	20.45	1.25	0.60
D27	20.83	1.63	0.32
D28	20.48	1.28	0.09
D29	18.49	-0.71	0.94
D31	17.48	-1.72	0.93
D32	19.22	0.02	-0.11
D34	20.36	1.16	0.36
D35	20.65	1.45	0.45

CLUSTER NO L20

REGION 2

STAR	V	MV	B-V
1A2	19.55	0.35	0.36
1A5	18.63	-0.57	0.67
1A7	18.94	-0.26	0.66
1A10	20.42	1.22	0.61
1A13	17.55	-1.65	1.06
1A18	20.58	1.38	0.38
1A19	19.34	0.14	0.69
1A25	20.15	0.95	-0.16
1A30	19.68	0.48	0.06
1A34	18.72	-0.48	0.36
1A35	19.32	0.12	0.23
1A37	19.28	0.08	1.42
1A40	18.67	-0.53	0.36
1A48	19.36	0.16	0.45
1A50	20.76	1.56	0.36
1A51	20.76	1.56	0.80
1A53	20.14	0.94	0.38
1A55	19.98	0.78	0.14
1A59	18.18	-1.02	1.08
1A60	20.65	1.45	-0.20
1A61	20.70	1.50	0.86
2A67	20.46	1.26	0.49
2A70	20.81	1.61	0.16
2A78	19.13	-0.07	0.33
2A79	18.32	-0.88	0.32
2A6	20.69	1.49	0.34
2A8	18.08	-1.12	0.79
2A11	17.65	-1.55	0.69
2A14	20.02	0.82	0.45
2A15	18.93	-0.27	0.60
2A16	20.49	1.29	0.41
2A23	20.54	1.34	0.46
2A25	18.50	-0.70	0.89
2A27	20.48	1.28	0.67
2A28	20.45	1.25	0.22
2A30	20.18	0.98	0.24
2A32	20.77	1.57	-0.09
2A33	19.12	-0.08	0.55
2A39	18.18	-1.02	0.97
2A43	20.90	1.70	-0.11
2A48	20.14	0.94	0.24
2A54	19.44	0.24	0.64
2A56	20.91	1.71	-0.01
2A58	18.68	-0.52	1.02
2A59	18.09	-1.11	0.89
2A81	20.78	1.58	0.28
2A86	16.72	-2.48	1.34
2A61	18.55	-0.65	0.71

END

&RUN;

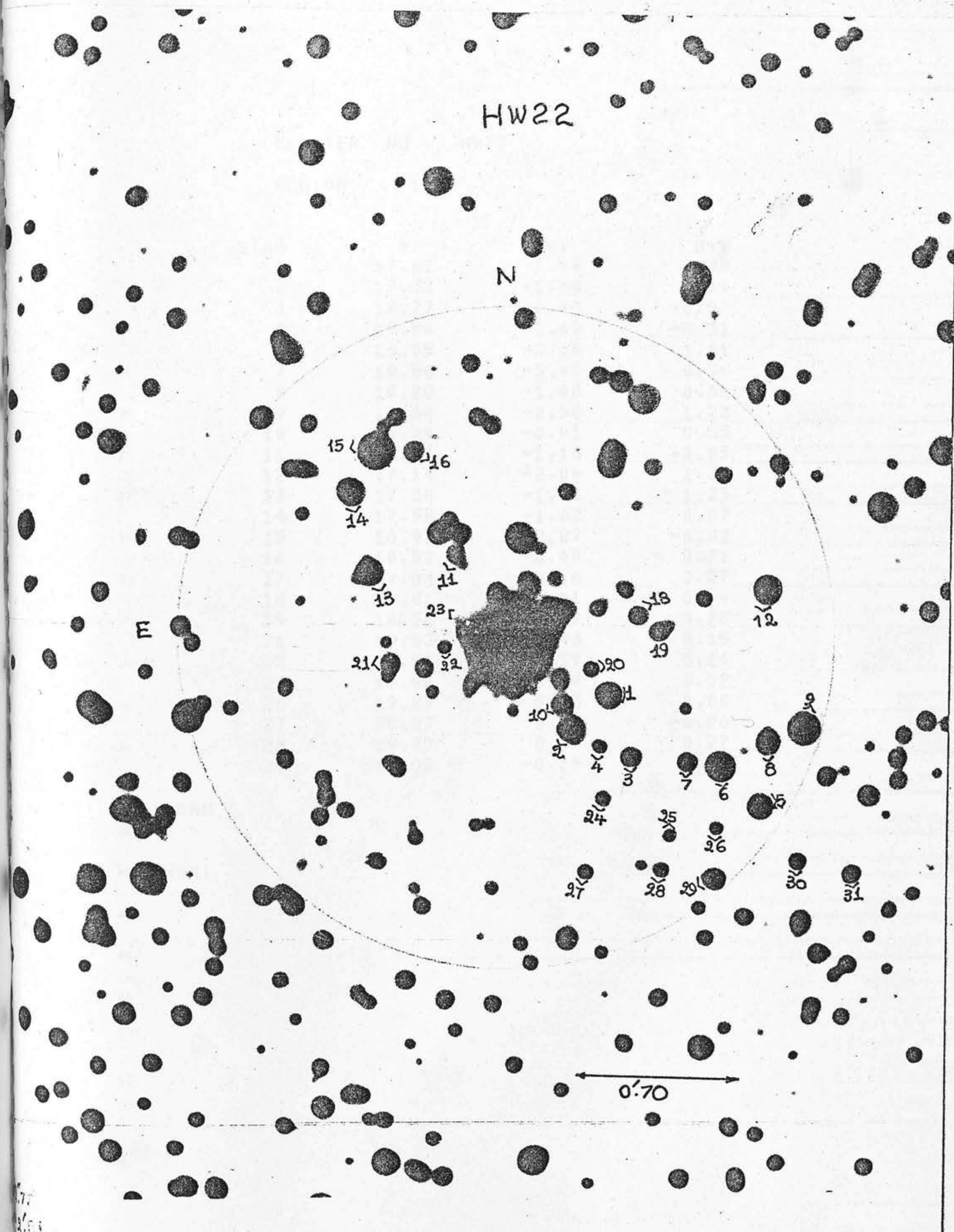
HW22
N
E
15
16
14
11
13
23
18
12
19
21
22
20
1
10
9
2
4
3
7
6
8
5
24
25
26
27
28
29
30
31
0'.70

CLUSTER NO HW22

REGION 1

STAR	V	MV	B-V
1	17.61	-1.59	0.88
2	17.32	-1.88	1.09
3	18.77	-0.43	-0.57
4	19.80	0.60	-0.31
6	16.55	-2.65	1.61
7	18.80	-0.40	0.51
8	18.20	-1.00	0.68
9	16.64	-2.56	1.23
10	18.29	-0.91	0.55
11	18.04	-1.16	-0.05
12	17.14	-2.06	1.34
13	17.30	-1.90	1.25
14	17.58	-1.62	0.87
15	16.93	-2.27	-0.02
16	18.52	-0.68	0.71
17	19.04	-0.16	0.37
18	19.81	0.61	0.54
19	18.58	-0.62	0.76
21	19.63	0.43	0.15
22	19.01	-0.19	0.14
24	19.06	-0.14	0.52
26	19.23	0.03	0.60
27	20.07	0.87	-0.26
28	19.27	0.07	0.27
29	19.02	-0.18	0.09

END

&RUN;

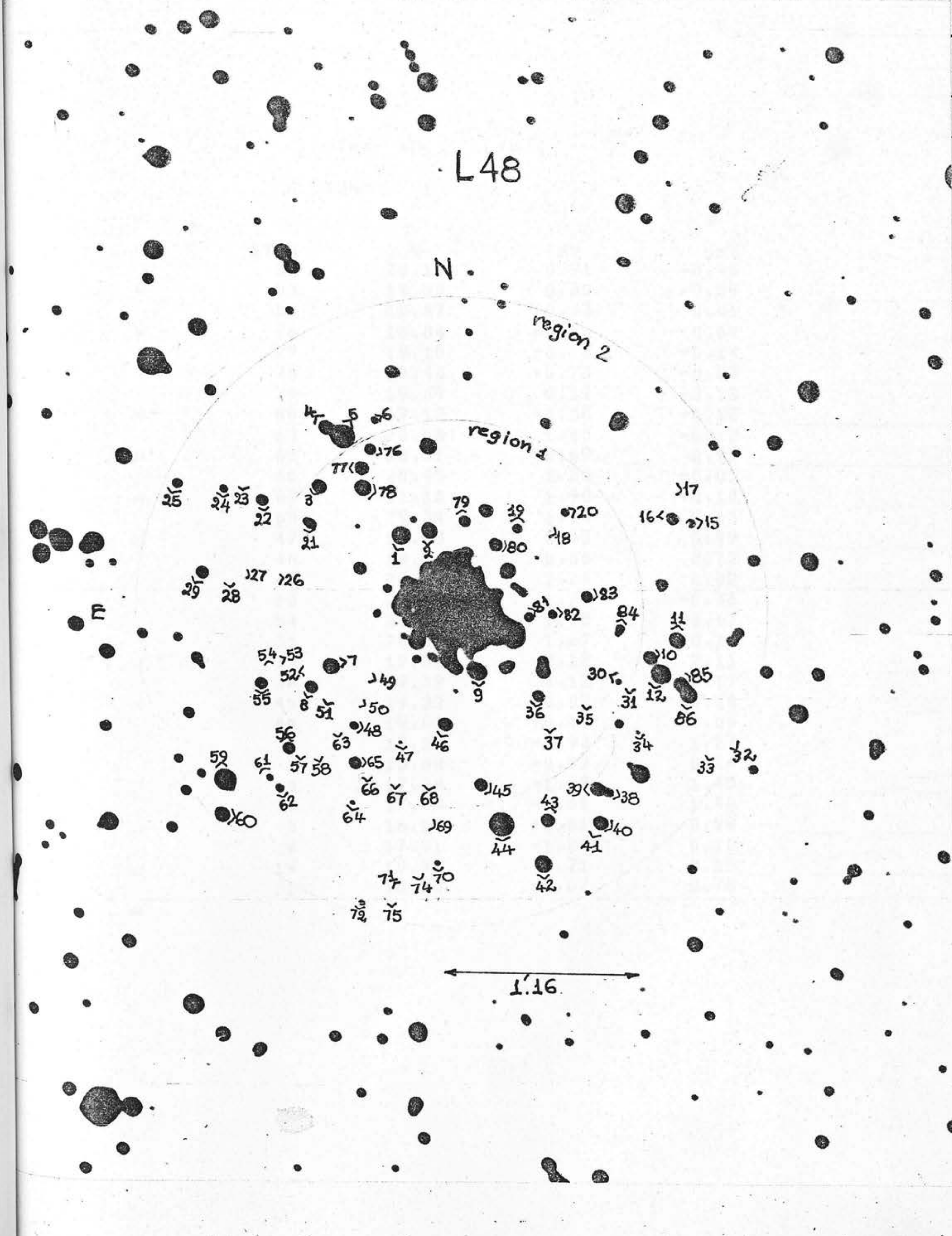
L48
N
E
region 2
region 1
1'.16

CLUSTER NO L48

REGION 1

STAR	V	MV	B-V
82	20.11	0.91	-0.46
83	19.50	0.30	-0.05
84	18.87	-0.33	0.61
76	18.84	-0.36	0.69
77	19.10	-0.10	-0.14
78	18.48	-0.72	-0.03
79	19.39	0.19	-0.13
80	19.12	-0.08	-0.12
63	20.68	1.48	-0.12
65	18.51	-0.69	0.95
66	20.45	1.25	-0.05
67	21.10	1.90	-0.10
68	20.34	1.14	0.63
47	19.53	0.33	0.49
48	19.14	-0.06	0.72
49	20.44	1.24	0.02
50	20.48	1.28	-0.36
54	21.18	1.98	-0.17
31	20.87	1.67	-0.12
35	19.08	-0.12	2.11
36	19.32	0.12	-0.17
45	19.22	0.02	0.10
46	19.05	-0.15	-0.05
1	17.27	-1.93	1.27
2	18.68	-0.52	0.14
3	17.98	-1.22	1.45
7	17.69	-1.51	1.40
8	18.59	-0.61	0.99
9	17.91	-1.29	0.10
19	19.91	0.71	0.15
21	18.53	-0.67	0.70

CLUSTER NO L48
REGION 2

STAR	V	MV	B-V
4	19.78	0.58	-0.52
5	16.38	-2.82	0.38
10	18.34	-0.86	1.04
11	18.65	-0.55	0.17
12	16.59	-2.61	1.92
15	19.15	-0.05	0.81
16	19.40	0.20	-0.15
17	20.75	1.55	0.07
22	18.75	-0.45	1.57
23	19.48	0.28	0.07
24	19.13	-0.07	1.06
25	19.02	-0.18	0.97
29	19.33	0.13	-0.07
32	20.69	1.49	-0.30
33	21.25	2.05	-0.20
34	19.98	0.78	0.09
39	18.61	-0.59	0.47
40	18.03	-1.17	1.15
41	20.46	1.26	0.19
42	18.32	-0.88	0.19
43	19.15	-0.05	-0.06
44	15.94	-3.26	0.91
55	19.15	-0.05	0.20
56	19.25	0.05	0.01
57	19.26	0.06	1.04
58	20.45	1.25	0.26
59	16.79	-2.41	-0.12
60	17.83	-1.37	1.27
61	19.71	0.51	0.05
62	18.97	-0.23	0.79
64	19.30	0.10	0.69
69	19.76	0.56	0.47
70	19.77	0.57	0.03
71	20.65	1.45	-0.05
75	20.90	1.70	0.43
85	18.11	-1.09	1.08
86	17.63	-1.57	0.81

END

&RUN;

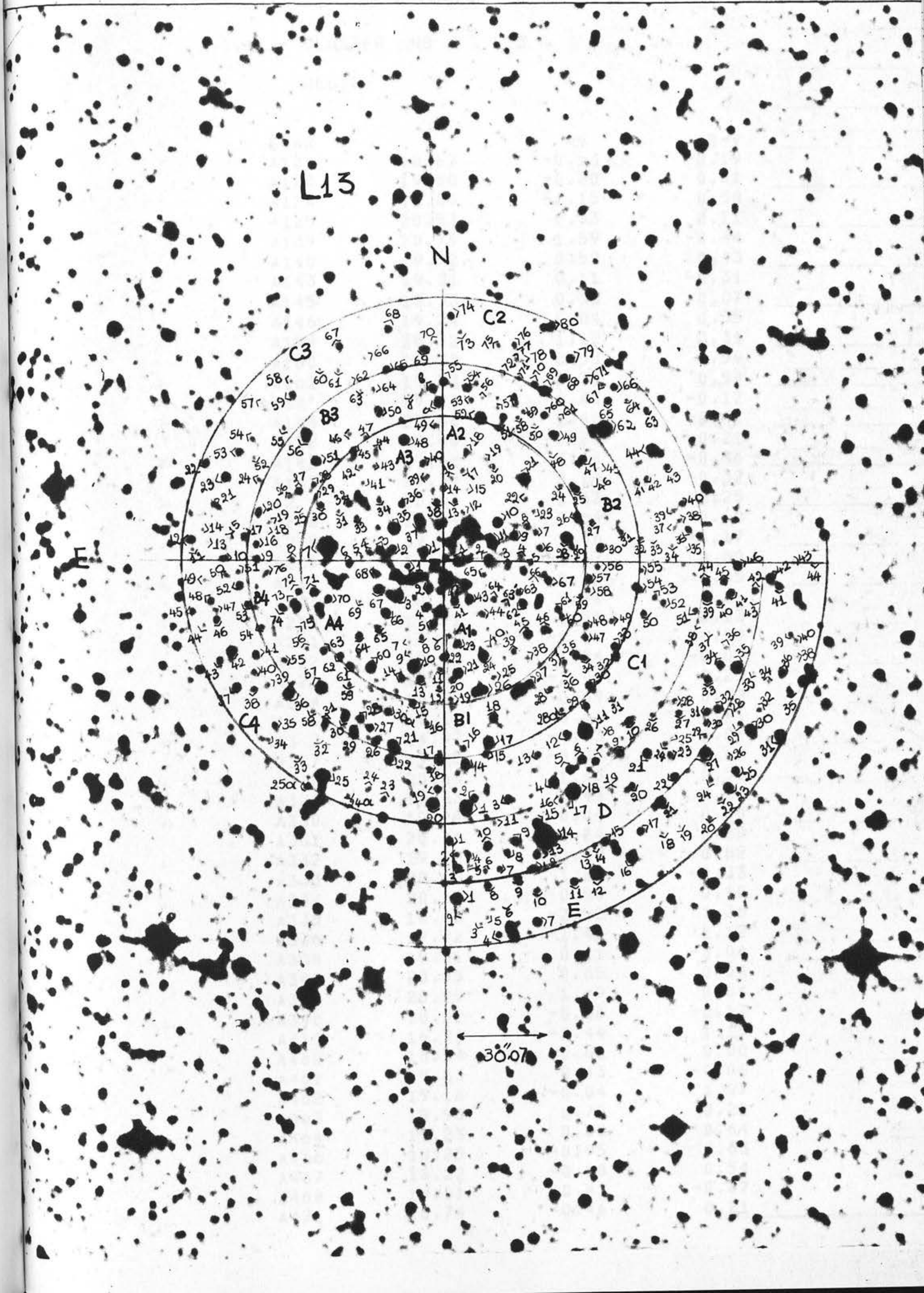
L13
N
E
C3
C2
B3
A2
A3
B2
B4
A4
A1
C1
C4
B1
D
E
30"07

CLUSTER NO L13

REGION 1

STAR	V	MV	B-V
A121	18.67	-0.53	-0.19
A123	19.00	-0.20	0.61
A124	18.05	-1.15	0.58
A125	20.53	1.33	0.11
A139	20.79	1.59	-0.44
A140	19.72	0.52	0.43
A143	19.31	0.11	-0.31
A145	19.53	0.33	0.07
A146	19.24	0.04	0.55
A159	20.32	1.12	0.31
A160	19.78	0.58	0.59
A161	19.53	0.33	0.54
A163'	19.63	0.43	-0.12
A164	20.66	1.46	-0.41
A22	19.00	-0.20	-0.21
A142	19.38	0.18	-0.36
A162	19.34	0.14	-0.32
A2 4	20.53	1.33	-0.25
A2 6	19.84	0.64	0.60
A2 9	19.56	0.36	-0.17
A210	17.73	-1.47	0.80
A212	19.67	0.47	0.65
A213	20.11	0.91	0.16
A214	19.71	0.51	0.03
A221	17.85	-1.35	0.59
A222	20.54	1.34	-0.07
A228	17.76	-1.44	0.25
A3 4	19.89	0.69	0.22
A3 6	19.19	-0.01	0.71
A3 7	14.97	-4.23	-0.01
A317	19.15	-0.05	0.62
A318	20.65	1.45	0.50
A320	19.63	0.43	0.28
A330	19.24	0.04	0.80
A331	20.44	1.24	0.29
A332	19.22	0.02	0.82
A333	20.28	1.08	-0.33
A334	20.10	0.90	0.10
A335	16.68	-2.52	1.36
A336	17.72	-1.48	2.12
A338	19.31	0.11	-0.04
A342	20.05	0.85	0.54
A344	20.29	1.09	0.04
A348	18.52	-0.68	-0.17
A410	16.76	-2.44	1.15
A460	18.54	-0.66	0.00
A461	19.63	0.43	-0.06
A462	19.16	-0.04	1.07
A463	19.90	0.70	0.20
A464	19.23	0.03	0.64
A466	18.25	-0.95	0.63
A467	18.22	-0.98	0.54
A468	19.61	0.41	-0.07
A471	18.74	-0.46	0.21

CLUSTER NO L13

REGION 2

STAR	V	MV	B-V
B114	18.58	-0.62	0.45
B116	19.85	0.65	0.26
B117	17.96	-1.24	0.67
B118	19.22	0.02	0.56
B128	19.91	0.71	0.62
B128'	20.09	0.89	0.59
B132	19.33	0.13	0.61
B134	19.79	0.59	0.55
B136	20.55	1.35	0.49
B147	20.33	1.13	0.06
B149	20.41	1.21	0.08
B157	19.85	0.65	0.05
B158	20.51	1.31	0.05
B225	19.24	0.04	0.32
B229	20.57	1.37	-0.05
B230	19.28	0.08	0.57
B245	21.18	1.98	-0.13
B249	19.03	-0.17	0.53
B252	17.76	-1.44	0.21
B260	19.41	0.21	0.79
B261	20.49	1.29	0.24
B3 9	19.33	0.13	0.33
B324	20.12	0.92	0.49
B325	20.58	1.38	0.52
B327	19.31	0.11	0.28
B349'	18.02	-1.18	0.48
B350	18.80	-0.40	0.53
B351	18.31	-0.89	0.87
B415	20.49	1.29	-0.49
B420	16.85	-2.35	1.38
B421	17.63	-1.57	1.18
B422	19.00	-0.20	0.31
B426	19.21	0.01	0.55
B427	19.08	-0.12	0.57
B429	17.85	-1.35	1.55
B431	19.27	0.07	0.65
B436	17.31	-1.89	1.16
B452	19.22	0.02	0.55
B453	19.19	-0.01	0.43
B457	16.96	-2.24	1.60
B458	20.55	1.35	0.15
B459	20.93	1.73	0.00
B472	19.69	0.49	0.06
B476	20.31	1.11	0.02

CLUSTER NO L13

REGION 3

STAR	V	MV	B-V
C1 1	17.02	-2.18	1.15
C1 2	19.29	0.09	0.41
C1 3	19.20	0.00	0.65
C1 4	18.01	-1.19	1.00
C1 5	18.71	-0.49	0.58
C1 6	19.06	-0.14	0.34
C1 7	19.28	0.08	0.56
C1 8	20.67	1.47	-0.20
C111	16.38	-2.82	0.76
C154	19.65	0.45	-0.01
C155	20.70	1.50	0.03
C234	20.90	1.70	0.17
C240	20.03	0.83	0.20
C243	19.78	0.58	0.69
C244	20.12	0.92	0.62
C244'	17.01	-2.19	1.42
C262	16.22	-2.98	0.44
C263	20.09	0.89	0.11
C265	19.07	-0.13	0.76
C266	19.21	0.01	0.75
C2670	19.99	0.79	0.38
C271	20.45	1.25	0.41
C273	20.21	1.01	0.57
C275	20.33	1.13	0.27
C277	20.65	1.45	0.36
C279	18.78	-0.42	0.88
C311	20.57	1.37	0.06
C312	19.32	0.12	0.17
C313	20.37	1.17	0.62
C314	20.25	1.05	0.49
C315	20.49	1.29	0.12
C321	19.95	0.75	0.15
C322	19.42	0.22	0.39
C323	17.72	-1.48	1.34
C352	20.43	1.23	0.59
C353	19.45	0.25	0.67
C354	19.96	0.76	0.81
C359	19.13	-0.07	0.92
C362	20.49	1.29	0.37
C367	19.38	0.18	0.75
C368	19.77	0.57	0.03
C420	16.85	-2.35	1.38
C424'	20.10	0.90	0.71
C425	17.06	-2.14	0.16
C469	18.79	-0.41	0.55
C433	20.84	1.64	-0.03
C435	19.93	0.73	0.35
C437	18.38	-0.82	1.02
C440	20.02	0.82	0.29
C442	18.23	-0.97	0.37
C443	19.83	0.63	0.02
C445	19.67	0.47	0.41
C448	19.58	0.38	0.56

CLUSTER NO L13

REGION 4

STAR	V	MV	B-V
D1	19.41	0.21	0.57
D4	20.07	0.87	-0.16
D6	20.44	1.24	0.25
D7	20.19	0.99	0.20
D8	20.07	0.87	-0.02
D9	19.40	0.20	0.29
D12	19.85	0.65	0.10
D13	18.94	-0.26	0.85
D14	13.55	-5.65	0.66
D18	16.31	-2.89	0.55
D21	18.72	-0.48	0.71
D22	19.29	0.09	0.37
D27	19.81	0.61	0.55
D32	19.36	0.16	0.48
D33	19.04	-0.16	0.58
D34	19.22	0.02	0.94
D35	17.72	-1.48	0.50
D37	20.88	1.68	0.15
D39	18.00	-1.20	0.90
D40	19.99	0.79	0.04
D41	19.30	0.10	0.42
D43	20.96	1.76	0.19
D44	19.07	-0.13	0.48
D45	19.50	0.30	0.46
D46	19.03	-0.17	0.40
E1	18.44	-0.76	-0.29
E5	20.89	1.69	-0.33
E7	18.88	-0.32	0.66
E9	19.17	-0.03	0.71
E11	19.68	0.48	0.01
E12	17.62	-1.58	-0.13
E13	20.57	1.37	0.18
E14	20.19	0.99	0.08
E15	19.26	0.06	0.41
E16	18.58	-0.62	-0.11
E17	19.34	0.14	0.56
E19	20.75	1.55	0.24
E20	20.49	1.29	0.01
E21	17.65	-1.55	0.87
E22	20.26	1.06	0.52
E23	18.25	-0.95	0.69
E24	20.72	1.52	-0.15
E27	18.09	-1.11	0.45
E29	20.43	1.23	0.11
E30	18.60	-0.60	-0.30
E31	17.89	-1.31	0.50
E32	20.42	1.22	0.29
E33	21.30	2.10	-0.28
E36	19.25	0.05	0.53
E38	20.83	1.63	0.21
E39	20.24	1.04	0.30
E40	20.97	1.77	-0.07
E41	19.14	-0.06	0.57
E42	18.59	-0.61	0.75
E43	20.82	1.62	0.49

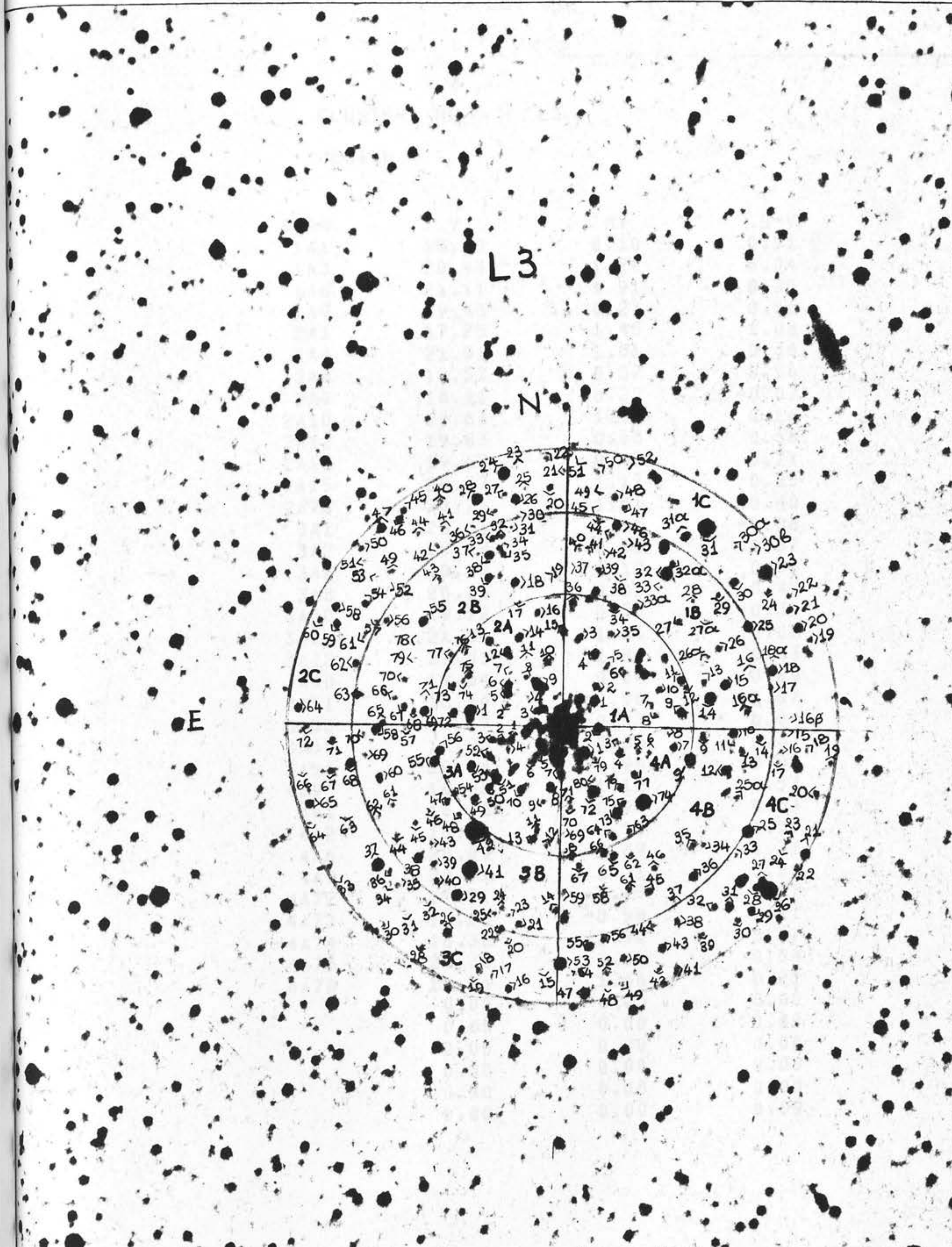
L3
N
E
1A
1B
1C
2A
2B
2C
3A
3B
3C
4A
4B
4C
20'6

CLUSTER NO L3

REGION 1

STAR	V	MV	B-V
1A1	19.30	0.10	0.51
1A3	20.44	1.24	0.04
1A6	21.11	1.91	0.25
1A9	19.43	0.23	0.56
2A1	17.75	-1.45	1.08
2A4	21.01	1.81	0.36
2A6	19.57	0.37	0.56
2A9	18.91	-0.29	-0.07
2A10	20.63	1.43	0.16
2A12	19.83	0.63	0.68
1A13	19.67	0.47	0.71
2A15	20.37	1.17	0.35
2A73	20.71	1.51	0.40
3A1	20.31	1.11	-0.06
3A2	20.18	0.98	0.07
3A6	20.32	1.12	0.02
3A8	20.03	0.83	0.49
3A10	19.72	0.52	0.36
3A11	21.16	1.96	0.02
3A12	21.01	1.81	0.43
3A50	19.54	0.34	0.89
3A51	18.64	-0.56	1.07
3A53	19.17	-0.03	0.84
3A55	19.25	0.05	0.87
3A56	20.14	0.94	-0.09
4A9'	18.08	-1.12	1.53
4A1	18.30	-0.90	0.63
4A2	18.29	-0.91	1.59
4A6	20.89	1.69	0.36
4A9	20.51	1.31	0.21
4A72	17.91	-1.29	1.27
4A73	18.62	-0.58	1.11
4A74	16.30	-2.90	0.87
4A75	20.38	1.18	0.54
4A78	20.86	1.66	0.21
	0.00	0.00	0.00
	0.00	0.00	0.00
	0.00	0.00	0.00
	0.00	0.00	0.00
	0.00	0.00	0.00
	0.00	0.00	0.00

CLUSTER NO L3

REGION 2

STAR	V	MV	B-V
1B11	20.11	0.91	0.26
1B14	17.91	-1.29	1.24
1B15	19.29	0.09	0.72
1B16	20.55	1.35	0.44
1B26'	20.99	1.79	0.31
1B32	18.09	-1.11	0.75
1B37	20.82	1.62	0.02
1B42	20.98	1.78	0.64
1B43	21.00	1.80	0.92
1B46	19.40	0.20	0.86
2B33	20.62	1.42	0.18
2B43	21.05	1.85	0.40
2B57	20.76	1.56	0.76
2B68	20.50	1.30	0.48
3B21	20.82	1.62	0.49
3B23	21.00	1.80	0.64
3B24	21.55	2.35	-0.22
3B25	21.42	2.22	-0.21
3B29	19.66	0.46	0.13
3B41	16.52	-2.68	0.76
3B42	15.11	-4.09	0.39
3B44	21.03	1.83	0.43
3B46	21.08	1.88	0.54
3B58	19.30	0.10	0.78
3B60	19.98	0.78	0.71
3B62	21.00	1.80	0.47
4B10	18.85	-0.35	1.50
4B12	18.14	-1.06	0.93
4B34	20.67	1.47	1.19
4B36	19.47	0.27	0.88
4B44	20.92	1.72	0.53
4B45	20.65	1.45	0.46
4B58	21.48	2.28	0.31
4B59	21.33	2.13	0.59
4B61	21.08	1.88	1.19
	0.00	0.00	0.00
	0.00	0.00	0.00
	0.00	0.00	0.00
	0.00	0.00	0.00
	0.00	0.00	0.00
	0.00	0.00	0.00

CLUSTER NO L3

REGION 3

STAR	V	MV	B-V
1C18	18.85	-0.35	0.98
1C20	19.82	0.62	0.52
1C22	20.83	1.63	0.90
1C25	18.84	-0.36	1.15
1C31	16.02	-3.18	0.61
1C31]	19.30	0.10	0.87
1C45	21.19	1.99	0.00
1C51	21.20	2.00	0.58
2C22	21.03	1.83	0.46
2C23	21.20	2.00	0.19
2C24	17.95	-1.25	1.06
2C26	18.66	-0.54	0.58
2C28	19.03	-0.17	0.68
2C29	20.79	1.59	0.43
2C30	20.76	1.56	0.50
2C40	21.05	1.85	0.35
2C49	21.03	1.83	0.88
2C51	21.34	2.14	0.16
2C53	20.69	1.49	0.76
2C57	20.76	1.56	0.76
2B58	19.60	0.40	0.81
2B60	20.89	1.69	0.35
3B15	17.50	-1.70	1.47
3C27	20.53	1.33	1.10
3C31	21.16	1.96	0.29
3C32	21.10	1.90	0.49
3C34	21.41	2.21	0.14
3C37	18.25	-0.95	0.86
3C38	19.55	0.35	1.08
3C66	21.15	1.95	0.78
3C68	19.85	0.65	0.02
4C21	19.25	0.05	0.86
4C25	18.34	-0.86	0.68
4C26	15.38	-3.82	1.16
4C31	19.59	0.39	0.84
4C39	21.06	1.86	0.59
4C42	21.09	1.89	0.55
4C43	20.27	1.07	0.41
4C47	19.48	0.28	0.35
4C51	20.55	1.35	0.37
4C64	20.47	1.27	0.12

END

°END:

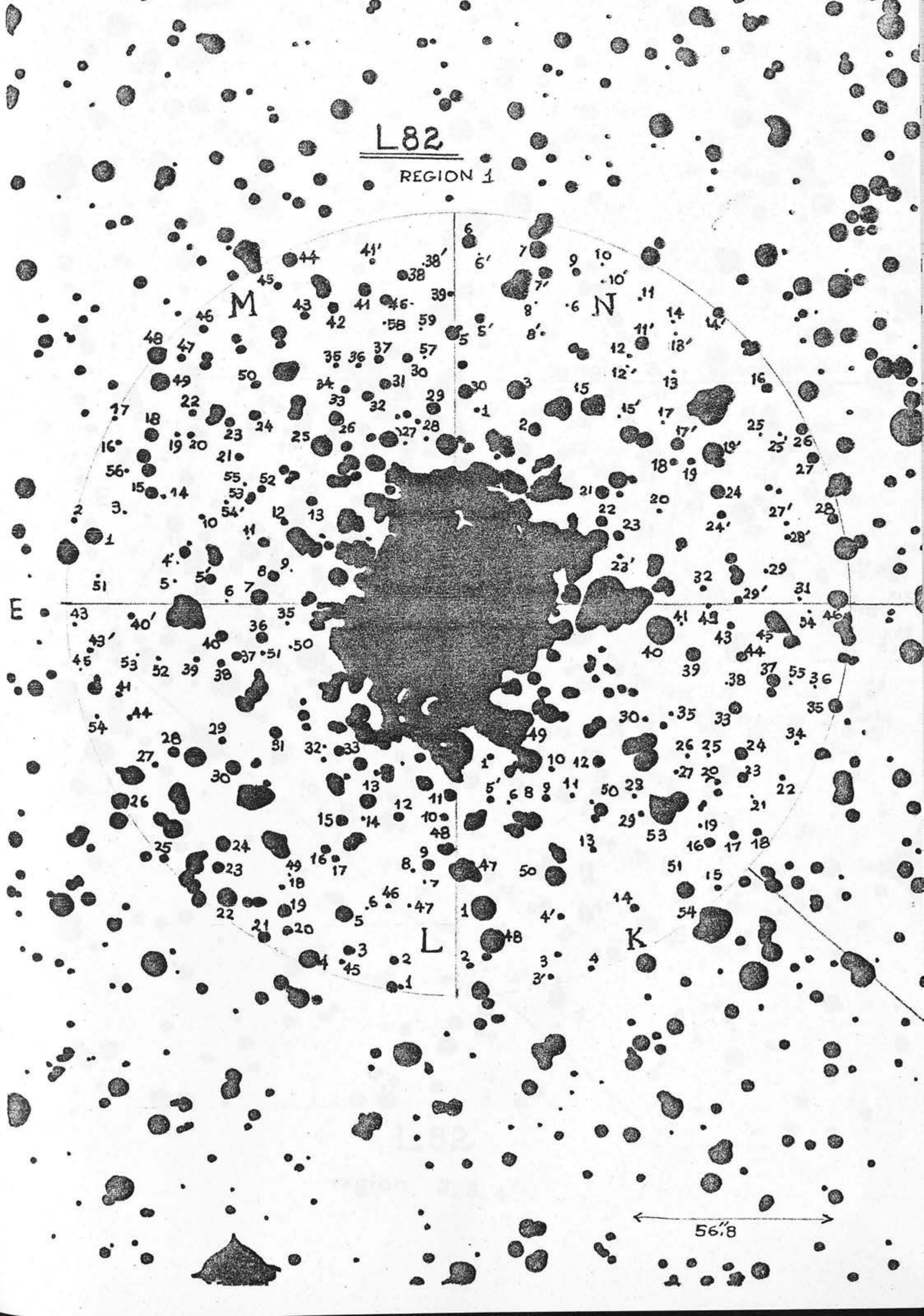
L82
REGION 1
E
M
N
L
K
56.8

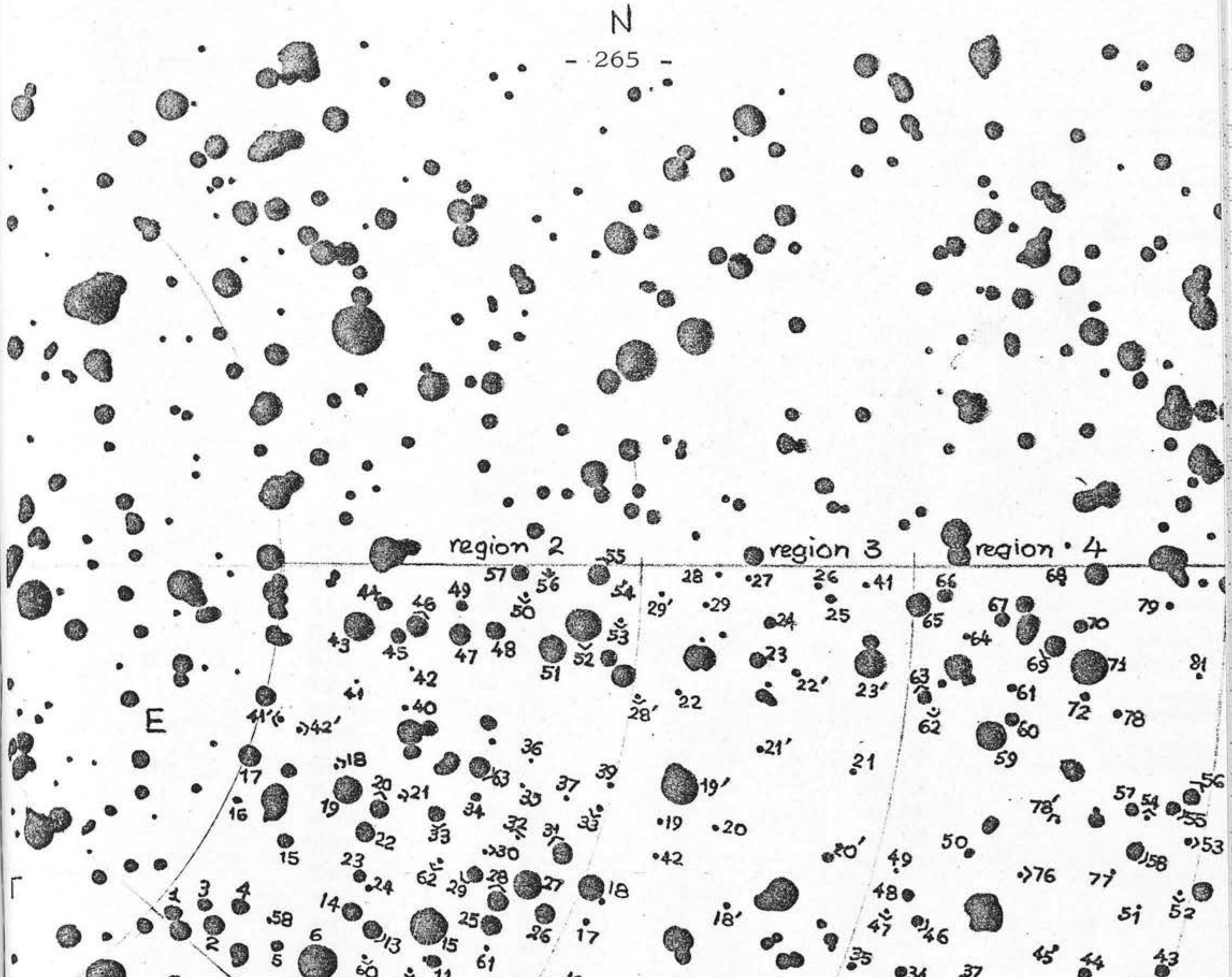

L82

region 2, 3, 4

CLUSTER NO L82

REGION 1

STAR	V	MV	B-V
K1	19.85	0.65	-0.43
K2	18.11	-1.09	0.32
K3	18.50	-0.70	0.16
K5	18.60	-0.60	0.39
K7	18.61	-0.59	0.20
K9	20.30	1.10	0.18
K10	20.11	0.91	0.00
K14	20.21	1.01	0.15
K15	16.28	-2.92	1.59
K16	18.90	-0.30	0.21
K20	19.76	0.56	-0.36
K22	18.31	-0.89	0.65
K23	18.63	-0.57	0.43
K24	18.56	-0.64	0.17
K25	20.52	1.32	-0.06
K27	19.04	-0.16	-0.28
K28	18.91	-0.29	0.74
K30	18.30	-0.90	0.94
K31	20.40	1.20	-0.10
K32	19.46	0.26	-0.16
K5'	19.41	0.21	-0.17
K7'	18.79	-0.41	-0.12
K11'	18.41	-0.79	0.67
K13'	20.01	0.81	0.33
K14'	18.82	-0.38	0.91
K15'	19.27	0.07	0.33
K19'	17.11	-2.09	0.86
K23'	19.56	0.36	0.13
K28'	20.24	1.04	0.38
K29'	18.86	-0.34	0.82
L1	18.43	-0.77	0.11
L2	20.04	0.84	-0.25
L3	19.89	0.69	0.28
L5	20.74	1.54	-0.32
L6	19.56	0.36	0.08
L7	18.17	-1.03	0.12

CLUSTER NO L82

REGION 1

STAR	V	MV	B-V
L13	18.69	-0.51	0.33
L14	20.29	1.09	1.09
L16	19.48	0.28	-0.22
L19	20.03	0.83	-0.20
L20	19.79	0.59	-0.20
L21	19.33	0.13	0.45
L22	19.66	0.46	-0.01
L23	19.24	0.04	-0.06
L25	17.08	-2.12	0.84
L26	18.25	-0.95	0.98
L29	19.01	-0.19	0.02
L32	18.90	-0.30	0.07
L36	18.86	-0.34	-0.01
L38	19.71	0.51	-0.22
L39	19.85	0.65	-0.31
L40	18.64	-0.56	-0.18
L41	18.60	-0.60	-0.29
L42	19.13	-0.07	-0.22
L43	19.11	-0.09	0.40
L44	18.96	-0.24	-0.03
L45	19.36	0.16	0.47
L47	19.55	0.35	0.11
L48	18.80	-0.40	-0.20
L49	18.29	-0.91	-0.10
L50	19.26	0.06	0.18
L51	20.75	1.55	0.34
L52	19.42	0.22	-0.25
L56	20.72	1.52	-0.28
L57	20.76	1.56	0.22
L58	20.75	1.55	0.17
L59	20.49	1.29	0.59
L38'	20.54	1.34	0.33
M1	18.73	-0.47	0.53
M3	18.96	-0.24	0.69
M4	18.40	-0.80	0.19
M5	17.89	-1.31	0.63
M7	20.14	0.94	-0.07
M9	19.14	-0.06	-0.11
M12	19.63	0.43	-0.10
M13	17.95	-1.25	0.68
M43'	19.35	0.15	0.51
M16	19.80	0.60	-0.24
M18	19.71	0.51	-0.27
M19	18.95	-0.25	-0.08
M20	19.12	-0.08	0.38

CLUSTER NO L82

REGION 1

STAR	V	MV	B-V
M21	19.42	0.22	0.02
M22	18.03	-1.17	0.26
M23	18.40	-0.80	0.87
M24	18.41	-0.79	0.02
M25	19.18	-0.02	0.22
M27	19.90	0.70	-0.05
M28	18.81	-0.39	0.38
M29	19.25	0.05	0.29
M30	17.80	-1.40	1.00
M31	18.33	-0.87	0.84
M40'	19.49	0.29	0.33
M54	20.56	1.36	0.32
M35	19.75	0.55	-0.19
M36	19.37	0.17	-0.58
M38	19.49	0.29	-0.06
M40	18.62	-0.58	-0.40
M41	19.98	0.78	-0.12
M43	20.51	1.31	-0.36
M47	20.72	1.52	-0.32
M48	18.67	-0.53	-0.07
M49	20.03	0.83	0.52
N1	17.23	-1.97	0.23
N2	19.73	0.53	-0.23
N3	19.43	0.23	0.31
N7	19.50	0.30	-0.10
N10	19.76	0.56	0.10
N11	19.82	0.62	0.08
N13	19.65	0.45	-0.09
N14	19.27	0.07	0.55
N16	18.96	-0.24	0.52
N19	19.40	0.20	-0.05
N22	19.15	-0.05	0.81
N24	18.46	-0.74	-0.08
N26	20.15	0.95	-0.07
N28	20.13	0.93	-0.44
N30	19.04	-0.16	0.37
N32	19.83	0.63	-0.18
N35	19.00	-0.20	-0.22
N36	19.85	0.65	0.14
N37	18.22	-0.98	0.79
N39	18.66	-0.54	-0.02
N40	16.10	-3.10	0.36
N41	19.86	0.66	-0.17
N43	18.60	-0.60	-0.22
N44	19.39	0.19	-0.03
N45	17.55	-1.65	0.37
N46	17.49	-1.71	1.18
N47	15.86	-3.34	1.61
N48	16.11	-3.09	1.65
N50	17.96	-1.24	0.74
N51	17.90	-1.30	0.81
N52	14.51	-4.69	1.28
N54	20.45	1.25	0.02
N3'	19.54	0.34	0.57

CLUSTER NO L82

REGION 2

STAR	V	MV	B-V
A3	19.73	0.53	-0.32
A4	18.49	-0.71	0.92
A5	19.66	0.46	-0.30
A6	16.07	-3.13	0.89
A7	20.49	1.29	0.25
A9	18.25	-0.95	1.02
A10	19.98	0.78	-0.07
A11	18.86	-0.34	0.42
A12	16.65	-2.55	0.29
A13	18.73	-0.47	-0.10
A14	18.92	-0.28	-0.20
A17	19.12	-0.08	-0.19
A18	19.86	0.66	-0.18
A19	16.87	-2.33	1.42
A20	18.91	-0.29	-0.08
A21	19.96	0.76	-0.38
A22	18.44	-0.76	0.63
A23	18.81	-0.39	0.42
A24	20.07	0.87	-0.01
A26	18.95	-0.25	-0.02
A27	16.51	-2.69	0.09
A28	18.17	-1.03	0.59
A30	20.00	0.80	-0.08
A31	18.66	-0.54	-0.05
A32	19.76	0.56	0.21
A33	19.02	-0.18	0.42
A37	19.86	0.66	-0.12
A39	19.35	0.15	0.36
A41	19.85	0.65	-0.08
A42	20.10	0.90	-0.34
A43	16.78	-2.42	1.25
A46	18.60	-0.60	-0.10
A47	18.93	-0.27	-0.04
A48	18.77	-0.43	0.63
A49	19.64	0.44	-0.05
A50	19.97	0.77	-0.23
A51	17.77	-1.43	0.06
A52	16.74	-2.46	0.52
A53	19.85	0.65	0.11
A54	19.90	0.70	-0.17
A56	20.15	0.95	-0.20

CLUSTER NO L82

REGION 3

STAR	V	MV	B-V
B1	18.30	-0.90	0.62
B2	18.37	-0.83	0.05
B3	19.24	0.04	-0.22
B4	19.99	0.79	-0.31
B5	19.37	0.17	-0.37
B6	19.32	0.12	0.45
B9	18.25	-0.95	1.12
B10	18.04	-1.16	0.63
B16	17.89	-1.31	1.16
B17	19.76	0.56	0.08
B18	18.16	-1.04	0.03
B20	20.57	1.37	-0.02
B22	19.80	0.60	0.04
B24	19.07	-0.13	0.53
B25	19.61	0.41	-0.22
B26	19.81	0.61	-0.08
B29	19.63	0.43	0.47
B32	18.36	-0.84	0.69
B33	20.29	1.09	0.08
B34	19.85	0.65	-0.07
B35	20.91	1.71	0.04
B39	18.01	-1.19	1.30
B19'	16.22	-2.98	1.22
B23'	17.29	-1.91	0.27
B29'	20.81	1.61	0.21

CLUSTER NO L82

REGION 4

STAR	V	MV	B-V
C1	18.35	-0.85	0.29
C2	17.59	-1.61	0.88
C4	17.95	-1.25	1.07
C5	19.54	0.34	0.06
C8	18.34	-0.86	0.18
C9	18.86	-0.34	-0.31
C11	17.70	-1.50	0.14
C18	19.57	0.37	-0.09
C19	18.91	-0.29	0.80
C21	18.25	-0.95	0.71
C22	18.37	-0.83	1.01
C24	19.93	0.73	-0.45
C25	18.58	-0.62	-0.03
C29	19.24	0.04	-0.07
C31	19.06	-0.14	0.60
C35	19.94	0.74	-0.36
C38	19.60	0.40	-0.28
C39	18.24	-0.96	0.72
C41	19.02	-0.18	-0.32
C43	18.39	-0.81	0.63
C45	20.11	0.91	-0.40
C50	19.78	0.58	-0.06
C55	18.18	-1.02	0.37
C58	18.93	-0.27	-0.35
C59	16.58	-2.62	1.20
C61	18.30	-0.90	1.65
C65	18.16	-1.04	0.26
C66	18.58	-0.62	1.11
C67	18.51	-0.69	1.12
C71	16.11	-3.09	0.79
C76	20.23	1.03	-0.14
C77	20.43	1.23	-0.47
C1′	20.19	0.99	0.12
C2′	20.60	1.40	0.69
C3′	20.26	1.06	-0.36
C5′	17.58	-1.62	0.85
C17′	20.53	1.33	0.35

END

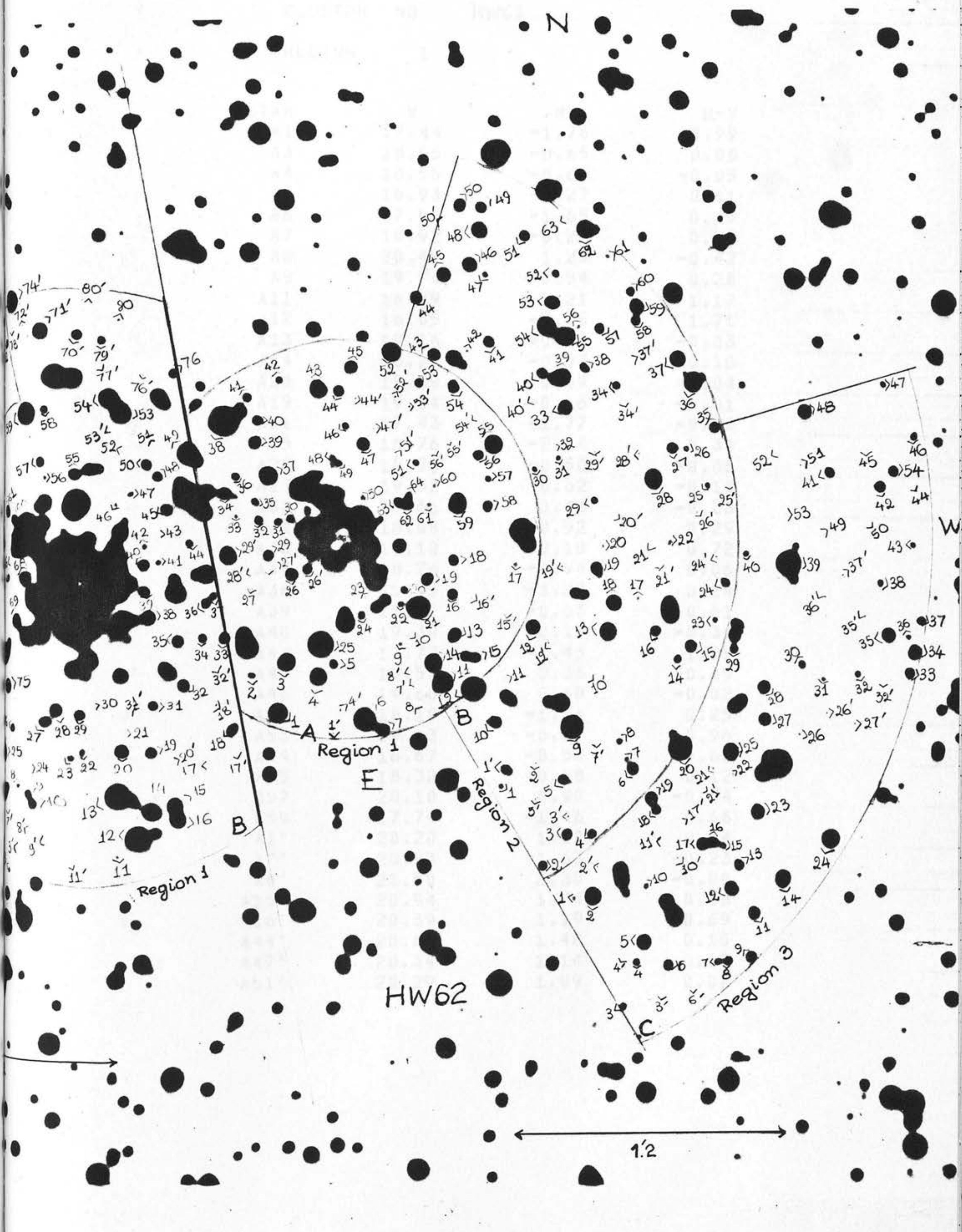
N
W
E
Region 1
Region 1
Region 2
Region 3
A
B
B
C
HW62
1.'2

CLUSTER NO **HW62**

REGION 1

STAR	V	MV	B-V
A1	17.44	-1.76	0.99
A3	18.55	-0.65	0.06
A4	18.56	-0.64	-0.05
A5	18.93	-0.27	0.61
A6	17.55	-1.65	0.25
A7	18.92	-0.28	0.23
A8	20.49	1.29	-0.42
A9	19.74	0.54	0.28
A11	16.99	-2.21	1.17
A12	16.05	-3.15	1.71
A13	19.16	-0.04	-0.03
A14	18.27	-0.93	0.18
A18	19.69	0.49	-0.04
A19	19.04	-0.16	-0.01
A21	17.43	-1.77	-0.20
A25	16.76	-2.44	0.34
A28	18.70	-0.50	-0.06
A29	19.52	0.32	-0.18
A32	19.66	0.46	-0.23
A34	18.68	-0.52	0.29
A36	19.10	-0.10	0.72
A37	18.26	-0.94	0.06
A38	15.93	-3.27	0.24
A39	18.57	-0.63	0.61
A40	19.39	0.19	-0.36
A43	17.77	-1.43	1.05
A45	19.56	0.36	-0.35
A46	19.60	0.40	-0.02
A52	18.19	-1.01	0.25
A53	19.13	-0.07	0.96
A54	18.67	-0.53	0.68
A55	18.32	-0.88	0.12
A57	20.10	0.90	-0.24
A59	17.74	-1.46	0.66
A1'	20.20	1.00	0.14
A7'	20.83	1.63	-0.23
A8'	21.50	2.30	-0.09
A15'	20.94	1.74	0.38
A16'	20.39	1.19	0.69
A44'	20.68	1.48	0.15
A47'	20.34	1.14	0.12
A51'	20.29	1.09	0.02

CLUSTER NO HW62

REGION 2

STAR	V	MV	B-V
B3	18.75	-0.45	1.11
B5	19.60	0.40	-0.05
B6	18.87	-0.33	0.78
B9	17.45	-1.75	0.34
B10	18.98	-0.22	0.39
B13	17.83	-1.37	0.83
B15	18.38	-0.82	1.16
B16	19.64	0.44	-0.20
B17	20.08	0.88	0.03
B18	18.73	-0.47	0.12
B19	18.60	-0.60	0.80
B20	20.06	0.86	-0.19
B25	19.35	0.15	0.78
B26	20.07	0.87	-0.20
B27	19.62	0.42	-0.31
B28	17.28	-1.92	1.14
B29	19.85	0.65	0.17
B33	18.94	-0.26	0.10
B34	19.90	0.70	-0.12
B36	17.80	-1.40	0.37
B37	17.88	-1.32	-0.18
B39	17.33	-1.87	0.93
B41	19.36	0.16	0.16
B44	19.13	-0.07	0.19
B45	18.28	-0.92	0.98
B46	17.55	-1.65	0.42
B48	18.07	-1.13	0.64
B49	19.53	0.33	-0.31
B50	19.06	-0.14	0.11
B51	18.93	-0.27	0.72
B53	18.45	-0.75	0.52
B55	16.87	-2.33	1.18
B57	19.31	0.11	0.21
B58	19.15	-0.05	0.66
B59	18.07	-1.13	0.88
B61	20.07	0.87	-0.09
B62	17.88	-1.32	0.37
B63	20.44	1.24	0.22
B2'	19.22	0.02	0.46
B5'	20.81	1.61	0.56
B14'	20.63	1.43	0.14
B20'	20.09	0.89	0.30
B24'	21.13	1.93	0.01
B34'	20.43	1.23	-0.07
B50'	21.00	1.80	-0.17
B52'	19.80	0.60	0.70

CLUSTER NO **HW62**

REGION 3

STAR	V	MV	B-V
C1	20.12	0.92	-0.20
C2	18.49	-0.71	0.13
C4	19.72	0.52	-0.05
C5	18.21	-0.99	1.01
C11	19.67	0.47	-0.44
C13	19.44	0.24	0.00
C14	17.77	-1.43	1.14
C18	19.61	0.41	-0.17
C20	16.60	-2.60	1.17
C21	20.27	1.07	-0.16
C23	18.82	-0.38	0.84
C24	18.25	-0.95	0.18
C25	18.13	-1.07	0.63
C26	20.32	1.12	-0.30
C27	18.98	-0.22	0.55
C28	19.43	0.23	-0.06
C31	19.74	0.54	0.35
C32	19.84	0.64	0.03
C34	18.77	-0.43	0.10
C35	19.12	-0.08	-0.23
C39	16.70	-2.50	0.22
C40	19.89	0.69	-0.24
C43	20.14	0.94	-0.07
C45	20.12	0.92	0.15
C47	19.95	0.75	-0.18
C48	18.86	-0.34	0.23
C49	20.49	1.29	-0.18
C51	20.84	1.64	0.17
C53	20.39	1.19	0.34
C55	20.11	0.91	-0.02
C6'	21.18	1.98	0.06
C11'	19.92	0.72	0.41
C17'	20.67	1.47	0.31
C21'	20.98	1.78	0.31
C23'	20.36	1.16	0.12
C30'	21.15	1.95	-0.01
C37'	20.52	1.32	0.10

END

&RUN;

L90

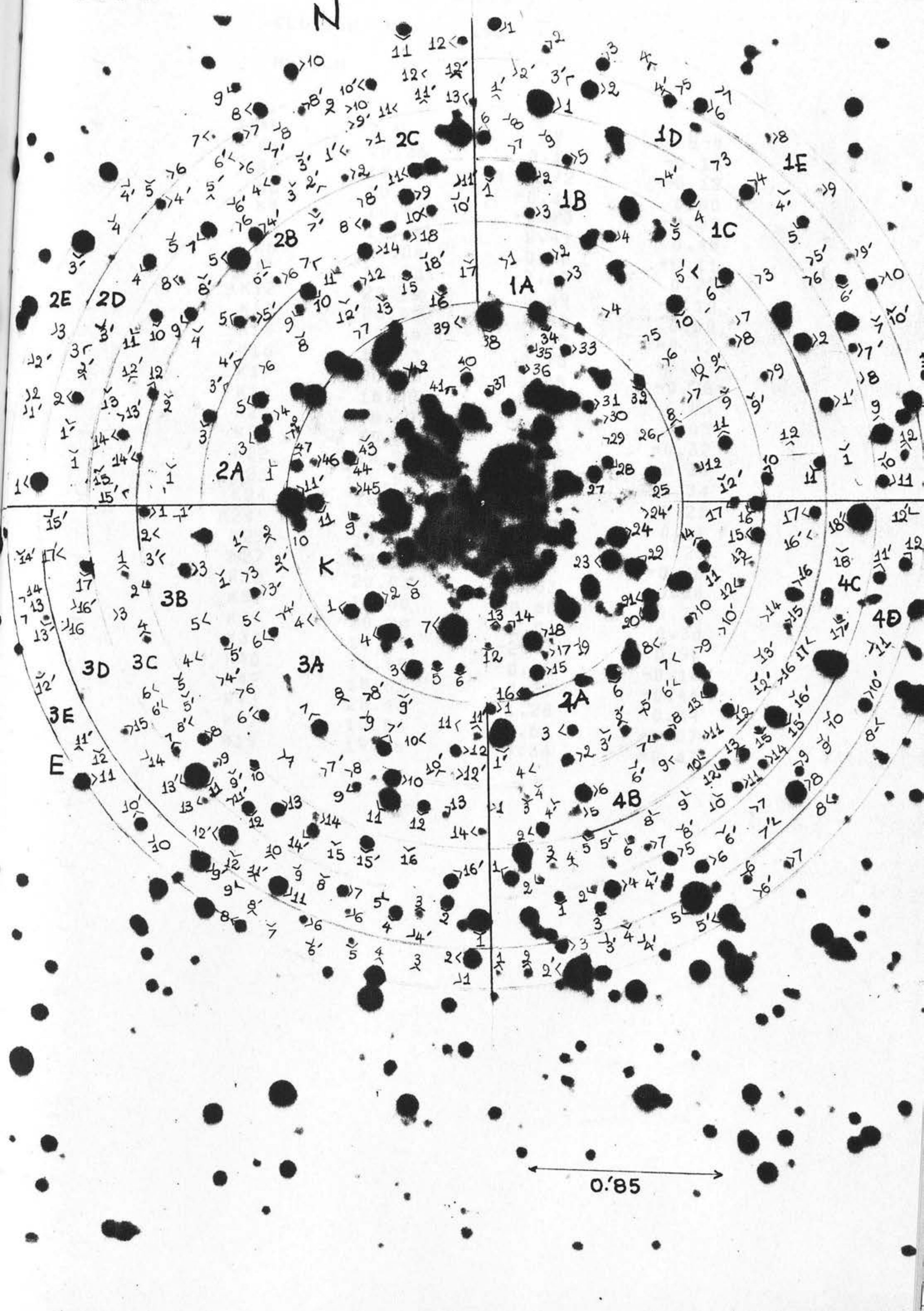

CLUSTER NO L90

REGION 1

STAR	V	MV	B-V
K1	19.36	0.16	-0.13
K2	18.48	-0.72	-0.12
K3	18.88	-0.32	0.00
K4	18.47	-0.73	-0.09
K5	19.61	0.41	0.45
K6	20.08	0.88	-0.11
K11'	16.33	-2.87	0.72
K12	20.09	0.89	-0.10
K13	20.06	0.86	0.08
K14	20.29	1.09	-0.12
K16	19.93	0.73	-0.33
K17	20.25	1.05	-0.28
K18	18.55	-0.65	-0.05
K20	18.47	-0.73	0.65
K21	19.21	0.01	-0.32
K22	18.30	-0.90	0.39
K23	18.55	-0.65	-0.34
K24	18.29	-0.91	-0.21
K24'	20.77	1.57	0.18
K25	19.42	0.22	-0.23
K27	19.56	0.36	-0.30
K28	20.03	0.83	-0.56
K32	19.80	0.60	-0.20
K35	20.28	1.08	0.30
K38	16.69	-2.51	0.90
K40	19.65	0.45	-0.18
K42	18.81	-0.39	-0.46
K43	20.48	1.28	0.34
K47	19.80	0.60	-0.07
K15	19.56	0.36	-0.37

CLUSTER NO L90

REGION 2

STAR	V	MV	B-V
1A2	19.86	0.66	-0.16
1A2	20.33	1.13	0.26
1A7	20.59	1.39	-0.17
1A9	20.78	1.58	-0.22
1A10	18.67	-0.53	0.06
2A1	20.35	1.15	0.74
2A3	19.45	0.25	0.08
2A4	19.71	0.51	0.14
2A5	18.96	-0.24	0.17
2A9	20.01	0.81	0.05
2A10	19.30	0.10	-0.32
2A12'	21.04	1.84	0.22
2A13	20.79	1.59	-0.10
2A15	20.20	1.00	0.02
2A12	20.15	0.95	-0.06
2A13'	20.94	1.74	-0.09
3A1	20.88	1.68	0.22
3A2	20.67	1.47	0.18
3A2'	20.57	1.37	0.18
3A4	20.59	1.39	0.09
3A6	20.15	0.95	-0.04
3A7	18.99	-0.21	0.09
3A7'	18.29	-0.91	0.68
3A8	20.40	1.20	0.14
3A12	19.47	0.27	0.07
3A12'	20.43	1.23	0.02
4A1	19.84	0.64	-0.47
4A1'	17.11	-2.09	-0.17
4A5	20.19	0.99	-0.07
4A6	19.37	0.17	-0.32
4A6'	20.97	1.77	0.00

CLUSTER NO L90

REGION 3

STAR	V	MV	B-V
1B2	18.53	-0.67	0.10
1B3	19.95	0.75	0.14
1B4	19.10	-0.10	0.48
1B5	20.54	1.34	-0.45
1B5'	20.57	1.37	0.67
1B6	19.37	0.17	-0.15
1B9	20.12	0.92	0.07
1B11	19.83	0.63	-0.16
2B1	20.75	1.55	0.08
2B2	20.44	1.24	-0.06
2B5	19.16	-0.04	0.67
2B6'	20.50	1.30	0.27
2B8	20.40	1.20	-0.21
2B8'	21.09	1.89	0.07
3B1	20,09	0.89	-0.01
3B5'	20.30	1.10	0.63
3B6'	18,12	-1.08	0.82
3B9	19.92	0.72	0.17
3B11	17,41	-1.79	0.57
3B13	19.98	0.78	0.13
3B14	20.08	0.88	-0.16
4B2	19.73	0.53	-0.43
4B4	20,42	1.22	0.04
4B5	19.98	0.78	0.02
4B6	18.91	-0.29	-0.11
4B10	20.62	1.42	-0.34
4B11	20.13	0.93	0.28
4B12	19.62	0.42	-0.29
4B13	19.37	0.17	-0.33
4B16	19.15	-0.05	-0.11
4B17	19.04	-0.16	0.52

CLUSTER NO L90

REGION 4

STAR	V	MV	B-V
1C1'	18.83	-0.37	0.62
1C2	18.83	-0.37	-0.06
1C4	19.39	0.19	-0.17
1C4'	20.88	1.68	0.60
2C2'	21.08	1.88	-0.21
2C4	19.65	0.45	0.65
2C5	17.35	-1.85	0.98
2C7	19.36	0.16	-0.32
2C9	18.76	-0.44	0.84
2C10	19.21	0.01	0.66
2C11	19.95	0.75	0.35
2C12	19.49	0.29	0.52
2C14	19.46	0.26	0.59
3C1	20.26	1.06	-0.04
3C9	20.50	1.30	-0.40
3C11	16.53	-2.67	0.64
3C11'	20.50	1.30	0.31
3C12	19.60	0.40	-0.15
3C13	18.87	-0.33	0.56
3C14	18.12	-1.08	1.54
C14'	20.01	0.81	-0.20
3C16	20.73	1.53	-0.25
3C16'	19.02	-0.18	0.02
4C2	19.90	0.70	-0.09
4C5	19.62	0.42	-0.36
4C5'	20.95	1.75	-0.24
4C7'	20.38	1.18	-0.34
4C8'	21.07	1.87	-0.20
4C12	19.59	0.39	0.33
4C15	19.99	0.79	-0.09
4C17'	19.98	0.78	0.12
4C18	20.66	1.46	-0.28
4C18'	17.16	-2.04	-0.36

CLUSTER NO L90

REGION 5

STAR	V	MV	B-V
1D4	19.50	0.30	-0.32
1D7'	19.97	0.77	0.08
1D8	21.24	2.04	0.09
1D9	18.25	-0.95	-0.10
1D12	20.13	0.93	-0.31
2D2	20.09	0.89	-0.09
2D6	21.08	1.88	-0.19
2D7	20.12	0.92	-0.15
2D8'	19.64	0.44	0.45
2D11	20.65	1.45	0.17
3D1	17.56	-1.64	-0.34
3D2	18.76	-0.44	0.41
3D4	19.60	0.40	-0.54
3D4'	20.69	1.49	0.08
3D6	20.63	1.43	-0.33
3D11	17.35	-1.85	1.27
3D12'	17.60	-1.60	0.85
3D13'	16.59	-2.61	0.53
3D16	20.62	1.42	0.25
4D1	19.34	0.14	0.43
4D4	19.79	0.59	-0.01
4D4	18.86	-0.34	-0.29
4D4'	20.43	1.23	0.46
4D8	18.20	-1.00	-0.16
4D9	20.16	0.96	0.39
4D9'	20.53	1.33	0.18
4D10'	19.70	0.50	-0.34
4D11'	18.91	-0.29	0.53
4D12	19.52	0.32	-0.08

CLUSTER NO L90

REGION 6

STAR	V	MV	B-V
1E1	18.19	-1.01	1.16
1E2	19.17	-0.03	0.62
1E3	18.45	-0.75	0.59
1E4	20.18	0.98	0.16
1E4'	19.72	0.52	-0.31
1E7	20.51	1.31	0.01
1E9'	20.15	0.95	0.06
E10'	20.97	1.77	0.45
1E12	17.71	-1.49	-0.34
1E13	19.89	0.69	0.01
1E14	20.07	0.87	0.18
2E1	18.85	-0.35	-0.03
2E3'	18.77	-0.43	-0.40
2E6	20.64	1.44	-0.02
2E10	18.85	-0.35	-0.14
2E11	19.01	-0.19	-0.20
2E12	19.15	-0.05	0.52
3E1	20.57	1.37	-0.10
3E2	18.45	-0.75	-0.12
3E8	19.56	0.36	-0.01
3E9'	17.58	-1.62	0.89
3E10'	19.05	-0.15	0.71
3E11	19.04	-0.16	-0.24
4E3	19.09	-0.11	0.50
4E4	20.49	1.29	-0.28
4E7	20.32	1.12	-0.41
4E8'	21.15	1.95	-0.32

END

&RUN;

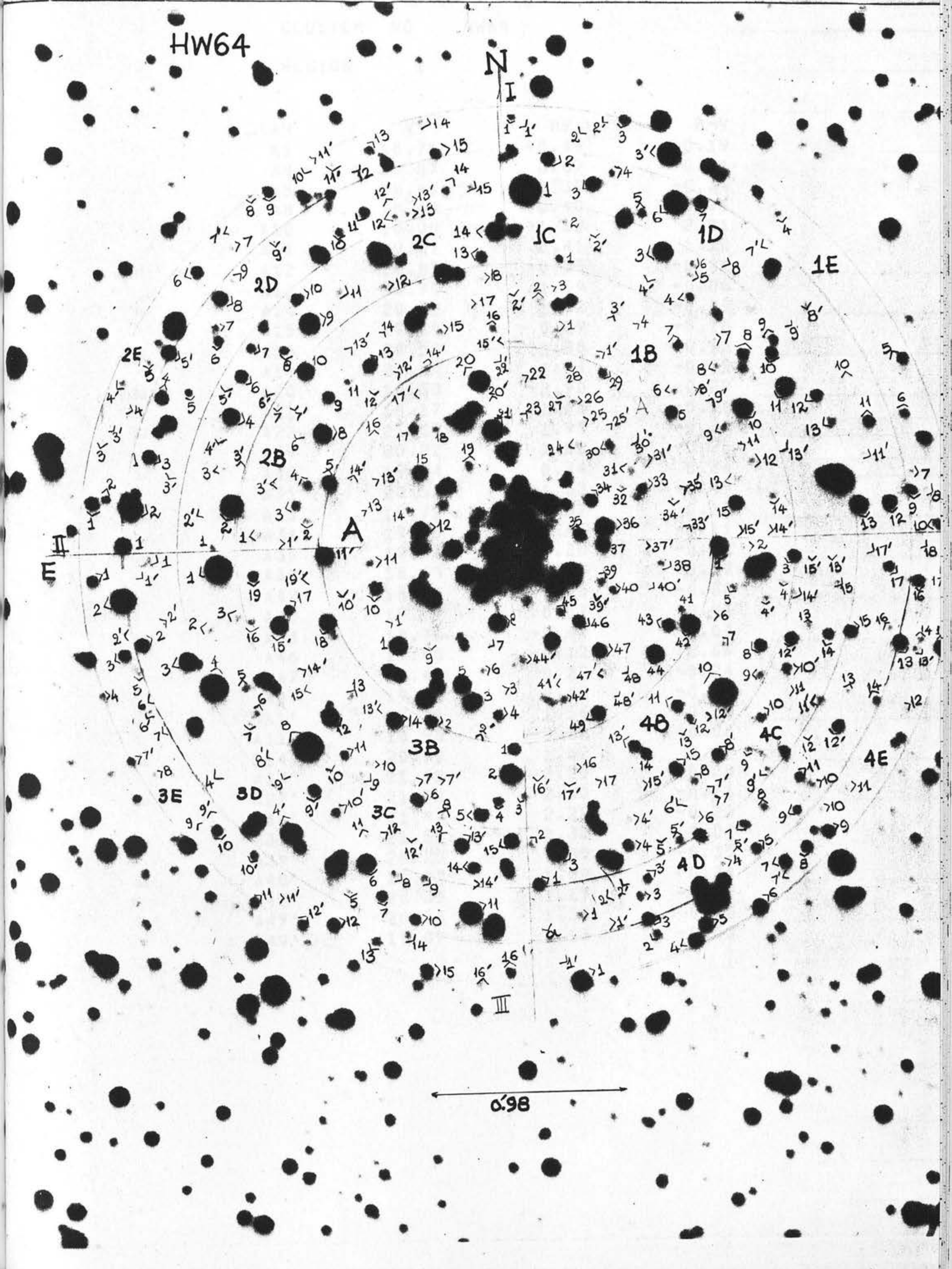
HW64
N
E
A
1B
1C
1D
1E
2B
2C
2D
2E
3B
3C
3D
3E
4B
4C
4D
4E
0'98

CLUSTER NO HW64

REGION 1

STAR	V	MV	B-V
A1	18.71	-0.49	-0.19
A4	20.07	0.87	0.01
A5	18.81	-0.39	-0.34
A8	18.80	-0.40	-0.11
A10	18.08	-1.12	2.01
A11	19.61	0.41	1.18
A12	18.85	-0.35	-0.21
A13	20.79	1.59	-0.06
A14	20.32	1.12	-0.09
A15	19.49	0.29	-0.16
A16	20.58	1.38	-0.13
A19	20.24	1.04	-0.32
A20	18.30	-0.90	-0.22
A21	18.17	-1.03	-0.11
A22	21.13	1.93	-0.39
A29	20.22	1.02	-0.21
A30	19.94	0.74	0.34
A31	20.53	1.33	-0.45
A33	19.72	0.52	0.15
A34	19.65	0.45	-0.11
A35	19.58	0.38	-0.31
A36	18.65	-0.55	-0.09
A42	18.67	-0.53	-0.30
A43	19.77	0.57	-0.41
A44	18.76	-0.44	-0.04
A46	19.08	-0.12	0.66
A47	19.42	0.22	-0.24
A49	19.62	0.42	-0.37
A1'	20.76	1.56	0.36
A11'	18.98	-0.22	-0.08
A14'	20.72	1.52	0.47
A17'	21.45	2.25	-0.28
A22'	21.50	2.30	-0.21
A34'	21.42	2.22	-0.23
A37'	21.52	2.32	0.04
A39'	20.25	1.05	-0.35
A40'	21.02	1.82	0.34
A42'	20.35	1.15	-0.22
A47'	20.56	1.36	0.30
A49'	19.07	-0.13	-0.03

CLUSTER NO HW64

REGION 2

STAR	V	MV	B-V
1B3	21.25	2.05	-0.40
1B4	20.62	1.42	0.14
1B7	20.03	0.83	-0.12
1B8	20.68	1.48	-0.23
1B10	18.65	-0.55	-0.14
1B13	20.08	0.88	0.37
1B1'	20.43	1.23	-0.04
1B3'	21.15	1.95	-0.11
1B8'	20.77	1.57	-0.13
1B14'	20.93	1.73	-0.11
2B1	20.42	1.22	-0.11
2B2	20.30	1.10	-0.17
2B4	20.08	0.88	-0.26
2B5	19.41	0.21	-0.25
2B8	18.90	-0.30	-0.32
2B9	19.00	-0.20	0.82
2B10	19.04	-0.16	-0.21
2B11	20.63	1.43	0.09
2B13	19.65	0.45	-0.18
2B17	20.38	1.18	0.44
2B3'	20.70	1.50	0.34
2B7'	21.58	2.38	-0.29
2B14'	19.88	0.68	0.65
3B2	18.44	-0.76	-0.24
3B3	20.62	1.42	0.02
3B6	19.63	0.43	-0.17
3B11	19.59	0.39	0.65
3B12	18.77	-0.43	-0.29
3B13	20.32	1.12	0.13
3B14	19.21	0.01	-0.13
3B17	19.72	0.52	0.07
3B18	19.10	-0.10	-0.37
3B19	20.05	0.85	-0.12
3B7'	20.74	1.54	0.28
3B14'	21.32	2.12	0.04
3B15'	18.05	-1.15	0.87
3B19'	21.22	2.02	-0.04
4B1	18.77	-0.43	-0.11
4B3	19.78	0.58	-0.22
4B5	20.08	0.88	0.21
4B7	20.32	1.12	0.40
4B9	20.48	1.28	0.24
4B10	16.89	-2.31	-0.28
4B11	19.85	0.65	-0.23
4B14	20.11	0.91	-0.28
4B15	19.38	0.18	0.02
4B16	20.89	1.69	0.16
4B17	20.76	1.56	0.08
4B13'	19.74	0.54	-0.22
4B15'	20.54	1.34	0.51

CLUSTER NO HW64

REGION 3

STAR	V	MV	B-V
1C2	20.87	1.67	-0.53
1C3	17.89	-1.31	0.72
1C5	20.58	1.38	-0.02
1C6	20.43	1.23	-0.12
1C7	20.90	1.70	-0.20
1C9	19.41	0.21	0.00
1C11	17.67	-1.53	1.07
1C12	19.47	0.27	-0.09
1C3'	20.72	1.52	0.35
1C13'	20.36	1.16	0.06
2C1	20.00	0.80	0.51
2C2	16.57	-2.63	1.34
2C4	18.13	-1.07	0.89
2C5	20.59	1.39	0.28
2C6	19.80	0.60	-0.35
2C8	19.60	0.40	0.53
2C9	18.23	-0.97	-0.10
2C11	20.90	1.70	-0.13
2C12	19.76	0.56	0.50
2C13	19.15	-0.05	0.51
2C14	18.78	-0.42	-0.45
2C5'	20.61	1.41	0.11
2C6'	21.35	2.15	-0.34
3C1	15.91	-3.29	0.79
3C4	16.41	-2.79	0.28
3C8	16.15	-3.05	0.07
3C9	21.07	1.87	0.10
3C14	19.31	0.11	0.51
3C15	19.44	0.24	-0.30
3C8'	20.88	1.68	0.43
3C9'	19.10	-0.10	0.61
3C10'	20.27	1.07	-0.21
3C12'	21.70	2.50	-0.30
3C13'	19.62	0.42	-0.26
4C3	18.06	-1.14	-0.06
4C4	19.40	0.20	-0.04
4C6	19.62	0.42	0.45
4C7	20.40	1.20	0.35
4C14	19.75	0.55	-0.06
4C4'	20.15	0.95	0.17
4C5'	20.17	0.97	-0.14
4C6'	20.28	1.08	0.20
4C7'	20.61	1.41	-0.12
4C10'	19.85	0.65	0.03
4C11'	19.80	0.60	0.45
4C12'	19.05	-0.15	0.45

CLUSTER NO HW64

REGION 4

STAR	V	MV	B-V
1D1	15.91	-3.29	-0.38
1D2	19.46	0.26	-0.12
1D3	19.25	0.05	-0.15
1D5	20.12	0.92	-0.06
1D6	16.79	-2.41	0.71
1D7	18.79	-0.41	0.67
1D12	19.21	0.01	-0.18
1D13	17.84	-1.36	0.77
1D7'	20.53	1.33	-0.08
1D8'	20.69	1.49	-0.15
2D1	19.17	-0.03	-0.27
2D2	17.53	-1.67	-0.27
2D3	19.65	0.45	-0.29
2D6	19.91	0.71	-0.11
2D7	20.08	0.88	-0.14
2D8	19.16	-0.04	-0.14
2D9	20.62	1.42	-0.03
2D11	19.97	0.77	-0.10
2D14	19.84	0.64	0.51
2D15	20.35	1.15	-0.24
2D5'	19.21	0.01	-0.22
2D8'	20.85	1.65	0.06
2D12'	21.18	1.98	-0.26
3D1	20.40	1.20	0.00
3D2	19.52	0.32	-0.29
3D3	17.88	-1.32	0.61
3D6	18.55	-0.65	-0.13
3D7	19.27	0.07	0.56
3D9	20.22	1.02	0.00
3D11	17.74	-1.46	-0.45
3D1'	21.01	1.81	-0.10
3D4'	16.93	-2.27	1.25
4D5	19.34	0.14	-0.14
4D6	19.98	0.78	-0.27
4D7	19.17	-0.03	0.58
4D9	20.00	0.80	-0.04
4D14	20.37	1.17	-0.38
4D15	19.76	0.56	-0.27
4D4'	20.10	0.90	-0.15
4D5'	21.10	1.90	-0.18

CLUSTER NO HW64

REGION 5

STAR	V	MV	B-V
1E3	19.68	0.48	-0.06
1E4	19.84	0.64	0.33
1E5	19.33	0.13	0.55
1E6	20.23	1.03	-0.05
1E7	20.40	1.20	0.07
1E9	19.70	0.50	-0.46
1E10	19.33	0.13	-0.29
1E1'	20.82	1.62	0.37
1E3'	17.46	-1.74	-0.21
2E1	19.76	0.56	-0.46
2E3	20.87	1.67	-0.01
2E5	20.29	1.09	-0.16
2E6	19.04	-0.16	0.88
2E7	20.70	1.50	0.54
2E8	20.41	1.21	0.27
2E9	19.30	0.10	0.72
2E11	20.54	1.34	0.03
2E4'	20.69	1.49	-0.07
3E1	20.01	0.81	-0.21
3E2	17.60	-1.60	-0.11
3E8	20.80	1.60	-0.12
3E11	19.36	0.16	0.70
3E13	19.59	0.39	0.09
3E15	18.97	-0.23	0.44
3E7'	20.27	1.07	-0.05
3E12'	19.85	0.65	-0.05
4E1	18.18	-1.02	1.77
4E3	19.40	0.20	-0.12
4E4	18.35	-0.85	0.87
4E5	18.86	-0.34	-0.06
4E6	18.93	-0.27	-0.10
4E7	19.62	0.42	-0.40
4E9	19.61	0.41	-0.33
4E13	19.27	0.07	-0.38
4E14	20.65	1.45	0.26
4E16	19.61	0.41	-0.17
4E2'	20.02	0.82	-0.06
4E7'	20.77	1.57	0.05
4E13'	20.08	0.88	0.22

END

&RUN;

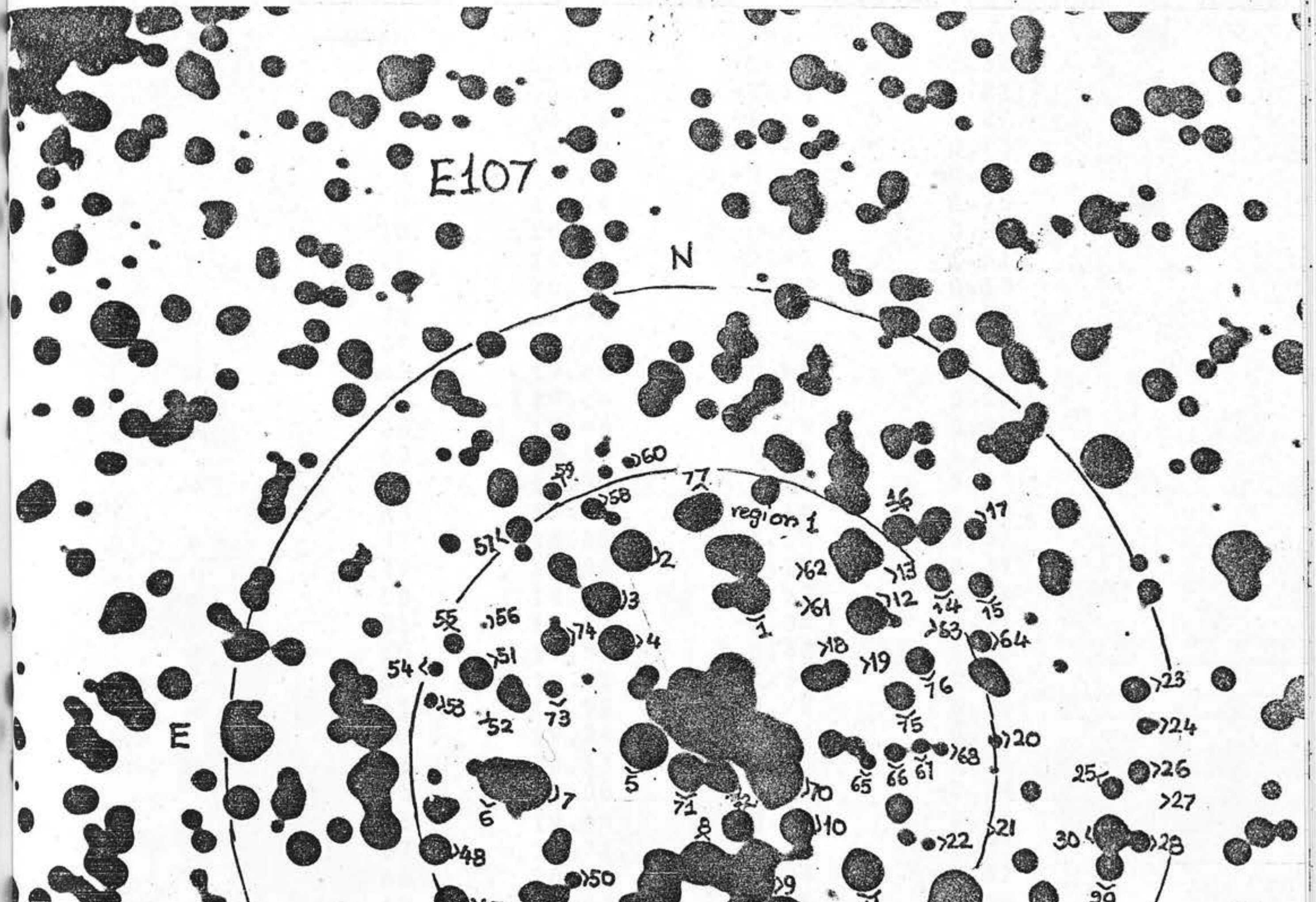
E107
N
E
region 1
region 2
0'.44

CLUSTER NO E107

REGION 1

STAR	V	MV	B-V
2	17.40	-1.80	0.32
3	18.09	-1.11	0.21
4	18.19	-1.01	0.27
5	16.42	-2.78	0.13
8	17.00	-2.20	-0.16
9	17.99	-1.21	0.96
10	18.38	-0.82	0.25
12	16.71	-2.49	1.41
13	20.15	0.95	0.18
22	19.93	0.73	0.10
34	19.72	0.52	0.20
35	19.88	0.68	0.12
37	19.18	-0.02	0.50
38	17.44	-1.76	0.99
39	19.48	0.28	0.14
42	19.55	0.35	0.03
43	19.04	-0.16	0.64
47	18.05	-1.15	0.57
49	19.08	-0.12	-0.37
50	19.77	0.57	0.06
51	18.14	-1.06	0.71
55	19.52	0.32	0.30
57	18.81	-0.39	0.59
61	19.99	0.79	0.05
62	19.94	0.74	0.30
63	20.13	0.93	0.51
65	20.08	0.88	-0.24
66	19.68	0.48	0.11
67	19.71	0.51	0.31
68	20.14	0.94	0.02
69	18.62	-0.58	0.68
70	15.97	-3.23	0.04
71	18.17	-1.03	-0.13
72	18.70	-0.50	-0.22
73	19.20	0.00	-0.13
75	18.74	-0.46	0.54
76	19.15	-0.05	0.04

REGION 2

STAR	V	MV	B-V
16	18.76	-0.44	-0.05
17	19.13	-0.07	0.72
21	19.72	0.52	0.53
23	18.75	-0.45	0.67
24	19.33	0.13	0.55
26	19.18	-0.02	0.31
27	20.32	1.12	-0.27
29	17.24	-1.96	1.07
30	19.39	0.19	-0.26
31	18.35	-0.85	0.93
32	19.45	0.25	0.34
33	18.85	-0.35	0.66
41	17.29	-1.91	1.25
44	17.31	-1.89	0.37
45	14.53	-4.67	-0.34
46	17.87	-1.33	0.13
48	19.18	-0.02	-0.30
59	19.58	0.38	0.37
60	20.25	1.05	0.33

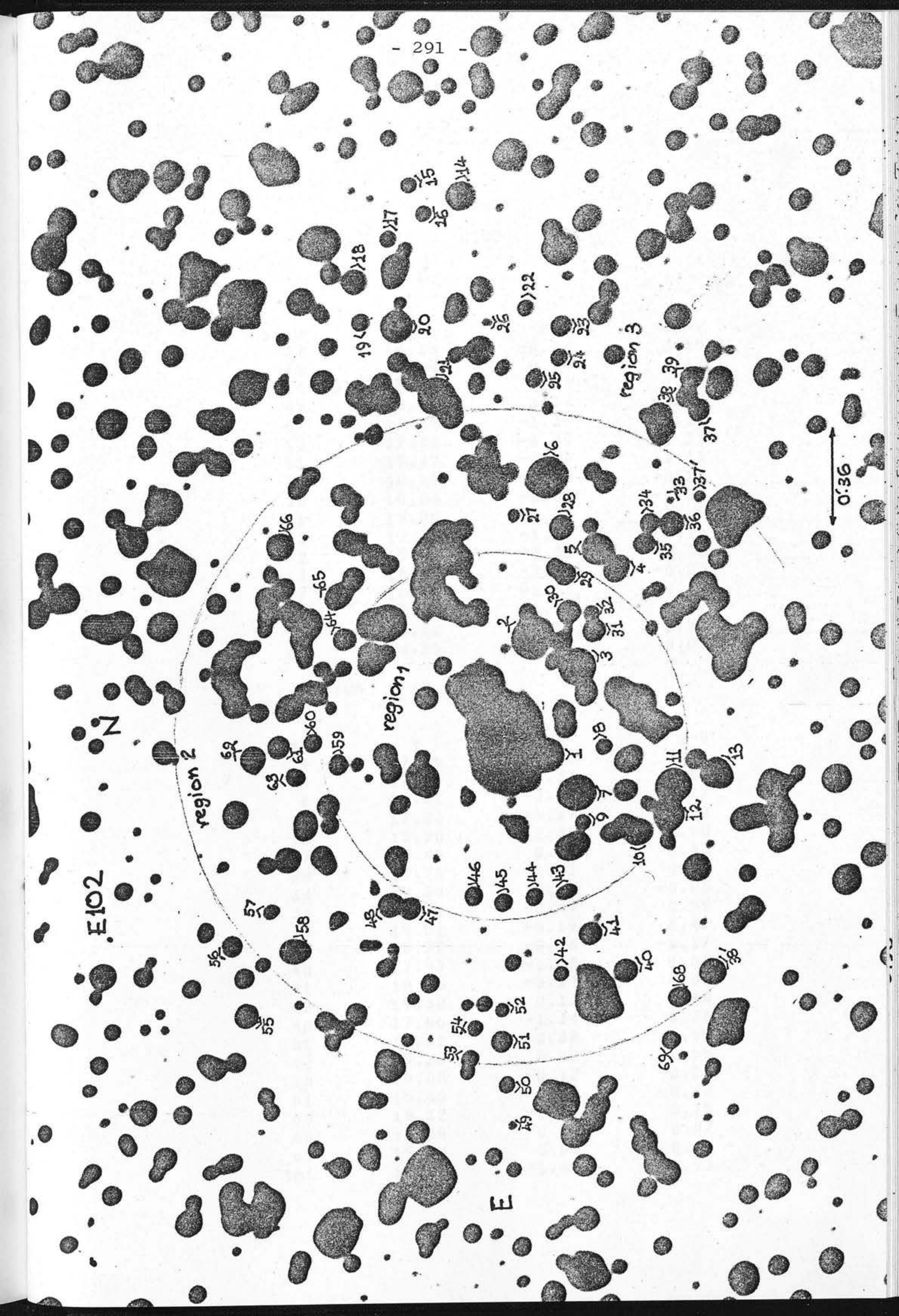
E102
N
E
region 1
region 2
region 3
0'.36

CLUSTER NO E102

REGION 1

STAR	V	MV	B-V
32	19.13	-0.07	0.65
43	19.34	0.14	0.17
44	19.34	0.14	0.13
45	19.54	0.34	-0.33
47	17.85	-1.35	1.14
10	17.80	-1.40	0.11
11	15.75	-3.45	1.11
29	18.99	-0.21	-0.18
30	18.88	-0.32	-0.07
31	19.05	-0.15	-0.35
1	17.39	-1.81	-0.16
2	15.75	-3.45	-0.18
3	16.67	-2.53	-0.22
7	16.70	-2.50	-0.17
9	18.20	-1.00	0.79
59	18.82	-0.38	0.51
64	18.85	-0.35	0.05

REGION 2

STAR	V	MV	B-V
4	17.65	-1.55	0.14
5	17.89	-1.31	1.07
6	15.81	-3.39	-0.77
12	17.23	-1.97	0.92
13	16.90	-2.30	0.98
27	19.40	0.20	0.43
28	17.79	-1.41	0.81
33	19.84	0.64	-0.06
34	18.71	-0.49	0.59
35	19.01	-0.19	0.47
36	18.72	-0.48	-0.17
40	17.97	-1.23	1.08
41	18.96	-0.24	0.04
42	19.32	0.12	0.46
48	17.86	-1.34	0.76
51	18.32	-0.88	0.95
52	19.25	0.05	0.55
58	19.08	-0.12	-0.16
61	18.60	-0.60	0.40
63	19.12	-0.08	0.15
66	18.30	-0.90	0.07
69	19.28	0.08	0.10
38'	17.72	-1.48	0.93

CLUSTER NO E102

REGION 3

STAR	V	MV	B-V
14	17.96	-1.24	-0.04
16	19.69	0.49	0.01
15	19.52	0.32	0.13
17	19.67	0.47	-0.29
18	18.51	-0.69	0.01
19	18.75	-0.45	0.73
20	17.39	-1.81	0.00
21	16,32	-2.88	0,23
22	19.73	0.53	-0.06
23	19.43	0,23	-0.09
24	19.10	-0.10	0.53
25	19.63	0.43	-0.07
26	19.53	0.33	0.63
49	19.86	0.66	0.29
50	19.47	0.27	0.03
54	19.30	0.10	0.47
60	18.95	-0.25	0.52
68	19.13	-0.07	0.00
39'	16.04	-3.16	0.09

END

&RUN;

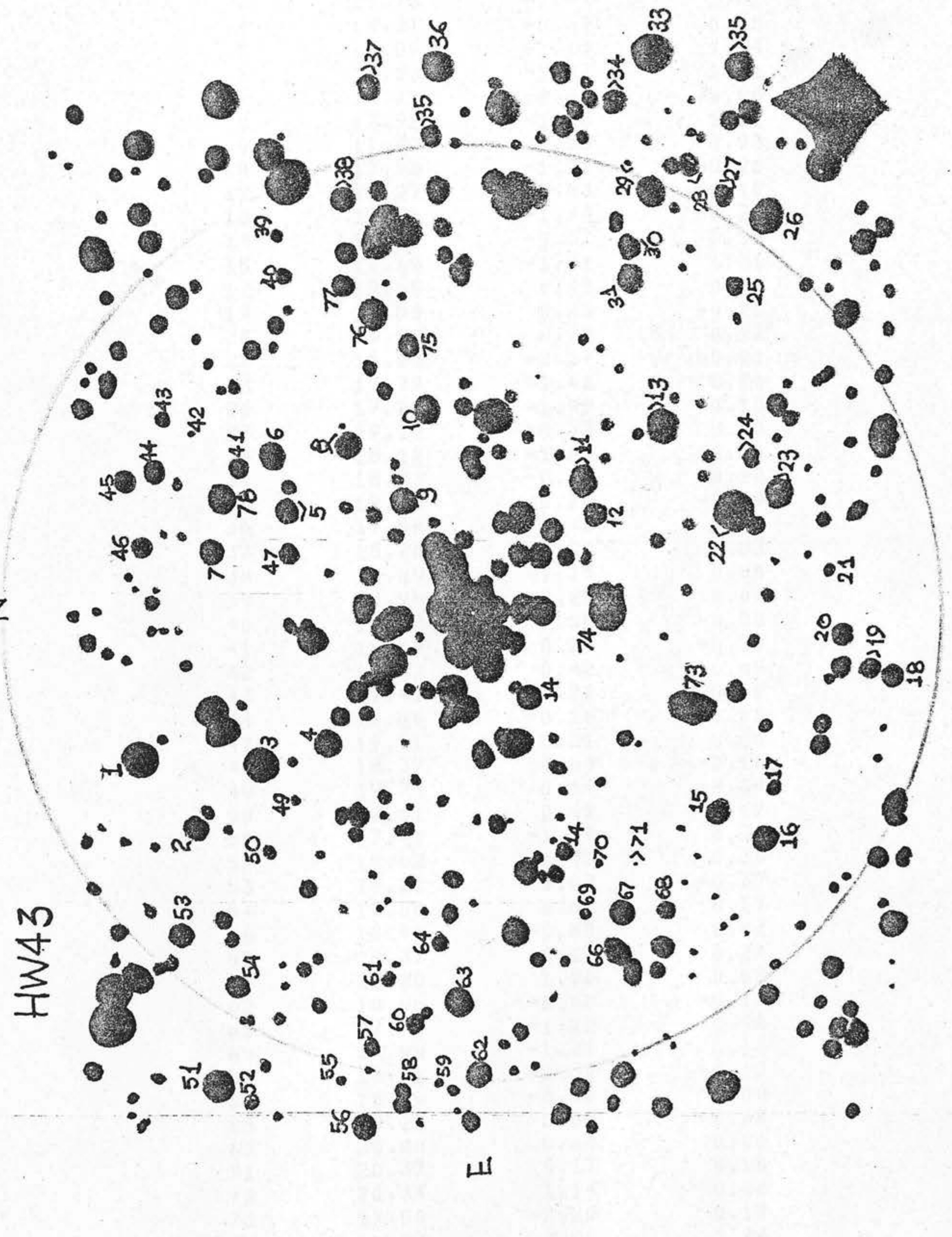
HW43
N
E
0'.90

CLUSTER NO HW43

REGION 1

STAR	V	MV	B-V
1	17.13	-2.07	0.23
2	18.40	-0.80	-0.11
3	16.73	-2.47	1.41
4	18.31	-0.89	0.18
5	17.09	-2.11	1.54
6	17.33	-1.87	1.31
7	18.11	-1.09	0.96
8	17.92	-1.28	1.11
9	17.62	-1.58	0.93
10	17.98	-1.22	0.28
12	18.27	-0.93	-0.10
13	17.46	-1.74	0.73
14	18.83	-0.37	0.13
15	17.69	-1.51	1.31
17	19.65	0.45	0.38
19	19.53	0.33	-0.20
20	19.90	0.70	0.12
22	16.63	-2.57	-0.01
23	17.79	-1.41	0.76
26	17.21	-1.99	0.10
27	19.12	-0.08	0.20
28	18.12	-1.08	0.56
34	18.73	-0.47	-0.28
35	19.46	0.26	-0.09
36	17.58	-1.62	0.78
37	18.20	-1.00	0.03
38	18.05	-1.15	0.86
39	18.95	-0.25	0.69
40	19.78	0.58	-0.08
41	19.44	0.24	-0.39
42	19.62	0.42	0.89
43	19.41	0.21	0.10
44	19.04	-0.16	-0.11
47	19.51	0.31	0.06
48	18.37	-0.83	-0.16
49	19.74	0.54	-0.04
50	19.61	0.41	0.17
51	17.41	-1.79	0.24
52	19.62	0.42	0.36
53	19.27	0.07	-0.37
54	19.80	0.60	0.17
56	18.40	-0.80	0.07
59	19.37	0.17	0.24
61	20.20	1.00	0.53
62	18.60	-0.60	-0.12
63	17.98	-1.22	0.98
65	17.99	-1.21	0.13
66	18.81	-0.39	-0.17
67	18.75	-0.45	1.09
68	19.22	0.02	0.58
69	20.00	0.80	0.20
71	20.37	1.17	0.16
72	20.34	1.14	0.08
73	17.00	-2.20	0.12
74	16.24	-2.96	0.24
75	18.54	-0.66	-0.14
76	18.48	-0.72	-0.07
77	18.67	-0.53	0.56
78	18.18	-1.02	-0.15

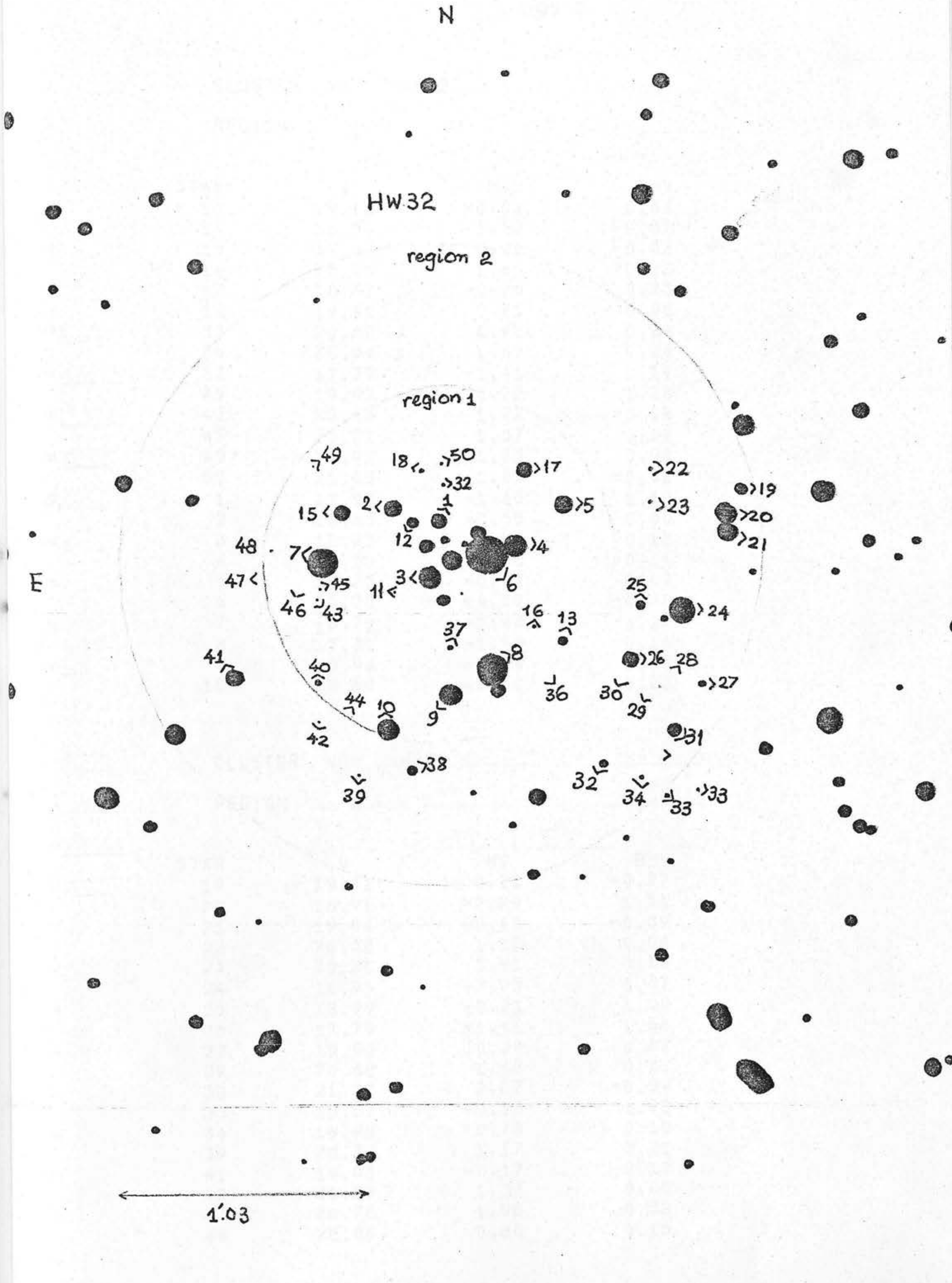
N
HW32
region 2
region 1
E
49
18
50
17
22
32
19
15
2
1
5
23
20
48
7
12
4
21
47
45
3
6
11
46
43
25
24
16
13
37
41
40
8
26
28
27
36
30
44
10
9
29
42
31
38
32
39
34
33
33
1'03

CLUSTER NO HW32

REGION 1

STAR	V	MV	B-V
13	19.16	-0.04	0.66
14	18.02	-1.18	-0.37
15	19.40	0.20	-0.32
16	20.85	1.65	-0.22
17	18.47	-0.73	0.73
18	19.41	0.21	0.58
32	20.62	1.42	0.24
36	20.89	1.69	0.24
37	17.79	-1.41	0.19
40	19.42	0.22	0.28
43	20.42	1.22	-0.14
45	20.27	1.07	0.19
49	21.05	1.85	0.02
50	21.05	1.85	-0.02
1	17.90	-1.30	1.40
2	18.65	-0.55	0.60
3	18.23	-0.97	0.18
4	18.00	-1.20	-0.11
5	18.23	-0.97	0.63
6	15.20	-4.00	-0.46
7	16.72	-2.48	0.27
8	17.30	-1.90	0.16
9	17.96	-1.24	0.93
10	18.60	-0.60	0.23

CLUSTER NO HW32

REGION 2

STAR	V	MV	B-V
19	19.41	0.21	-0.07
20	16.91	-2.29	1.51
21	19.04	-0.16	-0.89
22	20.38	1.18	0.04
23	20.21	1.01	0.13
24	16.95	-2.25	1.17
25	18.99	-0.21	1.00
26	17.79	-1.41	1.68
27	19.50	0.30	0.07
29	20.68	1.48	0.22
30	21.27	2.07	-0.09
33	19.07	-0.13	1.98
34	19.98	0.78	0.10
39	20.37	1.17	0.21
41	19.03	-0.17	0.17
42	20.53	1.33	0.06
47	20.76	1.56	0.32
48	20.06	0.86	0.15

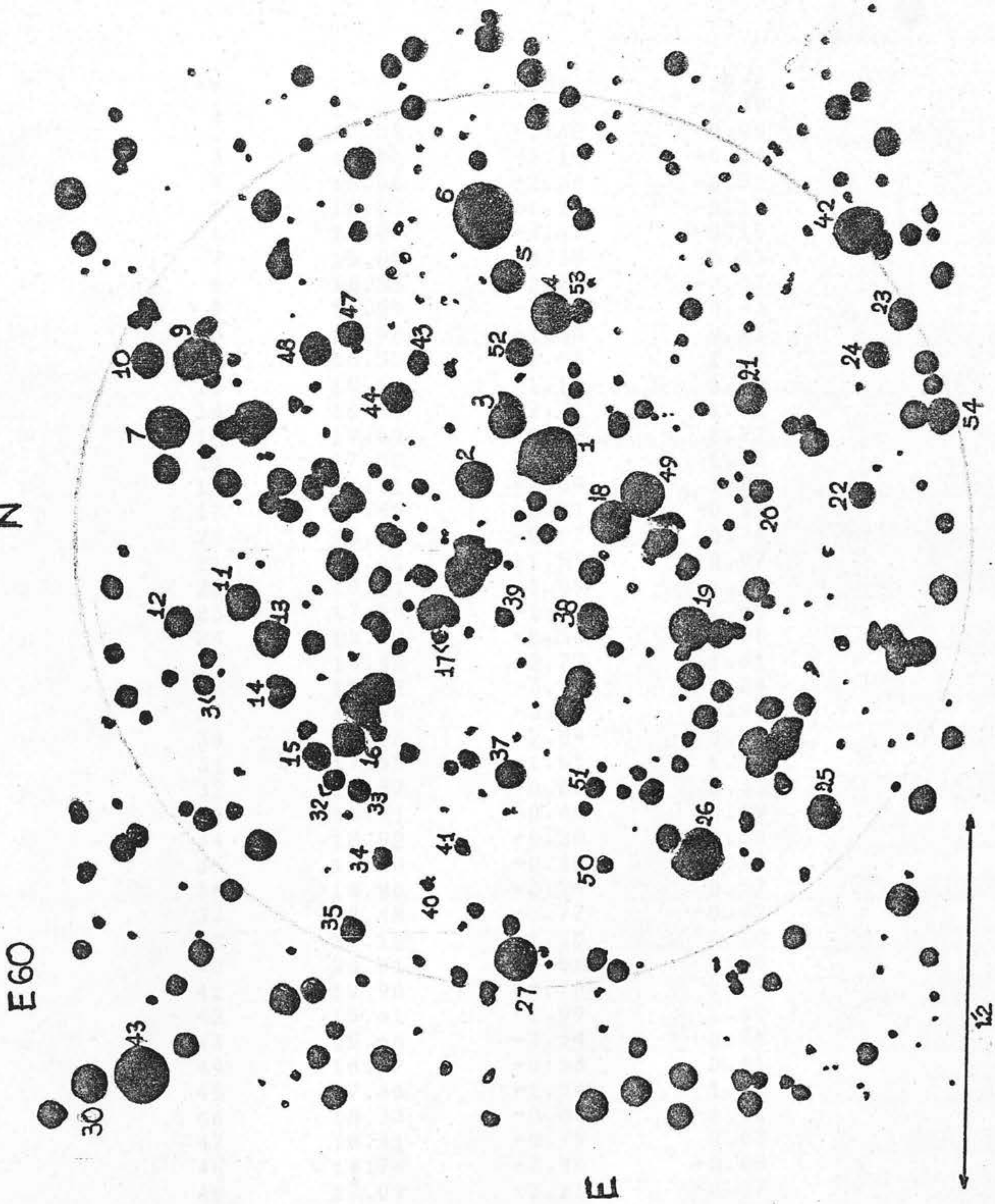
E60
N
E
1
2
3
4
5
6
7
9
10
11
12
13
14
15
16
17
18
19
20
21
22
23
24
25
26
27
30
31
32
33
34
35
37
38
39
40
41
42
43
44
47
48
49
50
51
52
53
54

CLUSTER NO E60

REGION 1

STAR	V	MV	B-V
1	15.08	-4.12	-0.39
2	17.58	-1.62	-0.09
3	17.06	-2.14	-0.04
4	16.86	-2.34	-0.51
5	18.07	-1.13	-0.17
6	14.77	-4.43	-0.15
7	15.82	-3.38	0.83
8	16.35	-2.85	-0.07
9	16.09	-3.11	0.43
10	17.90	-1.30	0.15
11	16.55	-2.65	1.24
12	18.10	-1.10	0.28
13	16.49	-2.71	1.01
14	19.69	0.49	1.22
15	17.50	-1.70	1.53
16	16.51	-2.69	1.93
17	16.49	-2.71	-0.39
20	18.28	-0.92	0.76
21	17.61	-1.59	0.97
22	18.11	-1.09	1.29
23	17.50	-1.70	1.50
24	18.62	-0.58	0.58
25	16.48	-2.72	1.61
26	15.22	-3.98	-0.04
27	15.98	-3.22	0.97
30	17.16	-2.04	0.01
31	17.55	-1.65	1.15
32	18.87	-0.33	0.33
33	18.71	-0.49	0.69
34	18.92	-0.28	0.60
35	19.10	-0.10	-0.10
36	18.96	-0.24	0.37
37	18.48	-0.72	-0.02
38	18.10	-1.10	0.30
40	20.01	0.81	0.08
41	19.90	0.70	0.23
42	15.61	-3.59	1.00
43	15.66	-3.54	0.74
44	18.67	-0.53	0.41
45	17.66	-1.54	1.02
46	18.33	-0.87	-0.11
47	18.41	-0.79	0.63
48	18.74	-0.46	-0.04
49	17.09	-2.11	-0.37
50	19.38	0.18	0.30
51	18.61	-0.59	-0.05
52	18.79	-0.41	-0.25
54	17.37	-1.83	-0.34

END

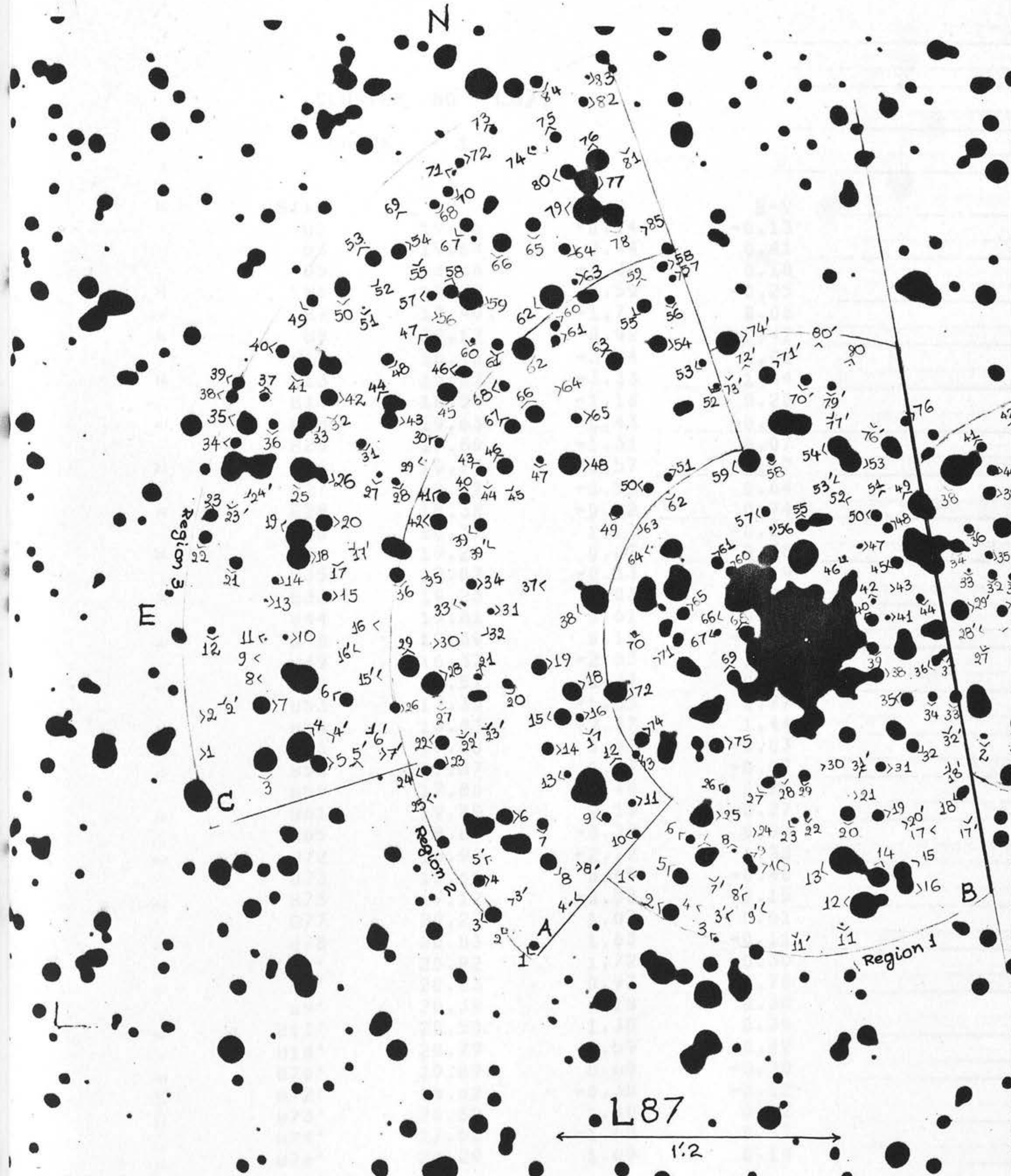
N
E
L87
1'.2
Region 1
Region 2
Region 3
A
B
C

CLUSTER NO L87

REGION 1

STAR	V	MV	B-V
B2	19.06	-0.14	-0.13
B3	19.64	0.44	0.41
B5	18.86	-0.34	0.10
B6	19.79	0.59	-0.25
B7	17.49	-1.71	0.08
B8	20.12	0.92	-0.42
B12	16.16	-3.04	1.01
B13	15.87	-3.33	1.44
B14	18.04	-1.16	0.28
B18	19.63	0.43	-0.09
B25	17.89	-1.31	0.07
B26	19.77	0.57	-0.17
B27	18.62	-0.58	0.64
B28	18.38	-0.82	0.74
B30	20.37	1.17	-0.24
B34	19.27	0.07	0.38
B35	19.07	-0.13	0.19
B38	19.23	0.03	-0.02
B44	19.81	0.61	0.11
B48	19.39	0.19	-0.17
B49	16.37	-2.83	1.46
B50	19.57	0.37	-0.16
B53	17.35	-1.85	0.77
B54	16.83	-2.37	1.44
B56	19.88	0.68	-0.03
B58	19.67	0.47	-0.07
B59	17.80	-1.40	0.25
B61	19.35	0.15	-0.27
B65	18.83	-0.37	0.03
B72	16.98	-2.22	1.30
B73	19.65	0.45	-0.40
B75	19.12	-0.08	-0.15
B77	20.27	1.07	0.61
B78	20.83	1.63	-0.11
B3'	20.92	1.72	-0.30
B7'	20.13	0.93	0.78
B9'	20.38	1.18	0.30
B11'	20.50	1.30	0.39
B18'	20.79	1.59	0.42
B70'	19.89	0.69	-0.30
B72'	18.82	-0.38	-0.12
B73'	20.60	1.40	0.42
B74'	17.52	-1.68	0.37
B76'	20.29	1.09	0.14

CLUSTER NO L87.

REGION 2

STAR	V	MV	B-V
A2	20.09	0.89	-0.05
A3	19.10	-0.10	-0.14
A4	19.59	0.39	0.01
A6	18.98	-0.22	-0.21
A7	19.71	0.51	-0.27
A8	18.86	-0.34	0.06
A9	19.09	-0.11	0.44
A10	19.19	-0.01	0.65
A14	19.68	0.48	-0.26
A15	18.76	-0.44	0.01
A18	18.36	-0.84	0.27
A19	19.00	-0.20	-0.11
A20	19.08	-0.12	0.21
A21	19.83	0.63	-0.47
A22	18.50	-0.70	1.09
A23	19.63	0.43	-0.16
A25	20.07	0.87	0.07
A27	20.04	0.84	-0.12
A28	17.70	-1.50	0.31
A29	17.99	-1.21	0.13
A34	19.15	-0.05	1.01
A35	20.42	1.22	-0.34
A37	19.23	0.03	-0.07
A38	16.95	-2.25	0.42
A39	18.91	-0.29	-0.10
A40	19.20	0.00	0.52
A41	18.71	-0.49	0.77
A42	18.97	-0.23	-0.08
A44	20.05	0.85	-0.30
A47	19.95	0.75	-0.08
A48	17.21	-1.99	1.14
A49	19.39	0.19	-0.19
A50	19.34	0.14	0.64
A51	19.91	0.71	-0.20
A52	20.10	0.90	0.04
A53	19.30	0.10	0.54
A54	18.77	-0.43	0.07
A60	19.75	0.55	-0.31
A61	19.55	0.35	-0.18
A62	18.04	-1.16	0.06
A66	18.49	-0.71	0.28
A67	19.18	-0.02	-0.06
A68	19.79	0.59	-0.49
A71	20.40	1.20	0.10
A74	20.52	1.32	0.27
A76	21.15	1.95	-0.15
A77	21.04	1.84	-0.18
A3'	21.29	2.09	-0.25
A5'	20.19	0.99	0.21
A22'	20.84	1.64	-0.06
A23'	20.86	1.66	0.19

CLUSTER NO L87

REGION 3

STAR	V	MV	B-V
C2	19.89	0.69	-0.11
C3	17.65	-1.55	0.23
C4	15.95	-3.25	1.19
C5	18.89	-0.31	-0.13
C6	18.73	-0.47	0.75
C7	18.64	-0.56	0.26
C9	19.98	0.78	0.04
C18	17,57	-1.63	0.49
C19	16.57	-2.63	1.09
C20	18.41	-0.79	0.41
C25	17.30	-1.90	0.10
C26	18,91	-0.29	0.46
C27	20.06	0.86	-0.35
C29	20,49	1.29	-0.32
C30	19.92	0.72	-0.30
C31	19,53	0,33	0.31
C33	18.44	-0.76	0.31
C34	19.40	0.20	-0.03
C35	16.96	-2.24	1.31
C38	18.47	-0.73	0.86
C41	17.56	-1.64	1.11
C42	18.71	-0.49	0.14
C44	18.67	-0.53	-0.07
C45	17.54	-1.66	1,08
C47	18.85	-0.35	0.18
C48	19.47	0.27	-0.10
C49	19.17	-0.03	0.31
C50	18.71	-0.49	-0.02
C51	20.15	0.95	0.03
C54	19.23	0.03	-0.11
C55	20.76	1.56	-0.29
C56	20.39	1.19	0.08
C58	18.50	-0.70	0.77
C59	17.65	-1.55	0.32
C62	16.67	-2.53	1.32
C63	19.20	0.00	0.69
C64	19.08	-0.12	0.51
C65	18.52	-0.68	1.03
C66	18.03	-1.17	0.81
C70	19.59	0.39	-0.19
C72	18.95	-0.25	0.47
C74	19.69	0.49	0.25
C76	16.86	-2.34	1.15
C78	17.01	-2.19	0.12
C79	16.06	-3.14	0.83
C80	17.98	-1.22	1.14
C83	19.48	0.28	-0.10
C84	17.95	-1.25	1.06
C85	20.21	1.01	0.04
C3'	20.80	1.60	0.13
C5'	20.89	1.69	0.24
C12'	21.37	2.17	-0.53
C17'	20.25	1.05	0.14
C23'	21.08	1.88	-0.06

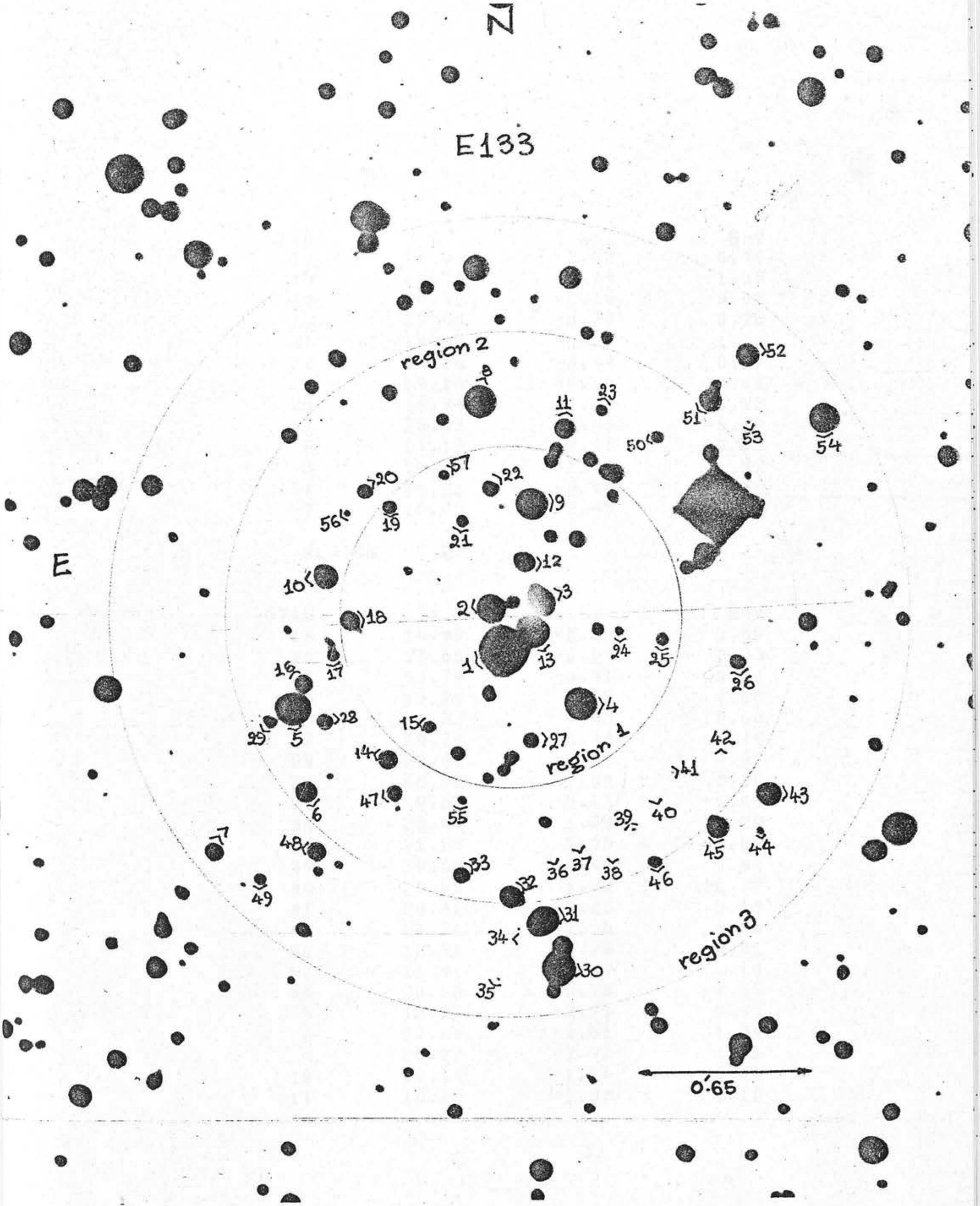
N
E
E133
region 1
region 2
region 3
1
2
3
4
5
6
7
8
9
10
11
12
13
14
15
16
17
18
19
20
21
22
23
24
25
26
27
28
29
30
31
32
33
34
35
36
37
38
39
40
41
42
43
44
45
46
47
48
49
50
51
52
53
54
55
56
57
0'65

CLUSTER NO E133

REGION 1

STAR	V	MV	B-V
13	16.68	-2.52	0.49
15	18.56	-0.64	1.09
18	18.90	-0.30	0.08
19	19.00	-0.20	0.76
21	19.05	-0.15	1.00
22	18.76	-0.44	0.37
24	19.10	-0.10	0.63
25	18.94	-0.26	0.92
57	20.03	0.83	-0.24
2	17.17	-2.03	0.58
3	16.79	-2.41	1.59
4	16.25	-2.95	1.09
9	16.75	-2.45	0.51

REGION 2

STAR	V	MV	B-V
14	18.95	-0.25	0.00
16	18.66	-0.54	0.73
20	18.79	-0.41	0.88
23	19.25	0.05	0.50
26	28.83	9.63	0.60
27	18.74	-0.46	0.74
29	19.06	-0.14	0.26
32	18.20	-1.00	0.10
33	19.32	0.12	-0.02
36	20.94	1.74	0.29
37	21.25	2.05	-0.02
39	19.60	0.40	0.84
40	20.55	1.35	-0.22
41	20.41	1.21	0.18
42	20.76	1.56	0.56
50	18.92	-0.28	0.81
51	18.41	-0.79	0.14
56	20.18	0.98	-0.19
5	16.25	-2.95	0.45
6	17.69	-1.51	1.49
8	16.27	-2.93	1.21
10	18.14	-1.06	0.41
11	18.12	-1.08	1.10

CLUSTER NO E133

REGION 3

STAR	V	MV	B-V
12	18.33	-0.87	0.36
17	19.26	0.06	0.15
28	19.28	0.08	-0.05
30	16.09	-3.11	0.31
31	16.09	-3.11	1.18
34	20.08	0.88	0.21
35	19.81	0.61	0.32
43	18.09	-1.11	0.15
45	17.53	-1.67	1.22
47	18.95	-0.25	0.41
48	18.86	-0.34	-0.02
49	19.20	0.00	0.63
52	17.57	-1.63	1.22
53	19.69	0.49	0.42
54	16.41	-2.79	1.13
7	17.99	-1.21	1.08

END

&RUN;

ACKNOWLEDGEMENTS

I owe the credit for this thesis to both of my supervisors, Dr. M.T. Brück and Dr. R.D. Cannon whose inspiration and encouragement have guided me over the past three years. I am deeply grateful to Professor V.C. Reddish for being so helpful and providing all necessary facilities for the completion of my project.

I am also indebted to Professor H.A. Brück for accepting me at Edinburgh University and making all the arrangements for the progress of my project during the first two years of my studies.

My thanks are also due to the Electronics Department of R.O.E. and especially Mr. G.A. Baldwin for being so helpful during my work with the iris photometer Becker 1 of R.O.E.

I am grateful to Mr. C.K. Barclay and Mrs. M. Fretwell for making blow-up prints of the measured regions and to the U.K. Schmidt Telescope Unit for allowing me ready access to the plate material and for the loan of plates.

I shall also thank again everybody on the staff of R.O.E. and University Department for being so hospitable and kind all these years. It has really been a pleasure working in this establishment.

I wish to thank the Greek Professors, D. Kotsakis, G. Contopoulos and M. Moutsoulas for their encouragement and help.

I was supported while working on this project by a grant from the Greek State Scholarship Foundation and I wish to address my thanks to all the staff and Director for being so helpful all these years.

REFERENCES

Ahmed, F., Lawrence, L.C., Reddish, V.C., 1965. ROE Publications, Vol. 3, No. 7.

Alcaino, G., 1973. "Atlas of galactic globular clusters with C-M diagrams".

Alcaino, G. and Contreras, C., 1971.. Astr. & Astroph. Suppl. Ser. 11, 14.

Alcaino, G., 1974. ESO/SRC/CERN Conference on"Research Programmes for the New Large Telescopes", Geneva, May 1974, p. 209.

Andrews, P.J., 1971. "The Magellanic Clouds", Reidel Publish Co. Dordrecht, p. 79.

Ambartsumian, V.A., 1971 "Nuclei of Galaxies", editor D.J.K. O'Connel. American Elsevier, New York, p. 9.

Argue, A.N., 1960. Vistas in Astronomy, 3, 184.

Arp, H.C. & Hartwick, F.D.A., 1971. Astroph. J., 167, 499.

Arp, H.C., 1958. Astr. J., 63, 273.

Arp, H.C., 1958. Astr. J., 63, 118.

Arp, H.C., 1958. Astr. J., 63, 487.

Arp, H.C., 1959. Astr. J., 64, 254.

Arp, H.C., 1959. Astr. J., 64, 175.

Baade, W., and Swope, H., 1961. Astr. J., 66, 300.

Baird, S., Flower, P.J., Hodge, P.W. Szkody, P., 1974. Astr. J., 70, 1365.

Basinski, J.T., Bok, B.J., Bok, P.J., 1966. PASP, 78, 439.

Barbaro, G., and Dallaporta, N., 1972. "Stellar Ages", Proceedings of the I.A.U. Colloquium No. 17, held at Meudon, France, September 1972, p. XVI-1.

Becker, W., 1972. Conference on "The role of Schmidt telescopes in the study of Galactic Structure", Hamburg, March 1972, p. 9.

Becker, W. and Biber, C., 1956. Zs. f. Ap., 41, 52.

van den Bergh, S., 1968. Astr. J., 73, 569.

van den Bergh, S., 1974. I.A.U. Symposium No. 58, 157.

Bok, B.J., 1966. An. Rev. of Astr. & Astrophys., 4, 95.

Brück, M.T., 1976. Occ. Reports of the ROE, No. 1.

Brück, M.T., 1972. Publ. of the ROE, Vol. 7, No. 7.

Brück, M.T., 1972. Publ. of the ROE, Vol. 7, No. 8.

Brück, M.T., 1975. Mon. Not. R. astr. Soc., 173, 327.

Brück, M.T., Lawrence, L.C., Nandy, K., Thackeray, A.D., Wood, R., 1970. Nature, 225, 531.

Butler, C.J., 1972. Dunsink Obs. Publ. No. 1, 133.

Butler, C.J., 1972. Ph.D. Thesis, Dunsink Observatory.

Cannon, R.D. and Stobie, R.S., 1976. Cluster NGC 288 (private communication).

Cannon, R.D., 1974. "Faint photoelectric standard in 47 TUC, (private communication).

Cannon, R.D., 1970. Mon. Not. R. astr. Soc., 150, 111.

Cannon, R.D., 1968. Ph.D. Thesis, Cambridge University.

Cannon, R.D., 1974. Mon. Not. R. astr. Soc., 167, 551.

Cannon, R.D. and Lloyd, C., 1970. Mon. Not. R. astr. Soc., 150, 279.

Cannon, R.D. and Stobie, R.S., 1973. Mon. Not. R. astr. Soc., 162, 227.

Cannon, R.D. and Stobie, R.S., 1973. Mon. Not. R. astr. Soc., 162, 207.

Cannon, R.D., 1974. ESO/SRC/CERN Conference, on Research Programmes for the New Large Telescopes, 207.

Chiosi, C. and Nasi, E., 1974. I.A.U. Symposium, No. 66, 102.

Clayton, D.D., 1968. "Principles of stellar evolution and Nucleosynthesis", McGraw-Hill Book Company, New York.

Clayton, D.D. and Woosley, S.E., 1974. Reviews of Modern Physics, 46, 755.

Davies, R.D., Elliot, K.H. and Meaburn, K., 1976. Mem. R. astr. Soc., 81, 89.

Dickens, R.J., 1972. Mon. Not. R. astr. Soc., 157, 281.

Dickens, R.J., 1974. ESO/SRC/CERN, Conference on "Research programmes for the New Large Telescopes, Geneva, 71.

Dickens, R.J., 1972. Mon. Not. R. astr. Soc., 157, 299.

Dluzheuskaya, O.B., Piskunov, A.E., 1976. I.A.U. Proceedings of the 3rd European Astr. Meeting, Tbilisi, July 1975, 513.

Eigenson, A.M. and Samus, N.N., 1975. Astrofisika, Vol. 11, translated July 1976, p. 247.

Eigenson, A.M., 1973. Astrofisika, Vol. 9, translated, p. 107.

Faulkner, D.J., and Cannon, R.D., 1973. Ap. J., 180, 435.

Feast, M.W., 1960. "The Observatory", 80, 104.

Feast, M.W. and Evans, L., 1973. Mon. Not. R. astr. Soc., 164, 15p.

Feast, M.W., 1974. ESO/SRC/CERN, Conference on Research Programmes for the New Large Telescope, Geneva, May 1974, p. 169.

Fehrenbach, C. and Duflot, M., 1962. Comptes Rendus de l'Acc. de Paris, 254, 1380.

Flower, P. and Hodge, P.W., 1975. Ap.J., 196, 369.

Freeman, K.C., 1974. ESO/SRC/CERN, conference on "Research programmes for the New Large Telescope", Geneva, May 1974, p. 177.

Freeman, K.C. and Munsuk, C., 1972. Proceedings Austr. Soc. of Astr. 2(3), October 1972, p. 15.

Freeman, K.C., 1976. "Galaxies and the Universe", Ed. A. Sandage, M. Sandage and J. Kristian. Stars and Stellar Systems Vol. IX, University Chicago Press, p. 42.

Gaposhkin, S., 1972. "Stellar ages". Proceedings of the I.A.U. Colloquium No. 17 held at Meudon France, September 1972, p. IV-1.

Gascoigne, S.C.B., 1963. "The Observatory", 83, 71.

Gascoigne, S.C.B., 1966. Mon. Not. R. astr. Soc., 134, 59.

Gascoigne, S.C.B., 1962. Mon. Not. R. astr. Soc., 124, 210.

Gascoigne, S.C.B., Norris, J., Bessell, M.S., Hyland, A.R. and Visvanathan, N., 1976. Ap. J. Letters, 209, L25.

Golay, M., 1974. "Introduction to Astronomical Photometry" Astroph. and Space Science Library, Vol. 41, p. 85.

Graham, J.A., 1975. Publ. astr. Soc. Pacific, 87, 641.

Graham, J.A., 1976. Irish Astr. Journal, 12, 138.

Graham, J.A., 1974. ESO/SRC/CERN Conference on Research programmes for the New Large Telescope, Geneva, May 1974, p. 159.

Grenstein, J. and Sargent, A., 1974. Ap.J. Suppl. Ser. 28, 157.

Hagen, G.L. and can den Bergh, S., 1974. Ap. J. Letters, 189, L103.

Harding, G.A., Harbour, R.S., Tritton, K.P., 1971. Royal Observatory Bulletins, No. 172.

Harris, W., 1974. Ap. J., 192, L161.

Hartwick, F.D.A. & van den Bergh, D.A., 1973. Publ. astr. Soc., Pacific, 85, 355.

Hartwick, F.D.A. and McClure, R.D., 1972. Ap.J. Letters, 176, L59.

Hayashi, C., Hoshi, R., Sugimoto, D., 1962. Suppl. of the Progress of Theoretical Physics, No. 22.

Hindman, J.V., 1976. Australian J. Phys., 78, 147.

Hodge, P.W., 1973. Astr. J. 78, 807.

Hodge, P.W., 1974. Astr. J., 79, 860.

Hodge, P.W. and Wright, F.W., 1974. Astr. J., 79, 858.

Hodge, P.W. and Flower, P.J., 1973. Ap. J., 185, 829.

Hodge, P.W., 1971. Smithsonian Astr. Obs. Special Report, 337.

Iben, I., 1971. Publ. Astr. Soc. Pacific, 83, 466.

Iben, I. and Rood, R.T., 1969. Ap.J., 159, 605.

Johnson, H.L., et al., 1961. Lowell Obs. Bull, Vol. V, No. 8, 133.

King, I.R., 1966. Astr. J., 71, 64.

Kron, G.E., 1956. Publ. astr. Soc. Pacific, 68, 125.

Kukarkin, B.V., 1974. "The Globular star clusters", The Academy of Sciences of the U.S.S.R., Publishing House, "NAUKA", Moscow, 1974.

Lequeux, J., 1966. "Structure and Evolution of Galaxies", Gordon and Breach Science Publishers.

Lindsay, E.M., 1958. Mon. Not. R. astr. Soc., 118, 172.

Lucke, P.B., 1974. Ap. J. Suppl. Ser., 28, 73.

MacGillivray, H.T., 1975. Mon. Not. R. astr. Soc., 170, 241.

Mallia, E.A., 1976. Astr. & Astrophys., 48, 129.

Mathewson, D.S., 1974. ESO/SRC/CERN conference on "Research programmes for the New Large telescope", Geneva May 1974, p. 189.

McClure, R.D., Forrester, W.T., Gibson, J., 1974. Ap. J. 189, 409.

McClure, R.D. and Norris J., 1974. Ap. J., 193, 144.

McCuskey, S.W., 1966. Vistas in Astronomy, 7, 141.

Meurers, J., 1953. Veröff. Univ. Sternw. Bon. no. 41.

Mihalas, D., 1968. "Galactic Astronomy, p. 232.

Miller, Wm. C., 1972. Conference on "The role of Schmidt telescopes in the study of the Galactic Structure", Hamburgh, March 1972, p. 148.

Norris, J., 1974. Ap.J., 191, 103.

Novotny, E., 1973. "Introduction to stellar atmospheres and interiors", Oxford University Press, New York.

Pagel, B.E.J., 1974. Mon. Not. R. astr. Soc., 167, 413.

Payne-Gaposhkin, C., 1972. "Stellar Ages", Proceedings of the I.A.U. colloquium No. 17 held at Meudon, France, September 1972, p. III-1.

Peimbert, M., 1974. I.A.U. Symp. 58, p. 141.

Reddish, V.C., 1974. "The physics of stellar interiors", Edinburgh University Press.

Reddish, V.C., 1966. Publ. Roy. Obs. Edinb., Vol. 5, 111.

Reddish, V.C., 1972. Conference on "The role of Schmidt telescopes in the study of Galactuc Structure", Hamburg, March, 1972, 148.

Robertson, J.W., 1974. Astr. & Astroph. Suppl. Ser., 15, 261.

Robertson, J.W., 1972. Ap.J., 177, 473.

Robertson, J.W., 1973. Ap. J., 180, 425.

Robertson, J.W., 1974. Ap. J., 191, 67.

Robertson, J.W., 1973. Ap. J., 185, 817.

Rood, R.T., 1973. Ap. J., 184, 815.

Rood, R.T., 1972. Ap. J., 177, 681.

Sandage, A., 1953. Astron. J., 59, 162.

Sandage, A., 1969. Ap. J., 157, 515.

Sandage, A. and Wildey, R., 1967. Ap. J., 150, 469.

Sandage, A., 1970. Ap. J., 162, 841.

Sanduleak, N., MacConnel, D.J. and Hoover, P.S., 1972. Nature, 237, 28.

Schild, R., 1970. Ap. J., 161, 855.

Schlesinger, B.M., 1969. Ap. J., 158, 1059.

Schlesinger, B.M., 1969. Ap. J., 157, 533.

Schwarzschild, M., 1958. "Structure and evolution of stars", Dover Publications, New York.

Simoda, M., 1959. Ap. J., 160, 133.

Tifft, W.G., 1963. Mon. Not. R. astr. Soc., 125, 199.

Tifft, W.G. and Snell, C.M., 1970. Mon. Not. R. astr. Soc., 151, 365.

Tifft, W.G., 1962. Mon. Not. R. astr. Soc., 126, 209.

de Vaucouleurs, G. and Freeman, K.C., 1973. "Vistas in Astronomy, 14, 163.

Vigroux, L., Andouze, J. and Lequeux, J., 1976. Astron. & Astroph., 52, 1.

Walker, M., 1970. Ap. J., 161, 835.

Walker, M., 1972. Mon. Not. R. astr. Soc., 159, 379.

Wayman, P.A., 1972. Conference on "The role of Schmidt telescopes in the study of the Galactic Structure", Hamburg , March 1972, p. 101.

Webster, B.L., 1975. Project report. GR 16/75.

Westerlund, B.E., 1972. "Vistas in Astronomy", 12, 335.

Westerlund, B.E., 1961. K.V.A. Handl 8:4.

Westerlund, B.E., 1972. "Galaxies and relativistic astrophysics", 1st European Astron. Meeting, Athens 1972. Proceedings Vol. 3, p. 39.

Wolf, B., 1973. Astr. & Astrophys., 28, 335.

Woolley, R.R., 1963. Royal Observatory Bulletins, No. 66.

Woolley, R.R. and Dickens, R.J. 1966. Royal Observatory Bulletins, No. 42.